PhD-FSTC-2015-60
The Faculty of Sciences, Technology and Communication

DISSERTATION

Defence held on 04/12/2015 in Luxembourg

to obtain the degree of

DOCTEUR DE L'UNIVERSITÉ DU LUXEMBOURG

EN BIOLOGIE

by

MAITI LOMMEL
Born on 9 January 1988 in Luxembourg (Luxembourg)

ANALYSIS OF SIGNAL TRANSDUCTION PATHWAYS LINKING L-PLASTIN SER5 PHOSPHORYLATION TO BREAST CANCER CELL INVASION

Dissertation defence committee

Dr. Elisabeth Schaffner-Reckinger, Dissertation Supervisor
University of Luxembourg

Dr. Serge Haan, Dissertation Co-supervisor and Vice Chairman
Professor, University of Luxembourg

Dr. Thomas Sauter, Chairman
Professor, University of Luxembourg

Dr. Christophe Ampe
Professor, University of Ghent

Dr. Guy Berchem
Medical Doctor, Luxembourg Institute of Health

Faculty of Science, Technology and Communication

UNIVERSITÉ DU LUXEMBOURG

Analysis of signal transduction pathways linking L-plastin Ser5 phosphorylation to breast cancer cell invasion

A dissertation by

Maiti Lommel

Life Sciences Research Unit, University of Luxembourg

Doctoral School in Systems and Molecular Biomedicine

Dissertation defence committee:

Supervisor:	Dr. Elisabeth Schaffner-Reckinger University of Luxembourg, Life Sciences Research Unit, Cytoskeleton and Cell Plasticity Group
Co-supervisor:	Dr. Serge Haan Professor, University of Luxembourg, Life Sciences Research Unit, Molecular Disease Mechanisms Group
Chairman:	Dr. Thomas Sauter Professor, University of Luxembourg, Life Sciences Research Unit, Systems Biology Group
Members:	Dr. Christophe Ampe Professor, University of Ghent, Department of Biochemistry, Molecular Cell Biology and of the Actin Cytoskeleton Group
	Dr. Guy Berchem Medical Doctor, Luxembourg Institute of Health, Department of Oncology, Laboratory of Experimental Hemato-Oncology

Acknowledgements

First and foremost I would like to express my deep gratitude to my supervisor, Dr. Elisabeth Schaffner-Reckinger, who has supported me throughout my thesis with a lot of energy and a great enthusiasm for the subject matter. Your guidance and encouragement largely contributed to the completion of my dissertation and I would also like to thank you for your openness and informality which made it a pleasure working with you.

I also thank my co-supervisor, Prof. Dr. Serge Haan, for always being available for giving advice and support and I thank Dr. Panuwat Trairatphisan and Prof. Dr. Thomas Sauter for their great collaboration on the modelling part of my dissertation.

I also express my gratitude to our collaborators at Ghent University in the groups of Prof. Dr. Christophe Ampe and Prof. Dr. Kris Gevaert for receiving me for a research stay.

Special thanks go to Dr. Laurent Vallar from the Luxembourg Institute of Health and his team members (Arnaud Muller, Tony Kaoma, François Bernardin and Petr Nazarov) for their help with the microarray experiments.

I am grateful to Christina Laurini, Karoline Gäbler and Alexandre Baron for their meaningful contribution to my experiments and to Monique Wiesinger, Andreas Girod and Sébastien Plançon for their guidance in the P2 lab, in the microscopy and in the flow cytometry facilities respectively. Thanks also go to Nicolas Beaume and Aurélien Ginolhac for their help with statistical data analysis. Big thanks also go to all current and alumni lab members for giving outstanding advice and for creating an enjoyable working atmosphere. I also wish to thank my colleagues from the LSRU for helping out with material and for providing a very pleasant working environment. Thanks also go to Prof. Dr. Evelyne Friederich as an initiator of my research project.

I would like to thank Prof. Dr. Christophe Ampe, Dr. Guy Berchem, Prof. Dr. Thomas Sauter, Prof. Dr. Serge Haan and Dr. Elisabeth Schaffner-Reckinger for accepting to be members of my Dissertation Defence Committee. A special thanks also goes to the members of my Dissertation Supervisory Committee, Dr. Thomas Clément and Prof. Dr. Serge Haan, for having accompanied my PhD project.

I wish to express my thankfulness to the FNR for financing my thesis.

Last but not least, I wish to express my deep gratitude to my family and my friends for their love and support and to my partner, Pit Ullmann, for constructive proofreading of my thesis and for his love and encouragement.

Table of contents

Abbreviations

Å	Angstrom
ABD	Actin-binding domain
ABP	Actin-binding protein
ADP	Adenosine diphosphate
ALS	Amyotrophic lateral sclerosis
AR	Amphiregulin
ATP	Adenosine triphosphate
BC	β-cellulin
BID	BI-D1870 (RSK inhibitor)
BSA	Bovine serum albumin
CAMK	Ca^{2+}/calmodulin-dependent protein kinase
CCR7	C-C chemokine receptor type 7
CD	Cluster of differentiation
CH	Calponin homology
CHO	Chinese hamster ovary
CPM	Counts per minute
CTKD	Carboxyl-terminal kinase domain
DEG	Differentially expressed gene
ECM	Extracellular matrix
EGF	Epidermal growth factor
EGFR	Epidermal growth factor receptor
EMT	Epithelial to mesenchymal transition
EGN	Epigen
EPR	Epiregulin
ER	Estrogen receptor
ERK	Extracellular signal regulated kinase (MAPK3)

FC	Fold change
FDA	US Food and Drug Administration
FDR	False discovery rate
G-actin	Globular actin
GF	GF109203X (PKC inhibitor)
GTP	Guanosine triphosphate
Grb2	Growth factor receptor-bound protein 2
GST	Glutathione S-transferase
H	Hour(s)
HBEGF	Heparin-binding EGF-like growth factor
HEK	Human embryonic kidney 293
Ig	Immunoglobulin
IL	Interleukin
IPA	Ingenuity Pathway Analysis
Kb	Kilo-base pair
kDa	Kilo Dalton
LC-MS/MS	Liquid chromatography-tandem mass spectrometry
LCP1	Lymphocyte cytosolic protein 1
LFA-1	Lymphocyte function-associated antigen 1
LIMMA	Linear models for microarray data
M	Molar
mAb	Monoclonal antibody
MAPK	Mitogen-activated protein kinase
MAPKK	Mitogen-activated protein kinase kinase
MAPKKK	Mitogen-activated protein kinase kinase kinase
MAPKAPK	Mitogen-activated protein kinase-activated protein kinase
MEK	Dual specificity mitogen-activated protein kinase kinase (MAPKK)
MET	Mesenchymal to epithelial transition

Min	Minute(s)
MMP	Matrix metalloproteinase
MS	Mass spectrometry
MSKs	Mitogen- and stress-activated kinases or ribosomal protein S6 kinases
MT	Mutant
NK cell	Natural killer cell
NRG	Neuregulin
NTKD	Amino-terminal kinase domain
P70S6K	p70 ribosomal protein S6 kinase
PBS	Phosphate-buffered saline
PBS-MgCa	PBS supplemented with 0.1 mM $MgCl_2$ and 0.1 mM $CaCl_2$
PD	PD98059 (MEK inhibitor)
PI3K	Phosphoinositide-3-kinase
PKA	Protein kinase A
PKC	Protein kinase C
PMA	Phorbol 12-myristate 13-acetate
PMN	Polymorphonuclear neutrophil
PR	Progesterone receptor
PTB	Phosphotyrosine-binding
RSKs	p90 ribosomal S6 kinases or ribosomal protein S6 kinases
RAF	RAF proto-oncogene serine/threonine-protein kinase
RT	Room temperature
SD	Standard deviation
SDS	Sodium dodecyl sulfate
Ser	Serine
SEM	Standard error of the mean
SGK	Serum and glucocorticoid- regulated kinase
SH2	Src homology 2

Src	Proto-oncogene tyrosine-protein kinase Src
Syk	Spleen tyrosine kinase
TBB	Tetra-bromo-benzo-triazole
TBCA	Tetra-bromo-cinnamic acid
TBS	Tris-buffered saline
TGF-α	Transforming growth factor α
Thr	Threonine
TKI	Tyrosine kinase inhibitors
TNBC	Triple-negative breast cancer
TNF	Tumour necrosis factor
Tyr	Tyrosine
WT	Wild type
2-D	Two-dimensional
8Br	8-Bromo-cAMP (PKA activator)

Summary

The organisation of the actin cytoskeleton is regulated by abundant actin-binding proteins. Functional alteration of these proteins contributes to pathologies such as cancer where structural and functional modifications of the actin cytoskeleton are linked to uncontrolled cell motility and signalling. The actin-bundling protein L-plastin has initially been detected in haematopoietic cells where it plays a role in the immune response. L-plastin is also ectopically expressed in several solid tumours and is often considered as a metastatic marker. L-plastin is known to be phosphorylated *in vitro* and *in vivo* with residue serine 5 (Ser5) being the major phosphorylation site. Ser5 phosphorylation increases the F-actin-binding and -bundling activity of L-plastin and regulates actin turn-over. Recent findings demonstrate that L-plastin Ser5 phosphorylation is crucial for invasion and metastasis formation. This research work has unravelled the signalling pathways leading to L-plastin Ser5 phosphorylation in breast cancer cells.

Previously, protein kinase A, protein kinase C and phosphoinositide-3-kinase have been reported to play a role in L-plastin Ser5 phosphorylation depending on the cell type and environment. This work however reveals that RSK kinases are the predominant kinases responsible for L-plastin Ser5 phosphorylation in breast cancer cells. *In vitro* kinase assays revealed that RSK1 and RSK2 are able to directly phosphorylate L-plastin on Ser5 and a whole genome microarray analysis pointed to an involvement of the ERK/MAPK pathway in this event. The involvement of this pathway was consolidated by activation and inhibition studies as well as by siRNA-mediated knockdowns. To our knowledge, this is the first evidence that L-plastin Ser5 phosphorylation occurs via the downstream ERK/MAPK pathway kinases, RSK1 and RSK2.

Moreover, a computational modelling approach enabled us to show that RSK is the most important activator of L-plastin in breast cancer cell lines compared to other previously identified kinases.

We performed migration and invasion assays which showed that RSK knockdown, besides reducing L-plastin Ser5 phosphorylation, also impaired breast cancer cell migration and invasion. The identification of a novel substrate of RSK kinases whose phosphorylation is important for cancer cell invasion underlines the importance of RSK in cancer progression and highlights RSK as a promising drug target in certain invasive carcinomas.

Chapter 1 Introduction

1.1 The actin cytoskeleton

1.1.1 Generalities

The 42 kDa actin monomer, which is the cornerstone of the actin cytoskeleton, has been discovered in muscle cells in the 1940's (Straub, 1942) and is found as the most abundant protein in almost all eukaryotic cells. Its sequence and structure are strongly conserved among species. Vandekerckhove and Weber revealed that six species-independent actin isoforms exist (Vandekerckhove and Weber, 1978): 2 smooth muscle actin isoforms (α-smooth and γ-smooth muscle), two striated muscle isoforms (α-skeletal and α-cardiac) and two cytoplasmic isoforms (β-cytoplasmic and γ-cytoplasmic). The α-actins are primarily expressed in muscle cells, β-actin is primarily expressed in non-muscle cells and γ-actins are expressed in both cell types.

Actin is a globular protein with overall dimensions of 67x40x37 Å. It consists of a single polypeptide chain of 375 residues comprising a small domain further divided into subdomains I and II and a large domain further divided into subdomains III and IV (Figure 1.1.1.1). The crystal structure of free globular actin (G-actin) was solved by (Otterbein et al., 2001).

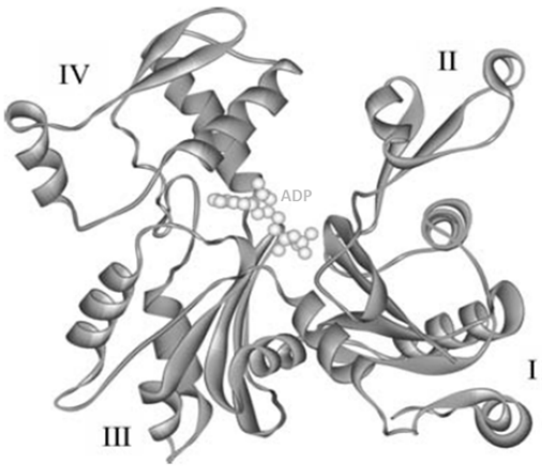

Figure 1.1.1.1 Atomic structure of free actin as revealed by (Otterbein et al., 2001). Subdomains are labelled I, II, III, IV. Adapted from (dos Remedios and Chhabra, 2008).

In animals, actin filaments complement with two other cytoskeletal polymers, microtubules and intermediate filaments (Figure 1.1.1.2). All three are involved in the maintenance of cell

shape. Microtubules are long, hollow cylinders made up of polymerised α- and β-tubulin dimers and involved in organelle transport, cell motility by flagella or cilia, membrane trafficking, and the formation of the mitotic spindle during cell division. Intermediate filaments are composed of fibrous proteins supercoiled into thicker cables that are localised underneath the cell cortex. Besides maintaining cell shape, they organise the internal tridimensional structure of the cell by anchoring the nucleus and other intracellular organelles. Actin filaments are composed of two intertwisted strands of actin. They are mainly concentrated just beneath the cell membrane and they are responsible for changes in cell shape, muscle contraction, endocytosis, cytokinesis, adhesion, signal transduction, intracellular organelle transport and cellular motility.

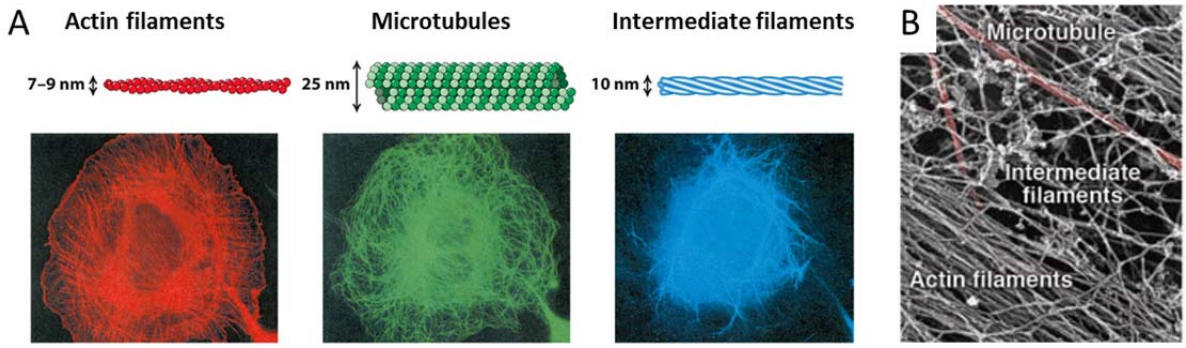

Figure 1.1.1.2 Cytoskeletal polymers. A) Schematic structure and cellular localisation of actin filaments, microtubules and intermediate filaments. Adapted from (Lodish et al., 2008). B) Electron micrograph of three types of cytoskeletal polymers in a cell permeabilised to release soluble components. After rapid freezing, the frozen water was sublimed away and cellular components were coated with platinum. Microtubules are highlighted in red. Adapted from (Pollard and Cooper, 2009).

1.1.2 Actin polymerisation

The assembly of globular actin monomers to form long, stable filaments (F-actin) with a helical arrangement of subunits (Figure 1.1.3) is essential in allowing the actin cytoskeleton to carry out its various functions. ATP-G-actin can polymerise into ATP-F-actin and occurs spontaneously under physiological conditions. Polymerisation starts slowly as small oligomers are unstable, but once filaments have been created, actin polymerises rapidly. The net rate of filament elongation is slightly less than 200 monomers/second (dos Remedios et al., 2003). Filaments are polar since all subunits point in the same direction. One end of the filament, the barbed end (also called + end) grows much faster than the other pointed end (also called – end) (Pollard et al., 2000; Wegner and Isenberg, 1983). Polymerisation can be divided into activation, nucleation, elongation and annealing (Gaszner et al., 1999). During

activation, actin-ATP binds an Mg^{2+} ion through its cation binding site which induces a conformational change that reduces the negative charge of the actin monomers, thus favouring an interaction between two monomers (Gaszner et al., 1999). Nucleation consists of the formation of a trimer of actin monomers. This is an energetically unfavourable process, the dimer intermediate being highly unstable (Wegner and Engel, 1975). Elongation refers to the association of actin monomers at both ends of the actin filament and annealing occurs when short actin filaments rapidly bind end-to-end to form longer filaments. All these steps are reversible and thus account for a highly dynamic actin turnover. As the actin filament is polar and as one end of the filament grows rapidly in length while the other end rather tends to shrink, this results in a section of filament seemingly moving. This phenomenon is called treadmilling (Wegner, 1976) (Figure 1.1.2).

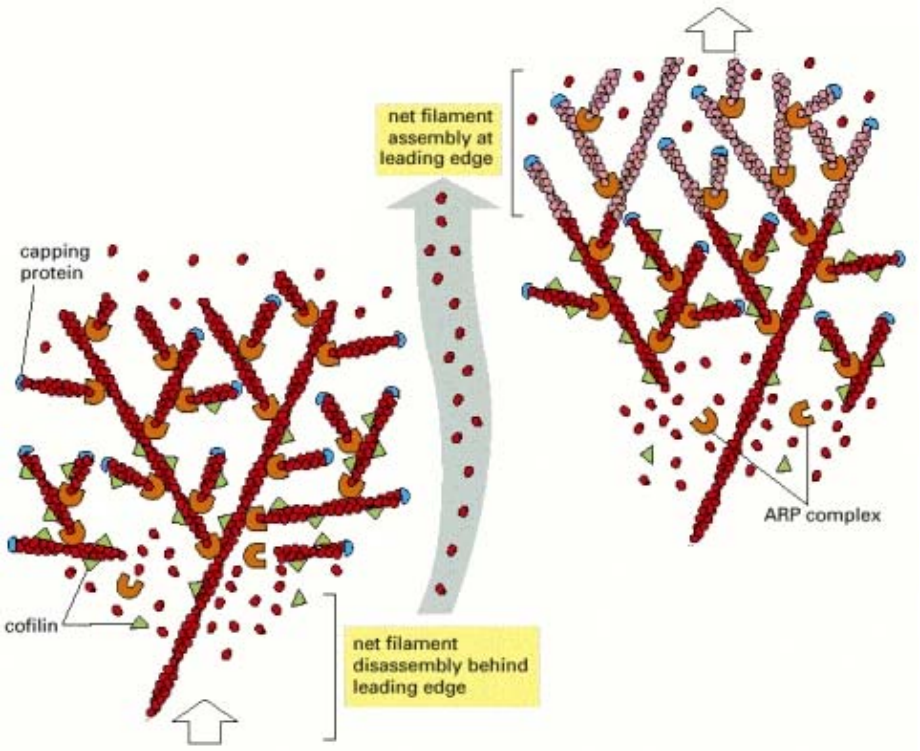

Figure 1.1.2 Illustration of actin treadmilling. Actin treadmilling occurs at the lamellipodium of migrating cells and consists of a cycle of actin polymerisation/depolymerisation. Actin nucleation occurs at the front of the leading edge and newly nucleated actin filaments are attached to the sides of pre-existing filaments. In addition, polymerisation of actin filaments occurs in the front and pushes the plasma membrane forward. At the rear end of the leading edge however, actin depolymerisation occurs. This polymerisation/depolymerisation cycle causes a spatial separation between net filament assembly at the front and net filament disassembly at the rear, so that the actin filament network as a whole can move forward, even though the individual filaments within it remain stationary with respect to the substratum. Adapted from (Alberts B. et al., 2008).

1.1.3 Actin-binding proteins (ABPs)

In the cell, actin polymerisation is controlled by over 100 so-called ABPs. The complex and dynamic properties of the actin cytoskeleton are regulated at multiple levels by a variety of ABPs that control the turn-over of actin filaments and their organisation into bundles or networks, which is required for the assembly of specific cytoskeletal structures (see (dos Remedios et al., 2003) for review). ABPs are classified in nine different groups but some ABPs can be classified in several groups:

1. **monomer binding** proteins that prevent actin polymerisation by sequestering G-actin (thymosin β4, DNase I),
2. **filament-nucleating** proteins that promote the formation of actin trimer nuclei (Arp2/3, formin),
3. **filament-depolymerising** proteins that induce the conversion of F- to G-actin (CapZ and cofilin),
4. **filament end-binding** proteins that cap the ends of the actin filament preventing the exchange of monomers at pointed (tropomodulin) and barbed (CapZ) ends,
5. **filament severing** proteins that shorten filament length by binding to the side of F-actin and cutting it into two pieces (gelsolin),
6. **filament branching** proteins (Arp2/3, WASP/SCAR/WAVE),
7. **crosslinking** proteins that contain at least two binding sites for F-actin, either inherent or through dimerisation, thus facilitating the formation of filament bundles (α-actinin, fascin, villin, L-plastin) and three-dimensional networks (filamin),
8. **stabilising** proteins that bind along the sides of actin filaments to prevent depolymerisation and stiffen the actin filament (tropomyosin),
9. **motor** proteins that use F-actin as a track upon which to move (myosin family of motors).

Crosslinking proteins will be described in more detail under 1.1.4.

1.1.4 Formation of higher order actin structures

F-actin filaments can be organised in more complex cytoskeletal structures for the implementation of diverse cellular functions, such as the maintenance of cell shape or the

generation of force for cell motility. Crosslinking proteins can organise the actin cytoskeleton to form three-dimensional networks of filaments (e.g. filamin) (Figure 1.1.4), which protect the cell from various shear stresses (Kasza et al., 2009). They can also form bundles of parallel filaments (e.g. fascin, α-actinin, villin and plastin) (Figure 1.1.4), which shield the cell against mechanical deformation and allow force generation. Actin bundles are found in filopodia where they exert protrusion forces at the leading edge of a motile cell, in microvilli which are passive structural elements that increase the surface area of the cells, in stress fibers which are essential for cell adhesion to the substratum and for changes in cell morphology and in invadopodia, which are matrix-degrading structures (Alberts B. et al., 2008; Schoumacher et al., 2010).

Crosslinking proteins contain actin-binding domains such as gelsolin domains (e.g. gelsolin, villin), spectrin domains (e.g. spectrin, α-actinin) or calponin homology (CH) domains (e.g. α-actinin, filamin and plastin). In order to be able to bind two actin filaments, many crosslinking proteins form dimers. Plastins are unique as they have tandem actin-binding domains consisting of pairs of CH domains (de Arruda et al., 1990). These closely positioned actin-binding domains allow plastins to form tight actin bundles. The formation of three-dimensional networks is mediated by proteins such as filamin containing actin-binding domains that are separated by longer, more flexible spacer regions, which allow a more perpendicular arrangement of actin filaments (Figure 1.1.4).

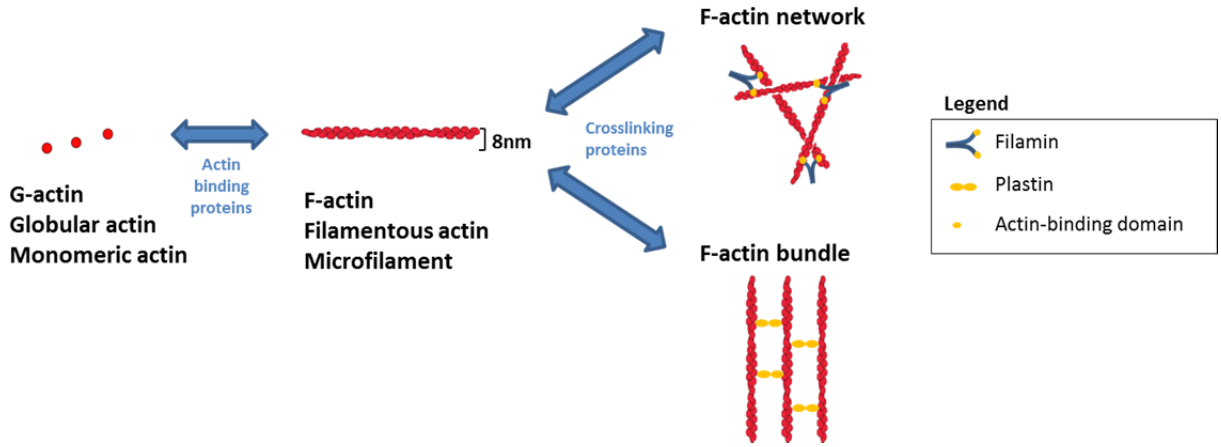

Figure 1.1.4 Organisation of the actin cytoskeleton by crosslinking proteins. Globular actin monomers are assembled to form long actin filaments with a helical arrangement of subunits. The equilibrium between G-actin and F-actin is regulated by ABPs. The organisation of actin into filaments is essential for the formation of higher-order actin structures such as actin networks or bundles governed by actin crosslinking proteins. Actin filaments in networks are organised into orthogonal arrays by large flexible proteins such as filamin. Actin bundles of parallel actin filaments are formed by actin-bundling proteins such as plastin.

1.1.5 Function of higher-order actin structures

The organisation of actin filaments into higher-order structures is a key step in the development of specialised cellular structures, such as filopodia (spike-like protrusions), lamellipodia (sheet-like protrusions), stress fibers (elastic contractile bundles), focal adhesions (plaques for mechanical linkage to the extracellular matrix), microvilli (finger-like surface protrusions) and invadopodia (invasive cell feet). Here we will focus on some structures that are required for cell motility.

Cell motility, important for numerous cellular functions including embryonic morphogenesis, wound healing and immune surveillance, is a tightly controlled multistep mechanism (reviewed in (Bailly and Condeelis, 2002)). First, the cell responds to an extracellular signal by localised actin polymerisation, which results in the rearrangement of the cell surface to form specialised cellular structures required for cell motility: filopodia, lamellipodia, podosomes or invadopodia. In a next step, these structures make contact with a neighbouring cell or with the extracellular matrix (ECM) to form an adhesion site. This subsequently generates signals resulting in actomyosin-based contraction, which in turn results in the development of tension between the adhesion sites of the cell. The last step can vary depending on the action to be completed. For locomotion of the cell, the tension developed by the contraction can lead to the detachment of the trailing edge of the cell and the pulling of the cell towards the adhesion site in the leading edge of the cell. Alternatively, the generated tension can lead to changes in cell shape during embryogenesis or to matrix remodelling during wound healing (Bailly and Condeelis, 2002).

1.1.5.1 Structures for migration

For migration on 2D substrates the cell polarises to form a leading edge and a trailing edge. The leading edge faces the direction of movement and contains dynamic actin structures called lamellipodium and filopodium (Figure 1.1.5.1). Lamellipodia are flat and wide membrane protrusions containing a complex bidimensional dendritic network of branched actin filaments. Fast elongation of actin filaments predominantly occurs at the barbed ends facing the leading edge (Lai et al., 2008; Urban et al., 2010) which allows pushing the membrane into the direction of movement. Filopodia are thin, finger-like protrusions that extend beyond the leading edge of protruding lamellipodia of migrating cells. They are formed by parallel bundles containing 15-20 actin filaments with their barbed ends facing the cellular membrane (Lewis and Bridgman, 1992). They sense the environment and determine the direction of movement.

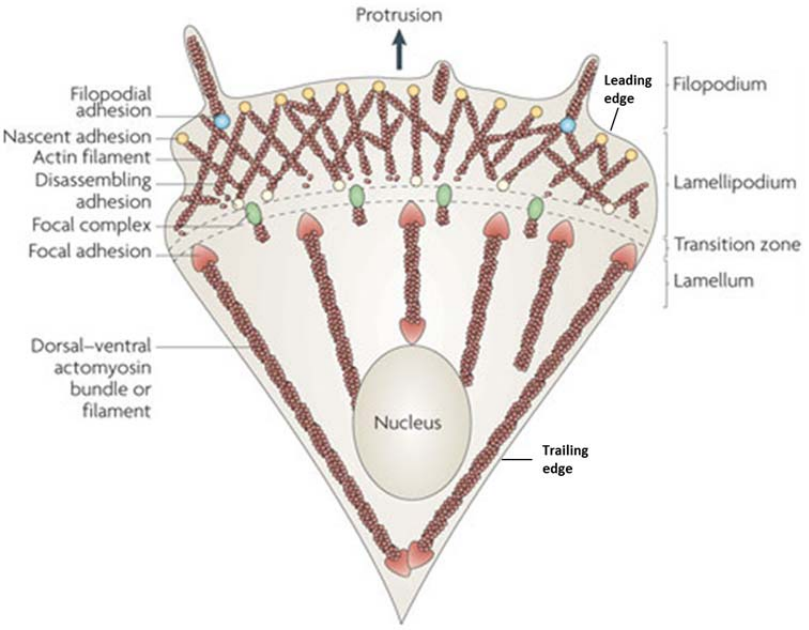

Figure 1.1.5.1 Organisation of the actin cytoskeleton in a migrating cell. Representation of various actin structures involved in cell migration. Adapted from (Parsons et al., 2010).

1.1.5.2 Structures for invasion

Podosomes and invadopodia (Figure 1.1.5.2) can be grouped as invadosomes (Linder et al., 2011). Podosomes are found in monocytic cells (Linder et al., 1999), dendritic cells (Burns et al., 2001), osteoclasts (Destaing et al., 2003), endothelial cells (Moreau et al., 2003) and smooth muscle cells (Burgstaller and Gimona, 2004) whereas invadopodia are found in invasive tumour cells. The structure of podosomes and invadopodia differs: Podosomes have a diameter of around 1 µm, a height of 0.4 µm and are non-protrusive whereas invadopodia have a diameter of up to 8 µm, a height of 5 µm and are protrusive (Artym et al., 2011; Linder, 2009). Furthermore, in podosomes the actin core is surrounded by a ring structure of adhesion proteins, such as vinculin or talin (Linder and Aepfelbacher, 2003), a structure that is not found in invadopodia (Gimona et al., 2008). Podosomes contain a branched network of actin filaments and possibly also a layer of unbranched radial actin filaments surrounding the central core (Linder et al., 2011). Invadopodia however contain parallel actin bundles and a meshwork of actin filaments at the base (Schoumacher et al., 2010). Podosomes have been shown to be surrounded by G-actin and short actin filaments that may be the source of raw material for turnover or podosome growth (Destaing et al., 2003; Hu et al., 2011). On 2D surfaces, invadosomes form at the ventral surface, which is in contact with the ECM, and they are involved in ECM degradation through the secretion of a variety of proteases, especially of the matrix metalloproteinase (MMP) family (reviewed in (Linder, 2007)). Podosomes seem to mediate a widespread but superficial matrix degradation whereas

invadopodia tend to a more focused and deeper degradation (Linder, 2007). Invadosomes are also involved in mechanosensing and it has been shown that matrix stiffness influences the spacing and the lifetime of podosomes (Collin et al., 2008; Collin et al., 2006) as well as matrix degradation by invadopodia (Parekh et al., 2011).

Podosomes are involved in adherence to the ECM and are thus enriched in matrix-binding proteins and integrins. It has been stated that podosomes may assist directional migration by stabilising short-lived cellular protrusions (Dovas et al., 2009).

Regarding invadopodia, it is not clear whether they adhere to the ECM and reports showing recruitment of integrins to invadopodia are rare (reviewed in (Linder et al., 2011)). Nevertheless, invadosomes appear to be involved in signal transduction by the fact that they contain a multitude of components similar to those in focal adhesions (Block et al., 2008).

The lifetime of podosomes is 2 to 12 minutes (Linder, 2007) and their actin is turned over around three times during their lifetime (Destaing et al., 2003). Invadopodia are more stable and can persist up to one hour (Linder, 2007). The lifetime of invadopodia has been shown to be dependent on cofilin expression (Yamaguchi et al., 2005a). Invadopodia formation and maturation is a dynamic process starting with the formation of a network of actin filaments and cortactin which is then followed by the recruitment of the proteinase MT1-MMP with subsequent matrix degradation (Artym et al., 2006). In tumour cells, expression of cortactin, Tks5, MT1-MMP as well as matrix degradation are unique markers of invadopodia (Bravo-Cordero et al., 2012). Membrane ruffling and filament-like protrusion from the invadopodia occur during maturation (Artym et al., 2011).

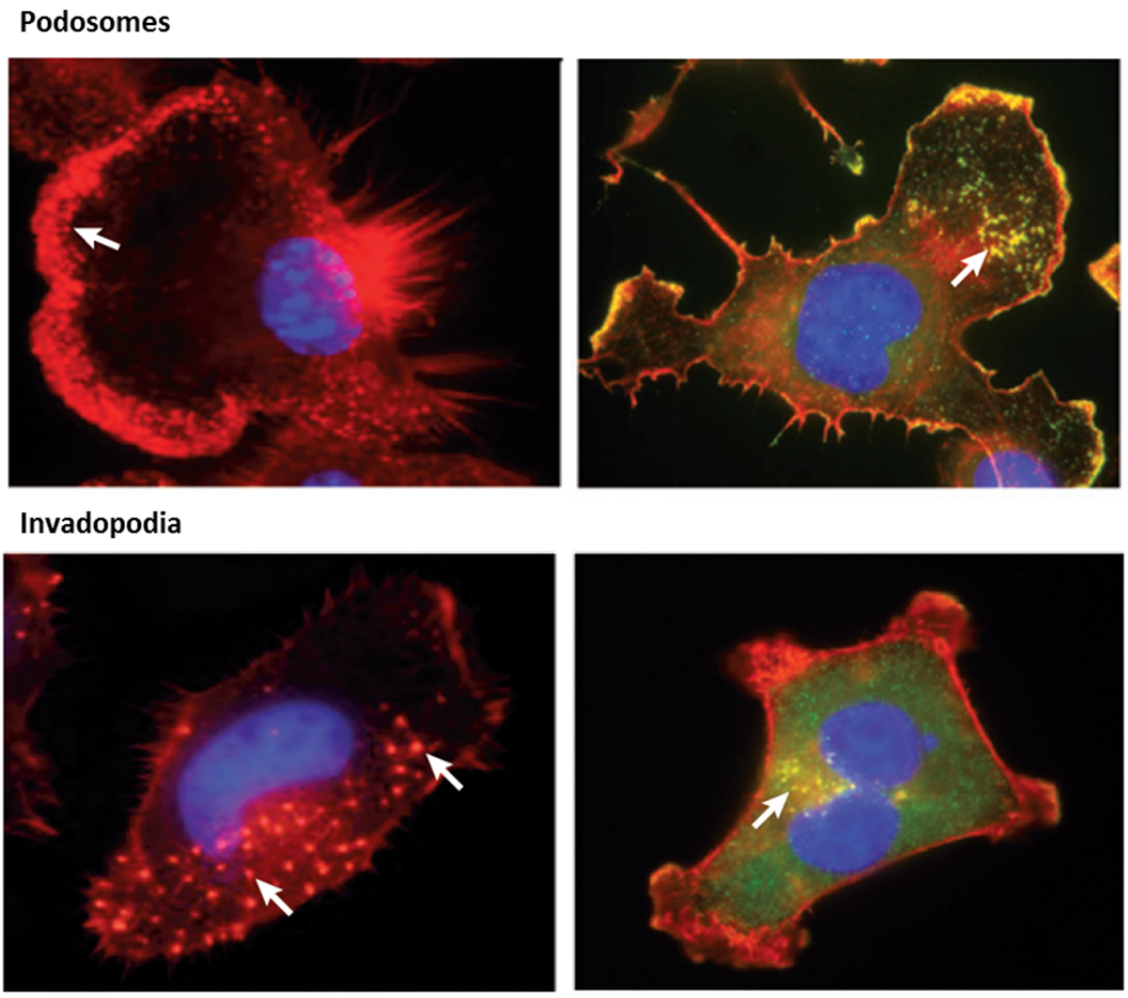

Figure 1.1.5.2 Invadosomes. The formation of invadosomes is visualised by co-immunostaining of F-actin (red) and the invadosome-associated protein cortactin (green) (the nucleus is shown in blue). Colocalisation of F-actin and cortactin (together indicated by yellow) is frequently used, among many markers, to confirm the presence of these structures in cells. Cortactin has been removed from the left panels. Podosomes are often found at the leading edge of cells. They are shown in macrophages (IC-21 cells; left) and neural crest stem cells (JOMA1.3 cells treated with 20 nM PMA to induce podosome formation; right). Invadopodia are often found surrounding the nuclei. They are shown in head and neck squamous carcinoma cells (SCC61 cells; left) and breast cancer cells (MDA-MB-231 cells; right). Arrows indicate individual puncta. Images were taken at ×40 magnification (MDA-MB-231) and ×60 magnification (JOMA1.3, IC-21 and SCC61) using a fluorescence microscope. Adapted from (Murphy and Courtneidge, 2011).

1.1.6 Actin cytoskeleton and cancer

Cancer figures among the leading causes of morbidity and mortality worldwide, with approximately 14 million new cases and 8.2 million cancer-related deaths in 2012 (Stewart and Wild, 2014). The word cancer is used for a large group of diseases that can affect any part of the body. One defining characteristic of cancer is the multiplication of abnormal cells

that grow beyond their usual boundaries, and that can then invade adjoining parts of the body and spread to other organs, the latter process being referred to as metastasising.

The progressive conversion of normal human cells into cancer cells involves genomic changes activating oncogenes and inhibiting tumour suppressor genes. Cancer development occurs similar to Darwinian evolution in which sequential genetic changes, each conferring one or another type of growth advantage, lead to the progressive transformation of normal human cells into highly malignant cells (Foulds, 1954; Nowell, 1976).

In 2000, Hanahan and Weinberg introduced six hallmarks of cancer, namely self-sufficiency in growth signals, insensitivity to anti-growth signals, limitless replicative potential, evasion of apoptosis, sustained angiogenesis and tissue invasion and metastasis (Hanahan and Weinberg, 2000). In 2011, they updated their model with the addition of four further cancer hallmarks: genome instability and mutation, deregulated cellular energetics, avoidance of immune destruction and tumour-promoting inflammation (Hanahan and Weinberg, 2011).

The metastatic process consists of a series of successive steps. In a first step, tumour cells detach from the primary tumour which involves an epithelial to mesenchymal transition (EMT) characterised by repression of E-cadherin expression, loss of cell adhesion, and increased cell motility. Thereafter the cells invade and migrate through the surrounding tissue and eventually enter blood vessels or the lymphatic system by intravasation. Subsequently, circulating tumour cells temporarily adhere to endothelial cells and extravasate. At a suitable location, the cells undergo mesenchymal to epithelial transition (MET), proliferate and form metastases (Engers and Gabbert, 2000; Nicolson, 1988; Orr et al., 2000; Stetler-Stevenson et al., 1996). Metastasis accounts for more than 90% of all cancer-related deaths (Siegel et al., 2011) and to date no drugs capable of blocking metastasis are available (Bravo-Cordero et al., 2012).

The cytoskeleton is important in normal cell function but it can be subverted in cancer cells where it contributes to cell growth, movement and invasiveness. Cell motility plays an important role in metastasis as its aberrant regulation drives the progression of cancer invasion (Condeelis et al., 2005; Sahai, 2005; Yamaguchi et al., 2005b). The ability of cancer cells to form invadopodia is associated with highly invasive and metastatic potentials and growing evidence exists that formation of invadopodia is part of the EMT process (Eckert et al., 2011; Yilmaz and Christofori, 2009).

Cell migration and invasion are triggered by a number of chemoattractants, which upon binding to surface receptors stimulate intracellular signalling pathways that regulate actin cytoskeleton reorganisation. Increased actin polymerisation activity and motility can result

from altered signalling pathways in invasive tumour cells (Wang et al., 2004; Wang et al., 2007b) and many signalling pathways are involved in the regulation of the actin cytoskeleton.

A critical chemotactic lamellipodia-inducing factor for breast cancer cells for example is epidermal growth factor (EGF) and activation of EGF signalling pathways is directly correlated with increased invasion, intravasation and metastasis (Xue et al., 2006). Downstream of EGF signalling pathways in invasive breast cancer cells, gene expression studies revealed an overexpression of components involved in lamellipodia formation such as Arp2/3 complex and the LIM-kinase/cofilin pathways (Wang et al., 2004). Arp2/3 complex, LIM-kinase/cofilin and cortactin are important proteins that mediate the signalling pathways involved in cytoskeleton regulation linked to cell migration and invasion.

Due to the large number of cellular processes involving the actin cytoskeleton, a fine-tuned regulation of the latter is required in order to prevent from disease.

1.2 The actin-bundling protein L-plastin

Three isoforms of plastins have been discovered in mammals: I-plastin, T-plastin and L-plastin. The first plastin isoform was discovered in microvilli from chicken intestinal brush border (Matsudaira and Burgess, 1979) and it was called fimbrin (from the latin word *fimbria*, meaning “border, fringe”) because it was associated with cell border structures, such as membrane ruffles, microvilli, microspikes and focal adhesions. Plastins are conserved and expressed in yeast, plant and animal cells. The strong evolutionary conservation of function of the plastin gene family can be highlighted by the fact that in yeast with mutations in its L-plastin homologue SAC6, human L-plastin and T-plastin can rescue the resulting defects in endocytosis (Adams et al., 1995).

Plastin expression is tissue-dependent. I-plastin is specifically expressed in microvilli of the small intestine, colon and kidney (Lin et al., 1994) whereas T-plastin is expressed in cells derived from solid tissue (Lin et al., 1988). L-plastin expression was first discovered in cells of the haematopoietic lineage (Matsushima et al., 1988) and is expressed as one of the most abundant proteins in normal, untransformed lymphocytes (Goldstein et al., 1985). Besides, L-plastin expression has been found in a great number of cancer cells where it is ectopically expressed. A study by Lin and colleagues showed that 68% of epithelial carcinomas and 53% of non-epithelial mesenchymal tumours express L-plastin (Lin et al., 1993b). Furthermore, Park and colleagues discovered that more than 90% of human tumour cell lines constitutively express L-plastin at varying degrees (Park et al., 1994).

1.2.1 L-plastin structure

L-plastin, also called lymphocyte cytosolic protein 1 (LCP1), is a protein with a size of approximately 68 kDa as determined by mobility rates in a sodium dodecyl sulfate (SDS)-polyacrylamide gel (de Arruda et al., 1990; Lin et al., 1988; Lin et al., 1990). The protein encompasses 627 amino acids and the description of the complete sequence of L-plastin revealed that this protein is organised into headpiece and core domains (de Arruda et al., 1990). Phosphorylation of L-plastin has been shown to occur specifically within a headpiece of 10 kDa (Messier et al., 1993).

I-, T- and L-plastin genes evolved from a common ancestor as revealed by the analysis of the exon-intron junction sequences and share approximately 70% similarity of their amino acid sequences (Lin et al., 1993b). Although L-plastin, T-plastin and I-plastin genes have evolved from a common ancestral gene, they are now dispersed on chromosome 13

(L-plastin), chromosome X (T-plastin) (Lin et al., 1993b) and chromosome 3 (I-plastin) (Lin et al., 1994) in human cells. In their N-terminal region the 3 human plastin isoforms contain two EF-hands implicated in calcium-binding, followed by 2 tandem actin-binding domains (ABDs), each composed of two CH domains (de Arruda et al., 1990) (Figure 1.2.1). An EF hand is a helix-turn-helix structural motif that consists of two alpha helices positioned roughly perpendicular to one another and linked by a short loop region that often binds calcium ions. CH domains are composed of 4 alpha helices of which one is oriented perpendicular to the other three which are forming a loose bundle. An isolated CH domain is able to bind to actin, but a pair of CH domains is required for a fully functional ABD (Korenbaum and Rivero, 2002). Plastins fold into a compact, horseshoe-like structure that can simultaneously bind two actin filaments and thereby crosslink the filaments into tight bundles (Shinomiya et al., 2007). For fimbrin of *Arabidopsis thaliana* it has been shown that the tandem ABDs are packed together in an approximately antiparallel arrangement with N- and C-terminal CH domains (CH1 and CH4) making direct contact and the same is believed to occur for L-plastin (Klein et al., 2004; Shinomiya et al., 2007).

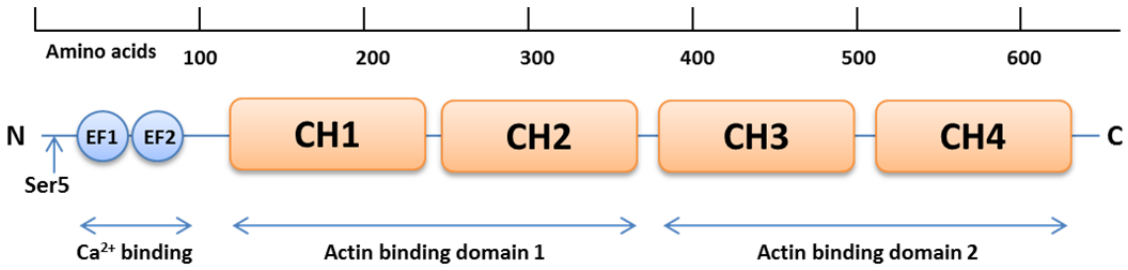

Figure 1.2.1 L-plastin structure. Human plastins contain two EF-hands implicated in calcium-binding in their N-terminal region and two tandem actin-binding domains, each composed of two calponin homology (CH) domains, in their C-terminal region. Residue serine 5 (Ser5) in the N-terminus is an important phosphorylation site involved in L-plastin activation.

L-plastin has been found to undergo co-translational modifications. Methionine removal and N-terminal acetylation of the subsequent alanine is reported for L-plastin in the UniProtKB/Swiss-Prot database (www.uniprot.org).

1.2.2 L-plastin regulation and function

As described above, L-plastin belongs to the family of actin crosslinkers and more precisely of actin-bundling proteins (Bretscher, 1981; de Arruda et al., 1990). L-plastin has no specificity towards different actin isoforms (Lebart et al., 2004). High resolution structural

analysis has been used to study the binding of L-plastin to F-actin and to establish a model stating that ABD2 of L-plastin initially binds to an actin filament which results in subsequent activation of ABD1, which can then bind to a second actin filament resulting in crosslinking of two actin filaments into parallel bundles (Galkin et al., 2008). The actin-bundling activity of L-plastin is positively regulated by phosphorylation (Janji et al., 2006) and negatively regulated by intracellular Ca^{2+} (Giganti et al., 2005; Namba et al., 1992; Pacaud and Derancourt, 1993). Human L-plastin is the only isoform that possesses all the conserved amino acids essential for calcium-binding (Delanote et al., 2005b). Significant conformational change is induced in the presence of Ca^{2+} (Shinomiya et al., 2007). As Ser5 is spatially close to the EF-hand Ca^{2+}-binding motif of the headpiece domain, it was investigated whether the presence of a negatively charged group at amino acid position 5 interfered with the inhibitory effect of Ca^{2+} (Janji et al., 2006). An almost identical decrease in F-actin-bundling was observed when non-phosphorylated wild type L-plastin or a Ser5 phosphorylation mimicking L-plastin variant were incubated with actin in the presence of increasing concentrations of free Ca^{2+}, suggesting that addition of a negative charge in amino acid position 5 does not influence Ca^{2+}- dependency of F-actin bundling (Janji et al., 2006).

Moreover, an interaction of L-plastin with Iba1, a macrophage/microglia-specific protein, was shown to increase the actin-bundling activity of L-plastin (Ohsawa et al., 2004).

Furthermore, the binding of L-plastin to monomeric actin is reduced by increasing amounts of phospholipids (Lebart et al., 2004) and recently the binding of L-plastin to actin was shown to be reduced following S-glutathionylation of L-plastin in human neutrophils (Dubey et al., 2015).

The use of a knockout nanobody in a human prostate cancer cell line suppressed L-plastin bundling activity that could not be compensated for by other resident endogenous cross-linking proteins (Delanote et al., 2010), which highlights an important role for L-plastin in the construction and/or rigidity of the cytoskeleton. L-plastin is located in the nucleus and the cytoplasm whereas T-plastin localises predominantly to the cytoplasm since it has a more conserved nuclear export signal than L-plastin (Delanote et al., 2005a). L-plastin was found to localise to actin-rich structures of the cellular cortex, such as focal adhesions, filopodia and membrane ruffles which are involved in adhesion, signalling or locomotion (Arpin et al., 1994; Janji et al., 2006). Besides crosslinking actin filaments, L-plastin also regulates actin turnover *in vitro* and *in vivo* (Al Tanoury et al., 2010).

During embryonic mouse development, L-plastin is expressed in the early stages of intestinal epithelial cell differentiation and in the visceral endoderm (Chafel et al., 1995). However, knockout of L-plastin has no influence on embryonic and neonatal development in

L-plastin -/- mice (Chen et al., 2003). In the early stages of intestinal epithelial cell differentiation, T- and I-plastin are localised at the apical surface and L-plastin at the basal surface which suggests that T- and I-plastin might be involved in the formation and extension of microvilli whereas L-plastin appears to play a role in controlling cell adhesion (Delanote et al., 2005b).

Whereas L-plastin expression in tumour cells is ectopic, its expression in leukocytes is normal and L-plastin plays a role in the immune response. Wang and colleagues showed that L-plastin -/- T cells were defective in proliferation and in T cell receptor-mediated cytokine production and demonstrated that L-plastin-dependent actin-bundling facilitates formation of lamellipodia and normal immunological synapses and thereby enables T cell activation (Wang et al., 2011). Furthermore, it was demonstrated that L-plastin and its interaction with the calcium-binding messenger protein calmodulin are required for the maintenance of L-plastin in the immune synapse between T cells and antigen presenting cells and for sustained Lymphocyte function-associated antigen 1 (LFA-1) clustering in the immunological synapse (Wabnitz et al., 2010). Another study showed an important role for L-plastin in the response to chemokines and in T lymphocyte polarity and migration (Freeley et al., 2012). Yet another study identified L-plastin as a molecule critical for C-C chemokine receptor type 7 (CCR7)-mediated motility in T lymphocytes (Morley et al., 2010). L-plastin polarises the chemokine receptor CCR7 and mediates directional migration. Confocal imaging showed that upon chemokine stimulation by ligand binding, colocalisation of F-actin and CCR7 in the lamellipodium was reduced in L-plastin -/- T cells. Defective migration resulted from defective cellular polarisation following CCR7 ligation. This suggests that the actin-bundling activity of L-plastin is required for cellular polarisation following CCR7 ligation.

L-plastin was also shown to be involved in natural killer (NK) cell migration (Serrano-Pertierra et al., 2014).

A certain number of studies point to a role for L-plastin in regulating integrin-mediated adhesion in macrophages and polymorphonuclear neutrophils (PMNs) (Correia et al., 1999; Jones et al., 1998; Messier et al., 1993; Wang et al., 2001). However, another study reported normal adhesion in PMNs isolated from an L-plastin knockout mouse (Chen et al., 2003). These cells also showed normal morphology, spreading, migration and phagocytosis but they had a defect in generating an adhesion-dependent respiratory burst in response to a variety of integrin ligands which was responsible for their inability to kill *Staphylococcus aureus* (Chen et al., 2003). Furthermore, spleen tyrosine kinase (Syk) and paxillin phosphorylation were abnormal in L-plastin -/- PMNs (Chen et al., 2003).

L-plastin is also involved in alveolar macrophage production which is required for combating pneumococcal infections (Deady et al., 2014).

In osteoclasts L-plastin is an integral component of the actin-core of podosomes (Babb et al., 1997). Here L-plastin contributes to sealing ring formation and bone resorption by inducing the formation of actin aggregates, functioning as a core in the recruitment of signalling molecules such as Src kinase, cortactin and integrin αvβ3 (Ma et al., 2010). This suggests that L-plastin may act as a scaffolding protein.

1.2.3 L-plastin phosphorylation and protein phosphorylation in general

Protein phosphorylation is the most widespread type of post-translational modification used in signal transduction. It plays a key regulatory role in nearly every aspect of eukaryotic cell biology and is a reversible and dynamic process that is mediated by protein kinases and phosphatases. These enzymes catalyse the transfer of phosphate between their substrates (Figure 1.2.3.1). Protein kinases catalyse the transfer of γ-phosphate from ATP (or GTP) to their protein substrates (protein-OH + $MgATP^-$ → protein-OPO_3^{2-} + MgADP + H^+) while protein phosphatases catalyse the transfer of the phosphate from a phosphoprotein to a water molecule (Protein-OPO_3^{2-} + H_2O → protein-OH + $HOPO_3^{2-}$). Based upon the nature of the phosphorylated –OH group, protein kinases are classified as serine/threonine (Ser/Thr) protein kinases or tyrosine (Tyr) protein kinases. Phylogenetic comparisons show that plants have relatively few tyrosine kinases and that unicellular organisms completely lack tyrosine kinases (Johnson, 2009). In eukaryotes, protein kinase genes constitute about 2% of genomes and phosphorylate more than 30% of the cellular proteins (Cohen, 2000; Pinna and Ruzzene, 1996).

Protein phosphorylation provides a control mechanism for various signalling processes and regulates protein functions by inducing conformational changes or by disruption and creation of protein-protein interaction surfaces (Holt and Corey, 2000; Serber and Ferrell, 2007).

The first 3D structure of a protein kinase was determined for protein kinase A by X-ray crystallography and revealed the basic bilobal scaffold structure that has now been observed in all protein kinases as shown below for CDK2 (Figure 1.2.3.2). The catalytic domain of protein kinases is about 250 amino acids long and consists of a small N-terminal lobe of β-sheets and a larger C-terminal lobe of α-helices (Ubersax and Ferrell, 2007). ATP binds in a cleft between the two lobes with the phosphate oriented outwards and the protein substrate binds along the cleft.

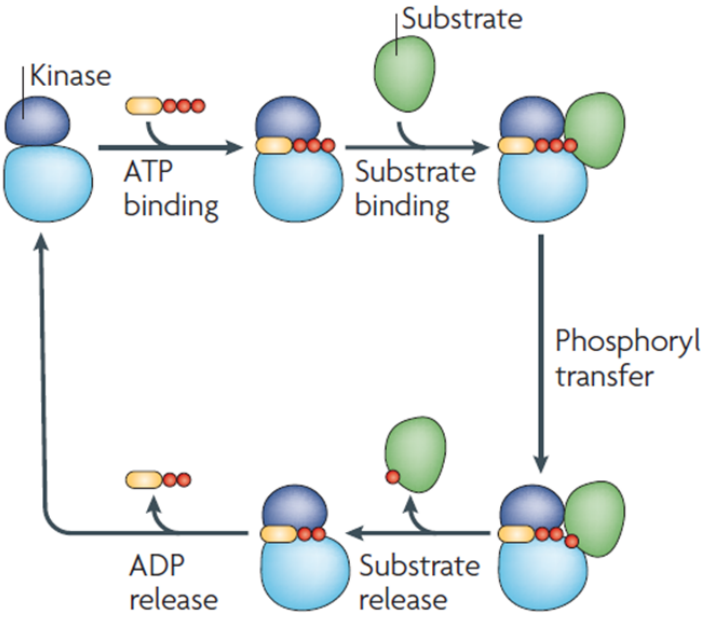

Figure 1.2.3.1 Catalytic cycle for substrate phosphorylation by a kinase. Starting top left: The active site of the kinase binds ATP and the substrate. Once bound, the γ-phosphate of ATP (red) is transferred to a Ser, Thr or Tyr residue of the substrate. After phosphorylation, the substrate and ADP are released from the kinase active site. Different kinases have varying orders for the binding or the release of the substrate or ATP/ADP respectively. Adapted from (Ubersax and Ferrell, 2007).

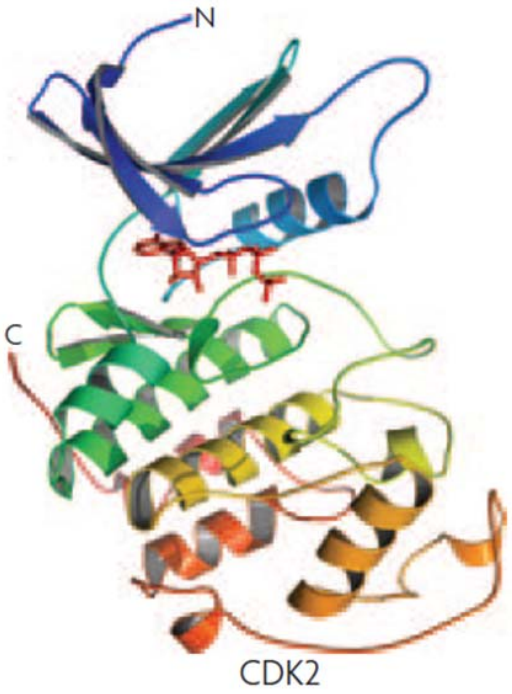

Figure 1.2.3.2 Basic protein fold of the catalytic domain of protein kinases. The protein fold of protein kinases comprises two lobes: an N-terminal lobe consisting of mainly β-sheets (blue) and a C-terminal lobe consisting of α-helices (green, orange and yellow). This lobe structure forms an ATP-binding cleft that constitutes the active site. The crystal structure of cyclin-dependent kinase-2 (CDK2) (Protein Data Bank (PDB) ID: 1QMZ) shows this representative fold. ATP is modelled bound in the cleft (red). Adapted from (Ubersax and Ferrell, 2007).

The common catalytic scaffold shared by the eukaryotic protein kinases switches between two extreme conformations for the “on” and the “off” states corresponding to high and low activity of the protein kinases. The transition from one state to the other can be mediated by a variety of strategies in different kinases such as through phosphorylation, interactions of additional domains within the protein kinase and/or binding to other regulatory proteins (Huse and Kuriyan, 2002).

A protein kinase must recognise between one and a few hundred phosphorylation sites in a background of about 700 000 potentially phosphorylatable residues that they might encounter (Ubersax and Ferrell, 2007). Multiple mechanisms exist to confer exquisite specificity. The first level of substrate specificity arises from structural characteristics of the kinase active site, its depth and charge or hydrophobicity, which will match with complementary characteristics of its substrates. Tyrosine kinases for example have a deeper catalytic cleft than Ser/Thr kinases (Brown et al., 1999; Hubbard, 1997). However, the specificity linked to the cleft depth is not absolute as several Ser/Thr kinases can phosphorylate Tyr residues (Zhu et al., 2000). A Tyr kinase that phosphorylates Ser or Thr residues appears to be rarer. The next level of substrate specificity is guaranteed by consensus sequences: the active site of the kinase usually interacts with four amino acids on either side of the phosphorylation site and the nature of these contributes substantially to kinase-substrate recognition. A next level includes distal interactions between docking motifs on the substrate and interaction domains on the kinases (Biondi and Nebreda, 2003; Holland and Cooper, 1999). These binding motifs are usually spatially separated from the kinase active site and the substrate phosphorylation site and increase the affinity of kinases for specific substrates. Another level of control is the “priming” of substrates which means that they have to be phosphorylated on a specific residue before they can become phosphorylated on another target residue. Priming makes the phosphorylation dependent on the activity of both the priming kinase and the ultimate kinase and it allows for a regulation in time. A further level of control is the subcellular localisation of kinases and substrates. Another important control of protein phosphorylation is mediated by scaffolds: sometimes the interaction between a protein kinase and its substrate occurs through the intermediary of adaptors or scaffolds, which act as organising platforms that recruit the kinase and the substrate to the same complex (Bhattacharyya et al., 2006; Pawson and Scott, 1997). Yet another mechanism for regulating phosphorylation is linked to organism-level. As opposed to *in vitro* where the interaction between a single kinase and a single substrate can be studied, in a cell the substrates of kinases are present in a mix of thousands of non-target proteins. A

kinase will have more than one substrate *in vivo* and each substrate can act as a competitive inhibitor for other substrates.

Protein kinases have become high-profile targets for drug development. Protein kinase inhibitors often target the ATP-binding site on the kinase. They can target active or inactive conformations of kinases. As kinases converge to a similar conformation in the active state, targeting this state often results in a less specific inhibition. However, targeting the active conformation is advantageous when the disease state has arisen from activating mutations which inappropriately maintain the protein kinases in an active state (Johnson, 2009).

Our protein of interest, human L-plastin, is the only plastin isoform that has been shown to be phosphorylated upon response to diverse stimuli (Henning et al., 1994; Jones and Brown, 1996; Matsushima et al., 1987; Shibata et al., 1993; Shiroo and Matsushima, 1990). Initially, phosphorylation of L-plastin has been shown to occur specifically within a headpiece of 10 kDa (Messier et al., 1993) and residues serine 5 (Ser5) and serine 7 (Ser7), both amino-terminally located, were revealed as the phosphorylation sites in haematopoietic cells (Shinomiya et al., 1995). A bit later it was shown that the presence of Ser5 is required for L-plastin phosphorylation in HeLa cells, but it was not ruled out that Ser7 might also be phosphorylated, with a requirement for Ser5 to achieve Ser7 phosphorylation (Jones et al., 1998). In non-haematopoietic cells, L-plastin was thought to be only phosphorylated on Ser5 (Lin et al., 1998; Messier et al., 1993; Shinomiya et al., 1995). More recent studies using proteomic discovery-mode MS revealed many more phosphorylation sites. L-plastin has been shown to be subject to multiple post-translational modifications as shown by a search on the PhosphoSitePlus® website (http://www.phosphosite.org/homeAction.do) (Figure 1.2.3.3). These include phosphorylations of serine, threonine and tyrosine residues as well as other post-translational modifications, such as acetylation or ubiquitination. However, the phosphorylation of Ser5 is the only post-translational modification that was found not only by proteomic discovery-mode mass spectrometry (MS) but also by site specific methods (such as amino acid sequencing, site-directed mutagenesis, modification site-specific antibodies and specific MS strategies) (Figure 1.2.3.3). Ser5 is also the only phosphorylation site that was described to influence L-plastin activity in many studies (Al Tanoury et al., 2010; Janji et al., 2006; Janji et al., 2010; Klemke et al., 2007; Riplinger et al., 2014).

A

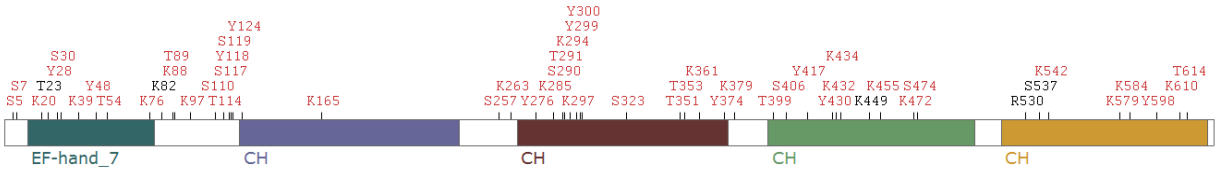

B

S.Sp.	M.S.	Human L-plastin	S.Sp.	M.S.	Human L-plastin
			0	1	K297-ac stDIkDSkAyyHLLE
8	34	S5-p ___MARGsVsDEEMM	0	2	K297-ub stDIkDSkAyyHLLE
0	17	S7-p _MARGsVsDEEMMEL	0	33	Y299-p DIkDSkAyyHLLEQV
0	1	K20-ac ELREAFAkVDTDGNG	0	128	Y300-p IkDSkAyyHLLEQVA
0	3	K20-ub ELREAFAkVDTDGNG	0	2	S323-p PAVVIDMsGLREKDD
0	1	T23 EAFAkVDTDGNGyIs	0	3	T351-p LGCRQFVtAtDVVRG
0	317	Y28-p VDTDGNGyIsFNELN	0	3	T353-p CRQFVtAtDVVRGNP
0	6	S30-p TDGNGyIsFNELNDL	0	2	K361-ac DVVRGNPkLNLAFIA
0	6	K39-ub NELNDLFkAACLPLP	0	4	K361-ub DVVRGNPkLNLAFIA
0	70	Y48-p ACLPLPGyRVREItE	0	83	Y374-p IANLFNRyPALHkPE
0	1	T54-p GyRVREItENLMATG	0	2	K379-ac NRyPALHkPENQDID
0	1	K76-ac ISFDEFIkIFHGLkS	0	1	T399-p GETREERtFRNWMNs
0	6	K76-ub ISFDEFIkIFHGLkS	0	13	S406-p tFRNWMNsLGVNPRV
0	1	K82 IkIFHGLKSTDVAkt	0	6	Y417-p NPRVNHLySDLSDAL
0	2	K82-ub IkIFHGLkSTDVAkt	0	2	Y430-p ALVIFQLyEkIkVPV
0	7	K88-ac LkSTDVAktFRKAIN	0	1	K432-ub VIFQLyEkIkVPVDW
0	2	K88-ub LkSTDVAktFRKAIN	0	1	K434-ub FQLyEkIkVPVDWNR
0	12	T89-p kSTDVAktFRKAINK	0	1	K449 VNKPPYPKLGGNMkK
0	1	K97-ub FRKAINKkEGICAIG	0	1	K455-ac PKLGGNMkKLENCNY
0	1	S110-p IGGTSEQsSVGtQHs	0	3	K472-ac ELGKNQAkFsLVGIG
0	5	T114-p SEQsSVGtQHsysEE	0	1	K472-ub ELGKNQAkFsLVGIG
0	7	S117-p sSVGtQHsysEEEKy	0	11	S474-p GKNQAkFsLVGIGGQ
0	13	Y118-p SVGtQHsysEEEKyA	0	1	R530 NWVNETLREAKKSSS
0	6	S119-p VGtQHsysEEEKyAF	0	2	S537 REAKKSSSISSFkDP
0	133	Y124-p sysEEEKyAFVNWIN	0	5	K542-ac SSSISSFkDPKISTS
0	2	K165-ub GDGIVLCkMINLSVP	0	22	K542-ub SSSISSFkDPKISTS
0	28	S257-p ALLREGEsLEDLMkL	0	1	K542 SSSISSFKDPKISTS
0	7	K263-ub EsLEDLMkLSPEELL	0	3	K579-ac ENLNDDEkLNNAkYA
0	250	Y276-p LLLRWANyHLENAGC	0	1	K584-ac DEkLNNAkYAISMAR
0	1	K285-ub LENAGCNkIGNFstD	0	2	K584-ub DEkLNNAkYAISMAR
0	4	S290-p CNkIGNFstDIkDSk	0	88	Y598-p RKIGARVyALPEDLV
0	8	T291-p NkIGNFstDIkDSkA	0	11	K610-ub DLVEVNPkMVMtVFA
0	3	K294-ac GNFstDIkDSkAyyH	0	1	T614-p VNPkMVMtVFACLMG

Figure 1.2.3.3 Post-translational modification sites of human L-plastin. A) L-plastin post-translational modification sites have been found in nearly all parts of the protein. B) L-plastin post-translational modification sites revealed by site-specific methods including amino acid sequencing, site-directed mutagenesis, modification site-specific antibodies and specific MS strategies (S.Sp.) or by proteomic discovery-mode mass spectrometry only (M.S.). (p – phosphorylation, ac – acetylation, ub – ubiquitination) Results obtained by PhosphoSitePlus® (http://www.phosphosite.org/homeAction.do).

L-plastin activity has been shown to be increased following phosphorylation on residue Ser5 *in vitro* and *in vivo*. Notably, the F-actin-binding and –bundling activities of L-plastin are increased upon Ser5 phosphorylation and this phosphorylation is required for efficient targeting of L-plastin to focal adhesions (Janji et al., 2006).

In leukocytes where L-plastin is normally expressed, phosphorylation of L-plastin is part of the cellular response to inflammation (Jones and Brown, 1996; Matsushima et al., 1987) and is involved in the regulation of leukocyte integrin-mediated adhesion (Jones et al., 1998). In addition, L-plastin is serine-phosphorylated after stimulation of leukocytes by inflammatory cytokines (including IL-8 and TNF), phorbol 12-myristate 13-acetate (PMA), and chemotactic peptides, all of which also induce an increase in actin polymerisation (Shibata et al., 1993; Shiroo and Matsushima, 1990). Furthermore, Messier and colleagues showed that in adherent macrophages stimulated with PMA, the majority of phosphorylated L-plastin associates with the cytoskeleton (Messier et al., 1993). Thus, L-plastin serine phosphorylation was proposed to be a mechanism to link signal transduction to cytoskeletal function.

Most interestingly, recent findings have demonstrated that L-plastin Ser5 phosphorylation is crucial for *in vitro* invasion and *in vivo* metastasis formation (Janji et al., 2006; Klemke et al., 2007; Riplinger et al., 2014).

So far, only protein kinase A (PKA) has been reported to directly phosphorylate L-plastin *in vitro* (Janji et al., 2006; Wang and Brown, 1999). Other kinases such as protein kinase C (PKC) delta, catalytic domain of PKC, casein kinase II, Pak1, protein kinase B, mitogen-activated protein kinase-activated protein kinase (MAPKAPK) 2, MAPKAPK3 and p38-regulated/activated protein kinase failed to phosphorylate L-plastin *in vitro* (Jones et al., 1998; Wang and Brown, 1999). In cells, distinct protein kinases have been reported to be involved in triggering L-plastin phosphorylation depending on the cell type and environment. Most frequent are reports of the involvement of PKA (Janji et al., 2006; Matsushima et al., 1987; Wang and Brown, 1999) and PKC (Al Tanoury et al., 2010; Freeley et al., 2012; Janji et al., 2010; Jones et al., 1998; Lin et al., 1998; Paclet et al., 2004; Pazdrak et al., 2011). Phosphoinositide-3-kinase (PI3K) has also been reported to play a role in L-plastin phosphorylation in human neutrophils (Jones et al., 1998; Paclet et al., 2004), but not in T

lymphocytes (Freeley et al., 2012). Nevertheless, the detailed signalling pathway(s) leading to L-plastin Ser5 phosphorylation remain(s) to be resolved.

1.2.4 L-plastin interaction partners

Besides binding to actin, L-plastin also binds a few other proteins. L-plastin has been shown to form a complex with cortactin in MCF7 cells (Al Tanoury et al., 2010). Cortactin is a major substrate of Src kinase and a regulator of actin dynamics by Rho-GTPases (Lai et al., 2009; Wu et al., 1991). It is an actin filament-binding protein that connects signalling pathways to cytoskeleton restructuring (Lai et al., 2009). It is found in lamellipodia, invadopodia, podosomes and at intercellular contact sites (El Sayegh et al., 2004; Linder and Aepfelbacher, 2003). Cortactin's regulation of cortical actin dynamics depends on its direct association with additional actin-associated proteins (reviewed in (Ammer and Weed, 2008)). Cortactin is activated by phosphorylation and can then recruit Arp2/3 complex proteins to existing actin microfilaments. Cortactin interacts with Arp2/3 and F-actin and stabilises nucleation sites both for branching and for formed branches.

L-plastin has also been shown to interact with grancalcin and this interaction is negatively regulated by Ca^{2+} (Lollike et al., 2001). Grancalcin is a calcium-binding protein that may play a role in the adhesion of neutrophils to fibronectin and in the formation of focal adhesions.

A yeast two-hybrid screen has revealed an interaction of L-plastin with the macrophage/microglia-specific calcium-binding and actin-bundling protein Iba1 (Ohsawa et al., 2004). Both proteins were shown to colocalise with F-actin in membrane ruffles and phagocytic cups in the microglial cell line MG5 (Ohsawa et al., 2004). The interaction is independent of Ca^{2+} and Iba1 was shown to increase the actin-bundling activity of L-plastin (Ohsawa et al., 2004).

L-plastin was also shown to bind Hsp70 in macrophages (Correia et al., 1999) and calmodulin in T cells which was required for the maintenance of L-plastin in the immune synapse between T cells and antigen presenting cells (Wabnitz et al., 2010).

In adherent macrophages, L-plastin binds the intermediate filament protein vimentin (Correia et al., 1999). Both proteins colocalise in podosomes, filopodia and retraction fibers. Vimentin binds L-plastin with its N-terminal domain and the vimentin-binding site localises to the first CH domain of L-plastin.

L-plastin can bind to the cytoplasmic portion of integrin subunits β1 and β2 through its actin-binding domains and these interactions are inhibited following μ-calpain activity (Le Goff et al., 2010). Despite the ability of calpain to cleave both proteins, only the cleavage of β

integrin hinders the formation of the L-plastin/integrin complex (Le Goff et al., 2010). Brown and colleagues suggest that in PMNs and in K562 lymphoblasts L-plastin peptides activate integrin $\alpha_M\beta_2$ (Jones et al., 1998) and $\alpha_v\beta_3$ (Wang et al., 2001).

Additionally, coimmunoprecipitation studies demonstrated a complex formation of phosphorylated L-plastin with protein kinase $C\beta_{II}$, GM-CSF receptor α-chain, and two actin-associated proteins, paxillin and cofilin (Pazdrak et al., 2011).

1.2.5 L-plastin and cancer

The ectopic expression of L-plastin has been observed in various cancer cells (Ang and Nice, 2010; Chaijan et al., 2014; Galiegue-Zouitina et al., 1999; Kim et al., 2010; Klemke et al., 2007; Lapillonne et al., 2000; Leavitt, 1994; Li and Zhao, 2011; Li et al., 2009; Lin et al., 1988; Lin et al., 1993a; Lin et al., 2000; Lin et al., 1993b; Otsuka et al., 2001; Park et al., 1994; Yuan et al., 2010; Zheng et al., 1997). Since L-plastin is normally expressed in immune cells required to quickly translocate to sites of infection, the ectopic expression of L-plastin in cancer cells may confer these cells with the ability to invade other parts of the body during metastasis. In accordance with this, it was shown that in carcinoma cells, similar as in haematopoietic cells, L-plastin localises to actin-rich structures of the cellular cortex involved in locomotion, adhesion or signalling, including focal adhesions, podosomes, filopodia and membrane ruffles (Arpin et al., 1994; De Clercq et al., 2013a; Janji et al., 2006).

L-plastin has been proposed as a biomarker for several human cancers: colorectal cancer (Ang and Nice, 2010), ovarian cancer (Kang et al., 2010), renal cell carcinoma (Kim et al., 2010), melanoma (Strickler et al., 2014), urinary bladder cancer (Harris et al., 2008) and choroid plexus tumours (Hasselblatt et al., 2006).

Lin and colleagues showed that L-plastin was one of the most abundant polypeptides in the majority of tumour cell lines in which its expression was detected (Lin et al., 1993b). Moreover, using a microarray chip specific to actin-related genes, our team showed that L-plastin is among the most significantly upregulated genes among actin-related genes in the invasive breast cancer cell line 1001 as compared to the non-invasive parental MCF-7 cell line (Janji et al., 2010). Furthermore, 1001 cells are resistant to TNFα cell death signals whereas the parental MCF-7 cells are sensitive to TNFα cytotoxicity (Cai et al., 1997; Janji et al., 2010). A former member of our group showed that TNFα resistance of 1001 cells was dependent on L-plastin phosphorylation on Ser5 (Janji et al., 2010).

Moreover, L-plastin is overexpressed in ovarian cancer interface zones corresponding to the invasive front between tumours and normal tissues (Kang et al., 2010) and it was shown that

L-plastin expression was responsible for increased invasion of the cholangiocarcinoma cell line RMCCA1 upon cultivation in matrigel (Chaijan et al., 2014). Furthermore, the expression of an L-plastin nanobody which reduced the bundling ability of L-plastin also inhibited filopodia formation, motility, and invasion of PC-3 prostate cancer cells (Delanote et al., 2010). Nanobodies are the smallest functional fragment of a naturally occurring single chain antibody which can be used to target a protein domain to inhibit a particular function. Interestingly however, L-plastin down-regulation showed no significant effect on filopodia extension and a less pronounced effect on motility as compared to nanobody expression (Delanote et al., 2010).

The strong 5,1 kb L-plastin gene promoter contains a classic TATA box and control elements which are involved in its suppression in normal non-haematopoietic cells and in its activation in human tumour cells (Lin et al., 1993a). The L-plastin promoter harbours hormone receptor-responsive elements: one estrogen-responsive element and three imperfect androgen-responsive elements (Lin et al., 1993a; Lin et al., 2000). This might explain why in some tumour cells of the steroid-regulated female reproductive tract such as breast, ovary, uterus and placenta, the frequency of L-plastin induction seems to be especially high (Lin et al., 1993b). In addition, a further study demonstrated that L-plastin expression in a prostate cancer cell line is up-regulated by both dihydrotestosterone and estradiol (Zheng et al., 1997). However, another study states that L-plastin expression is hormone-independent during malignancy (Leavitt, 1994).

One study shows that nasopharyngeal tumours with down-regulated L-plastin tend to have a more advanced clinical stage and a poorer differentiation than tumours with higher levels of L-plastin (Li et al., 2009). However, several other studies rather indicate a positive correlation between L-plastin expression and tumour progression (Foran et al., 2006; Harris et al., 2008; Kim et al., 2010; Otsuka et al., 2001; Zheng et al., 1999). Notably, for colorectal cancer a correlation between L-plastin expression and tumor stages was observed (Otsuka et al., 2001) and for prostate carcinoma cells it was reported that L-plastin downregulation decreased proliferation, migration and invasion rates (Zheng et al., 1999). In the metastatic colon cancer cell line SW620 L-plastin is upregulated as compared to its premetastatic counterpart SW480 and overexpression of L-plastin in SW480 leads to higher rates in proliferation and invasion and to loss of E-cadherin protein expression (Foran et al., 2006). E-cadherin is an epithelium-specific tumour suppressor gene whose loss of expression is directly associated with increased proliferation and invasion (Behrens et al., 1991). In renal cell carcinoma L-plastin was upregulated and proposed as candidate biomarker (Kim et al., 2010) and for urinary bladder cancer a correlation was described between the expression of

L-plastin and clinically important pathologic features such as tumour grade, stage, and growth pattern (Harris et al., 2008).

Surprisingly, no clear correlation between L-plastin expression and tumour stage was found in other cancer types (Lapillonne et al., 2000 & Klemke et al., 2007). Lapillonne and colleagues detected L-plastin expression in malignant epithelial cells of the mammary gland in around 14% of the breast carcinoma tumours analysed whereas no L-plastin expression could be detected in untransformed epithelial cells (Lapillonne et al., 2000). However, they found that in breast cancer the expression of L-plastin does not relate to tumour size, histological grade and lymph node status (Lapillonne et al., 2000). It has to be noted that this study by Lapillonne and colleagues (Lapillonne et al., 2000) is based on only 29 breast tumour samples. In contrast to Lapillonne's findings, a study by Schulz and colleagues (Schulz et al., 2009) identified L-plastin to be 1.43-fold upregulated in triple-negative (HER2-, ER-, PR-) as compared to HER2+, ER-, PR- breast cancers. As in the literature it is so far not clear whether L-plastin expression is linked to tumour progression in breast cancer, we performed survival curves with the Kaplan Meier plotter tool (www.kmplot.com) (Gyorffy et al., 2010). The results indicate that L-plastin expression is not an optimal biomarker for breast cancer prognosis as no significant survival differences were obtained for patients with high versus low L-plastin expression for overall survival, relapse-free survival and distant metastasis-free survival (the survival curves can be found in the appendix). Overall, the level of L-plastin expression does thus not seem to be linked to breast cancer stage and outcome.

Concerning melanoma, Klemke and colleagues (Klemke et al., 2007) found that even though knockdown of endogenous L-plastin by siRNA treatment reduced haptotactic migration of the melanoma cell line IF6, in melanoma patients, L-plastin expression was not significantly higher in tumours with bad prognosis compared to tumours with good prognosis. The fact that no correlation existed between L-plastin expression and the penetration depths or tumour stages of the malignant melanomas implied that additional factors such as phosphorylation of L-plastin may influence its function in tumour cells. Indeed, invasion into matrigel was up to three-fold increased for melanoma cells expressing the phosphorylatable wild type L-plastin as compared to cells expressing a non-phosphorylatable L-plastin mutant or a transfection-control protein (Klemke et al., 2007). In contrast to invasion, haptotactic migration of human melanoma cells was similarly enhanced for wild type and non-phosphorylatable L-plastin-expressing cells compared to transfection-control protein expressing cells and migration was thus independent of the L-plastin phosphorylation state (Klemke et al., 2007). Klemke and colleagues also analysed the well-established mouse melanoma model of two isogenic variants of the mouse melanoma cell line B16 with different metastatic capabilities. In line with the invasion-related previous findings, they revealed that

the highly metastatic B16F10 cells expressed higher amounts of L-plastin than the low metastatic B16F1 cells. Furthermore, only the highly metastatic cells contained substantial amounts of phosphorylated L-plastin. Therefore, endogenous expression of phosphorylated L-plastin correlates with enhanced *in vivo* metastasis in the mouse B16F1/B16F10 melanoma model. Interestingly, these data indicate that an increase in melanoma cell invasion and metastasis potential might require not only expression but also phosphorylation of L-plastin.

More recently, the same group also found that knockdown of endogenous L-plastin in human prostate carcinoma cells led to reduced tumor cell growth and metastasis and more importantly that L-plastin Ser5 phosphorylation was involved in *in vivo* metastasis formation in melanoma (Riplinger et al., 2014). L-plastin wild type was ectopically expressed and spontaneously phosphorylated in melanoma MV3 cells which were then intracardially injected in mice. This led to an increase in the number of metastases as compared to mice that were injected with MV3 cells lacking L-plastin. No increase in the number of metastases was observed for mice injected with MV3 cells expressing a non-phosphorylatable L-plastin mutant (Riplinger et al., 2014).

Similarly to what Klemke et al. showed for melanoma cells, it was also found that a decrease in L-plastin Ser5 phosphorylation inhibits invasion of HEK293T cells whereas the phosphorylation state of L-plastin was not important for migration (Janji et al., 2006).

Taken together, these findings indicate that L-plastin expression alone might not be sufficient but that Ser5 phosphorylation of L-plastin may be additionally required for endowing cancer cells with aggressive properties.

1.3 Deregulation of signalling pathways in cancer

The human body consists of a wide variety of cell types that must be able to communicate with each other and to respond to their environment in a process called signal transduction. The sensing of stimuli such as growth factors, cytokines, hormones, cell-ECM contact and cell-to-cell contacts occurs by the corresponding receptors including transmembrane receptors such as G protein-coupled receptors (GPCRs), receptor tyrosine kinases (RTKs) and integrins as well as intracellular receptors such as the nuclear steroid hormone receptors. Following ligand binding, these receptors trigger a biochemical chain of events inside the cell. The most common route of transducing signals is phosphorylation and dephosphorylation of signalling molecules by protein kinases and phosphatases. Common signal transduction pathways include the extracellular signal-regulated kinase/mitogen-activated protein kinase (ERK/MAPK), the PI3K, the phospholipase C gamma/protein kinase C (PLCγ/PKC), the cAMP-dependent as well as the Janus kinase and signal transducer and activator of transcription (JAK/STAT) pathways. Depending on the cell type, the induced response alters the cellular metabolism, shape, gene expression, or ability to divide. Signal transduction pathways can thus govern various cellular functions such as proliferation, differentiation, growth and division, cell death and cell motility.

Biochemical signals can be amplified at any step so that one receptor or signalling molecule can cause many responses. Moreover, a large number of regulatory mechanisms occur to modulate signal transduction processes. These include dephosphorylation by phosphatases, proteasomal degradation following ubiquitination and the formation of inactive protein complexes. Besides, multiple crosstalk interactions between intracellular signalling pathways occur and can fine-tune signals or compensate for disturbed canonical pathways (Mendoza et al., 2011).

Signal transduction pathways are crucial for regulating various biological processes and a large number of diseases are attributed to their deregulation. For example, mammalian cells require stimulation for cell division and survival and in the absence of such stimuli they undergo apoptosis. Thus, requirements for extracellular stimulation are necessary for controlling cell behaviour and perturbations in signal transduction due to mutation or overexpression of receptors or key signalling molecules can lead to pathological phenotypes of the cells.

Cancer is driven by genetic and epigenetic alterations leading to changes in cell growth and division, cell survival, cell fate and cell motility. As all of these events are controlled by signalling pathways and the deregulation of signal transduction cascades is an important

trigger of many cancers (Sever and Brugge, 2015). An examination of the ERK/MAPK pathway illustrates how deregulated signalling can lead to the development of cancer.

1.3.1 ERK/MAPK pathway activation and activity

The conventional MAPK family consists of four major subfamilies of related proteins, ERK1/2, p38 MAPK (α,β,γ,δ), JNK (1,2,3) MAPK, ERK5, that are interconnected by signal transduction cascades activated by external stimuli, such as growth factors, stress, cytokines and inflammation. Each group of conventional MAPKs is composed of three evolutionarily conserved, sequentially acting kinases: a MAPK, a MAPK kinase (MAPKK) and a MAPKK kinase (MAPKKK) (Figure 1.3.1). In response to extracellular stimuli, a small GTP-binding protein of the Ras/Rho family interacts with and activates a MAPKKK. MAPKKK then leads to the phosphorylation of a MAPKK which then phosphorylates a MAPK by dual phosphorylation on Threonine and Tyrosine residues in the activation loop. Scaffolding proteins can simultaneously bind several components of the MAPK cascade and thereby mediate specificity and organise pathways in specific modules.

A wide range of functions are regulated by the MAPKs through phosphorylation of several substrates including members of the MAPK-activated protein kinase (MAPKAPK) family. This family is composed of RSKs, MSKs, MNKs, MK2/3 and MK5 (Figure 1.3.1).

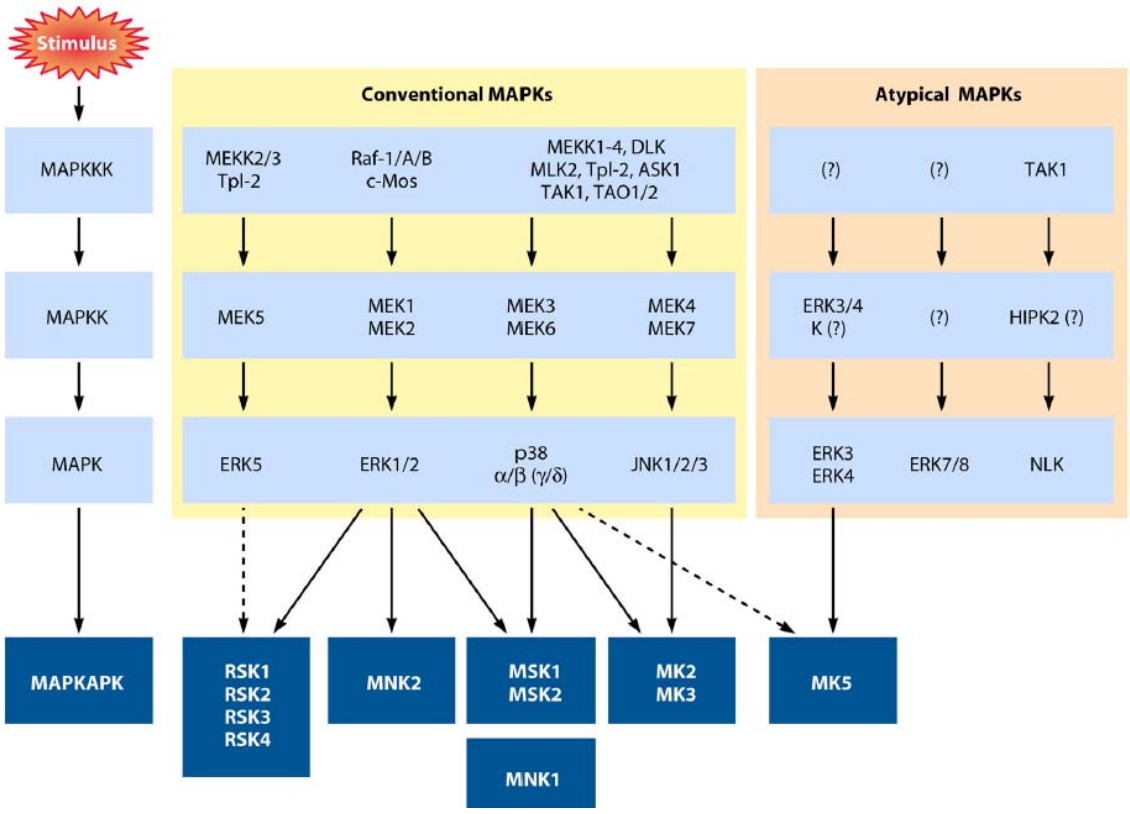

Figure 1.3.1 MAPK signalling cascade. External stimuli such as mitogens, cytokines and cellular stress factors can lead to the activation of diverse MAPKKKs in turn leading to activation of diverse MAPKKs and finally to activation of MAPKs. The latter can extend the MAPK phosphorylation cascade by phosphorylating MAPKAPKs. Dotted lines indicate interactions that need further demonstration. γ and δ isoforms of p38 are in brackets as these have not been shown to promote MAPKAPK activation. Adapted from (Cargnello and Roux, 2011).

This dissertation will focus on the ERK1/2 module. ERK1 was the first mammalian MAPK to be cloned and characterised. ERK1 and ERK2 share 83% amino acid identity and are expressed ubiquitously. The ERK1/2 module is activated by growth factors (epidermal growth factor, platelet-derived growth factor and nerve growth factor), insulin, ligands for GPCRs, cytokines, osmotic stress and microtubule disorganisation (Raman et al., 2007). The MAPKs ERK1 and ERK2 are activated by the MAPKKs MEK1 and MEK2 which are activated by the MAPKKKs A-Raf, B-Raf and Raf-1. ERK1 and ERK2 activations occur following cell surface receptor activation upon ligand binding and receptor dimerisation. The phosphorylated intracellular domains of the receptor can bind proteins containing Src homology 2 (SH2) or phosphotyrosine-binding (PTB) domains such as the adaptor proteins Shc and the growth factor receptor-bound protein 2 (Grb2). The guanine nucleotide exchange factor SOS is recruited to the plasma membrane by binding Grb2 and it activates Ras which in turn sequentially activates the MAPKKKs, the MAPKKs and the MAPKs. In resting cells, ERK1 and ERK2 are localised in the cytoplasm. Upon activation however, a significant proportion accumulates in the nucleus (Chen et al., 1992; Lenormand et al., 1993). ERK1 and ERK2 phosphorylate numerous substrates (reviewed in (Yoon and Seger, 2006)) located in the cytoplasm, the nucleus and at the membranes or the cytoskeleton.

ERK1 and ERK2 mainly control cell proliferation. Sustained activation of these kinases is required for progression from G1 to S phase. ERK1/2 activate the transcription factor Elk-1 which is involved in expression of immediate early genes such as c-Fos (Gille et al., 1995).

ERK1/2 extends the MAPK cascade by phosphorylating the MAPKAPKs p90 ribosomal S6 kinases (RSKs), mitogen- and stress-activated kinases (MSKs) and MAPK-interacting kinases (MNKs) (Figure 1.3.1).

Of particular importance for our work were RSK kinases. The human RSK family is a group of highly conserved Ser/Thr kinases which contains 4 isoforms, RSKs 1-4, that are 80% identical. The RSK family is unique because their isoforms all contain 2 kinase domains: the carboxyl-terminal kinase domain (CTKD), which is activated by ERK1/2, subsequently activates the amino-terminal kinase domain (NTKD) by autophosphorylation which can then

phosphorylate substrates. Only the NTKD has been shown to be involved in substrate phosphorylation. The CTKD belongs to the Ca^{2+}/calmodulin-dependent protein kinase (CAMK) family and the NTKD belongs to the AGC family of kinases. RSK 1-3 are expressed ubiquitously whereas RSK4 has a much lower and more restricted expression. RSK4 is found mainly in the cytoplasm and does not translocate to the nucleus upon stimulation (Dummler et al., 2005). On the other hand, RSK 1-3 are found in the cytoplasm in resting cells and, upon stimulation, a significant proportion translocates to the nucleus (Chen et al., 1992; Lenormand et al., 1993; Richards et al., 2001; Vaidyanathan and Ramos, 2003; Zhao et al., 1995). RSK1 was shown to accumulate at the plasma membrane within minutes upon stimulation, where it may receive activating inputs before nuclear translocation (Richards et al., 2001).

Different phosphorylation events are important for the activation of RSK (Figure 1.3.2). Upon stimulation, ERK1/2 docks at the C-terminus of RSK and phosphorylates Thr573 in the activation loop of the CTKD (Ranganathan et al., 2006; Shaul and Seger, 2006; Smith et al., 1999) and might also phosphorylate Thr359/Ser363 in the linker region (Dalby et al., 1998). The activated CTKD autophosphorylates RSK at Ser380 which allows access of PDK1 to RSK (Frodin and Gammeltoft, 1999) which is required for stimulation of RSK 1-3. RSK4 does not seem to require PDK1 to be fully active and it is fully phosphorylated and activated in unstimulated cells (Dummler et al., 2005). PDK1 phosphorylates Ser221 in the activation loop of the NTKD (Richards et al., 1999) leading to the full activation of the protein and subsequent substrate phosphorylation (Anjum and Blenis, 2008). The NTKD can then phosphorylate Ser749 which in some cases results in dissociation of ERK1/2 from RSK.

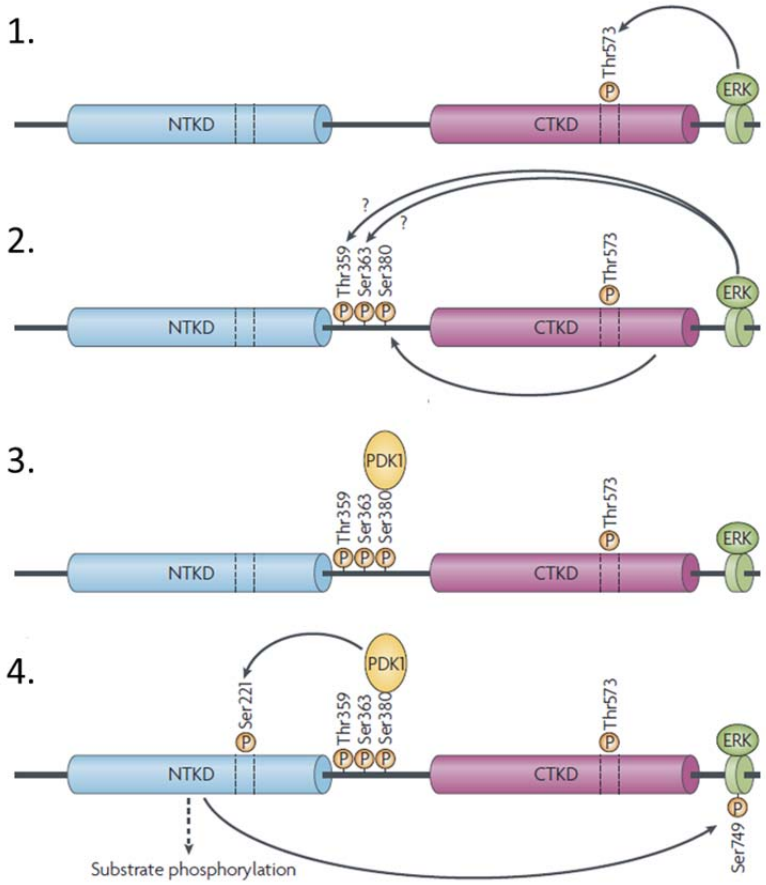

Figure 1.3.2 Current model of RSK activation. RSK activation relies on several phosphorylation events with a final phosphorylation step by PDK1 leading to RSK substrate phosphorylation. Adapted from (Anjum and Blenis, 2008).

The RSK1 consensus sequence for substrate phosphorylation is Arg/Lys-X-Arg-X-X-pSer/Thr or Arg-Arg-X-pSer/Thr (Leighton et al., 1995). RSK1 has a five-fold preference for phosphorylating Ser than Thr residues and indeed most of the so far identified RSK substrates are phosphorylated on Ser residues. The identification of RSK substrates indicates roles for RSK in gene transcription, nuclear signalling, cell cycle progression, cell proliferation, cell growth, protein synthesis, cell survival and cell motility. Although most studies have not determined isoform specificity, most substrates have been identified for RSK2 as compared to the other isoforms. However, many known substrates for RSK2 may be shared by different RSK family members.

In physiological conditions, MAPK signalling is activated in a controlled manner in response to environmental stimuli and leads to a controlled response. MAPK signalling is involved in cell proliferation, differentiation, survival and death. In pathological conditions in contrast, deregulation of MAPK signalling can lead to aberrant cellular responses resulting in various

diseases including Alzheimer's disease, Parkinson's disease, amyotrophic lateral sclerosis (ALS) and various types of cancers (Kim and Choi, 2010).

Various tumours and tumour cell lines display constitutive activation of the MAPK pathway and approximately 30% of all human cancers contain a constitutively-activating mutation in one of the ras oncogenes (Bos, 1989). K-Ras is frequently mutated in many human cancers including lung and colon cancer (Schubbert et al., 2007). Mutations in B-Raf are responsible for approximately 66% of melanomas (Halilovic and Solit, 2008). Also ERK1/2 was identified as a crucial contributor to the pathogenesis of cancer (Land et al., 1983) and many tumour cell lines show high levels of activated ERK1/2 (Hoshino et al., 1999). Moreover, hyperactive RSK signalling is found in several human cancers and RSKs are overexpressed in approximately 50% of human breast cancer tissues (Smith et al., 2005). However, RSK function is dependent on the RSK isoform as well as on the specific type of cancer.

Since the ERK/MAPK signal transduction cascade is activated upon epidermal growth factor receptor (EGFR) stimulation and since the overexpression of RTKs plays a role in cancer development and progression, the next section of this dissertation will focus on the EGFR family upregulation in cancer.

1.3.2 EGFR signalling in breast cancer

The EGFR (also called ErbB1 or HER1) belongs to the ErbB receptor family which also contains ErbB2 (or HER2 or HER2/neu), ErbB3 (or HER3) and ErbB4 (or HER4). Seven ligands are known for the EGFR: EGF, transforming growth factor α (TGF-α), amphiregulin (AR), epigen (EGN), epiregulin (EPR), β-cellulin (BC) and heparin-binding EGF-like growth factor (HBEGF). ErbB2 has no known ligands, ErbB3 binds neuregulins (NRGs) 1 and 2 and ErbB4 binds NRGs 1-4, EPR, BC and HBEGF (Figure 1.3.2). All ligands exist as membrane-anchored precursors and are released as soluble factors upon cleavage by metalloproteases. Ligand binding induces a dramatic conformational change that exposes a dimerisation arm which induces the extracellular region of the ErbB receptor to dimerise (Burgess et al., 2003). For most RTKs, ligand-mediated receptor dimerisation is thought to position the two cytoplasmic tyrosine kinase domains for efficient trans-phosphorylation of tyrosine residues in the kinase activation loop. For ErbB family receptor activation however, such trans-phosphorylation is not required. Instead, following ligand-mediated dimerisation of the ErbB receptors, the two receptor kinase domains form an asymmetric dimer in which one kinase activates the other allosterically (Jura et al., 2009; Red Brewer et al., 2009; Zhang et al., 2006). The activator kinase interacts with the receiver and induces conformational changes leading to the activation of the latter.

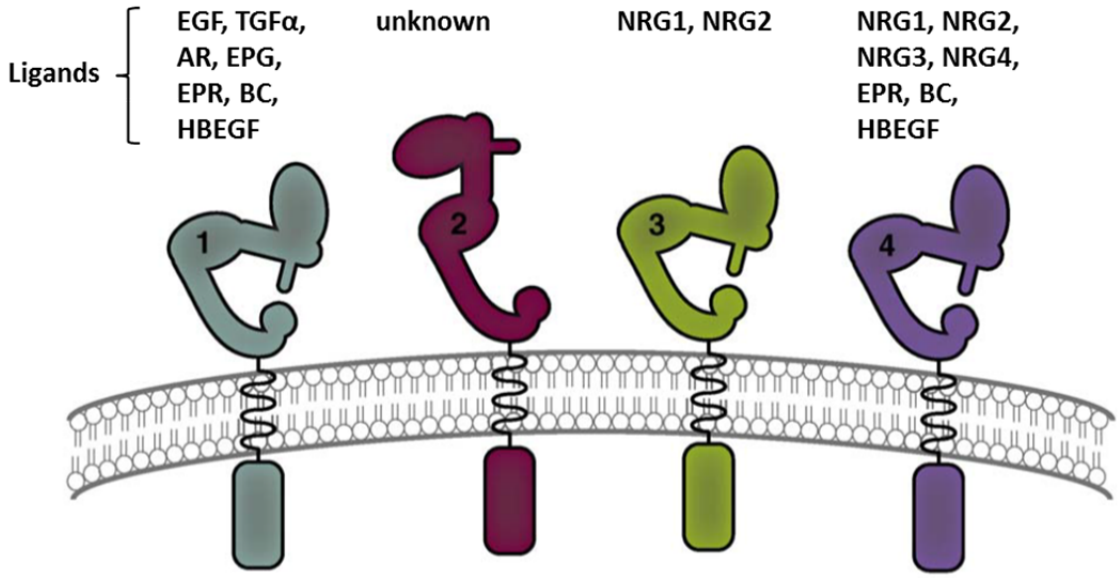

Figure 1.3.2 ErbB family receptors and their ligands. The ErbB receptor family is composed of four different members: 1 – EGFR (also ErbB1 or Her1), 2 – ErbB2 (or Her2), 3 – ErbB3 (or HER3) and 4 – ErbB4 (or HER4). Diverse ligands can bind to the respective receptors and induce receptor homo –or heterodimerisation. ErbB2 has no known ligands but is the preferred dimerisation partner of all family members due to an extended interaction loop rendering it constitutively available for dimerisation. (AR, amphiregulin; EPG, epigen; EPR, epiregulin; BC, β-cellulin; HBEGF, heparin-binding EGF-like growth factor; NRG, neuregulin). Adapted from (Hynes and MacDonald, 2009) and (Yarden and Pines, 2012).

Homo- and heterodimerisation of ErbB family receptors enables 10 possible combinations. Even though ErbB2 has no known ligands, it is the preferred partner of all family members due to an extended interaction loop rendering it constitutively available for dimerisation (Figure 1.3.2). ErbB3 is kinase dead and has no ability to phosphorylate other proteins. Nevertheless, it can form an active signalling complex with another member of the ErbB receptor family, especially ErbB2, where it acts as an allosteric activator (Eccles, 2011).

Upon activation, the EGFR can bind a vast range of direct substrates and/or adaptor proteins depending on the mode of activation and the dimerisation partner (Schulze et al., 2005). The major signal transduction cascades activated by ErbB receptors are mediated by ERK/MAPK, JNK, PLCγ and PI3K pathways. ErbB receptor signalling can result in the induction of proliferation, the regulation of adhesion and motility, the avoidance of apoptosis and the promotion of invasion and angiogenesis. (Eccles, 2011). In normal mammary gland physiology, the ErbB receptors play a key role during puberty, pregnancy and lactation when the steroid hormones upregulate the production of many growth factors including those of the EGF family (Eccles, 2011).

Breast cancer is the most common cancer in women worldwide (Tinoco et al., 2013) and the major signalling pathways involved in breast cancer tumour progression and metastasis formation are still incompletely understood. Breast cancers are often classified based on the presence and absence of three cellular receptors. Hormone receptor positive cancers express estrogen and/or progesterone receptors (ER/PR) and represent approximately 60% of all breast cancers, the HER2/neu receptor is overexpressed in approximately 20% of all breast cancers and approximately 20% of breast cancers are negative for ER, PR and HER2/neu and are known as triple-negative breast cancers (TNBCs) (Tinoco et al., 2013). Receptor positive breast cancer patients receive treatments targeting the expressed receptors whereas patients with the aggressive TNBC do not have these targeted treatment options. In this regard it is interesting to note that 50-70% of TNBCs exhibit EGFR expression, that TNBCs show a high frequency of EGFR dysregulation and that EGFR status negatively correlates with patient survival (Burness et al., 2010; Lehmann and Pietenpol, 2014). Altogether this has turned focus on the EGFR as a potential clinical target for TNBCs.

The EGFR and its relatives are known as oncogenic drivers in various cancers, including lung cancer (Mok, 2011), breast cancer (Arteaga et al., 2012) and glioblastoma (Lee et al., 2006; Libermann et al., 1985; Vivanco et al., 2012). An overview of the pathological role of the EGFR in breast cancer is given in (Foley et al., 2010). Particularly EGFR and ErbB2 are mutated to constitutively active forms in a large number of epithelial tumours. ErbB receptors become activated by receptor overexpression, ligand-dependent or ligand-independent mechanisms. Ligand-independent activity can occur due to forms of the receptor that have a deletion of the extracellular domain which results in constitutive receptor activation (Frederick et al., 2000). The most common mutation of the EGFR is an in-frame deletion in the tyrosine kinase domain which leads to uncontrolled activation of downstream signalling (Paez et al., 2004).

EGFR signalling is one of the most targeted signalling pathways for the treatment of cancers. Two types of drugs against ErbB receptors have shown clinical activity and were approved for the treatment of cancer. One type consists of small-molecule tyrosine kinase inhibitors (TKIs) competing with ATP for binding to the receptor's kinase pocket (drug names ending with –inib) and the other type consists of humanised monoclonal antibodies targeted against the receptor's ligand-binding extracellular domain (drug names ending with –mab). Seven such drugs have so far been approved for cancer treatment by the US Food and Drug Administration (FDA), all targeting the EGFR, ErbB2 or both (Table 1.3.2).

Table 1.3.2 ErbB inhibitors approved for cancer treatment by the FDA.

Drug	Target	FDA approval for
Cetuximab	EGFR	-head and neck cancer
		-colorectal cancer
Panitumumab	EGFR	-colorectal cancer
Gefitinib	EGFR	-non-small-cell lung cancer
Erlotinib	EGFR	-non-small-cell lung cancer
		-pancreatic cancer
Trastuzumab	ErbB2	-gastric or gastroesophageal junction adenocarcinoma
		-breast cancer
Pertuzumab	ErbB2	-breast cancer
Lapatinib	EGFR+ErbB2	-breast cancer

Three ErbB targeting drugs have been approved for breast cancer treatment (Table 1.3.2). However, trials using small-molecule TKIs or antibodies only targeting the EGFR have been largely disappointing in breast cancer monotherapy (Burness et al., 2010; Foley et al., 2010). A possibility to circumvent this problem might be combination therapies of antibodies and TKIs which are currently investigated in clinical trials and which already suggest additive or even synergistic antitumor activity (Tebbutt et al., 2013).

Chapter 2 Aims and outline of the thesis

Several studies highlight aberrant L-plastin expression in diverse cancer types (Ang and Nice, 2010; Chaijan et al., 2014; Galiegue-Zouitina et al., 1999; Kim et al., 2010; Klemke et al., 2007; Lapillonne et al., 2000; Leavitt, 1994; Li and Zhao, 2011; Li et al., 2009; Lin et al., 1988; Lin et al., 1993a; Lin et al., 2000; Lin et al., 1993b; Otsuka et al., 2001; Park et al., 1994; Yuan et al., 2010; Zheng et al., 1997). In some cancers, including breast cancer, there is however no correlation between L-plastin expression and cancer progression (Klemke et al., 2007; Lapillonne et al., 2000). Findings showing that Ser5 phosphorylation of L-plastin increases its F-actin-binding activity and promotes its targeting to sites of actin assembly in cells (Janji et al., 2006) and providing evidence that L-plastin Ser5 phosphorylation is involved in cell invasion and metastasis formation (Janji et al., 2006; Klemke et al., 2007; Riplinger et al., 2014) indicate that it is rather the phosphorylation of L-plastin on Ser5 than mere L-plastin expression which plays a role in cancer progression.

Since the signal transduction pathway and the identity of the kinase responsible for L-plastin Ser5 phosphorylation are still a matter of debate, the main objective of this study was to decipher the signalling pathway(s) upstream of this phosphorylation event and to identify the kinase(s) involved in L-plastin Ser5 phosphorylation in breast cancer cells.

As we observed that baseline phosphorylation of L-plastin Ser5 was high in invasive breast cancer cell lines and absent or low in non-invasive breast cancer cells, a whole-genome microarray analysis approach was applied in order to compare cells with differential L-plastin Ser5 phosphorylation focusing on deregulated signalling pathways. In order to narrow down the potential candidate kinases for the phosphorylation of L-plastin Ser5, an *in vitro* kinase assay screen was performed in parallel with the company Kinexus. Both experiments pointed to an involvement of the ERK/MAPK signalling pathway and of its downstream kinases RSK1 and RSK2 in Ser5 phosphorylation of L-plastin. We then performed *in vitro* kinase assays on the full-length wild type L-plastin protein as well as activation and inhibition studies to deepen the analysis of this pathway. These investigations led to our most significant and novel findings that L-plastin Ser5 phosphorylation is mediated by the ERK/MAPK pathway in breast cancer cells and that the downstream effector kinases of this pathway RSK1 and RSK2 are able to directly phosphorylate L-plastin on residue Ser5. siRNA-mediated knockdown and a

systems biology approach using computational modelling also confirmed that RSK is an important activator of L-plastin in all studied breast cancer cell lines.

The next part of the work was dedicated to the investigation of a functional outcome of L-plastin Ser5 phosphorylation. We performed migration and invasion assays which showed that RSK knockdown, besides reducing L-plastin Ser5 phosphorylation, also impaired MDA-MB-435S breast cancer cell migration and invasion.

A third aim of the study was to identify L-plastin interaction partners. To this end we performed coimmunoprecipitation assays using GFP-Trap and thereby identified the proto-oncogene tyrosine kinase Src as a binding partner of L-plastin. Moreover we performed high performance liquid chromatography mass spectrometry and identified prothymosin α and heterogeneous nuclear ribonucleoprotein M as potential L-plastin binding partners.

Chapter 3 Materials and methods

3.1 Cell culture

SK-BR-3 and BT-20 cells were grown in McCoy's 5A and EMEM (Eagle's minimal essential medium) media respectively and MCF7 and MDA-MB-435S cells were cultured in RPMI (Roswell Park Memorial Institute) medium. Human embryonic kidney 293 (HEK) cells were grown in DMEM (Dulbecco's modified Eagle's) medium. All media were supplemented with 10% fetal bovine serum, 2 mM of L-glutamine and 100 units/ml of penicillin and streptomycin. Cells were grown at 37°C in a humid 5% CO_2 atmosphere. All cells were bought from or authentified by ATCC (American Type Culture Collection, Manassas, VA, USA).

3.2 Antibodies and reagents

Mouse monoclonal immunoglobulin (Ig) G1 antibody against L-plastin (LPL4A.1, MA5-11921) used for immunoblotting was purchased from Thermo Scientific (Erembodegem, Belgium). Rabbit polyclonal IgG antibody against L-plastin used for immunofluorescence was characterised in (Lapillonne et al., 2000). Rabbit polyclonal anti-Ser5-P antibody specifically recognising L-plastin phosphorylated at Ser5 was raised against a peptide encoding L-plastin residues 2-17 in which Ser5 was phosphorylated (ARGS(P)VSDEEMMELREA) (characterised in (Janji et al., 2006)). Rabbit polyclonal antibodies against RSK1 (sc-231) or RSK2 (#9340) were purchased from Santa Cruz Biotechnology (Heidelberg, Germany) and Cell Signaling Technology (Leiden, Netherlands) respectively. Mouse anti-β-actin (A5441), mouse anti-α-tubulin (T5168) and mouse anti-GFP (G-6539-1) antibodies were obtained from Sigma-Aldrich (Diegem, Belgium). Anti-EGFR (#2232), anti-src (#2109), anti-phosphorylated PKA substrates (#9624), anti-PKCδ (#2058) and a P-RSK1/2 antibody specifically recognising the phosphorylated forms of RSK1 and RSK2 (Ser221, respectively Ser227) (#3556) were from Cell Signaling Technology. Rabbit anti-β-tubulin (sc-9104) antibody was from Santa Cruz Biotechnology. Anti-N-cadherin (33-3900) and anti-claudin-3 (341700) were from Life Technologies (Carlsbad, CA, USA) and anti-E-cadherin (610182) from BD Biosciences (Franklin Lakes, NJ, USA) and anti-vimentin (sc-6260) and anti-cytokeratin-18 (sc-6259) from Santa Cruz Biotechnology.

Phorbol 12-myristate 13-acetate (PMA), epidermal growth factor (EGF), 8-Bromo-cAMP (8Br-cAMP or 8Br), H89, PP2, endothelin-1, β-estradiol and progesterone were obtained

from Sigma, GF109203X (GF), SL0101, BI-D1870 (BID), SU6656 and Src inhibitor I from Calbiochem Merck Millipore (Nottingham, UK) and PD98059 (PD) from Cell Signaling Technology.

3.3 Treatment of cells with pharmacological agents

Cells were treated with PMA at a concentration of 0.1 µM for 1 hour (h), with EGF at 1 ng/ml for 15 minutes (min), with 8-Bromo-cAMP at 1 mM for 1 h, with endothelin-1 at 100 nM for 5 to 30 min, with β-estradiol at 10 nM for 1 to 48 h, with progesterone at 100 nM for 1 to 48 h, with GF109203X at 1 µM for 3 h, with H89 at 50 µM for 1 h, with PP2 at 10 µM for 1 h, with SU6656 at 5 µM or 10 µM for 3 h, with Src inhibitor I at 10 µM for 3 h, with PD98059 at 10 µM for 1 h, with BI-D1870 at 5 µM for 30 min, or with SL0101 at 80 µM for 4 h. In case of combined treatment with activators and inhibitors, the incubation with the inhibitor was performed before the incubation with the activator. For serum starvation prior to EGF treatment cells were cultured in the absence of serum for 24 h.

3.4 Plasmid constructs

L-plastinWT, L-plastinS5A (unphosphorylatable) and L-plastinS5E (phosphomimic) constructs in pEGFP-N1 and in pDsRed-Monomer-N1 vectors (both from Clontech, Saint-Germain-en-Laye, France) were available in the lab and generated as described in (Al Tanoury et al., 2010).

GFP-PKCδ was generated by cloning a cDNA corresponding to the full-length PKCδ protein into the pEGFP-C3 vector (Clontech) using Xho1-Kpn1 restriction sites. For constitutively active PKCδ, a fragment of PKCδ was replaced by a synthesised fragment leading to a point mutation of AA144 arginine to alanine and of AA145 arginine to alanine using restriction enzymes Sal1-Hind3. For dominant negative PKCδ, a fragment of PKCδ was replaced by a synthesised fragment leading to a point mutation of AA278 lysine to arginine using restriction enzymes Hind3-Xmn1.

The v-Src-DsRed vector was a kind gift from Gerhard Müller-Newen (Uniklinik RWTH Aachen, Germany).
All constructs were verified through sequencing by LGC Genomics.

3.5 Transfections and siRNA knockdown

Calcium phosphate transfections were performed on HEK cells prior to GFP-Trap immunoprecipitation. A solution of 30-65 µg DNA and 160 µl of 2.5 M $CaCl_2$, completed to 1300 µl with H_2O (for a 145 cm^2 dish) was added drop-wise to an equal amount of HEPES-buffered saline 2x, pH 7.0 (Alfa Aesar, Ward Hill, MA, USA). After 30 min of incubation at room temperature (RT) the solution was added to the cells at ≥70% confluence. Cells were analysed 24-48 h post transfection.

Small interfering RNA against RSK-1 (Hs_RPS6KA1_10), RSK-2 (Hs_RPS6KA3_5) and PKCδ (Hs_PRKCD11) were purchased from Qiagen GmbH (Venio, Netherlands). 60 nM and 80 nM of RSK-1 & RSK-2 and PKCδ siRNA respectively were transfected using Lipofectamine®2000 (Life Technologies, Gent, Belgium). A solution of 625 µl of OptiMEM medium with 25 µl of Lipofectamine®2000 (or 50 µl for the combined addition of two siRNAs) was added to a solution of 625 µl of OptiMEM medium with 15 µl of corresponding siRNA. The solution was mixed by pipetting and incubated for 10-15 min at RT. 4 ml of RPMI medium were added to the mix and 100 µl of this mix were added to each well of a 96-well plate. After 4 h of incubation with the transfection solution, the medium was replaced by fresh RPMI supplemented with 10% fetal bovine serum, 2 mM of L-glutamine and 100 units/ml of penicillin and streptomycin.

3.6 Immunofluorescence

Epithelial and mesenchymal marker assay

Cells were washed with phosphate-buffered saline (PBS) supplemented with 0.1 mM $MgCl_2$ and 0.1 mM $CaCl_2$ (PBS-MgCa), fixed with 3% paraformaldehyde in PBS-MgCa for 20 min at RT, saturated with NH_4Cl 50 mM in PBS-MgCa for 10 min at RT and permeabilised with Triton 0.4% in PBS-MgCa for 5 min at RT. In-between steps the cells were washed with PBS-MgCa. Cells were incubated with primary antibodies against N-cadherin, vimentin, E-cadherin, cytokeratin-18 and claudin-3 during 1 h at RT, followed by staining with secondary antibodies for 30 min at RT. Labelled cells were analysed by a Zeiss laser scanning confocal microscope (LSM-510 Meta, Carl Zeiss, Jena, Germany) with a 63x-1.4 oil objective. Image acquisition was performed using Zen 2009 software and image analysis using ImageJ software.

L-plastin and Ser5 phosphorylated L-plastin localisation assay

Cells were plated on fibronectin-coated (20 µg/ml) glass coverslips 16 h before serum starvation which was performed for 24 h. Then the cells were treated with vehicle or EGF (100 ng/ml) with or without prior treatment with BI-D1870 (5 µM). 1 h following treatment the cells were fixed with 4% paraformaldehyde in PBS with 0.5% Triton X-100 for 10 min, permeabilised with 0.5% Triton X-100 in PBS for 5 min and blocked in 2% BSA in PBS-Tween 0.05% for 10 min. In-between steps, the cells were washed with PBS-Tween. The cells were stained with phalloidin and antibodies against L-plastin or Ser5 phosphorylated L-plastin. Imaging was performed on an Andor Spinning Disk Revolution system (CSU-W1) (Andor Technology, Belfast, United Kingdom) based on a Nikon Ti microscope (Nikon, Konan, Minato-ku, Tokyo, Japan) with an Andor iXon Ultra EMCCD camera and a 100x-1.4 NA oil objective. Image acquisition was performed using Andor iQ3 software and image analysis using ImageJ software.

3.7 Microarrays

RNA extraction was performed using Trizol reagent. RNA quality and concentration were evaluated spectroscopically using a NanoDrop2000c instrument (Thermo Scientific). RNA integrity was subsequently analysed on an Agilent 2100 Bioanalyzer (Agilent Technologies, Palo Alto, CA, USA). Only good quality RNA with integrity numbers > 9 was used. Transcriptome profiling assays were performed using the Affymetrix Human GeneChip 1.0 ST arrays (Affymetrix, Santa Clara, CA, USA). Briefly, 250 ng of total RNA were reverse transcribed into cDNA, then transcribed into cRNA and labelled into biotinylated cRNA using the GeneChip WT PLUS Reagent kit (Affymetrix) according to the manufacturer's protocols (P/N 4425209 Rev.B 05/2009 and P/N 702808 Rev.6). Labelled cRNA products were randomly fragmented and hybridised onto Affymetrix GeneChips. Arrays were washed and stained with Affymetrix GeneChip WT Terminal Labelling and Hybridization kit, before being scanned using a GeneChip Scanner 3000. Cell intensity files containing hybridization raw signal intensities were imported into the Partek GS software (Partek, St. Louis, MO, USA) using default options. Resulting expression data (transcript cluster level) were imported into R statistical environment for further analysis. Transcript clusters without chromosome location were removed. Quality of the data was assessed through boxplot, relative log expression and Pearson's correlation. Linear Model for Microarray Data (LIMMA) was used to compare transcript cluster expression between different conditions, according to author's recommendations [LIMMA User's Guide section 9.5]. Resulting p-values were adjusted for false discovery rate (FDR) with Benjamini and Hochberg's FDR (Benjamini and Hochberg,

1995) and transcript clusters with FDR < 0.05 and absolute fold change (FC) ≥ 1.5 were considered as significantly differentially expressed and used for further analyses. The Ingenuity Pathway Analysis (IPA) software (Ingenuity Systems, Redwood City, CA, USA, www.ingenuity.com) was used for transcript cluster mapping which led to the identification of differentially expressed genes (DEGs) and for data mining, including functional analyses and gene network reconstruction. Right-tailed Fisher's exact test was used to calculate a p-value for functional enrichment analysis (threshold: -log(p-value) > 1.301). Microarray expression data are available in the ArrayExpress database (www.ebi.ac.uk/arrayexpress) under the accession number E-MTAB-3487.

3.8 Kinase screening

The phosphorylation prediction algorithm *Kinase substrate predictor version 2.0 (KSPv2)* from KINEXUS Bioinformatics Corporation (Vancouver, Canada) identified the 50 best scored candidate kinases for L-plastin phosphorylation on residue Ser5, out of which 43 were subsequently screened by KINEXUS for their ability to phosphorylate L-plastin peptides in *in vitro* kinase assays. The following peptides corresponding to the L-plastin N-terminus and comprising residue Ser5 were chosen to be used in the kinase assays: ARG**S**V**S**DEERR (WT) and ARG**S**V**A**DEERR (MT), both starting with an N-acetylalanine (taking into account co-translational modifications described by the UniProtKB/Swiss-Prot database), as well as native MARG**S**V**S**DEERR (M-WT) and MARG**S**V**A**DEERR (M-MT), both still comprising the initial methionine residue. Residue Ser7 was substituted by an alanine in order to be able to distinguish between Ser5 and Ser7 phosphorylation and to exclude false positives. Two arginine residues were added at the C-terminal end of the peptides to ensure adhesion of the peptides to the capture phosphocellulose filter paper following the kinase assay, and were placed far enough from the Ser5 site so as not to affect the kinase recognition of this site. Briefly, L-plastin peptides were mixed with individual protein kinases in the presence of [γ-^{33}P] ATP for 20-40 min, depending on the protein kinase tested. The assay was terminated by spotting 10 µl of the reaction mixture onto a multiscreen phosphocellulose P81 plate. After removing unreacted [γ-^{33}P] ATP from the reaction, radioactivity was quantified in a scintillation counter.

3.9 In vitro kinase assays of full-length recombinant L-plastin

10 µg of full-length recombinant L-plastin were incubated with 50 µM of ATP and 100 ng of recombinant kinase (RSK1, RSK2, MSK1 or PKCδ) obtained from SignalChem (Richmond, British Columbia, Canada) in a reaction volume of 25 µl according to the manufacturer's protocol. For the controls the respective kinase was omitted. Following an incubation of 15 min at 30°C, Laemmli buffer was added, the samples were boiled at 100°C for 5 min and then analysed by immunoblotting.

3.10 In vitro kinase assay of recombinant glutathione S-transferase (GST)-tagged L-plastin-deltaABD2

64 µg of recombinant GST-L-plastin-deltaABD2 were incubated with 100 ng of recombinant PKCδ with or without 50 ng recombinant Src and 0.1 mM Na_3VO_4 and with 50 µM of ATP in a reaction volume of 25 µl according to the manufacturer's protocol. For the negative controls PKCδ was omitted. Samples were incubated for 15 min at 30°C. Laemmli buffer was added and the samples were boiled at 100°C for 5 min and analysed by immunoblotting. As a control for the immunoblotting procedure an MDA-MB-435S cell lysate was included.

3.11 Immunoblotting

Cells were lysed *in situ* in ice-cold lysis buffer (50 mM Tris-HCl pH 7.5, 150 mM NaCl, 0.1% SDS, 5 mM EDTA, 1% Nonidet P-40, 1% Triton X-100, 1% Na-deoxycholate, 1 mM Na_3VO_4, 10 mM NaF, 100 µM leupeptin, 100 µM E64D) containing a cocktail of protease inhibitors (Roche Diagnostics GmbH, Mannheim, Germany). Lysates were cleared by centrifugation at 13200 rpm for 15 min at 4°C. The total protein concentration was determined by Bradford assay (Bio-Rad, Temse, Belgium). Protein separation was performed by SDS-PAGE gel electrophoresis under reducing conditions and proteins were transferred onto nitrocellulose membranes by semi-dry transfer. The membranes were saturated with 1% bovine serum albumin (BSA) in Tris-buffered saline (TBS) pH 7.4 supplemented with 0.1% Tween for 1 h at RT, then incubated with primary antibodies overnight (except for the RSK2 antibody which was incubated over 4 nights) at 4°C and with secondary antibodies coupled to a fluorescent dye for 1 h at RT. Antibody incubations were followed by membrane washings with TBS supplemented with 0.1% Tween. Signal intensities were detected by the Odyssey® infrared image system (LI-COR, Westburg, Leusden, Netherlands). For quantification the ratio

between the intensities obtained for phosphorylated L-plastin (or phosphorylated PKA substrates) versus total L-plastin was determined to make individual samples comparable and then normalised to the mean of all the values obtained in one experiment to make blots comparable by accounting for technical day-to-day variability. For presentation purposes, data were scaled to the highest signal and are represented as means +/- standard deviation (SD). Statistical significance was determined by an unpaired T-test with Welch's correction. $P < 0.05$ was considered significant.

3.12 Two-dimensional (2-D) gel electrophoresis

BT-20 cells were treated with PMA, EGF or EGF + BI-D1870 and then lysed in a buffer containing 7 M urea, 2 M thiourea, 1% CHAPS detergent, 5 mg/ml dithiothreitol, 1 µg/ml pepstatin A, 1 mM Na_3VO_4, 10 mM NaF and protease inhibitor cocktail. Lysates were kept on ice for 30 min, sonicated and then centrifuged at 13000 rpm for 10 min at 4°C. Supernatants were collected and total protein concentrations were determined by Bradford assay (Bio-Rad). Lysates were prepared to contain 80 µg in 200 µl and 2 µl (1%) IPG buffer pH 4-7 (GE Healthcare, Little Chalfont, Buckinghamshire, UK) was added right before starting the first dimension. For isoelectric focusing, each sample was then loaded in a strip holder of a Multiphore electrophoresis system (GE Healthcare) and an 11 cm Immobiline DryStrip with a pH range from 4 to 7 (GE Healthcare) was placed on top of the sample with the gelside facing down. To prevent evaporation, a mineral oil solution (Immobiline DryStrip Cover Fluid, GE Healthcare) and a lid were added on top of the strip. The following programme was applied: 11 h of rehydration at 50 µA/strip, 1 h at 300 V, 3 h with a gradient from 300 to 6000 V, 9 h at 6000 V, 1 h at 8000 V. Following isoelectric focusing, the gelstrips were equilibrated for 15 min at RT in 10 ml of a solution containing 50 mM Tris-HCl pH 6.8, 6 M urea, 30% glycerol, 1% SDS, 10 mg/ml dithiothreitol, followed by another 15 min equilibration step at RT in a 10 ml solution containing 50 mM Tris-HCl pH 6.8, 6 M urea, 30% glycerol, 1% SDS and 0.45 g iodoacetamide. For the second dimension, protein separation according to the molecular weight was performed by SDS-PAGE placing the gelstrips on top of a stacking gel with the high pH side (negatively charged side) next to the molecular weight marker. Proteins were then transferred onto nitrocellulose membranes by wet transfer. The membranes were saturated with a 1:1 solution of PBS 1x and Odyssey® Blocking Buffer (LI-COR) for 1 h at RT, then incubated with an anti-L-plastin antibody overnight at 4°C and with a secondary antibody coupled to a fluorescent dye for 1 h at RT. Antibody incubations were followed by membrane washings with TBS supplemented with 0.1% Tween. Signal intensities were detected by the Odyssey® infrared image system (LI-COR). Subsequently the same

procedure was repeated on the same membranes with an anti Ser5-phosphorylated L-plastin antibody and a secondary antibody coupled to a different fluorescent dye.

3.13 Invasion and migration assays

Cancer cell lines were seeded in collagen I-coated (200 µg/ml) 96-well plates (Essen Imagelock, Essen Bioscience, Hertfordshire, UK). At appoximately 90% confluence, a wound was scratched across each well with the Cellplayer^{TM} 96-well woundmaker (Essen Bioscience). (For siRNA knockdown, cells were transfected with siRNA 24 h before wound scratching.) To study invasion, cells were covered with collagen I (1.5 mg/ml) diluted in cell culture medium. To study migration, only cell culture medium was added to the cells. Wound confluence was monitored with the IncuCyte LiveCell Imaging System (Essen Bioscience) by measuring cell confluence every 3 h for a total of 72 h. The IncuCyte software calculates a relative wound density for every time point, measuring the spatial cell density in the wound area relative to the spatial cell density outside of the wound area. It is designed to be 0 at t=0 and 100% when the cell density inside the wound is the same as the cell density outside the initial wound. The graphs depict means +/- standard error of the mean (SEM) from all technical replicates obtained from three independent experiments, each including at least five technical replicates.

3.14 Modelling

The literature-derived model topology of L-plastin signalling including the interactions between Src, PKC, PKA and the ERK/MAPK pathway were described as Boolean rules with corresponding selection probabilities in the probabilistic Boolean network (PBN) framework (see review in (Trairatphisan et al., 2013)). The experimental data obtained from immunoblot analysis of activation/inhibition studies for ratios of phosphorylated L-plastin versus total L-plastin (P-LPL/LPL) and phosphorylated PKA substrates versus total L-plastin (P-PKAsubstrates/LPL) from the four cell lines were used for model contextualisation. Normalisation of immunoblot data was performed as described above in the immunoblotting paragraph. Data generated from different experimental sets were normalised to the calibrator PMA, subsequently pooled and scaled to the maximal value. We applied an improved version of the optPBN toolbox (Trairatphisan et al., 2014) to optimise the selection probabilities of the L-plastin signalling model in PBN format. Optimisation was performed on a stand-alone machine (Intel CPU Xeon @3.50GHz, 16GB Ram) for the different model

variants based on random initial conditions. Bootstrapping was performed by randomly sampling 100 artificial datasets based on means and SD as acquired from our experimental datasets. Optimisation was subsequently performed 100 times to identify the distribution of the identified selection probabilities.

3.15 GFP-Trap

GFP-Trap is an immunoprecipitation technique based on monovalent Lama antibodies directed against GFP (Rothbauer et al., 2008). The antibody is fixed to beads allowing the purification of GFP fusion proteins and their interacting partner proteins. 24 h post-transfection for immunoblot analysis and 48 h post-transfection for mass spectrometry analysis, transfected cells were harvested on ice with a lysis buffer containing 10 mM Tris-HCl pH 7.5, 100 mM NaCl, 0.5 mM EDTA, 0.5% Nonidet P-40, 1 mM PMSF, complemented with protease inhibitor cocktail 7X (Roche Diagnostics GmbH). The cells were then incubated in the lysis buffer for 30 min on ice. After centrifugation at 20000 g at 4°C for 10 min, the supernatant was recovered and the protein concentration was determined by Bradford assay. 50 µl of the supernatant were diluted in 50 µl of Laemmli buffer and used as input. For every condition 30 µl of GFP-Trap beads (ChromoTek GmbH, Planegg-Martinsried, Germany) were used. In a first step, the beads were washed 3 times in 500 µl dilution buffer (10 mM Tris-HCL pH 7.5, 100 mM NaCl, 0.5 mM EDTA, 1 mM PMSF, complemented with protease inhibitor cocktail 7X), followed by a centrifugation at 2700 g at 4°C for 5 min. The cell extracts were incubated with the beads for 2 h, followed by a centrifugation at 2700 g at 4°C for 5 min. 50 µl of the supernatant were diluted in 50 µl of Laemmli buffer and were used as non-bound samples. The beads were washed 2 times with 500 µl dilution buffer followed by a centrifugation at 2700 g and 4°C for 5 min. For immunoblot analysis, the beads were then resuspended in 100 µl Laemmli buffer and boiled at 100°C for 10 min for elution, followed by a centrifugation at 2700 g for 5 min. The supernatant was recovered and considered as bound fraction. For mass spectrometry, the samples were loaded to an affinity column and eluted with 4% formic acid.

3.16 Mass spectrometry

Sample preparation

Stable isotope labelling by amino acids in cell culture (SILAC) of HEK cells was performed in SILAC DMEM medium supplemented with 10% dialysed fetal bovine serum, 2 mM of L-glutamine, 50 units/ml of penicillin and streptomycin, 146 mg/l lysine (C^{12} or C^{13}) and 16.8

mg/l arginine (C^{12} or C^{13}). Cultured cells were transfected with constructs of interest, lysed and subjected to GFP-Trap.

Liquid chromatography-tandem mass spectrometry (LC-MS/MS) analysis

Following GFP-Trap, protein complexes were eluted from the affinity column using 4% formic acid. These protein samples were vacuum-dried and re-dissolved in 100 µl 50 mM triethylammonium bicarbonate pH 8.0. Digestion occurred overnight at 37°C using sequencing-grade porcine trypsin (Promega, Leiden, Netherlands). The resulting peptide mixtures were acidified with 10% trifluoroacetic acid for subsequent LC-MS/MS analysis. Of each sample, 2.5 µl were first analysed on the LTQ-Orbitrap Velos (Thermo Scientific) in LC-MS/MS mode (operated as described in (De Antonellis et al., 2014)) to determine the quantity of the material present in the sample. For final analysis, 5 µl of each sample were subjected to LC-MS/MS analysis using a Q Exactive mass spectrometer (Thermo Scientific) that was operated as previously described (Stes et al., 2014). Data were converted to Mascot generic format files using Mascot Distiller (Matrix Science, London, United Kingdom) and, using the Mascot database search engine (Matrix Science), these were presented to the Swiss-Prot database restricted to human proteins. Peptide-to-spectrum matches were allowed with confidence settings of 99% and were withheld only if ranked first and if scores were above the corresponding threshold.

Chapter 4 Results

Parts of the discussion section are taken from a manuscript which can be found in the appendix and which was recently published in The FASEB Journal: *L-plastin Ser5 phosphorylation in breast cancer cells and in vitro is mediated by RSK downstream of the ERK/MAPK pathway* (Lommel et al., 2015).

4.1 Characterisation of four breast cancer cell lines

The four breast cancer cell lines MCF7, SK-BR-3, BT-20 and MDA-MB-435S chosen as a working model for this study were carefully selected in order to cover different molecular profiles (Kao et al., 2009; Kenny et al., 2007; Subik et al., 2010) with the main prerequisite being the expression of our protein of interest L-plastin. Figure 4.1 shows that L-plastin is present in all four cell lines at different expression levels.

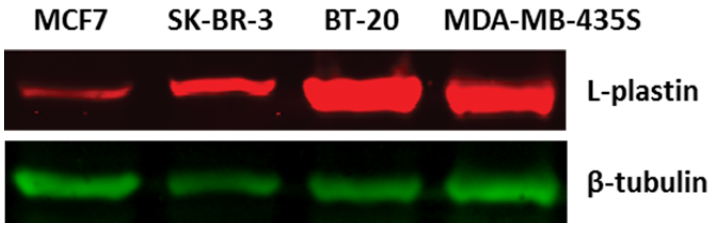

Figure 4.1 Protein level of L-plastin in four breast cancer cell lines. Cell extracts were subjected to immunoblot analysis using antibodies specific for L-plastin and β-tubulin as a loading control.

4.1.1 Epithelial and mesenchymal signature

For the characterisation of our cell lines, we investigated the morphology as well as typical epithelial and mesenchymal markers. Invasive cell lines usually have a more mesenchymal phenotype whereas non-invasive cell lines are more epithelial. Figure 4.1.1.1 shows phase contrast images of breast cancer cells and indicates an epithelial phenotype for MCF7 and SK-BR-3 for which cells adhere to each other and do not show an elongated, fibroblast-like phenotype whereas for MDA-MB-435S cells a clear mesenchymal phenotype with a fibroblast-like morphology is observed. BT-20 cells display an intermediate phenotype.

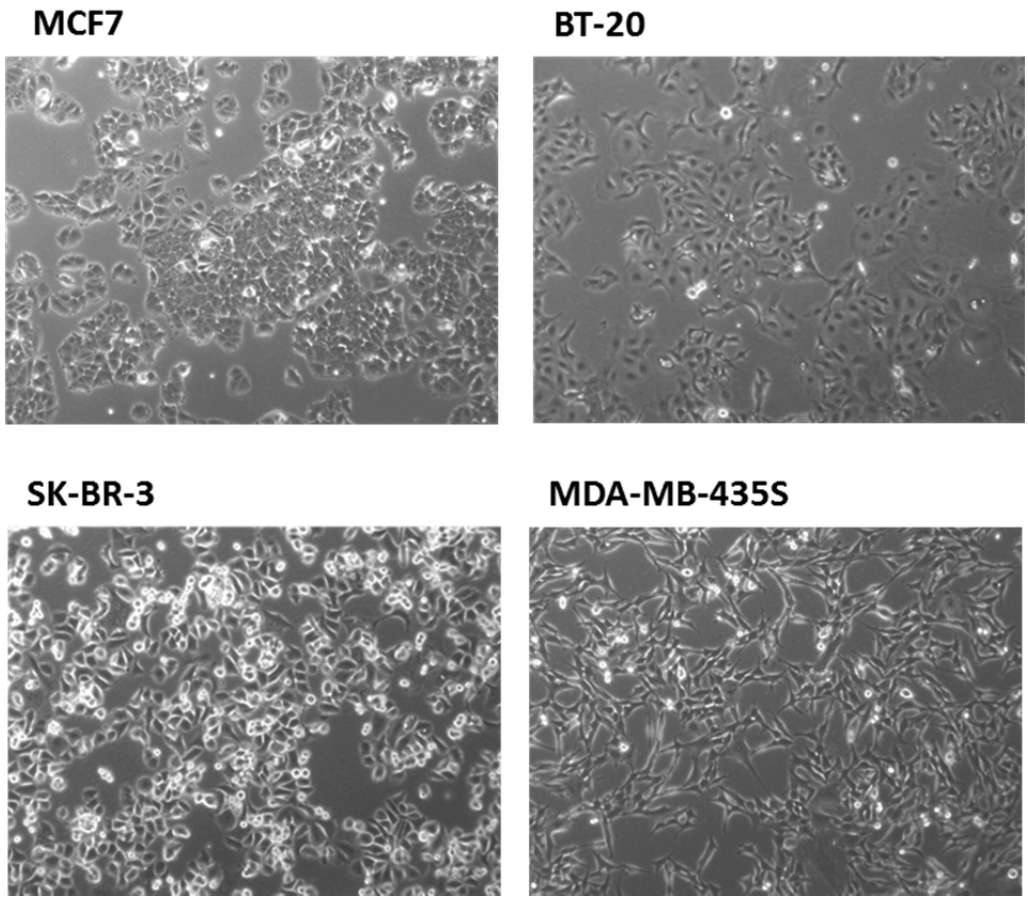

Figure 4.1.1.1 Epithelial and mesenchymal phenotypes of breast cancer cell lines. Phase contrast images were taken with a Leica phase contrast microscope with a 10x objective.

The expression of epithelial and mesenchymal markers in the four cell lines was assessed by immunoblot analysis (Figure 4.1.1.2) as well as by immunofluorescent staining (Figures 4.1.1.3-7) and the results are summarised in Table 4.1.1. Notably we analysed the expression of two mesenchymal markers, N-cadherin, a transmembrane protein that is found in adherens junctions, and vimentin, a type III intermediate filament protein, and of three epithelial markers, E-cadherin, a transmembrane protein found in adherens junctions, cytokeratin-18, an intermediate filament protein and claudin-3, a tight junction protein.

Immunoblot as well as immunofluorescence assays show that both mesenchymal markers are present in the most invasive cell line MDA-MB-435S. Immunoblot analysis shows that the epithelial marker E-cadherin is expressed in MCF7 and BT-20 and immunofluorescent staining shows its localisation in cell membranes as expected. Staining for E-cadherin is also weakly observed in dot-like structures for some SK-BR-3 cells and extremely rarely in MDA-MB-435S cells. However the dot-like staining in these cells does not correspond to the expected localisation of this transmembrane protein. Both analyses also reveal that the epithelial marker cytokeratin-18 is expressed in MCF7, SK-BR-3 and BT-20 and not in MDA-

MB-435S cells. Immunoblot analysis shows similar levels of cytokeratin-18 for the three cell lines whereas immunofluorescence shows a strong staining in MCF7 and BT-20 and a weaker staining in SK-BR-3. Both analyses show strong expression of the epithelial marker claudin-3 in MCF7.

Overall the expression of epithelial markers roughly corresponds to the invasive capacity of the cells. According to the expression of epithelial and mesenchymal markers, MDA-MB-435S is the most mesenchymal of the four cell lines as it is positive for all tested mesenchymal markers and negative for all epithelial markers. MCF7 presents the most pronounced epithelial phenotype as it is positive for all tested epithelial markers and negative for all mesenchymal markers. SK-BR-3 and BT-20 do not express mesenchymal markers but they are also not positive for all epithelial markers and they thus have an intermediate phenotype.

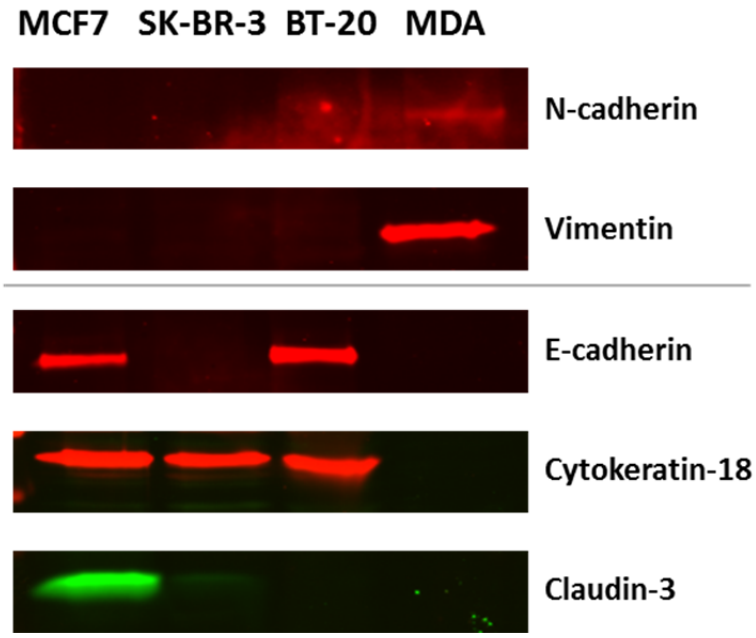

Figure 4.1.1.2 Protein level of epithelial and mesenchymal markers of breast cancer cell lines. Cell extracts were subjected to immunoblot analysis using antibodies specific for N-cadherin, vimentin, E-cadherin, cytokeratin-18 and claudin-3. Loading controls were used for all membranes to confirm loading of equal protein amounts. (MDA refers to MDA-MB-435S).

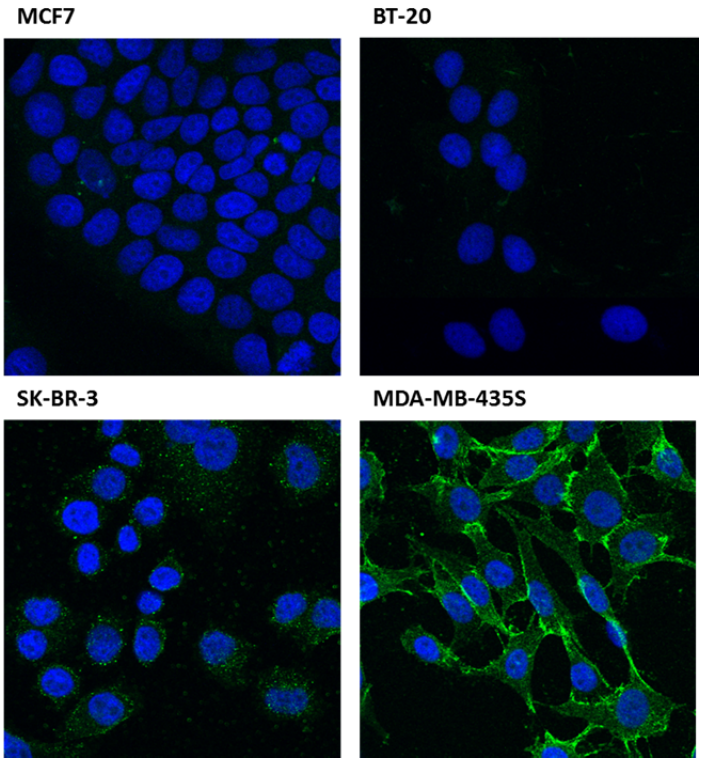

Figure 4.1.1.3 N-cadherin expression and localisation in breast cancer cell lines. Breast cancer cells were fixed and processed for immunofluorescence. Cells were stained using DAPI (in blue) and an antibody against N-cadherin (in green) and analysed with a laser scanning confocal microscope.

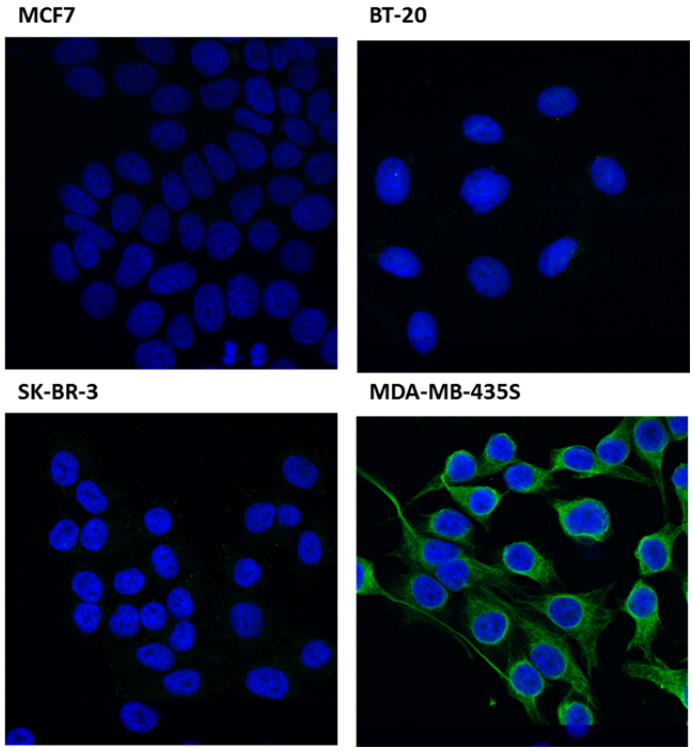

Figure 4.1.1.4 Vimentin expression and localisation in breast cancer cell lines. Breast cancer cells were fixed and processed for immunofluorescence. Cells were stained using DAPI (in blue) and an antibody against vimentin (in green) and analysed with a laser scanning confocal microscope.

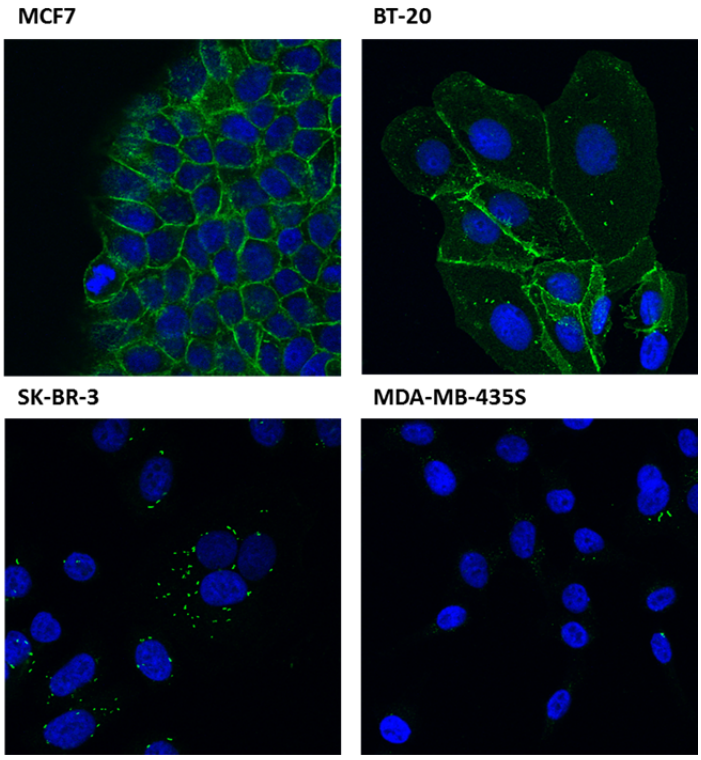

Figure 4.1.1.5 E-cadherin expression and localisation in breast cancer cell lines. Breast cancer cells were fixed and processed for immunofluorescence. Cells were stained using DAPI (in blue) and an antibody against E-cadherin (in green) and analysed with a laser scanning confocal microscope.

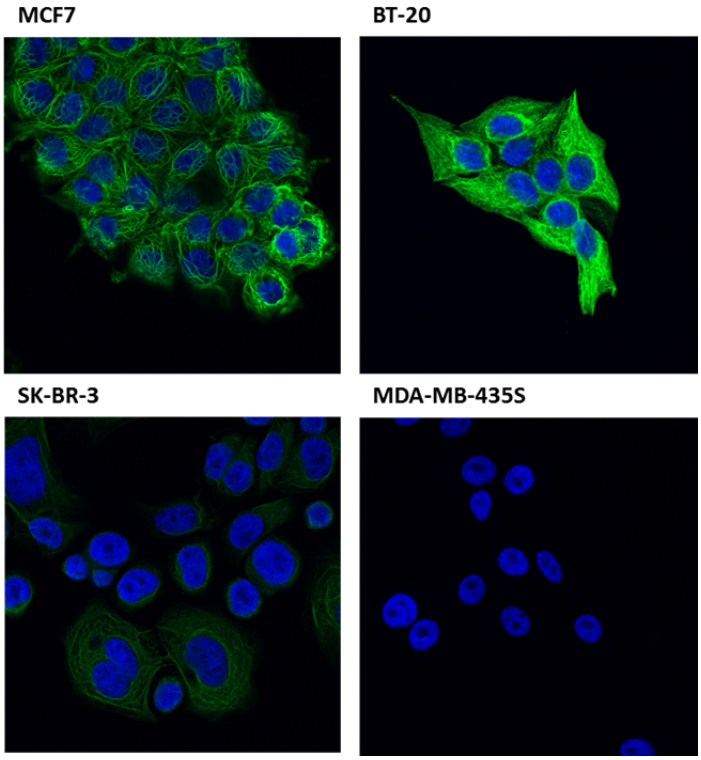

Figure 4.1.1.6 Cytokeratin-18 expression and localisation in breast cancer cell lines. Breast cancer cells were fixed and processed for immunofluorescence. Cells were stained using DAPI (in blue) and an antibody against cytokeratin-18 (in green) and analysed with a laser scanning confocal microscope.

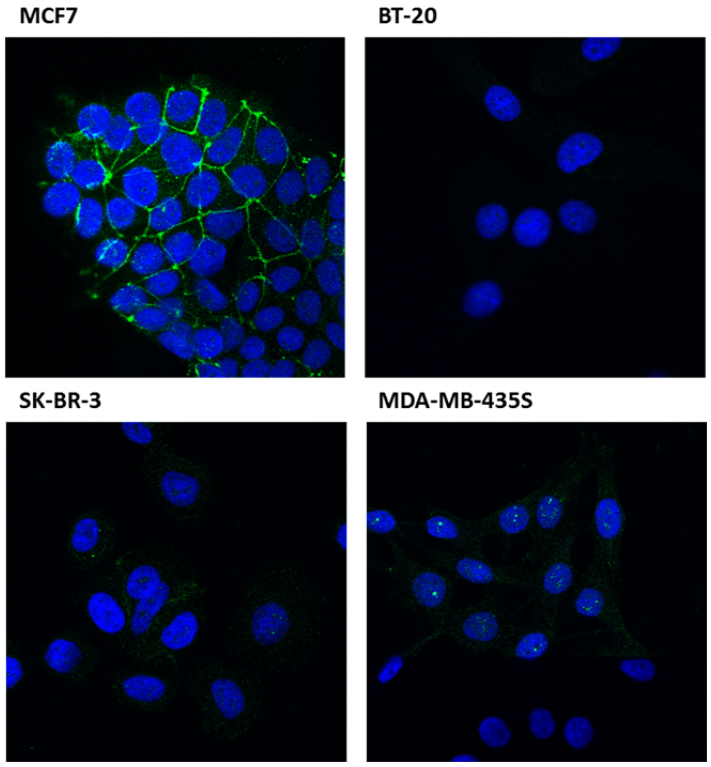

Figure 4.1.1.7 Claudin-3 expression and localisation in breast cancer cell lines. Breast cancer cells were fixed and processed for immunofluorescence. Cells were stained using DAPI (in blue) and an antibody against claudin-3 (in green) and analysed with a laser scanning confocal microscope.

	N-cadherin		Vimentin		E-cadherin		Cytokeratin-18		Claudin-3	
	WB	IF	WB	IF	WB	IF	WB	IF	WB	IF
MCF7	/	/	/	/	MCF7	MCF7	MCF7	MCF7	MCF7	MCF7
SKBR3	/	/	/	/	/	SKBR3 in dot-like structures	SKBR3	SKBR3 faint	SKBR3 faint	/
BT20	/	/	/	/	BT20	BT20	BT20	BT20	/	/
MDAMB435S	MDA faint	MDA	MDA	MDA	/	MDA rarely in dot-like structures	/	/	/	/

Table 4.1.1 Combined western blotting and immunofluorescence results on the presence of epithelial and mesenchymal markers in the four breast cancer cell lines.

4.1.2 Epidermal growth factor receptor (EGFR)

As the EGFR plays key roles in normal mammary gland physiology as well as in breast cancer (Eccles, 2011), we tested the presence of the EGFR in the four breast cancer cell lines by immunoblot analysis. As previously decribed by others (Subik et al., 2010), both SK-BR-3 and BT-20 cells expressed high levels of EGFR, whereas in MCF7 and MDA-MB-435S cells the expression was very low or absent (Figure 4.1.2).

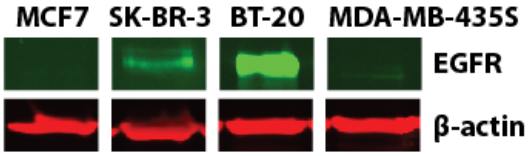

Figure 4.1.2. EGFR is expressed in SK-BR-3 and BT-20 breast cancer cells. Cell extracts were analysed by immunoblotting using antibodies specific for the EGFR and β-actin as a loading control. Adapted from (Lommel et al., 2015).

4.1.3 Migration and invasion capacities

The migration and invasion capacities of our four breast cancer cell lines were assessed by performing *in vitro* scratch wound assays. MDA-MB-435S had the highest migration capacity, relatively tightly followed by MCF7 and BT-20 whereas SK-BR-3 had a remarkably lower migration capacity (Figure 4.1.3.1).

MCF7 and SK-BR-3 cells are only weakly invasive whereas invasiveness was considerably more important in BT-20 and most prominent in MDA-MB-435S cells (Figure 4.1.3.2). These results are in line with the literature, MCF7 and SK-BR-3 being considered as non- or merely weakly invasive cell lines in contrast to BT-20 and MDA-MB-435S which have been described as invasive cell lines (Lacroix and Leclercq, 2004; Zajchowski et al., 2001).

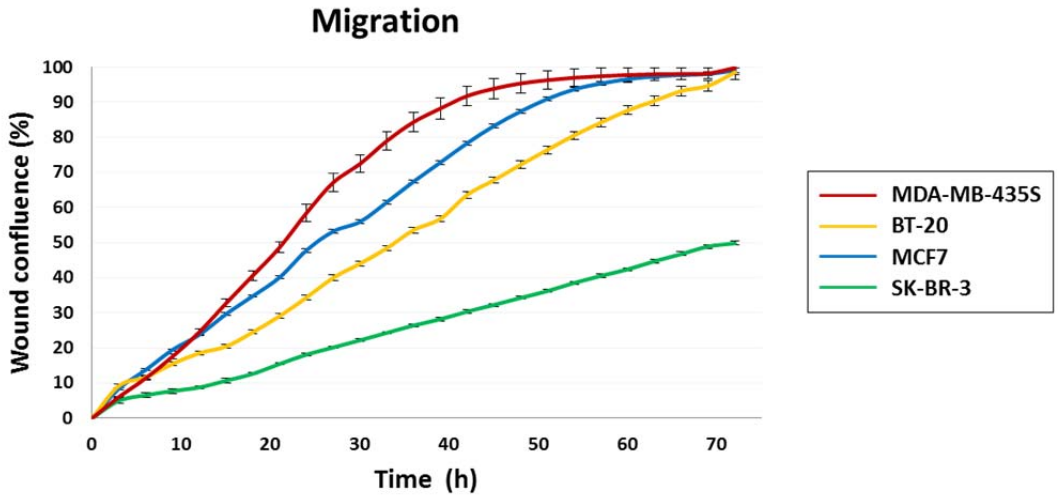

Figure 4.1.3.1 Migration assays for the four model breast cancer cell lines. Cells were seeded in collagen I-coated (200 µg/ml) 96-well plates. At appoximately 90% confluence, a wound was scratched across each well with the Cellplayer 96-well woundmaker. Cells were covered with cell culture medium and wound confluence was monitored with the IncuCyte LiveCell Imaging System by measuring cell confluence every 3 h over a total period of 72 h. The graph depicts means +/- SEM from all technical replicates obtained from three independent experiments.

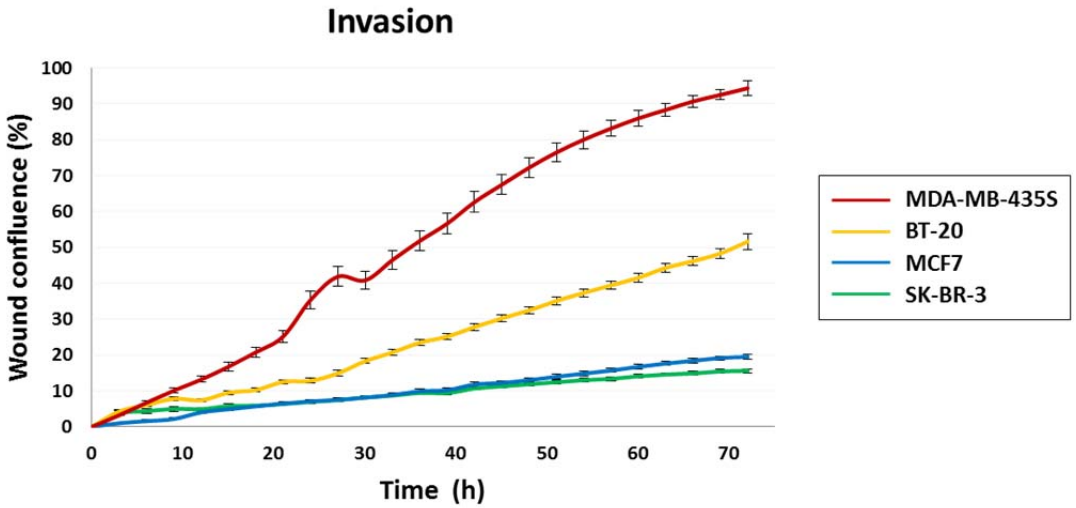

Figure 4.1.3.2 Invasion assays for the four model breast cancer cell lines. Cells were seeded in collagen I-coated (200 µg/ml) 96-well plates. At appoximately 90% confluence, a wound was scratched across each well with the Cellplayer 96-well woundmaker. Cells were covered with collagen I (1.5 mg/ml) diluted in cell culture medium. Wound confluence was monitored with the IncuCyte LiveCell Imaging System by measuring cell confluence every 3 h over a total period of 72 h. The graph depicts means +/- SEM from all technical replicates obtained from three independent experiments. Adapted from (Lommel et al., 2015).

4.1.4 L-plastin Ser5 phosphorylation levels

Since a correlation between the invasive capacity of cells and the phosphorylation state of L-plastin on Ser5 has been suggested before (Janji et al., 2006; Klemke et al., 2007; Riplinger et al., 2014), we continued by investigating baseline L-plastin Ser5 phosphorylation in the four breast cancer cell lines. To this end, we used an antibody specifically recognising Ser5-phosphorylated L-plastin (anti-Ser5-*P* antibody) raised and characterised by our group (Al Tanoury et al., 2010; Janji et al., 2006; Janji et al., 2010). Although the L-plastin expression level is higher in the invasive as compared to the non-invasive cell lines, our results clearly show high baseline L-plastin Ser5 phosphorylation in the invasive cell lines BT-20 and MDA-MB-435S as compared to absent or extremely weak phosphorylation in the non-invasive cell lines MCF7 and SK-BR-3 (Figure 4.1.4).

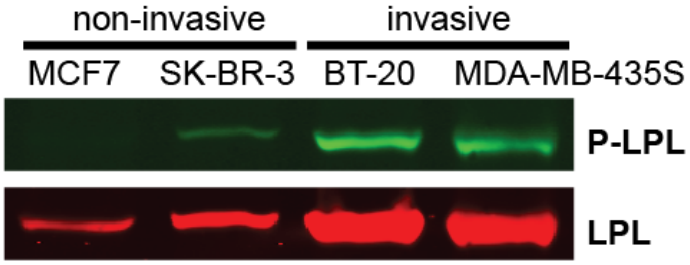

Figure 4.1.4 High baseline L-plastin Ser5 phosphorylation in highly invasive versus low baseline L-plastin Ser5 phosphorylation in non- or weakly invasive breast cancer cell lines. Cell extracts were analysed by immunoblotting using antibodies specific for Ser5 phosphorylated L-plastin (anti-Ser5-*P* antibody, P-LPL) and total L-plastin (LPL). Adapted from (Lommel et al., 2015).

4.1.5 Arguments in favour of a breast cancer origin of MDA-MB-435S

It is noteworthy that considerable doubt had been raised about the origin of the cell clone MDA-MB-435S (Ross et al., 2000). Concerning the issue of the identity of MDA-MB-435S, the scientific community appears to agree that MDA-MB-435S and the M14 melanoma cell line are essentially identical with respect to cytogenetic characteristics and gene expression as confirmed by microsatellite analyses (Hollestelle et al., 2010; Rae et al., 2007). Nevertheless there is no agreement whether both cell lines should be classified as breast (Chambers, 2009; Hollestelle and Schutte, 2009; Sellappan et al., 2004) or melanoma (Ellison et al., 2002; Rae et al., 2007) cancer cell lines. *Cell Lines Service GmbH* sells MDA-MB-435S as breast cancer cell line (http://www.clsgmbh.de/p513_MDA-MB-435S.html) whereas *American Type Culture Collection* (ATCC) sells it as melanoma cell line

(http://www.lgcstandards-atcc.org/Products/All/HTB-129.aspx#characteristics) refering to publications from 2000 to 2007. They thus ignored the more recent publication from Chambers (Chambers, 2009) pointing to the fact that MDA-MB-435S and M14 cells currently in circulation have female karyotypes whereas M14 was originally derived from a male patient which implies that current cultures of both cell lines are more likely to be derived from MDA-MB-435S.

Another important publication favoring the breast origin of MDA-MB-435S shows that these cells express breast and epithelial-specific markers and that these cells can be induced to express breast differentiation-specific proteins and secrete milk lipids, as observed in other well-established breast cancer cell lines (Sellappan et al., 2004). They also detected some melanocyte-specific proteins in MDA-MB-435S but these were also expressed at lower levels in BT-474, another breast cancer cell line. Overall they concluded that MDA-MB-435S is most likely a breast epithelial cell line which has undergone lineage infidelity.

Be that as it may, the experiments performed in this study were conducted in four cancer cell lines including MDA-MB-435S and three other cell lines being undoubtedly of breast origin.

4.2 Signal transduction cascade leading to L-plastin Ser5 phosphorylation

As the detailed signalling cascade leading to L-plastin Ser5 phosphorylation remains elusive, we decided to investigate the pathways upstream of L-plastin Ser5 phosphorylation.

4.2.1 Analysis of protein kinases previously described to play a role in L-plastin Ser5 phosphorylation

As stated in the introduction (under 1.2.3 L-plastin phosphorylation), mainly PKC and PKA have been described to play a role in L-plastin Ser5 phosphorylation. Most of these studies have been performed in cells of the immune system where L-plastin is typically expressed. Only two studies investigated L-plastin phosphorylation in cancer cells and showed that siRNA-mediated knockdown of PKCδ reduced L-plastin Ser5 phosphorylation in MCF7 cells (Al Tanoury et al., 2010) and in the MCF7-derived invasive 1001 cells (Janji et al., 2010).

We thus started by investigating the involvement of PKC in L-plastin Ser5 phosphorylation in all our model breast cancer cell lines. Indeed the activation of PKC by PMA led to a significant increase in L-plastin Ser5 phosphorylation in all tested cell lines regardless of their baseline phosphorylation level (Figure 4.2.1.1).

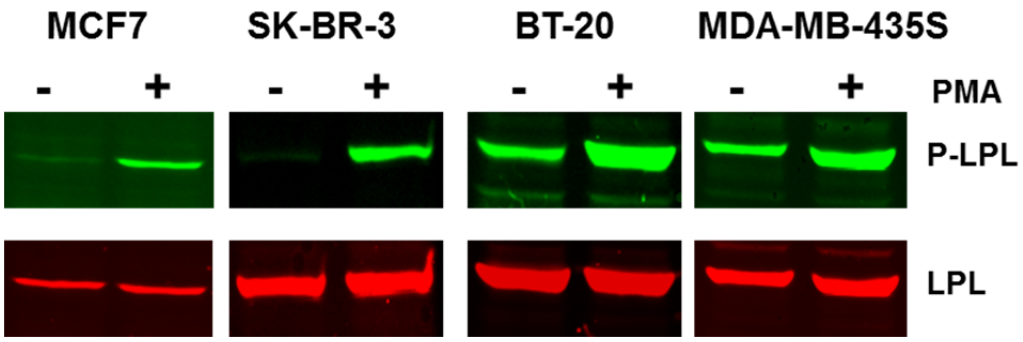

Figure 4.2.1.1 PKC activation increases L-plastin Ser5 phosphorylation in the four breast cancer cell lines. Cells were treated with PMA 0.1 µM for 1 h and cell extracts were analysed by immunoblotting using antibodies specific for Ser5 phosphorylated L-plastin (anti-Ser5-P antibody, P-LPL) and total L-plastin (LPL).

As it was suggested that it is the PKCδ isoform that is responsible for L-plastin Ser5 phosphorylation in MCF7 and 1001 cells, we investigated whether this isoform was also involved in L-plastin Ser5 phosphorylation in SK-BR-3, BT-20 and MDA-MB-435S cells. To this end we proceeded to PKCδ knockdown which resulted in efficiently decreased levels for

all cell lines. We observed a significant decrease in L-plastin Ser5 phosphorylation in MDA-MB-435S cells, a small decrease in BT20 and no decrease in SK-BR-3 cells (Figure 4.2.1.2). The involvement of PKCδ in L-plastin Ser5 phosphorylation appeared thus to be cell type-dependent.

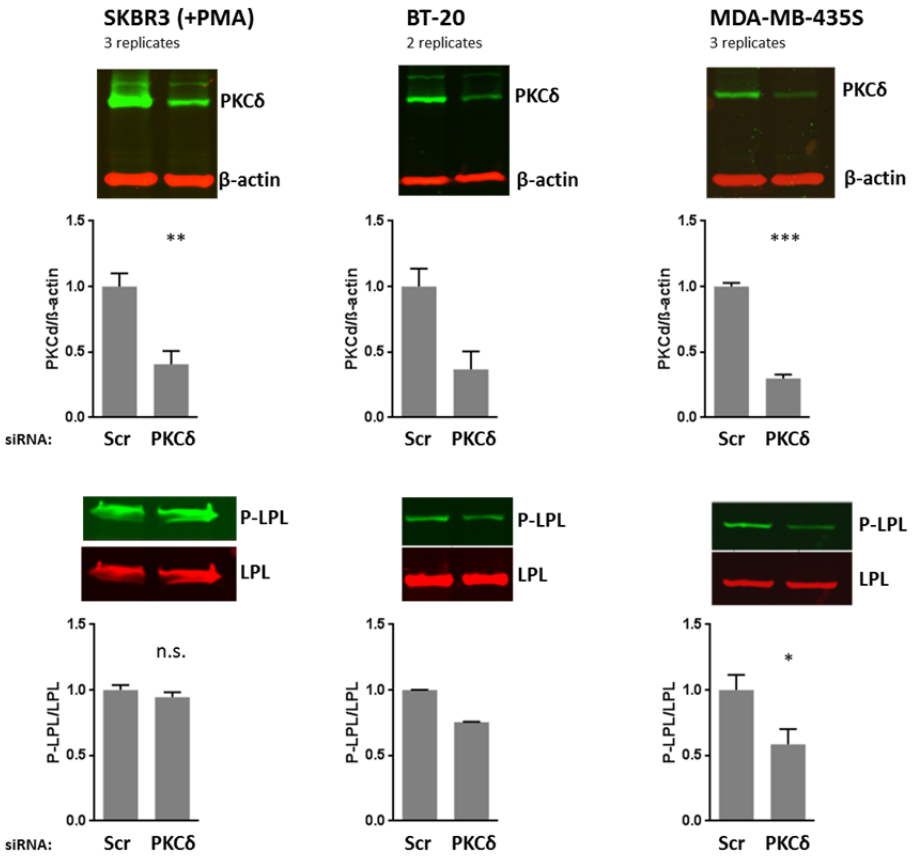

Figure 4.2.1.2 Effect of PKCδ knockdown on L-plastin Ser5 phosphorylation in breast cancer cells. siRNA against PKCδ was transfected in SK-BR-3, BT-20 and MDA-MB-345S cells and L-plastin Ser5 phosphorylation and PKCδ levels were assessed by immunoblot analysis 48 h post transfection. SK-BR-3 cells were treated with PMA 1 h before cell lysis. For quantification the ratio between the intensities obtained for phosphorylated L-plastin (P-LPL) versus total L-plastin (LPL) and for PKCδ versus β-actin respectively were determined to make individual samples comparable and then normalised to the mean of all the values obtained in one experiment to make blots comparable by accounting for technical day-to-day variability. For presentation purposes, data were scaled to the highest signal and are represented as means +/- standard deviations (SD). For experiments with at least 3 replicates, statistical significance was determined by an unpaired T-test with Welch's correction. *P<0.05, **P<0.01, ***P<0.001 and n.s. – non-significant. (Scr refers to scrambled)

In parallel to the PKCδ knockdown experiments, we cloned a wild type construct of PKCδ as well as dominant negative and constitutively active PKCδ into a pEGFP-C3 vector. Dominant negative PKCδ contains a lysine to arginine mutation at amino acid position 378 in the C-terminal ATP binding site which impairs ATP binding (Soh et al., 1999). Constitutively

active PKCδ contains two arginine to alanine mutations at amino acid positions 144 and 145 in the pseudosubstrate domain of the regulatory domain of PKCδ (Ueda et al., 1996). The three constructs were transfected into MCF7 and MDA-MB-435S cells using lipofectamine transfection. None of these transfections had an effect on L-plastin Ser5 phosphorylation (data not shown). As the transfection efficiency in these cells was low, the same experiment was performed in human embryonic kidney 293 (HEK) cells where a transfection efficiency of about 95% was reached using calcium-phosphate transfection. We observed that constitutively active PKCδ increases L-plastin Ser5 phosphorylation (Figure 4.2.1.3). This confirms previously obtained data showing a role for PKCδ in the signalling pathway leading to L-plastin Ser5 phosphorylation (Al Tanoury et al., 2010; Freeley et al., 2012; Janji et al., 2010; Jones et al., 1998; Lin et al., 1998; Paclet et al., 2004; Pazdrak et al., 2011).

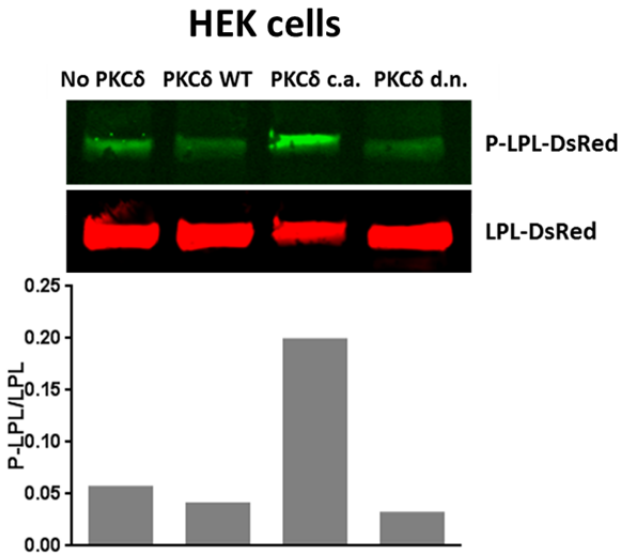

Figure 4.2.1.3 Constitutively active PKCδ increases L-plastin Ser5 phosphorylation in HEK cells. HEK cells were transfected with L-plastinWT-DsRed and with a pEGFP-C3 vector containing the indicated PKCδ variant. Cell lysates were analysed by immunoblotting using antibodies specific for Ser5 phosphorylated L-plastin and L-plastin.

In cells, PKC can be activated in response to physiological stimuli inducing inositol phospholipid hydrolysis such as endothelin-1 (Griendling et al., 1989). Endothelin-1, a peptide derived from endothelial cells, is a constrictor of vascular smooth muscle. We tested whether this PKC activator had an effect on L-plastin Ser5 phosphorylation in our four breast cancer cell lines and in HEK cells. No effect was observed in the four breast cancer cell lines whereas in HEK cells endothelin-1 led to a significant increase in L-plastin Ser5 phosphorylation (Figure 4.2.1.4).

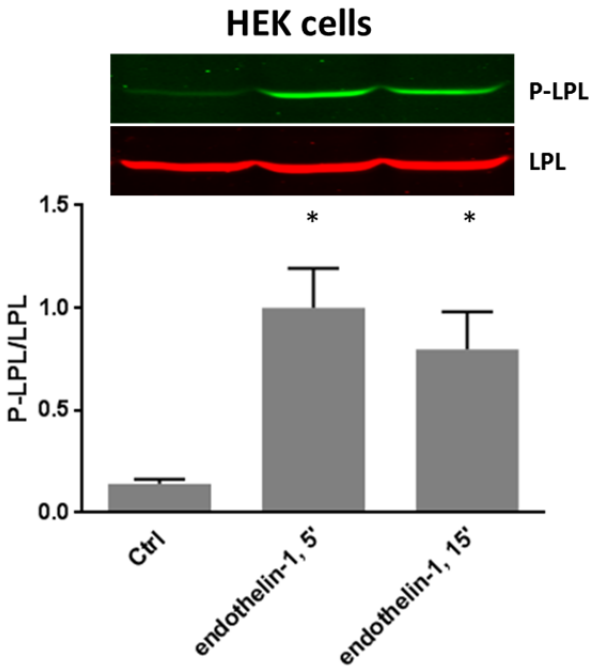

Figure 4.2.1.4. Endothelin-1 increases L-plastin Ser5 phosphorylation in HEK cells. HEK cells were treated with 100 nM of endothelin-1 for 5 or 15 min. Quantification was performed as described in Figure 4.2.1.2. Data are represented as means +/- SD. Statistical significance was determined by an unpaired T-test with Welch's correction. *P<0.05, **P<0.01 and ***P<0.001.

In order to get a more complete overview of L-plastin Ser5 phosphorylation by PKC and PKA, we treated our four model breast cancer cell lines with PKC and PKA activators and inhibitors as well as with combinations of activators and inhibitors. PMA was used for PKC activation, GF109203X (GF) for PKC inhibition, 8-Bromo-cAMP (8Br) for PKA activation and H89 for PKA inhibition. After treatment, the cells were lysed and the samples were loaded on SDS-PAGE and blotted against phosphorylated L-plastin (P-LPL) and L-plastin (LPL) or phosphorylated PKA substrates (P-PKAsubstrates) and L-plastin respectively (Figures 4.2.1.5-8).

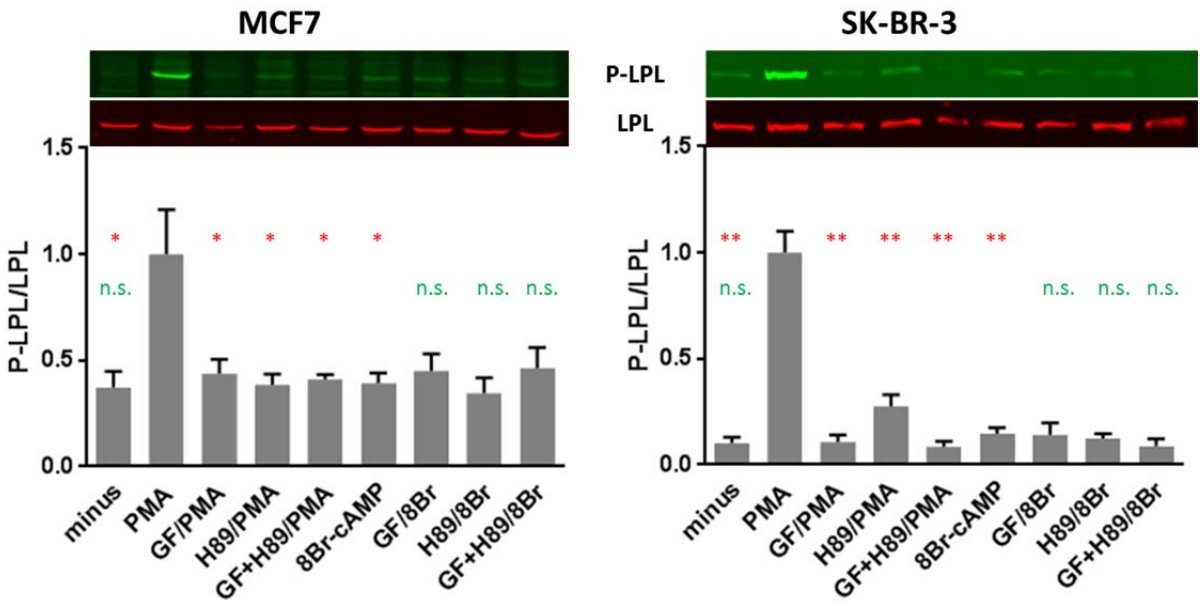

Figure 4.2.1.5. Effect of PKC or PKA activation with or without prior inhibition on L-plastin Ser5 phosphorylation in non-invasive cell lines. Cells were treated with the indicated inhibitors and/or activators before being lysed and analysed by immunoblotting. Quantification was performed as described in Figure 4.2.1.2. Data are represented as means +/- SD. Statistical significance was determined by an unpaired T-test with Welch's correction. *P<0.05, **P<0.01, ***P<0.001 and n.s. – non-significant with comparisons to PMA in red and to 8Br-cAMP in green.

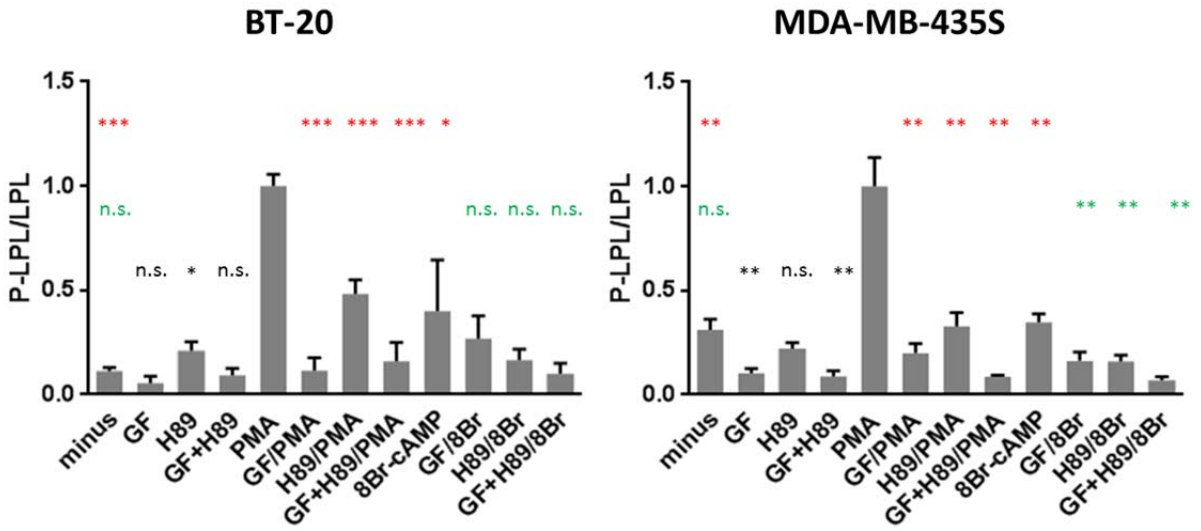

Figure 4.2.1.6 Effect of PKC or PKA activation with or without prior inhibition on L-plastin Ser5 phosphorylation in invasive cell lines. Cells were treated with the indicated inhibitors and/or activators before being lysed and analysed by immunoblotting. Quantification was performed as described in Figure 4.2.1.2. Data are represented as means +/- SD. Statistical significance was determined by an unpaired T-test with Welch's correction. *P<0.05, **P<0.01, ***P<0.001 and n.s. – non-significant with comparisons to PMA in red, to 8Br-cAMP in green and to minus in black.

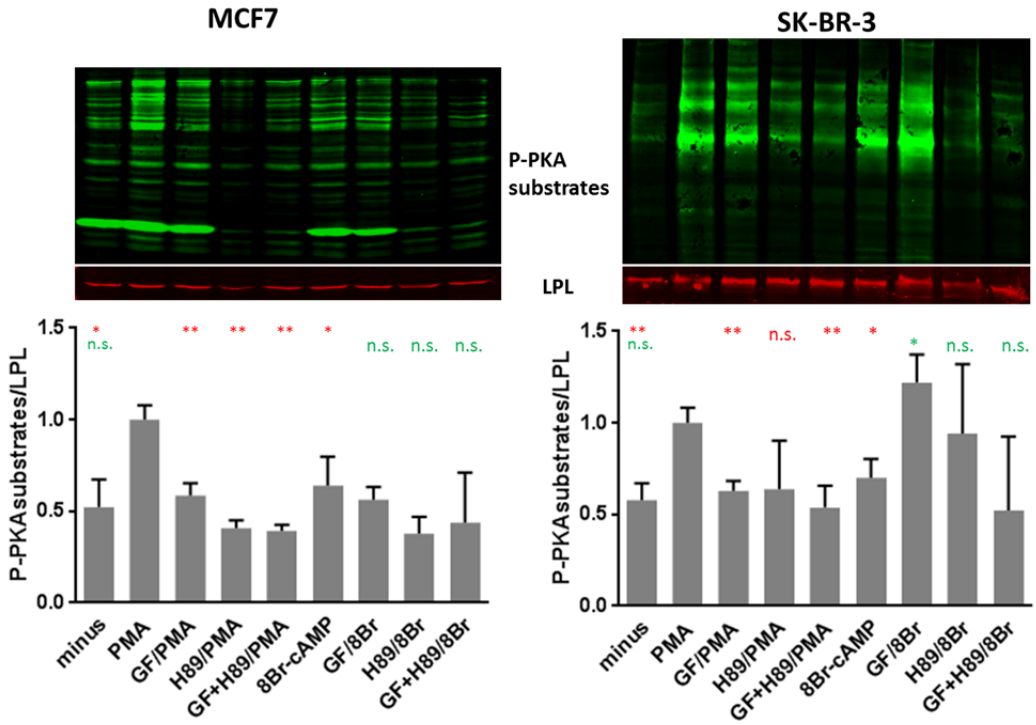

Figure 4.2.1.7 Effect of PKC or PKA activation with or without prior inhibition on PKA substrate phosphorylation in non-invasive cell lines. Cells were treated with the indicated inhibitors and/or activators before being lysed and analysed by immunoblotting. Quantification was performed as described in Figure 4.2.1.2. Data are represented as means +/- SD. Statistical significance was determined by an unpaired T-test with Welch's correction. *P<0.05, **P<0.01, ***P<0.001 and n.s. – non-significant with comparisons to PMA in red and to 8Br-cAMP in green.

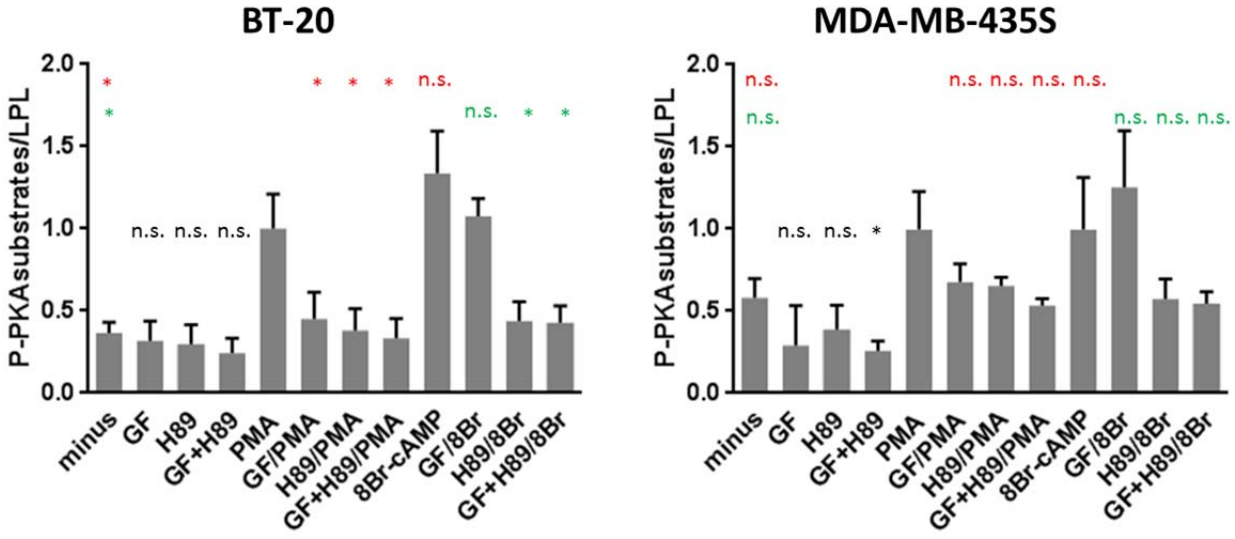

Figure 4.2.1.8 Effect of PKC or PKA activation with or without prior inhibition on PKA substrate phosphorylation in invasive cell lines. Cells were treated with the indicated inhibitors and/or activators before being lysed and analysed by immunoblotting. Quantification was performed as described in Figure 4.2.1.2. Data are represented as means +/- SD. Statistical significance was determined by an unpaired T-test with Welch's correction. *P<0.05, **P<0.01, ***P<0.001 and n.s. – non-significant with comparisons to PMA in red, to 8Br-cAMP in green and to minus in black.

In contrast to PKC activation, PKA activation with 8-Bromo-cAMP had no significant effect on L-plastin Ser5 phosphorylation in MCF7, SK-BR-3, BT-20 and MDA-MB-435S cells (Figures 4.2.1.5 and 4.2.1.6). Looking at the phosphorylation of PKA substrates, an increase is observed as expected in all cell lines for treatment with the PKA activator 8-Bromo-cAMP (Figures 4.2.1.7 and 4.2.1.8). Strikingly, the phosphorylation of PKA substrates was also increased with the treatment of the PKC activator PMA (Figures 4.2.1.7 and 4.2.1.8). This could be an indication that PKC is an upstream activator of PKA.

In order to be able to draw more conclusions from this relatively large dataset, the data represented in figures 4.2.1.5-8 were analysed (together with data from the following sections) by a systems biology approach using computational modelling detailed under 4.2.5.

Preliminary experiments performed by the former group member Ziad Al Tanoury (Al Tanoury, 2009) and by myself suggest that L-plastin interacts with the proto-oncogene tyrosine-protein kinase Src (see under 4.4.1). In this regard we investigated whether Src might be indirectly involved in L-plastin Ser5 phosphorylation. Indeed the inhibition of Src by three different inhibitors led to a considerable decrease in L-plastin Ser5 phosphorylation in all cell lines except MCF7 (Figures 4.2.1.9 and 4.2.1.10).

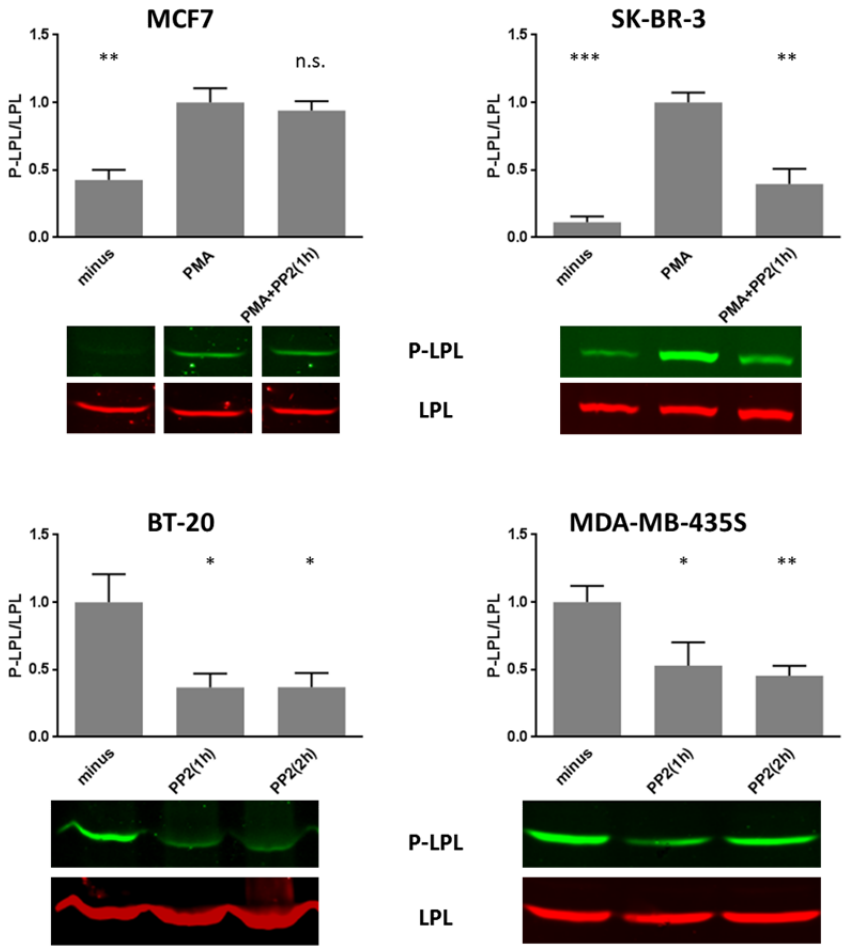

Figure 4.2.1.9 The Src inhibitor PP2 decreases L-plastin Ser5 phosphorylation in SK-BR-3, BT-20 and MDA-MB-435S cells. Cells were treated with the Src inhibitor PP2 with or without subsequent PMA stimulation. L-plastin Ser5 phosphorylation was determined by immunoblot analysis. Quantification was performed as described in Figure 4.2.1.2. Data are represented as means +/- SD. Statistical significance was determined by an unpaired T-test with Welch's correction. P<0.05 was considered significant. *P<0.05, **P<0.01, ***P<0.001 and n.s. – non-significant. For each immunoblot shown, samples were run on the same gel, but for the MCF7 blot bands were cut and put in another order for presentation purposes.

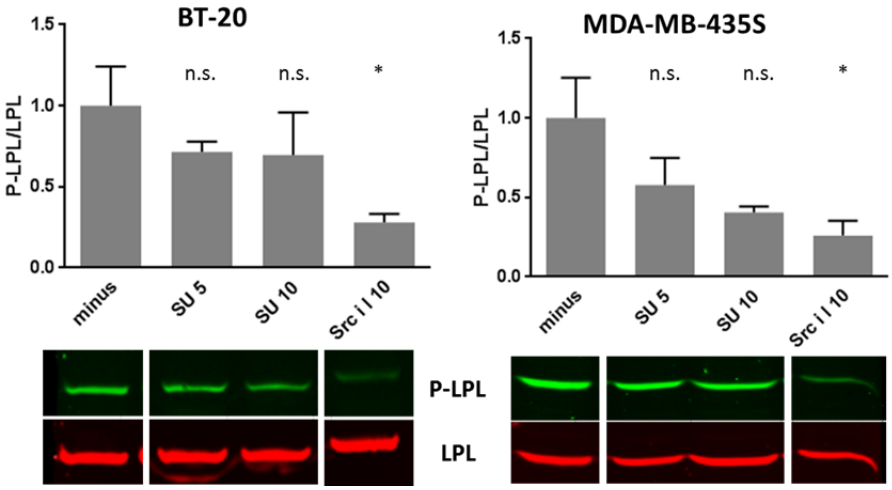

Figure 4.2.1.10. The Src inhibitors SU6656 (SU) and Src inhibitor I (Src i I) decrease L-plastin Ser5 phosphorylation in invasive breast cancer cells. Cells were treated with Src inhibitors and L-plastin Ser5 phosphorylation was determined by immunoblot analysis. Quantification was performed as described in Figure 4.2.1.2. Data are represented as means +/- SD. Statistical significance was determined by an unpaired T-test with Welch's correction. P<0.05 was considered significant. *P<0.05, **P<0.01, ***P<0.001 and n.s. – non-significant. For each immunoblot shown, samples were run on the same gel, but bands were cut and put in another order for presentation purposes.

Moreover, we transfected cells with viral Src (v-Src) which has a constitutively active tyrosine kinase activity. Compared to human Src, v-Src is truncated in the C-terminal region and thus is devoid of residue Tyr530, the phosphorylation of which inactivates human Src. Transfection of v-Src-DsRed into all four cell lines led to a considerable increase in L-plastin Ser5 phosphorylation compared to cells transfected with DsRed alone (Figure 4.2.1.11). When cells were treated with the PKC inhibitor GF109203X following transfection, a decrease in L-plastin Ser5 phosphorylation was observed compared to the non-treated transfected cells (Figure 4.2.1.11). This is an indication that PKC might act downstream of Src in mediating L-plastin Ser5 phosphorylation. Interestingly, only the PKCδ isoform can be tyrosine phosphorylated and activated by Src (Li et al., 1994; Steinberg, 2004) and this is the isoform that was suggested to be involved in L-plastin phosphorylation in breast cancer cells (Al Tanoury et al., 2010; Janji et al., 2010). Tyrosine phosphorylation is specifically implicated in the regulation of only the PKCδ isoform as, in contrast to serine/threonine residues, tyrosine phosphorylation residues are not conserved across PKC family members (Steinberg, 2004). Tyrosine phosphorylation of PKCδ has been shown to involve Src kinase (Li et al., 1994; Sumandea et al., 2008). However, studies on the effects of Src-mediated tyrosine phosphorylation of PKCδ exhibit some discrepancy as tyrosine phosphorylation has been described to activate PKCδ (Gschwendt et al., 1994; Li et al., 1994), to modifiy PKCδ substrate specificity (Haleem-Smith et al., 1995), or to decrease PKCδ activity (Denning et al., 1993; Zang et al., 1997). These studies differ in several aspects such as cell type, nature of stimulus and whether PKCδ was tyrosine phosphorylated *in vitro* after purification or extracted from stimulated cells. Overall, tyrosine phosphorylation by Src seems to have two main effects: It increases the specific activity of PKCδ and it causes the protein to become unstable and prone to degradation (Blake et al., 1999). Moreover, alongside the studies showing that Src activation influences PKC activity (Gschwendt et al., 1994; Zang et al., 1995), it has also been shown that PKC can lead to Src activation (Brandt et al., 2002; Brandt et al., 2003; Levi et al., 1998). Some studies indicated that PKC directly activates Src by phosphorylation of Ser12 and Ser48 (Gould et al., 1985; Moyers et al., 1993) and some report that other proteins such as PTPα and AFAP-110 play a role by relaying signals from

PKC to Src kinase (Brandt et al., 2003; Gatesman et al., 2004). In any case, our results suggest that Src acts upstream of PKC in the phosphorylation of L-plastin.

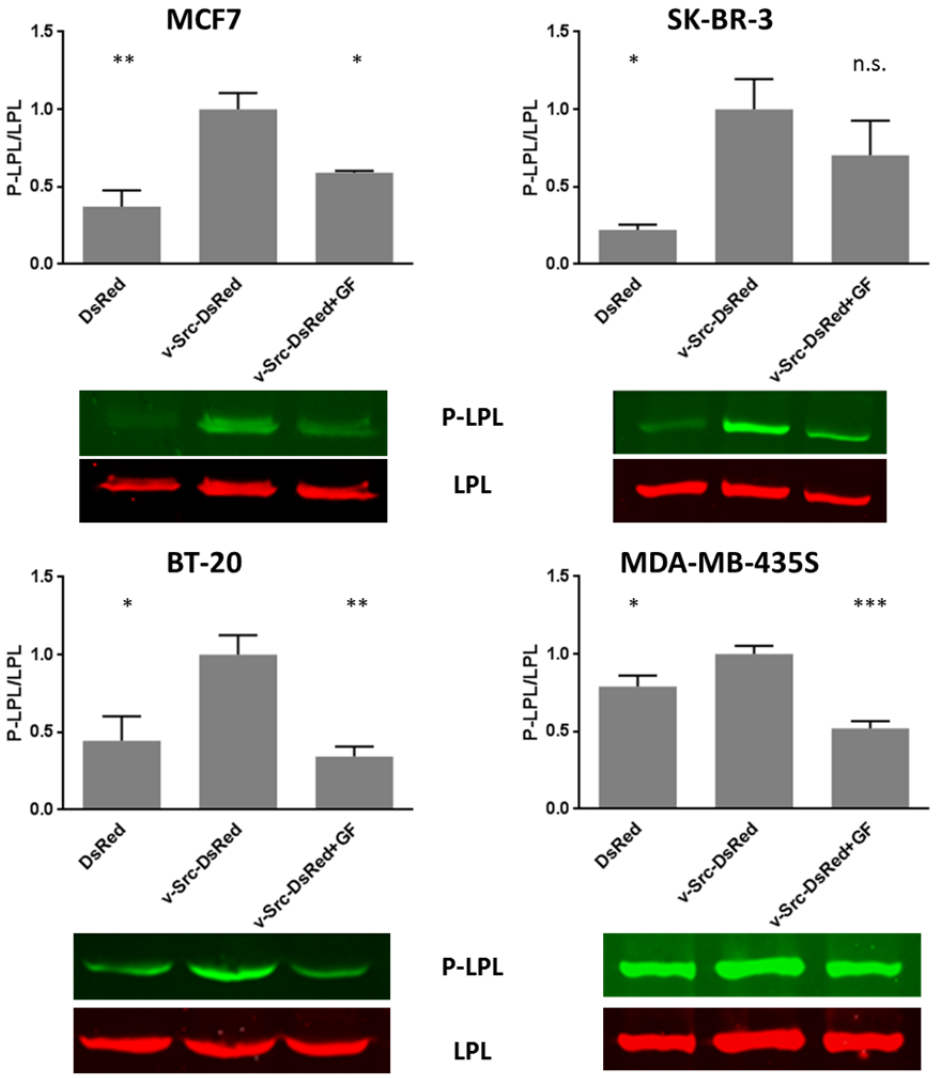

Figure 4.2.1.11 Viral Src (v-Src) increases L-plastin Ser5 phosphorylation in breast cancer cells and this effect is abolished with PKC inhibition. Cells were transfected with v-Src-DsRed or DsRed alone. PKC inhibition with GF was performed before lysis as indicated. L-plastin Ser5 phosphorylation was determined by immunoblot analysis. Quantification was performed as described in Figure 4.2.1.2. Data are represented as means +/- SD. Statistical significance was determined by an unpaired T-test with Welch's correction. P<0.05 was considered significant. *P<0.05, **P<0.01, ***P<0.001 and n.s. – non-significant.

Overall, the above mentioned results show an involvement of Src and PKC and to a lesser extent PKA in L-plastin Ser5 phosphorylation. *In vitro* kinase assays already showed that PKA can directly phosphorylate L-plastin (Janji et al., 2006; Wang and Brown, 1999). *In vitro* L-plastin Ser5 phosphorylation by any isoform of PKC could not be shown (Jones et al.,

1998). Accordingly, we performed an *in vitro* kinase assay to investigate whether PKCδ was able to directly phosphorylate L-plastin Ser5 with or without activation of PKCδ by Src and tyrosine phosphatase inhibition with Na_3VO_4. The addition of Src was performed on the basis of our finding that Src might act upstream of PKC in L-plastin Ser5 phosphorylation and of studies that provided evidence that Y311 phosphorylation of PKCδ was required to "fine tune" the PKCδ substrate specificity and was a prerequisite for the phosphorylation of cardiac troponin at T144 by PKCδ (Steinberg, 2012). However, in none of the tested conditions PKCδ was able to directly phosphorylate L-plastin Ser5 (Figure 4.2.1.12). Regrettably, we have to admit that we were lacking a known PKCδ substrate to be used as a proper positive control for this experiment.

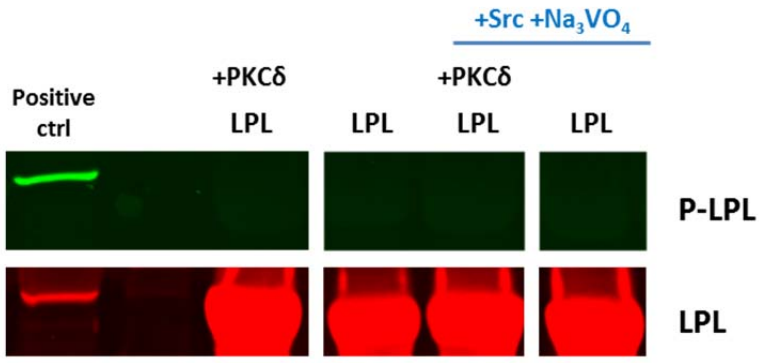

Figure 4.2.1.12 PKCδ cannot directly phosphorylate L-plastin Ser5 *in vitro*. 64 µg of recombinant GST-L-plastin-deltaABD2 were incubated with 100 ng of recombinant PKCδ with or without 50 ng recombinant Src and 0.1 mM Na_3VO_4 and with 50 µM of ATP in a reaction volume of 25 µl according to the manufacturer's protocol. For the negative controls PKCδ was omitted. The "positive control" is an MDA-MB-435S cell lysate and is a control for the correct functioning of the immunoblotting procedure. Samples were incubated for 15 min at 30°C. Following incubation, Laemmli buffer was added, the samples were boiled at 100°C for 5 min and analysed by immunoblotting, visualising Ser5 phosphorylated L-plastin (P-LPL) and total L-plastin (LPL).

As L-plastin Ser5 matches the consensus phosphorylation sequence for the Ser/Thr casein kinase II (CKII) (along with PKC and PKA), we also investigated whether this kinase is involved in L-plastin Ser5 phosphorylation by using the CKII-specific inhibitors tetra-bromo-benzo-triazole (TBB) and tetra-bromo-cinnamic acid (TBCA). Moreover, as phosphatidylinositol 3-kinase (PI3K) was described to play a role in L-plastin phosphorylation in human neutrophils (Jones et al., 1998; Paclet et al., 2004), we investigated its effect in breast cancer cells by using the inhibitor wortmannin. None of these three inhibitors showed consistent effects on L-plastin Ser5 phosphorylation in the four breast cancer cell lines.

Since the hormones estrogen and progesterone play important roles in the regulation of normal mammary gland biology as well as in breast cancer, we investigated their effect on the estrogen and progesterone receptor-positive MCF7 cells (SK-BR-3, BT-20 and MDA-MB-435S being negative for both receptors). β-estradiol was used at 10 nM for incubation times between 1 h and 48 h and progesterone was used at 100 nM for 1 h to 48 h. However, we could not observe an increase of L-plastin Ser5 phosphorylation upon treatment with these hormones.

Altogether, so far we can state that in our breast cancer cell lines PKC appears to be more important than PKA for mediating L-plastin Ser5 phosphorylation and that the tyrosine kinase Src appears to be an important contributor acting upstream of L-plastin Ser5 phosphorylation. Nevertheless, since knockdown of PKCδ by siRNA was not equally efficient for reducing L-plastin Ser5 phosphorylation in all breast cancer cell lines and since no evidence for direct L-plastin phosphorylation by PKC could be provided, other yet to be identified kinases are likely to be involved in this process.

4.2.2 Whole genome microarrays reveal enrichment of the ERK/MAPK pathway in breast cancer cells with high L-plastin Ser5 phosphorylation

This part was accomplished in collaboration with Dr. Laurent Vallar, Arnaud Muller and Tony Kaoma from the Genomics Research Unit of the Luxembourg Institute of Health.

In parallel to the analysis of the potential involvement of various kinases in L-plastin Ser5 phosphorylation, a whole genome microarray study was set up in order to compare non-invasive breast cancer cell lines with low baseline Ser5 phosphorylation (MCF7 and SK-BR-3) versus invasive breast cancer cell lines with high baseline Ser5 phosphorylation (BT-20 and MDA-MB-435S) in order to detect differences in signal transduction pathways. In addition, we treated the two non-invasive cell lines with PMA to obtain a strong L-plastin Ser5 phosphorylation and compared the PMA-treated to untreated cells (Fig. 4.2.2 left). In order to perform microarray analysis total RNA was isolated from triplicate cell cultures and microarray data were obtained using Affymetrix technologies. Lists of differentially expressed transcript clusters were established as described in the Materials and Methods section and transcript cluster mapping and analysis was performed using Ingenuity Pathway Analysis® (IPA). For the comparison of PMA-treated cells versus untreated controls, we thus obtained a

first list of DEGs for MCF7 and a second for SK-BR-3 cells. For the comparison of our two invasive and two non-invasive cancer cell lines, we obtained another four lists of differentially expressed transcript clusters (Fig. 4.2.2 right), the intersection of which was mapped by IPA to obtain a third list of DEGs. Taking the intersection of the four lists enabled us to focus on the genes that are differentially expressed between all comparisons of invasive versus non-invasive cells, thus setting a stringent filter. The three lists can be found in the appendix.

In order to assess a difference in signalling pathways between the compared conditions, we focused on canonical signalling pathways in IPA. For each of the three comparisons of interest, IPA revealed a list of canonical signalling pathways (see appendix) from which we selected those that were significant (-log(p-value)>1.301) and thus enriched by genes that are significantly differentially expressed. Interestingly, we identified three canonical signalling pathways that were common to the three lists: ERK/MAPK Signalling, UVA-Induced MAPK Signalling and Role of Osteoblasts, Osteoclasts and Chondrocytes in Rheumatoid Arthritis (Fig. 4.2.2 bottom). These results suggest an involvement of one or more of these pathways in L-plastin Ser5 phosphorylation.

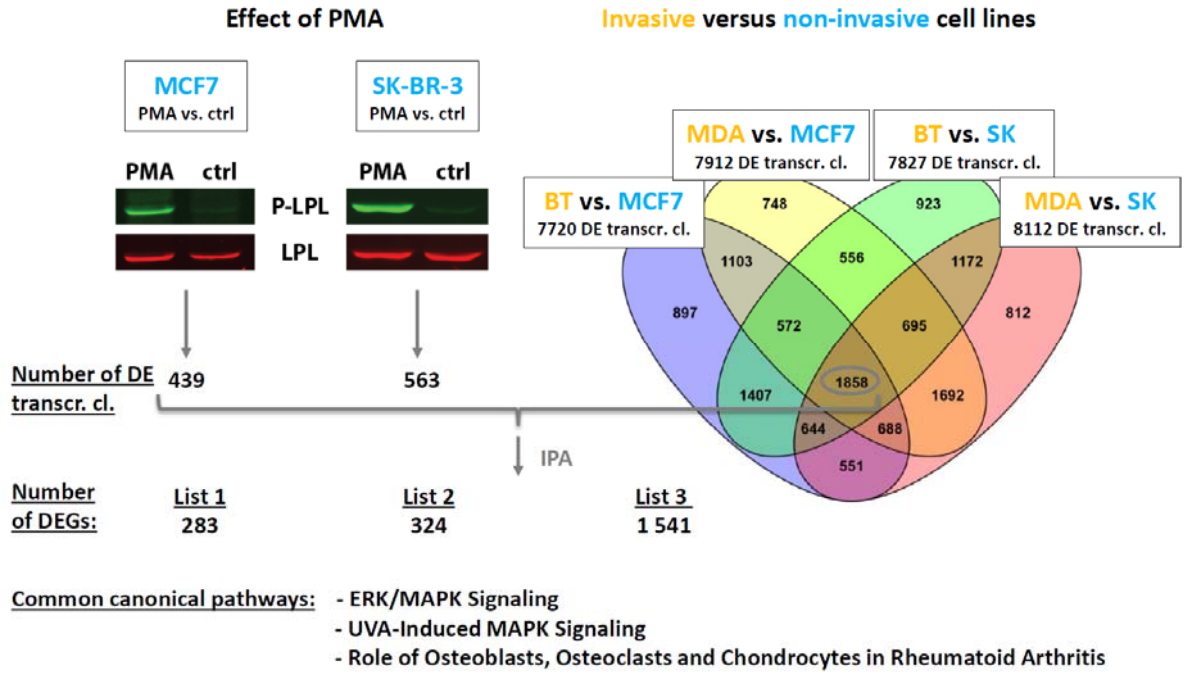

Figure 4.2.2 Enrichment of the ERK/MAPK pathway in breast cancer cells with high L-plastin Ser5 phosphorylation. Non-invasive cell lines were treated with PMA and resulting L-plastin Ser5 phosphorylation was determined by immunoblot analysis. Whole genome microarray analysis was then used to compare breast cancer cells with differential L-plastin Ser5 phosphorylation levels and invasive capacities. Three comparisons were analysed: 1. PMA-treated versus untreated MCF7 cells; 2. PMA-treated versus untreated SK-BR-3 cells; 3. intersection between comparisons of invasive versus non-invasive cells (BT-20 vs. MCF7, MDA-MB-435S vs. MCF7, BT-20 vs. SK-BR-3 and MDA-MB-435S vs. SK-BR-3). Differentially expressed transcript clusters (DE transcr. cl.) were identified for the three

comparisons and were mapped and analysed by IPA. For each of the three comparisons of interest, IPA revealed a list of canonical signalling pathways (see Supplemental microarray data in the appendix) from which we selected those that were significant (-log(p-value) > 1.301) and thus enriched by genes that are differentially expressed. Three canonical signalling pathways were common to the three lists: ERK/MAPK Signalling, UVA-Induced MAPK Signalling and Role of Osteoblasts, Osteoclasts and Chondrocytes in Rheumatoid Arthritis. Adapted from (Lommel et al., 2015).

4.2.3 RSK1 as well as RSK2 specifically phosphorylate residue Ser5 of L-plastin in vitro

L-plastin peptides were synthesised and screened for Ser5 phosphorylation by 43 candidate kinases identified using the phosphorylation prediction algorithm *KSPv2* from KINEXUS. In addition to PKA, which was previously shown to be able to phosphorylate L-plastin Ser5 *in vitro* (Janji et al., 2006; Wang and Brown, 1999), our screening identified RSKs as well as MSK1 as top candidate kinases for phosphorylating this residue. As shown in Table 4.2.3, these kinases led to high radioactivity counts for the wild type L-plastin peptide (WT) as well as for the Ser7-to-alanine mutated peptide (MT), both peptides being devoid of the initiator methionine and acetylated on the N-terminal alanine. The WT peptide displayed higher counts for the named kinases than the MT peptide indicating that phosphorylation occurs not only at residue Ser5, but also at Ser7. It is however noteworthy that Ser7 phosphorylation is not required for Ser5 phosphorylation by the investigated kinases, as significant Ser5 phosphorylation was always also observed in the absence of the Ser7 residue. This is in line with the finding of Jones and colleagues, showing that Ser5 is necessary for L-plastin phosphorylation and that Ser7 might also be phosphorylated but with a requirement for Ser5 phosphorylation to achieve Ser7 phosphorylation (Jones et al., 1998). Importantly, the same kinases appear in the top positions for both WT and MT peptides. Validation experiments as well as experiments with the WT and MT peptides still containing the initiator methionine were performed and showed higher radioactivity counts for methionine containing peptides but always similar rankings (in appendix).

Table 4.2.3 For *in vitro* kinase assays on L-plastin peptides, the peptides were mixed with individual protein kinases in the presence of [γ-33P] ATP for 20-40 min, depending on the protein kinase tested. The assay was terminated by spotting 10 µl of the reaction mixture onto a multiscreen phosphocellulose P81 plate. After removing unreacted [γ-33P] ATP from the reaction, radioactivity was quantified in counts per minute (cpm) in a scintillation counter. Adapted from (Lommel et al., 2015).

Ranking	Kinases	Counts (cpm) *ARG**S**V**S**DEERR (WT)	Kinases	Counts (cpm) *ARG**S**V**A**DEERR (MT)
1	RSK2	116698	RSK1	55774
2	PKAca	109766	PKAca	53986
3	RSK1	101952	MSK1	53254
4	MSK1	86947	RSK2	48800
5	RSK3	71917	PKAcb	34148
6	PKAcb	54673	PKAcg	33572
7	RSK4	45174	RSK3	32917
8	PKAcg	40167	PRKG2	26041
9	SGK3	32646	RSK4	22477
10	SGK2	32129	SGK2	22249
11	PRKG2	29921	SGK3	20290
12	PKCh	29273	STK33	10761
13	p70S6Kb	19894	PKCh	10007
14	AURORA B	12688	AURORA B	9696
15	STK33	9990	PRKG1	9110
16	PKCq	9671	PRKX	8113
17	VRK1	9054	DCAMKL1	5899
18	PRKX	8310	VRK1	5745
19	PRKG1	8189	VRK2	5470
20	CAMK1b	8126	MNK1	5430
21	VRK2	7876	PKCe	5053
22	CAMK4	6955	CAMK4	4668
23	PKCe	6779	DCAMKL2	4447
24	DCAMKL2	5726	p70S6Kb	4242
25	MNK1	5718	CAMK1b	3996
26	DCAMKL1	5437	NDR	3797
27	NDR	5072	PKCq	3589
28	PKCd	4597	IKKe	3422
29	PIM2	4405	NDR2	3284
30	SGK1	4243	ASK1	2771

31	NDR2	3821	SGK1	2540
32	MSK2	3741	PKCd	2329
33	IKKe	3437	AKT1	1920
34	AKT1	3257	p70S6K	1911
35	ASK1	3241	PIM2	1813
36	PIM3	2732	PIM3	1537
37	p70S6K	2454	AKT3	1460
38	AKT3	2196	AKT2	1242
39	AKT2	2142	MSK2	1005
40	PIM1	892	PIM1	922
41	CK2a2	892	AURORA C	663
42	AURORA C	588	CHK1	256
43	CHK1	176	CK2a2	44

*N-terminal alanine is acetylated

As the *in vitro* kinase assays performed on L-plastin peptides identified RSK1, RSK2 and MSK1 as candidate kinases (Table 4.2.3), we also tested these kinases for their ability to phosphorylate recombinant full-length L-plastin on residue Ser5 *in vitro*. As shown in Figure 4.2.3, both RSK1 and RSK2 were able to strongly phosphorylate L-plastin on residue Ser5 while MSK1 was merely able to induce a weak L-plastin Ser5 phosphorylation. In parallel, PKCδ was again tested here on the full-length recombinant L-plastin and did again not show any phosphorylation activity towards L-plastin Ser5.

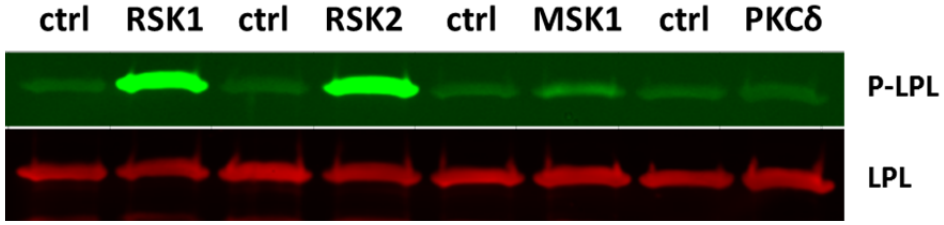

Figure 4.2.3 RSK1 and RSK2 are able to directly phosphorylate L-plastin Ser5 *in vitro*. 10 µg of recombinant full-length L-plastin were incubated with 100 ng of recombinant kinase and with 50 µM of ATP in a reaction volume of 25 µl according to the manufacturer's protocol. For each kinase assay a control was performed by omitting the respective kinase. Samples were incubated for 15 min at 30°C. Following incubation, Laemmli buffer was added, the samples were boiled at 100°C for 5 min and analysed by immunoblot visualising Ser5 phosphorylated L-plastin (P-LPL) and total L-plastin (LPL). Adapted from (Lommel et al., 2015).

4.2.4 RSK1/2 protein expression levels largely correlate with the invasive status of breast cancer cell lines whereas RSK protein activity levels do not

Following our findings that RSK1 and RSK2 mediate *in vitro* L-plastin Ser5 phosphorylation and because in invasive breast cancer cell lines we have higher L-plastin Ser5 phosphorylation than in non-invasive cell lines, we analysed whether there is a correlation between RSK1/2 expression and/or activity level and the invasive status of breast cancer cell lines.

We started by performing IPA upstream analysis to investigate whether RSK1/2 proteins are differentially activated in invasive compared to non-invasive cell lines, making use of our 4 lists (corresponding to *invasive versus non-invasive*) and applying the parameters false discovery rate FDR<0.01 and absolute fold change FC>4. As a result, we could not infer *in silico* significant enrichment of RSK1/2 activity in any of the 4 lists. Thus, no upregulation of RSK1 or RSK2 activity upstream of transcriptional regulation could be detected in any of the four invasive versus non-invasive comparisons.

Since RSK activity is not limited to transcriptional regulation, we proceeded by directly comparing RSK1/2 protein levels as well as the levels of the phosphorylated, active form of RSK1/2 between the different investigated cell lines. RSK1 protein levels were found to be higher in the two invasive cell lines BT-20 and MDA-MB-435S compared to the two non-invasive cell lines MCF7 and SK-BR-3 (Figure 4.2.4.1). RSK2 was highly expressed in the invasive cell lines BT-20, MDA-MB-435S as well as in MCF7 cells and at a lower level in SK-BR-3 cells (Figure 4.2.4.1).

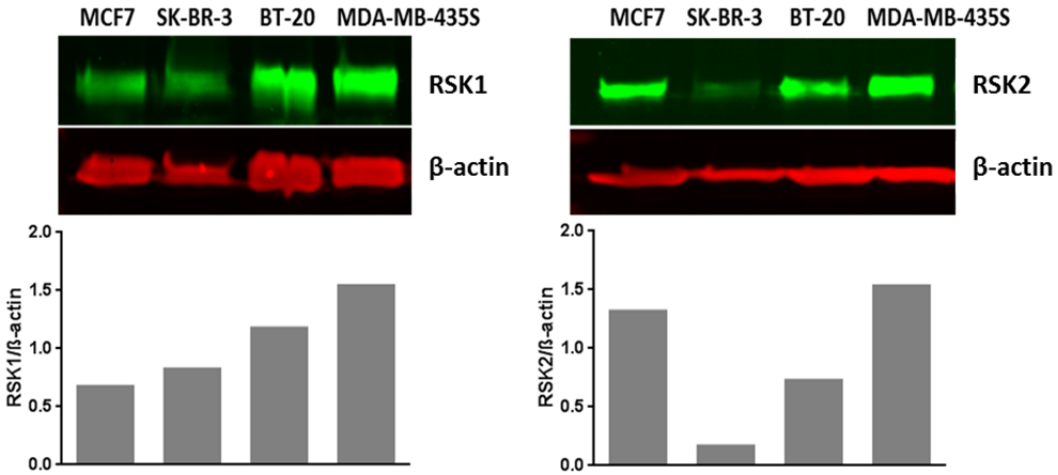

Figure 4.2.4.1 Protein levels of RSK1 and RSK2 in four breast cancer cell lines. Cell extracts were subjected to immunoblot analysis using antibodies specific for RSK1, RSK2 and β-actin as a loading control.

Using an antibody specifically recognising the phosphorylated forms of RSK1 and RSK2, we investigated the phosphorylation levels in our four cell lines (Figure 4.2.4.2). Our results indicate that SK-BR-3 and MDA-MB-435S have higher RSK1/2 phosphorylation levels than MCF7 and BT-20. In addition, phosphorylation of RSK1/2 was increased upon EGF or PMA stimulation in the four cell lines.

So far, higher RSK1 and RSK2 protein levels in invasive versus non-invasive cells seem to largely correlate with higher baseline L-plastin Ser5 phosphorylation in invasive versus non-invasive cells. However, the levels of the phosphorylated RSK1/2 forms do not correlate with the invasiveness of the respective cell lines.

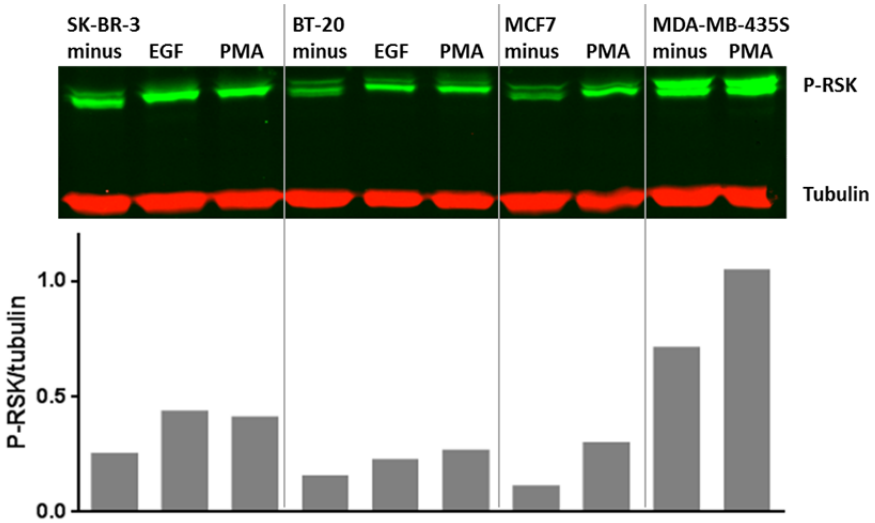

Figure 4.2.4.2 Levels of phosphorylated RSK1/2 in four breast cancer cell lines with or without EGF or PMA stimulation. Cell extracts were subjected to immunoblot analysis using antibodies specific for P-RSK1/2 and tubulin as a loading control. (Note: MDA refers to MDA-MB-435S.)

4.2.5 The ERK/MAPK pathway and its downstream RSK kinases are involved in L-plastin Ser5 phosphorylation in breast cancer cells

The two newly identified prime candidate kinases capable of phosphorylating L-plastin on Ser5 *in vitro*, RSK1 and RSK2, are downstream effectors of the ERK/MAPK pathway (Anjum and Blenis, 2008). In addition, the results of our microarray experiments have also suggested an involvement of the ERK/MAPK pathway in L-plastin Ser5 phosphorylation. Altogether these findings prompted us to further investigate the role of the ERK/MAPK pathway in

L-plastin Ser5 phosphorylation. In a first step, we inhibited selected signalling molecules of this pathway and we showed that PKC inhibition with the widely-used pan-PKC inhibitor GF109203X, MEK1/2 inhibition with PD98059 as well as RSK inhibition with BI-D1870 decreased baseline L-plastin Ser5 phosphorylation in invasive cells (Fig. 4.2.5.1).

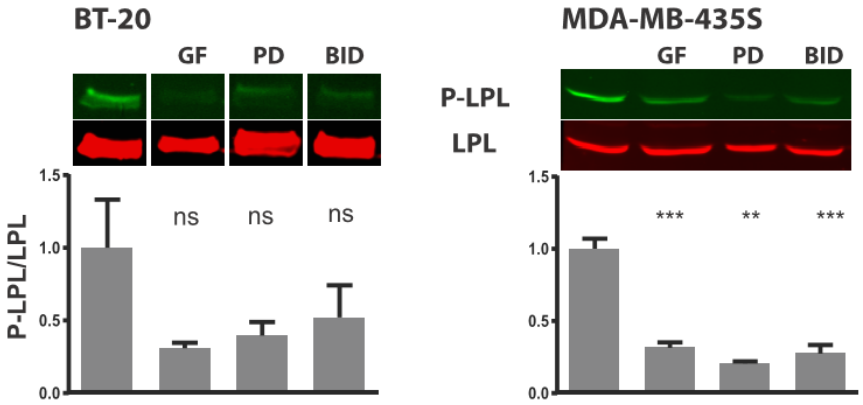

Figure 4.2.5.1 Inhibitors of molecules of the ERK/MAPK pathway reduce L-plastin Ser5 phosphorylation in invasive breast cancer cells. Invasive cell lines exhibiting high baseline L-plastin Ser5 phosphorylation were treated with inhibitors of selected signalling molecules of the ERK/MAPK pathway GF109203X (GF), PD98059 (PD) and BI-D1870 (BID). Subsequent to inhibitor treatment, residual L-plastin Ser5 phosphorylation was determined by immunoblot analysis. Quantification was performed as described in Figure 4.2.1.2. Data are represented as means +/- SD. Statistical significance was determined by an unpaired T-test with Welch's correction. $P<0.05$ was considered significant. *$P<0.05$, **$P<0.01$, ***$P<0.001$ and n.s. – non-significant. Samples were run on the same gel, but for BT-20 bands were cut and put in another order for presentation purposes. Adapted from (Lommel et al., 2015).

In a second step, we took advantage of the fact that the ERK/MAPK pathway is one of the major signalling pathways activated upon binding of various growth factors to the corresponding receptor tyrosine kinases. Knowing that the EGFR family plays a key role in normal breast development and in breast cancer (Eccles, 2011), and as the EGFR is capable to trigger cell migration through ERK/MAPK pathway signalling (Tarcic et al., 2012), we investigated L-plastin Ser5 phosphorylation in our breast cancer cells after EGF stimulation. As expected, stimulation with EGF did not increase L-plastin phosphorylation in the two EGFR-negative cell lines MCF7 and MDA-MB-435S, even when stimulated with high EGF concentrations (Figure 4.2.5.2). However, EGF treatment highly increased L-plastin Ser5 phosphorylation in SK-BR-3 and BT-20 cells at all tested concentrations (Figure 4.2.5.2).

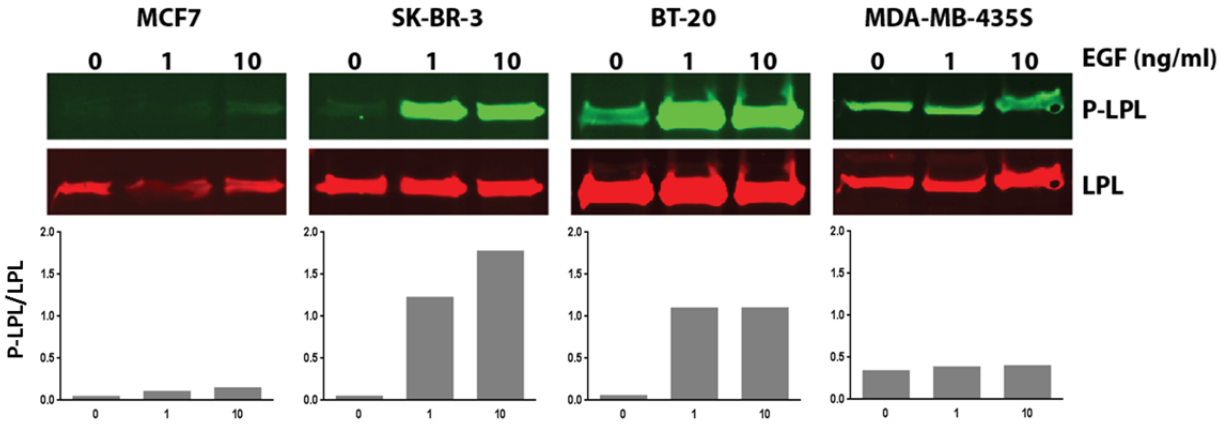

Figure 4.2.5.2 Analysis of EGF-dependent L-plastin Ser5 phosphorylation. Cells were stimulated for 15 min with different EGF concentrations and cell extracts were subjected to immunoblot analysis using antibodies specific for Ser5 phosphorylated L-plastin (P-LPL) and total L-plastin (LPL). Adapted from (Lommel et al., 2015).

Importantly, preincubation with inhibitors of the ERK/MAPK pathway impaired L-plastin phosphorylation upon PMA or EGF stimulation in all tested cell lines (Figure 4.2.5.3A). To exclude off-target effects, we confirmed our results with a second RSK inhibitor, SL0101, which also impaired EGF-triggered L-plastin phosphorylation in SK-BR-3 and BT-20 cells and decreased baseline L-plastin phosphorylation in invasive cell lines (Figure 4.2.5.4). Interestingly, the strongest decrease of L-plastin Ser5 phosphorylation was obtained for the combined inhibition of RSK and PKC (Figure 4.2.5.3A). Finally, Trametinib, a clinical MEK inhibitor approved by the U.S. Food and Drug Administration for melanoma treatment (trade name Mekinist), clearly reduced baseline L-plastin Ser5 phosphorylation in invasive cell lines and prevented an EGF-triggered increase of L-plastin Ser5 phosphorylation in SK-BR-3 and BT-20 cells (Figure 4.2.5.3B). Altogether these results provide solid evidence for a major involvement of the ERK/MAPK signalling pathway in L-plastin Ser5 phosphorylation.

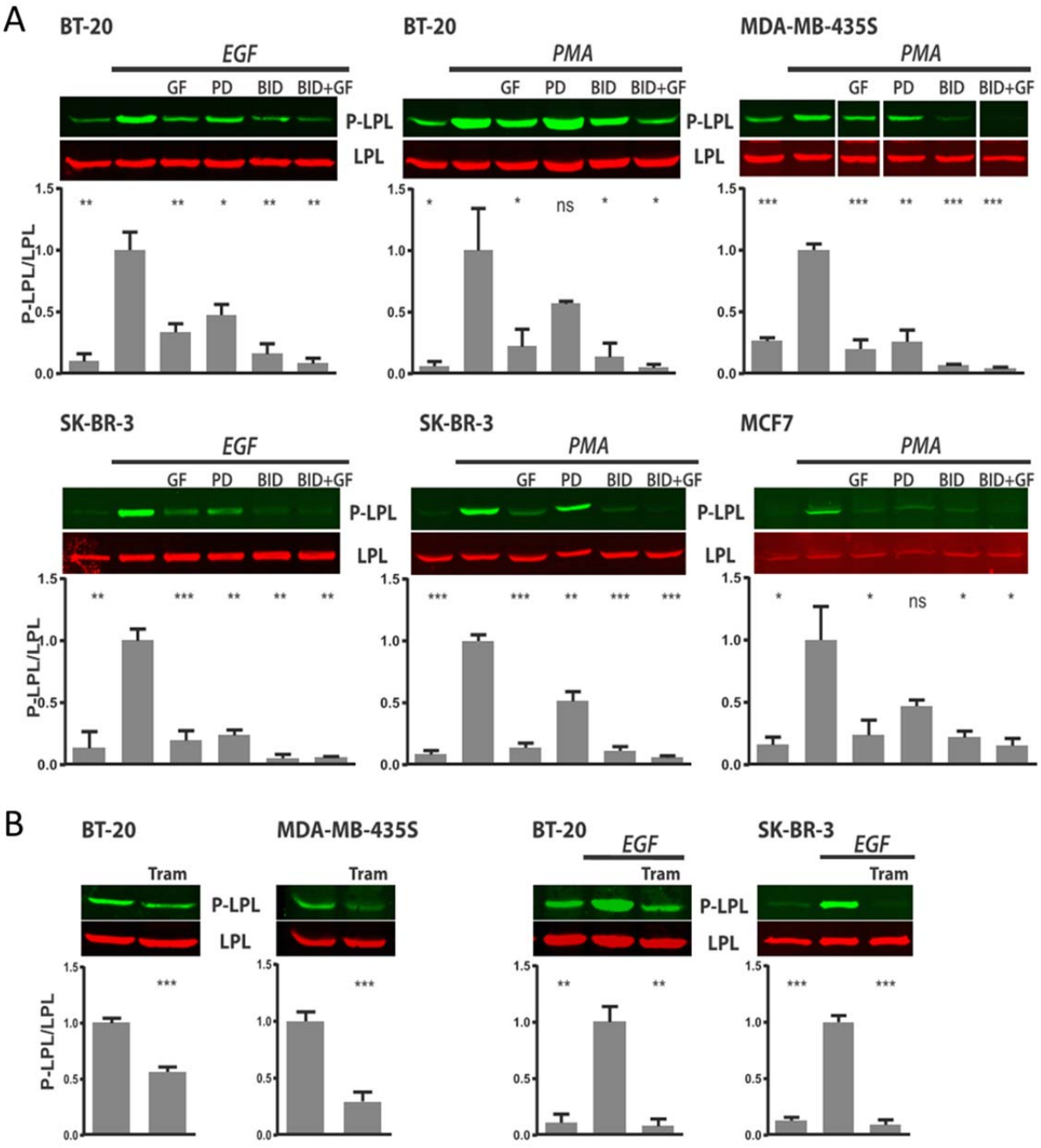

Figure 4.2.5.3 Involvement of the ERK/MAPK pathway in L-plastin Ser5 phosphorylation in breast cancer cells. A) Cells were preincubated with inhibitors of the ERK/MAPK pathway, GF109203X (GF), PD98059 (PD) and BI-D1870 (BID), and then stimulated with EGF (for the two EGFR expressing cell lines) or PMA (for the four cell lines). Quantification was performed as described in Figure 4.2.1.2. Data are represented as means +/- SD. For each immunoblot shown, samples were run on the same gel, but for MDA-MB-435S bands were cut and put in another order for presentation purposes. B) Cells were treated with Trametinib (Tram) with or without subsequent EGF stimulation. Quantification was performed as described in Figure 4.2.1.2. Data are represented as means +/- SD. Statistical significance was determined by an unpaired T-test with Welch's correction. $P<0.05$ was considered significant. *$P<0.05$, **$P<0.01$, ***$P<0.001$ and n.s. – non-significant. Adapted from (Lommel et al., 2015).

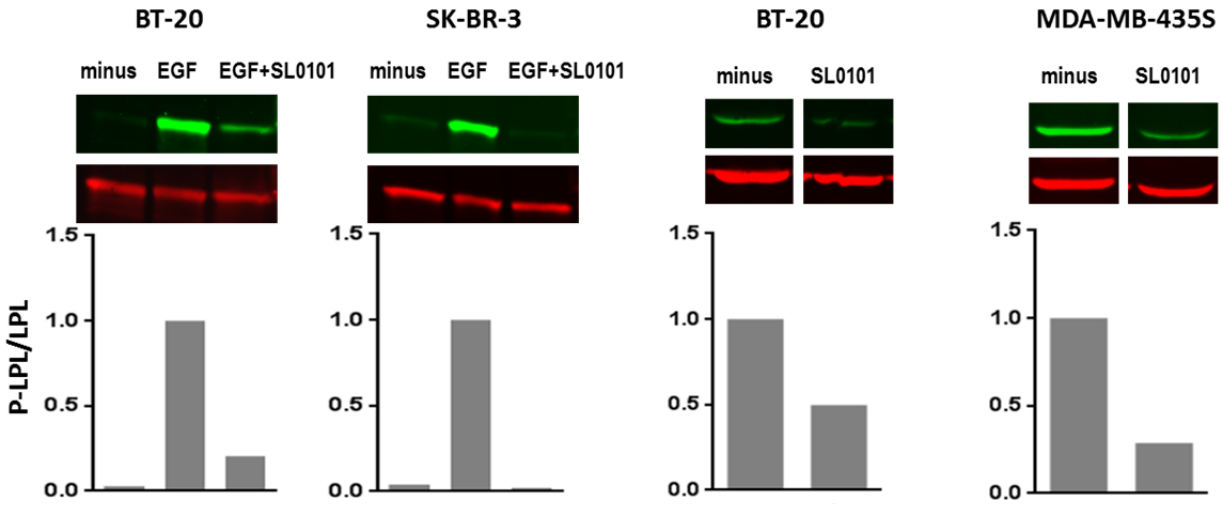

Figure 4.2.5.4 The RSK inhibitor SL0101 decreases L-plastin Ser5 phosphorylation. Cells were treated with SL0101 and with EGF as indicated. For quantification the ratio between the intensities obtained for phosphorylated L-plastin (P-LPL) versus total L-plastin (LPL) was determined. For each immunoblot shown, samples were run on the same gel, but in some cases bands were cut and put in another order for presentation purposes.

4.2.6 2-D gel electrophoresis suggests that RSK phosphorylates L-plastin on Ser5 but not on other residues

These experiments were performed in collaboration with Prof. Christophe Ampe and Prof. Marleen van Troys from the University of Ghent.

In order to analyse the phosphorylation of L-plastin in more detail, with a specific focus on the extent of phosphorylation in response to different treatment conditions, we performed two-dimensional gel electrophoresis with lysates of differentially treated BT-20 cells. Using the PhosphoSitePlus® website we found the isoelectric point of L-plastin to be 5.29 for the unsphosphorylated form, 5.24 for L-plastin with one phosphorylated residue and 5.2, 5.15, 5.11, 5.07 for increasing numbers of phosphorylated residues. As the isoelectric point corresponds to the pH level at which L-plastin has no global electrical charge, we performed isoelectric focusing in a pH range from 4 to 7. Figure 4.2.6 shows blots after isoelectric focusing (horizontal separation) and SDS-PAGE (vertical separation). Highly negatively charged and thus highly phosphorylated proteins are found on the '+' side and less phophorylated proteins are found on the '-' side. In contrast to our expectation to see clearly seperated spots corresponding to L-plastin proteins with distinct numbers of phosphorylated residues, we rather detected a line where only some spots can be recognised. As we count five to six spots, L-plastin seems to be phosphorylated on five to six residues. Since the

spots corresponding to phosphorylated L-plastin were not clearly distinguishable from the spot of non-phosphorylated L-plastin, we were not able to calculate an exact ratio of phosphorylated versus non-phosphorylated protein. Interestingly however, with the staining for Ser5 phosphorylated L-plastin, we reveal that Ser5 is a crucial phosphorylation site as all L-plastin spots except the very left, non-phosphorylated spot, are phosphorylated on Ser5. We can thus also conclude that an important part of L-plastin is Ser5 phosphorylated. This is true for non-treated cells as well as for cells treated with PMA or EGF. However, upon treatment with the RSK inhibitor BID, L-plastin Ser5 phosphorylation is dramatically decreased whereas overall L-plastin phosphorylation seems to be largely unaffected. This indicates that RSKs are involved in the phosphorylation of L-plastin on Ser5 but not of other L-plastin phosphorylation residues.

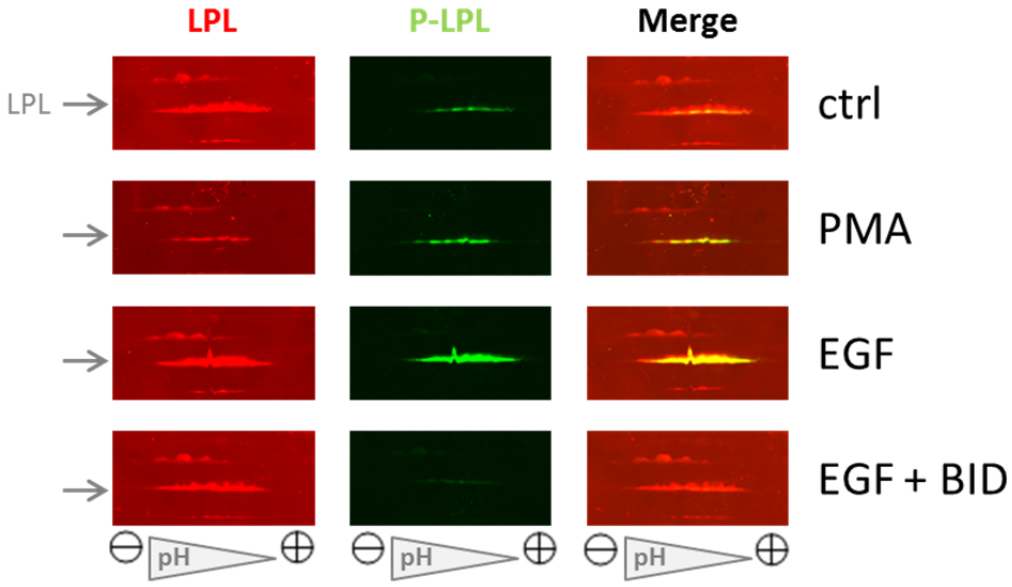

Figure 4.2.6 Analysis of L-plastin phosphorylation by 2-D gel electrophoresis. BT-20 cells were treated with PMA, EGF or EGF + BI-D1870 and then lysed. Isoelectric focusing and SDS-PAGE were performed and membranes were blotted against L-plastin (LPL) and Ser5 phosphorylated L-plastin (P-LPL)-specific antibodies.

4.2.7 Modelling of the L-plastin signalling pathway using a probabilistic Boolean network (PBN) approach

This part was accomplished in collaboration with Dr. Panuwat Trairatphisan and Prof. Thomas Sauter from the Systems Biology Group of the University of Luxembourg, who performed probabilistic Boolean network modelling on our experimental data.

Literature reports as well as our experimental data presented before (section 4.2.1) show the involvement of PKA (Janji et al., 2006; Wang and Brown, 1999) and PKC (Al Tanoury et al., 2010; Freeley et al., 2012; Janji et al., 2010; Jones et al., 1998; Lin et al., 1998; Paclet et al., 2004; Pazdrak et al., 2011) in L-plastin Ser5 phosphorylation, and most importantly, our newest results also highlight a role for RSK kinases in this process. As the network of signalling events that control L-plastin Ser5 phosphorylation is not clearly understood, quantitative computational simulation of signalling cascades was applied for a better understanding of the hierarchy of these regulatory events. We applied the optPBN toolbox to further study and analyse these pathways in the PBN framework (Trairatphisan et al., 2014). We built a PBN model which represents the network topology of signalling pathways upstream of L-plastin Ser5 phosphorylation based on literature information and own findings (Figure 4.2.7.1). Our model is mainly focused on the ERK/MAPK pathway (downstream of the EGFR) and includes Src, PKC and PKA kinases which are known to interact with this pathway. Then, we fitted the PBN model to our extensive dataset comprising activation and inhibition of various network nodes which modulate the signals towards the two measured output nodes, i.e. L-plastin Ser5 phosphorylation and PKA substrate phosphorylation in four breast cancer cell lines. To this end, we took into account the described off-target effects of the inhibitors GF109203X and H89 on RSK (Alessi, 1997; Davies et al., 2000). As a result, we obtained a model which explained well our experimental data for all four cell lines as shown in Figure 4.2.7.2.

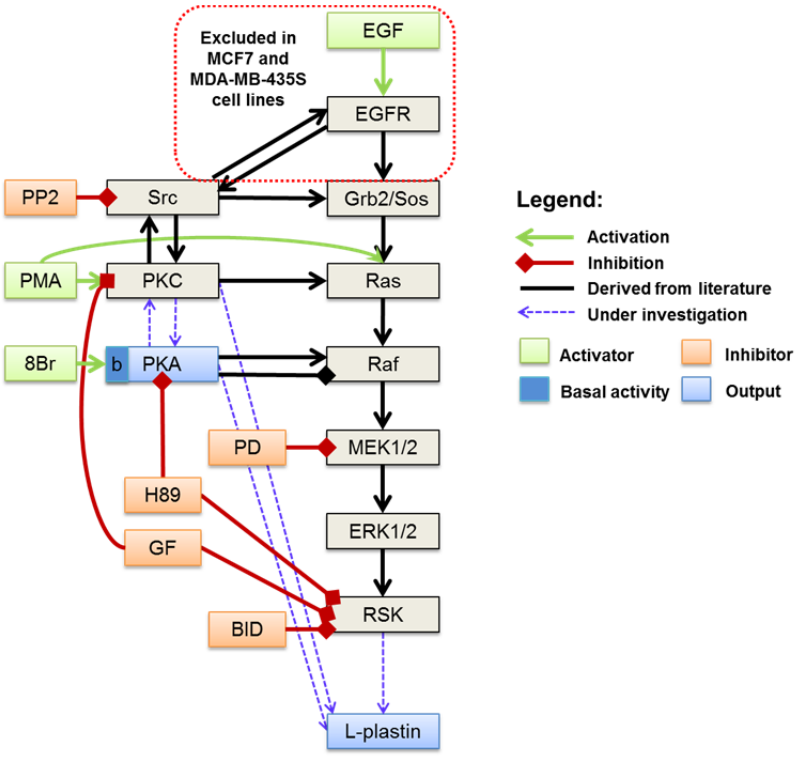

Figure 4.2.7.1 Literature-derived and experiment-based L-plastin signalling network. A candidate network for the signalling pathways upstream of L-plastin Ser5 phosphorylation was built based on literature information and own experimental findings. The network interactions were analysed by applying a probabilistic Boolean network approach taking into account cell line-specific immunoblot-based quantifications of phosphorylated L-plastin and phosphorylated PKA substrates. Various conditions were tested in breast cancer cell lines including activation by EGF, PMA or 8-Bromo-cAMP (8Br) and/or inhibition by GF109203X (GF), H89, PP2, PD98059 (PD) or BI-D1870 (BID). Adapted from (Lommel et al., 2015).

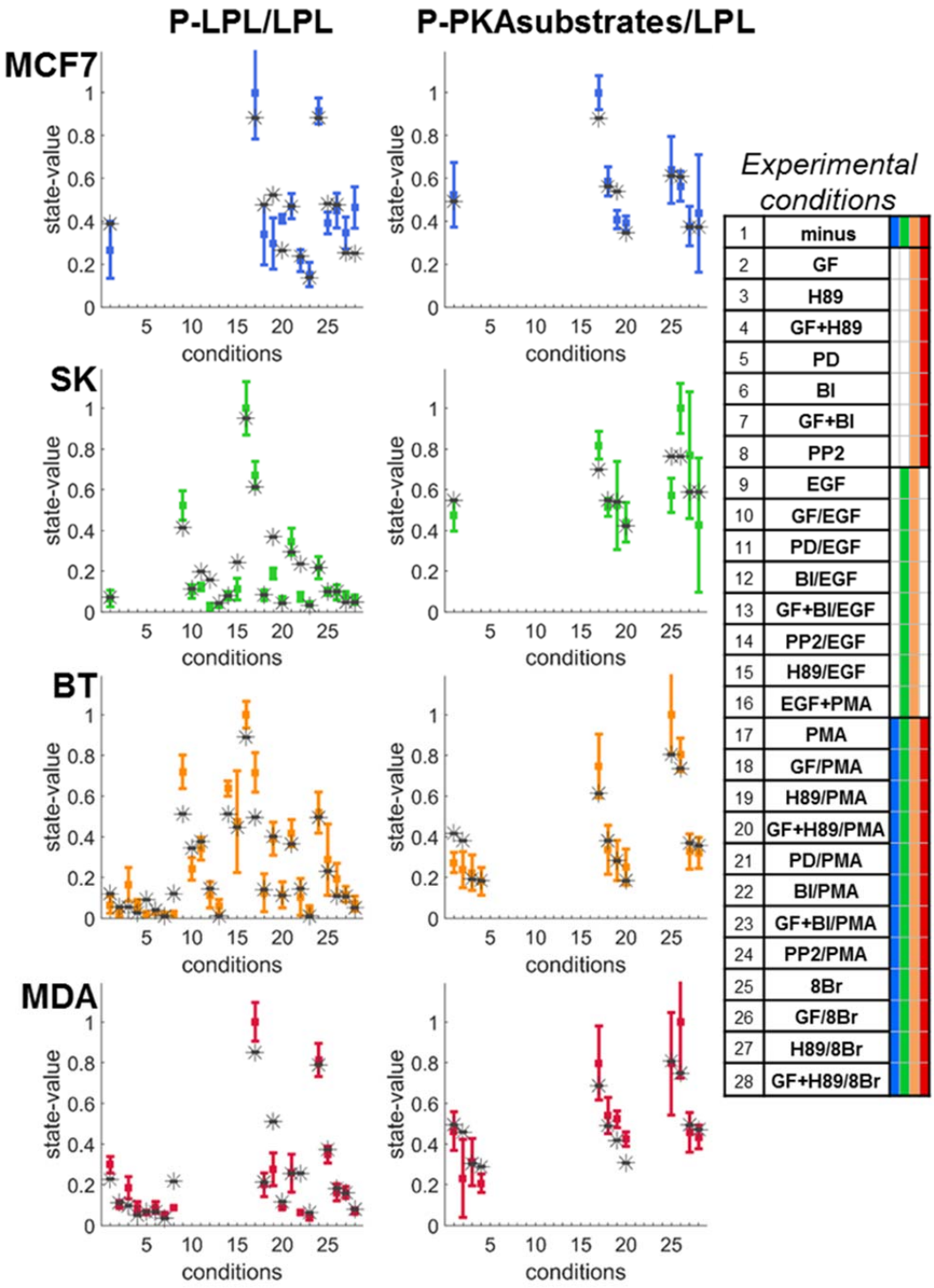

Figure 4.2.7.2 PBN model fitting results in comparison to experimental data for the various tested conditions. Coloured bars at the right of the figure indicate the conditions tested for the individual cell lines MCF7, SK-BR-3 (SK), BT-20 (BT), MDA-MB-435S (MDA). For quantification the ratios between the intensities obtained for phosphorylated L-plastin (P-LPL) respectively phosphorylated PKA substrates (P-PKAsubstrates) versus total L-plastin (LPL) were determined to make individual samples comparable and then normalised to the mean of all the values obtained in one experiment to make blots comparable by accounting for technical day-to-day variability. Data generated from different experimental sets were normalised to the calibrator PMA, subsequently pooled and scaled to the highest signal (of each respective graph) for presentation purposes. Means of ten simulated values from the

PBN model (black stars) were compared against the experimental data (multi-coloured squares [mean] and error bars [SD]). Adapted from (Lommel et al., 2015).

As we found RSK kinases to be essential for L-plastin Ser5 phosphorylation, the fitted PBN model was used to investigate whether RSK kinases have a larger effect on L-plastin in the four cell lines than PKA and PKC. In addition, we analysed whether the crosstalk interactions between PKC and PKA suggested in the literature (Sugita et al., 1997; Yao et al., 2008) are important to modulate the signal transduction upstream of L-plastin Ser5 phosphorylation. We therefore applied an *in silico* knockout approach where we removed an interaction from the model one-at-a-time and checked if the removal affected the fitting quality. Five interactions situated in close proximity to our output nodes were analysed, i.e. RSK→L-plastin, PKC→L-plastin, PKA→L-plastin, PKC→PKA and PKA→PKC (Table 4.2.7.1). We found that removing the interactions RSK→L-plastin and PKC→PKA led to a dramatic increase of the model fitting costs in all four cell lines, meaning that the networks missing one of these two interactions fitted our experimental data less well. The individual knockout of the other three interactions only led to minor changes in fitting costs, suggesting that none of these three interactions is necessary to explain our experimental data.

Table 4.2.7.1 The fitting costs of model variants after removing individual interactions were compared to those of the initial model structure prior to removal. The fitting cost is the sum of squared error between simulated state values and the mean values of the experimental data. Adapted from (Lommel et al., 2015).

	MCF7	SK-BR-3	BT-20	MDA-MB-435S
Initial model	0.2298	0.2942	0.2961	0.3126
RSK → LPL removed	0.7872	1.0344	0.6921	1.2369
PKC → LPL removed	0.2298	0.2942	0.2962	0.3126
PKA → LPL removed	0.2318	0.2942	0.2966	0.3126
PKC → PKA removed	0.7163	0.4520	0.4245	0.4622
PKA → PKC removed	0.2298	0.2942	0.3045	0.3452

We then proceeded by examining the optimised selection probability weights of each interaction and their distributions obtained via bootstrapping (see Materials and Methods section). A subset of the obtained weight distributions of the interactions is shown in Table 4.2.7.2. All weights are illustrated in Figure 4.2.7.3. Strikingly, in all four cell lines the

activation of L-plastin by RSK is largely predominant as compared to its activation by PKC or PKA. In addition, the weights attributed to the investigated interactions indicate that in all four cell lines the PKC-PKA interaction appears to be directed from PKC to PKA rather than from PKA to PKC. The relatively low standard deviations on the weights ensured that these findings are robust against experimental variation in the dataset. Figure 4.2.7.4 shows the final structure of the L-plastin signalling pathway as revealed by PBN modelling.

Table 4.2.7.2 The distributions of identified weights obtained via bootstrapping have been investigated for the five interactions in the four cell lines. The obtained weights are shown as mean and (standard deviation). Adapted from (Lommel et al., 2015).

	MCF7	SK-BR-3	BT-20	MDA-MB-435S
RSK → LPL	0.888 (0.081)	1.000 (0.000)	0.948 (0.070)	1.000 (0.000)
PKC → LPL	0.004 (0.023)	0.000 (0.000)	0.025 (0.058)	0.000 (0.000)
PKA → LPL	0.108 (0.073)	0.000 (0.000)	0.027 (0.023)	0.000 (0.000)
PKC → PKA	0.407 (0.060)	0.236 (0.049)	0.262 (0.059)	0.252 (0.093)
PKA → PKC	0.072 (0.112)	0.005 (0.017)	0.256 (0.189)	0.204 (0.068)

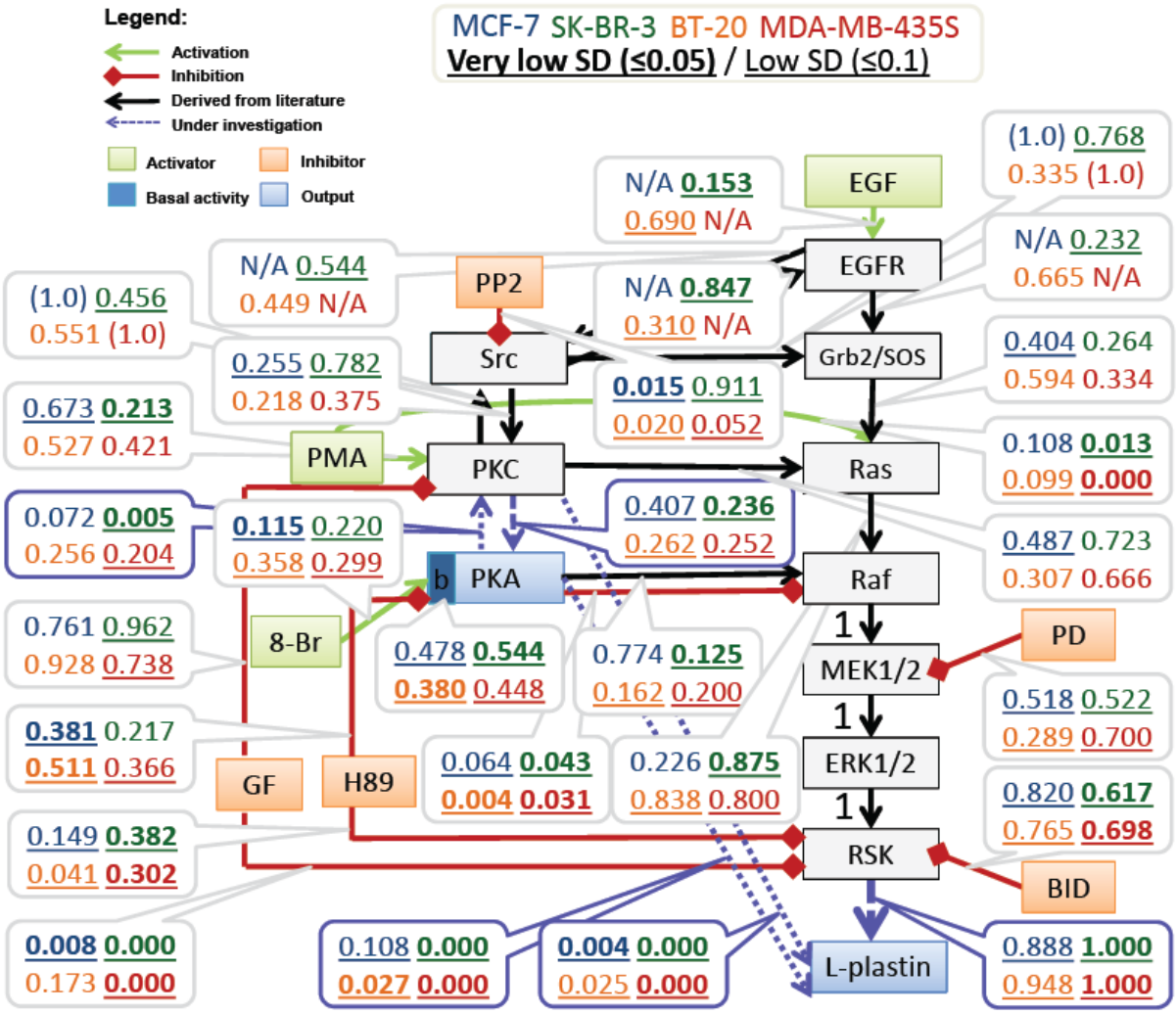

Figure 4.2.7.3 Optimised weights of interactions for the L-plastin signalling network. Bootstrapping was performed by randomly sampling 100 artificial datasets based on means and standard deviations as acquired from the experimental data. Optimisation was subsequently performed 100 times to identify the distribution of the identified selection probabilities. Means and standard deviations of the weights of the interactions were compared among the four cell lines. Adapted from (Lommel et al., 2015).

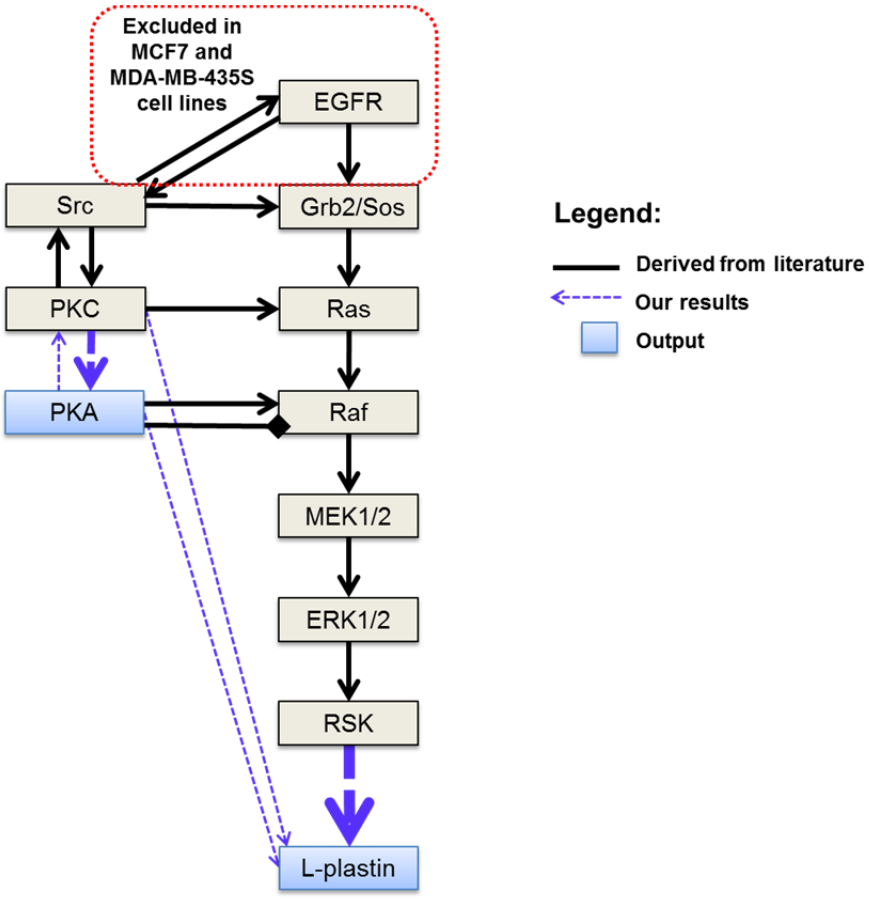

Figure 4.2.7.4 L-plastin signalling pathway as revealed by PBN modelling. A PBN modelling approach based on cell line-specific immunoblot-based quantifications of Ser5 phosphorylated L-plastin and phosphorylated PKA substrates revealed that RSK is crucial for L-plastin Ser5 phosphorylation whereas PKC and PKA play a minor role in this event in the four tested cell lines. In addition, our PBN modelling results indicate that in all four cell lines the PKC-PKA interaction appears to be directed from PKC to PKA rather than from PKA to PKC. Adapted from (Lommel et al., 2015).

4.2.8 Combined RSK1 and RSK2 knockdown by siRNA decreases L-plastin Ser5 phosphorylation

Altogether, we provide evidence that RSK kinases are involved in L-plastin Ser5 phosphorylation by *in vitro* kinase assays, by inhibition with two different RSK inhibitors as well as by computational modeling. To further consolidate our findings, we simultaneously knocked down RSK1 and RSK2 by an siRNA approach. Albeit RSK knockdown was not equally efficient in all the investigated cell lines, we were able to observe a decrease of Ser5 phosphorylated L-plastin in all four cell lines following the combined knockdown of RSK1 and RSK2 (Figure 4.2.8). It is interesting to note that for SK-BR-3 and MDA-MB-435S, for which an efficient RSK knockdown could be obtained, the decrease in L-plastin Ser5 phosphorylation was more important than for MCF7 and BT-20, with a less efficient RSK

knockdown. The remaining L-plastin Ser5 phosphorylation might be due to residual RSK1 and RSK2 protein presence after knockdown. Altogether, even though phosphorylation was not completely abolished, our data clearly confirm an important role for RSKs in L-plastin Ser5 phosphorylation.

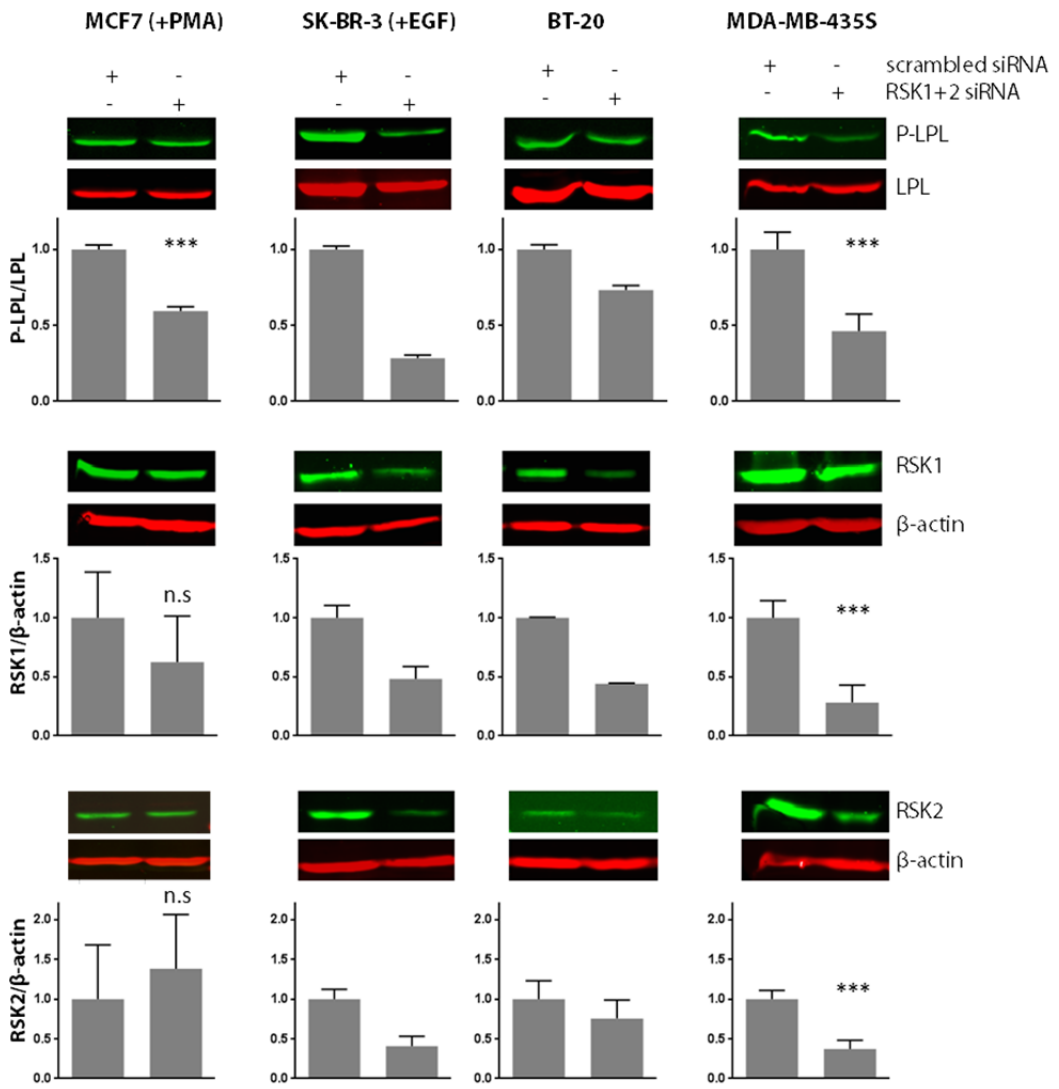

Figure 4.2.8 Combined RSK1 and RSK2 knockdown decreases L-plastin Ser5 phosphorylation in breast cancer cells. siRNA against RSK1 and RSK2 or scrambled siRNA were transfected in the four cancer cell lines as indicated and L-plastin Ser5 phosphorylation, RSK1 and RSK2 expression were assessed by immunoblot analysis 72 h post transfection. Non-invasive cell lines were treated with EGF or PMA as indicated. Quantification was performed as described in Figure 4.2.1.2. For presentation purposes, the values obtained with RSK1+2 siRNA were scaled to the signal obtained with scrambled siRNA. The resulting graphs depict means +/- SD from two (for SK-BR-3 and BT-20 cells), three (for MCF7 cells) and six (for MDA-MB-435S cells) biological replicates. For experiments with at least 3 replicates, statistical significance was determined by an unpaired T-test with Welch's correction (*P<0.05, **P<0.01, ***P<0.001 and n.s. – non-significant). Representative blots are shown. Adapted from (Lommel et al., 2015).

Overall, our data presented in section 4.2 clearly reveal a role for the ERK/MAPK pathway and its downstream kinases RSK1 and RSK2 in L-plastin Ser5 phosphorylation in breast cancer cells. Notably, a whole genome microarray analysis pointed to the involvement of the ERK/MAPK pathway in this phosphorylation step and this finding was confirmed by a detailed analysis of this pathway performing activation/inhibition studies. Moreover, *in vitro* kinase assays and siRNA-mediated knockdown experiments revealed the implication of RSK1 and RSK2 in this phosphorylation. Finally, a computational modelling approach corroborated that in all four cell lines RSK is largely predominant as compared to PKC and PKA in the event of L-plastin Ser5 phosphorylation.

4.3 Link between L-plastin Ser5 phosphorylation by RSK and invasion and migration of breast cancer cells

In order to investigate whether there is a link between RSK activity responsible for L-plastin Ser5 phosphorylation and cell migration and invasion capacities, we investigated the effect of RSK knockdown on migration and invasion in MDA-MB-435S cells. This cell line was selected as it has the highest invasive capacity as shown in Figure 4.1.3.2. *In vitro* scratch wound assays revealed that the combined knockdown of RSK1 and RSK2 considerably slowed down MDA-MB-435S cell migration and invasion by up to 30% (Figure 4.3.1) whereas cell proliferation remained largely unaffected (data not shown).

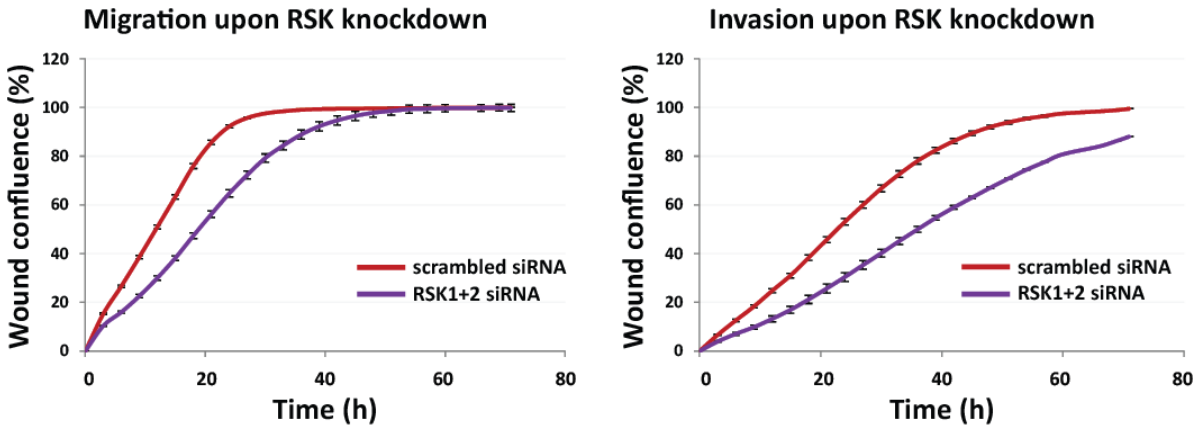

Figure 4.3.1 Combined RSK1 and RSK2 knockdown impairs migration and invasion in breast cancer cells. MDA-MB-435S cells were seeded in collagen I-coated (200 µg/ml) 96-well plates and transfected with siRNA against RSK1 and RSK2 or with scrambled siRNA. After 24 h, a wound was scratched across each well with the Cellplayer 96-well woundmaker. To study invasion, cells were covered with collagen I (1.5 mg/ml) diluted in cell culture medium. To study migration, cell culture medium was added to the cells. Migration and invasion were monitored by measuring wound confluence every 3 h for a total of 72 h with the Incucyte LiveCell Imaging System. The graphs depict means +/- SEM from all technical replicates obtained from three independent experiments. Efficient knockdown of RSK1 and RSK2 as well as efficient decrease of L-plastin Ser5 phosphorylation were confirmed by immunoblot analysis (quantifications included in Figure 4.2.8). Adapted from (Lommel et al., 2015).

Moreover, we investigated whether endogenous RSK activity affects actin, L-plastin and Ser5 phosphorylated L-plastin localisation in migrating cells. To this end, SK-BR-3 cells were plated on glass coverslips coated with fibronectin and at approximately 90% confluence a wound was scratched. Immunofluorescent staining of L-plastin, Ser5 phosphorylated L-plastin and actin was performed after EGF treatment with or without prior treatment with the RSK inhibitor BI-D1870 in cells migrating into the scratched wound. As a result we

observed that EGF treatment led to an increased formation of ruffling membranes, microspikes and even longer filopodia-like structures embedded in the cortical region of the cell, all of which are structures playing a role in cell migration. Strikingly, L-plastin was highly enriched in these structures. Interestingly, RSK inhibition with BI-D1870 treatment prior to EGF stimulation did not abolish, but clearly reduced the formation of these migratory structures and the redistribution of L-plastin to these structures. Ser5 phosphorylated L-plastin could only be visualised in the cells following EGF treatment and was also found in ruffling membranes and in microspikes. The staining for Ser5 phosphorylated L-plastin completely disappeared with RSK inhibition. The same experiment was performed with BT-20 cells and led to similar conclusions although the phenotype was less obvious as these cells display a less well-organised actin cytoskeleton at all tested conditions (data not shown). Altogether, these results indicate a qualitative link between L-plastin Ser5 phosphorylation by RSK and its localisation to migratory structures upon EGF stimulation.

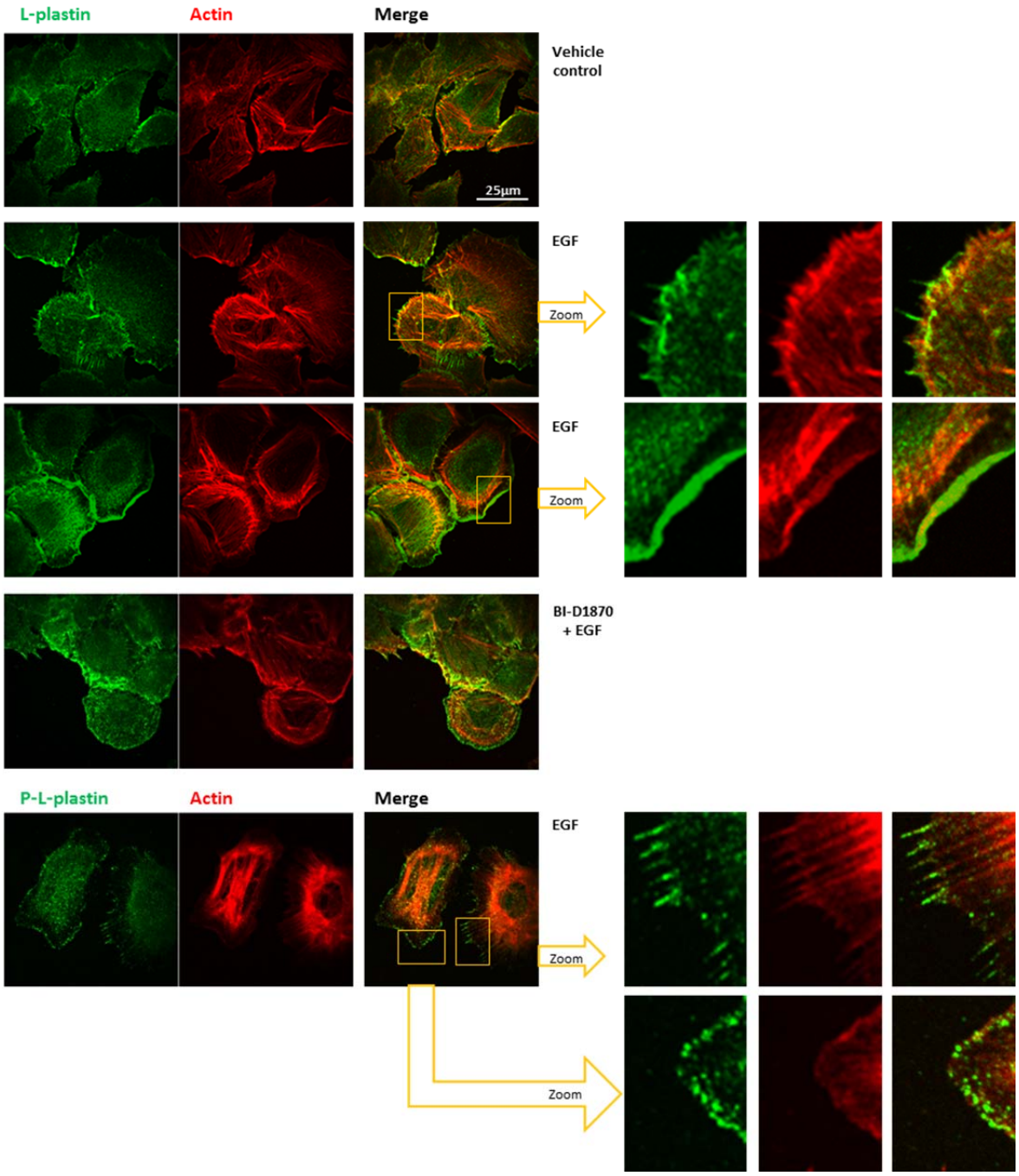

Figure 4.3.2 L-plastin Ser5 phosphorylation and localisation in migratory structures upon EGF stimulation is dependent on RSK activity. SK-BR-3 cells were plated on fibronectin-coated coverslips and were serum-starved for 24h. At approximately 90% confluence a wound was scratched with a micropipette tip and cells were subsequently treated with vehicle or EGF (100 ng/ml) with or without prior treatment with BI-D1870 (5 µM). 1 h following treatment, the coverslips were fixed and subsequently stained with phalloidin and an antibody specific for L-plastin or Ser5 phosphorylated L-plastin (anti-Ser5-*P* antibody, P-L-plastin) before being analysed by confocal microscopy. The scale bar shown represents 25 µm. Adapted from (Lommel et al., 2015).

4.4 L-plastin interaction partners

4.4.1 GFP-Trap followed by immunoblotting

In osteoclasts, L-plastin has been found to induce the formation of actin aggregates functioning as a core in the recruitment of signalling molecules (Ma et al., 2010) which suggests that L-plastin may act as a scaffolding protein. Indeed, L-plastin has been shown to form a complex with cortactin in MCF7 cells (Al Tanoury et al., 2010). Cortactin is an actin filament-binding protein that connects signalling pathways to cytoskeleton restructuring for migration and invasion (Lai et al., 2009). It is found in lamellipodia, invadopodia, podosomes, and at intercellular contact sites (El Sayegh et al., 2004; Linder and Aepfelbacher, 2003). Cortactin is a major substrate of the tyrosine kinase Src (Wu et al., 1991) and previous pulldown assays performed in our lab have pointed to an interaction of L-plastin with Src in HEK cells (Al Tanoury, 2009). These preliminary pulldown results prompted us to perform coimmunoprecipitation experiments using the GFP-Trap assay (Rothbauer et al., 2008) in HEK cells. This assay makes use of bead-linked monovalent lama antibodies directed against GFP and allows fast and efficient purification of GFP fusion proteins and their associated complexes formed in the cell. HEK cells transiently expressing GFP, L-plastinWT-GFP, L-plastinSA-GFP (unphosphorylatable L-plastin variant due to substitution of Ser5 into alanine) or L-plastinSE-GFP (mimics L-plastin phosphorylation by the substitution of Ser5 into glutamic acid) were harvested and precipitated with the GFP-Trap beads followed by immunoblot analysis. The GFP-Trap efficiently precipitated the GFP fusion proteins from cell extracts (Figure 4.4.1). Importantly, immunoblot analysis revealed that Src efficiently coprecipitated with all L-plastin variants for all treatment conditions (Figure 4.4.1), indicating that L-plastin is present in a complex with Src and that this interaction is independent of the PMA treatment and the phosphorylation status of L-plastin. Ser5 phosphorylation is thus not required for binding of Src. These data suggest that L-plastin may play a role in the assembly of signalling complexes, containing cortactin and Src kinase, two proteins known to promote cell invasiveness.

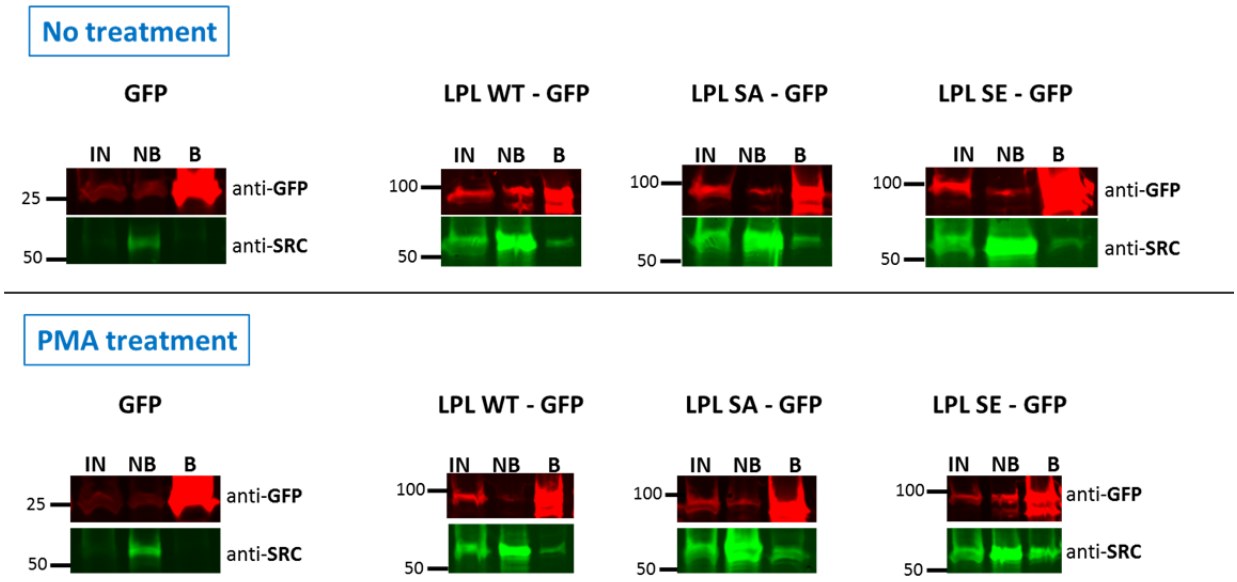

Figure 4.4.1. Coimmunoprecipitation of GFP fusion proteins in HEK cells. HEK cells transfected with GFP or L-plastin-GFP variants were treated with 0.1 µM PMA for 1 h at 37°C as indicated. Following cell lysis, protein extracts were subjected to immunoprecipitation with GFP-Trap. Aliquots of input (In), non-bound (NB) and bound (B) fractions were separated by SDS-PAGE and visualised by immunoblot analysis using GFP- and Src-specific antibodies.

4.4.2 GFP-Trap followed by mass spectrometry

In order to identify further interaction partners of L-plastin, we performed mass spectrometry experiments in collaboration with Prof. Christophe Ampe and Prof. Kris Gevaert from the University of Ghent, in the framework of the PRIME-XS consortium.

Stable isotope labelling by amino acids in cell culture (SILAC) of HEK cells was performed. Four cultures of HEK cells were grown in light medium containing the natural isotype amino acids ^{12}C arginine and ^{12}C lysine and one culture of HEK was grown in heavy medium containing ^{13}C arginine and ^{13}C lysine (Figure 4.4.2). After thirteen days of culture, three light cultures were transfected with GFP and the remaining cultures (one light and one heavy) were transfected with the construct of interest (Figure 4.4.2). This procedure was performed for two constructs of interest: L-plastinWT-GFP and L-plastinSE-GFP. This was meant to allow the identification of L-plastin binding partners and to determine whether some partners only bind to one of these two constructs. In that case, the binding would depend on the phosphorylation status of L-plastin. For each of these two experiments we performed five immunoprecipitations using GFP-Trap and afterwards the precipitates were mixed. The resulting mixture was then analysed by LC-MS/MS in order to determine the ratio of the ^{12}C

and ^{13}C peptides of the identified proteins. A ratio of 4 light to 1 heavy represents unspecific binding to GFP and to L-plastin-GFP and a ratio of 1 light to 1 heavy represents specific binding to L-plastin-GFP only (Figure 4.4.2).

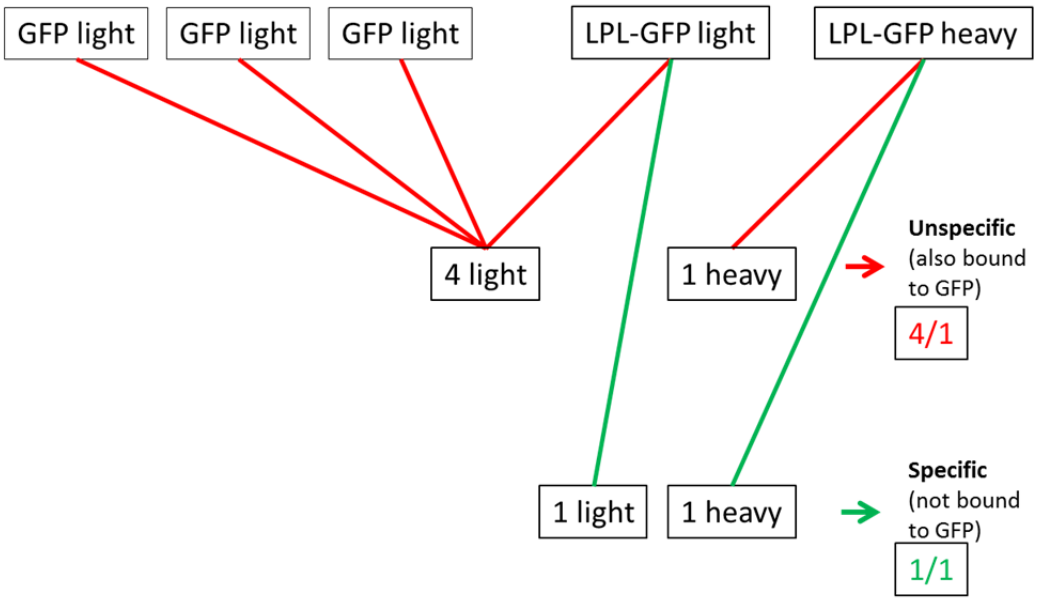

Figure 4.4.2. SILAC labelling performed in HEK cells for the identification of L-plastin binding partners. Four cultures of HEK cells were grown in light medium and one was grown in heavy medium. After a cultivation period of thirteen days, three light cultures were transfected with GFP and one light and one heavy culture were transfected with L-plastin-GFP. Five immunoprecipitations using GFP-Trap were subsequently mixed and analysed by LC-MS/MS to determine the ratio of light and heavy peptides of the identified proteins.

For L-plastinWT-GFP only L-plastin was identified in the 1/1 ratio distribution and for L-plastinSE-GFP, L-plastin and also prothymosin α were identified in the 1/1 ratio distribution (Table 4.5.2). Prothymosin α is a 12.5 kDa protein with a highly conserved primary structure and a wide cellular distribution. It has been described to suppress cell proliferation (Kobayashi et al., 2006). Prothymosin α can also be found in the blood and its extracellular functions include cytokine-like, antiviral, antifungal and anti-ischemic activities (Mosoian, 2011). Prothymosin α was shown to be overexpressed in different cancer types but it was also reported to exhibit anticancer activity (Shiau et al., 2001). Our result that this protein interacts with L-plastin is highly interesting but deserves further investigation and validation.

Two other proteins, heterogeneous nuclear ribonucleoprotein M (HNRPM) and β-actin, displayed one peptide with good ratios indicating their binding to L-plastinSE (Table 4.4.2). Even though these proteins only had one peptide found in the 1/1 ratio distribution, the fact that we know that β-actin is a partner of L-plastin strengthens the prothymosin α data and

supports a possible interaction between HNRPM and L-plastin which however also needs further validation.

For the L-plastinWT experiment it seems that the incorporation of the SILAC labels has not functioned properly, thus explaining the lack of identification of interaction partners. For the L-plastinSE experiment a shift in the ratios was observed so that ratios indicating a specific interaction are around 0.5 instead of 1.

Full lists of proteins identified with the mass spectrometry analysis can be found in the appendix.

Table 4.4.2 L-plastin interaction partners identified by LC-MS/MS.

L-plastinWT interaction peptides

accession	description	sequence	ratio
P13796	PLSL_HUMAN Plastin-2 OS=Homo sapiens GN=LCP1 PE=1 SV=6	NH2-IGNFSTDIK<c13>DSK<c13>-COOH	0,928
		NH2-AYYHLLEQVAPK<c13>-COOH	1,002
		NH2-AYYHLLEQVAPK-COOH	1,002
		NH2-VNK<c13>PPYPK<c13>-COOH	1,031
			1,031
		NH2-VNKPPYPK-COOH	1,031
			1,031
		NH2-TENLNDDEK<c13>LNNAK<c13>-COOH	0,908
		NH2-TENLNDDEKLNNAK-COOH	0,908
			0,928

L-plastinSE interaction peptides

accession	description	sequence	ratio
P06454	PTMA_HUMAN Prothymosin alpha OS=Homo sapiens GN=PTMA PE=1 SV=2	Ace-SDAAVDTSSEITTK<c13>-COOH	0,563
		NH2-RAAEDDEDDDVDTK-COOH	0,672
P13796	PLSL_HUMAN Plastin-2 OS=Homo sapiens GN=LCP1 PE=1 SV=6	NH2-IGNFSTDIK<c13>DSK<c13>-COOH	0,509
		NH2-AYYHLLEQVAPK-COOH	0,565
		NH2-VNK<c13>PPYPK<c13>-COOH	0,520
			0,520
			0,520
		NH2-VNKPPYPK-COOH	0,520
			0,520
		NH2-ISTSLPVLDLIDAIQPGSINYDLLK<c13>-COOH	0,581
			0,581
			0,579
		NH2-ISTSLPVLDLIDAIQPGSINYDLLK-COOH	0,579
		NH2-TENLNDDEK<c13>LNNAK<c13>-COOH	0,508
		NH2-VYALPEDLVEVNPK<c13>-COOH	0,563
		NH2-VYALPEDLVEVNPK-COOH	0,563
P52272	HNRPM_HUMAN Heterogeneous nuclear ribonucleoprotein M OS=Homo sapiens GN=HNRNPM PE=1 SV=3	Ace-AAGVEAAAEVAATEIK<c13>-COOH	0,574
P60709	ACTB_HUMAN Actin, cytoplasmic 1 OS=Homo sapiens GN=ACTB PE=1 SV=1	NH2-HQGVMVGMGQK<c13>-COOH	0,703

Chapter 5 Discussion and perspectives

5.1 Discussion

Parts of the discussion section are taken from a manuscript which can be found in the appendix and which was recently published in The FASEB Journal: *L-plastin Ser5 phosphorylation in breast cancer cells and in vitro is mediated by RSK downstream of the ERK/MAPK pathway (Lommel et al., 2015)*.

Previous studies by our group have shown that the phosphorylation of L-plastin on residue Ser5 increases the F-actin-binding and -bundling activity of L-plastin (Al Tanoury et al., 2010; Janji et al., 2006). Furthermore, L-plastin Ser5 phosphorylation was shown to be essential for cell invasion and metastasis formation (Janji et al., 2006; Klemke et al., 2007; Riplinger et al., 2014). The signalling pathways leading to L-plastin Ser5 phosphorylation being unclear, this thesis focused on unravelling the signalling pathways leading to L-plastin Ser5 phosphorylation in breast cancer cells.

Even though PKC, PKA and PI3K were shown to be involved in L-plastin Ser5 phosphorylation in different studies, mainly PKC seems to mediate L-plastin Ser5 phosphorylation in cancer cells (Al Tanoury et al., 2010; Janji et al., 2010). This observation led us to initially focus on investigating the implication of PKC in our four breast cancer cell lines. Indeed we could show a role for PKC in this phosphorylation event by diverse experiments. Notably, L-plastin Ser5 phosphorylation was increased by the PKC activator PMA and this increase was prevented by the PKC inhibitor GF109203X in all four breast cancer cell lines. Moreover, also the PKC activator endothelin increased L-plastin Ser5 phosphorylation in HEK cells. In addition, constitutively active PKCδ was shown to increase this phosphorylation in HEK cells and knockdown of endogenous PKCδ decreased this phosphorylation in BT-20 and MDA-MB-435S cells. Nevertheless, as we showed that PKC knockdown was not decreasing L-plastin Ser5 phosphorylation in SK-BR-3 cells and as an *in vitro* kinase assay could not show direct phosphorylation of L-plastin Ser5 by PKC, we concluded that other kinases must be responsible for this phosphorylation event and we emitted the hypothesis that signalling pathways leading to this phosphorylation might be cell type-dependent.

Following these observations and knowing that also PKA has been described in the literature to be involved in L-plastin Ser5 phosphorylation in cells of the immune system (Janji et al., 2006; Matsushima et al., 1987; Wang and Brown, 1999), in HEK cells (Janji et al., 2006) and *in vitro* (Janji et al., 2006; Wang and Brown, 1999), we also investigated the involvement of this protein kinase in L-plastin Ser5 phosphorylation in our four model breast cancer cell lines. Interestingly, the PKA activator 8-Bromo-cAMP only weakly increased L-plastin Ser5 phosphorylation in BT-20 cells and did not increase L-plastin Ser5 phosphorylation in MCF7, SK-BR-3 and MDA-MB-435S cells. Interestingly, even though PKA seems to play a less important role than PKC in L-plastin Ser5 phosphorylation in breast cancer cells, our results also point to a crosstalk between these two kinases in this phosphorylation event. Indeed, PKA inhibition prevented PKC activation-mediated increase in L-plastin Ser5 phosphorylation in all four breast cancer cell lines.

To further investigate such a potential crosstalk between PKC and PKA, we took the approach of analysing PKA substrate phosphorylation upon PKA or PKC stimulation. We found that the phosphorylation of PKA substrates was not only increased with the PKA activator 8-Bromo-cAMP but also with the PKC activator PMA which could be an indication that PKC is an upstream activator of PKA. Another less plausible explanation would be that PMA does not only activate PKC but also PKA. However, even though PMA is a widely used PKC activator, PMA-dependent PKA activation has never been described in the literature. Furthermore in that case the phosphorylation of PKA substrates should not decrease with PMA+GF compared to PMA alone, assuming that GF is specific for PKC and has no effect on PKA. However, we observe such a decrease for all four cell lines. A further explanation could be that the antibody we are using does not only recognise phosphorylated PKA but also PKC substrates. Even though this is likely to occur it is probably not the only reason for our observation that phosphorylated PKA substrates increase with the PKC activator PMA. If this observation was due to the recognition of phosphorylated PKC then we would not expect a considerable decrease upon PMA+H89 treatment compared to PMA alone which we observe in all four cell lines. Overall, the most likely scenario is that PKC is an upstream activator of PKA.

In the literature, crosstalks of PKC and PKA have already been suggested for other cell types but the detailed mechanisms of this interplay remained unclear (Fricke et al., 2004; Mau et al., 1997; Motzkus et al., 2000; Sugita et al., 1997; Yao et al., 2008). Our hypothesis that PKC acts upstream of PKA was further validated by a probabilistic Boolean network

modelling approach applying two different strategies. First, an *in silico* knockout study and second, a study analysing optimised selection probability weights of all interactions, demonstrated the importance of the PKC-PKA crosstalk and indicated that in all four cell lines the interaction appears to be directed from PKC to PKA rather than from PKA to PKC.

As pulldown experiments performed by a former group member Ziad Al Tanoury (Al Tanoury, 2009) and GFP-Trap co-immunoprecipitation performed by myself suggest that L-plastin interacts with the proto-oncogene tyrosine protein kinase Src, we investigated whether Src would be indirectly involved in L-plastin Ser5 phosphorylation. Indeed, L-plastin Ser5 phosphorylation was increased following transfection with constitutively active v-Src in all four model cell lines and decreased upon Src inhibition with three different inhibitors in SK-BR-3, BT-20 and MDA-MB-435S cells but not in MCF7 cells. Src being a tyrosine kinase, it cannot be responsible for direct L-plastin Ser5 phosphorylation. Our results thus suggest that Src acts upstream of the serine kinases responsible for L-plastin Ser5 phosphorylation. In addition, this observation is in line with the suggestion of Ma and colleagues (Ma et al., 2010) that L-plastin might act as a scaffolding protein functioning as a core in the recruitment of signalling molecules.

As we found that L-plastin Ser5 phosphorylation correlates with the invasive capacity of breast cancer cell lines, we chose to take a whole genome microarray-based gene expression profiling approach to compare cells with differential L-plastin Ser5 phosphorylation in order to detect underlying differences in signal transduction pathways. In the context of the cofilin pathway in breast cancer invasion and metastasis (Wang et al., 2007a), the authors have pointed out that not only individual genes, but whole pathways with differential regulation and activity states of the corresponding molecules should be taken into account for phenotype interpretation. Similarly, in our study the whole genome microarray analysis approach allowed us to identify three canonical pathways enriched in DEGs, namely ERK/MAPK signalling, UVA-induced MAPK signalling and role of osteoblasts, osteoclasts and chondrocytes in rheumatoid arthritis. The latter pathway can only be linked to cancer progression in the broadest sense considering that both cancer and rheumatoid arthritis involve inflammation but this pathway cannot explain differential L-plastin Ser5 phosphorylation. UVA-induced MAPK signalling, in contrast to UVB and UVC-induced signalling, involves ERK/MAPK signalling (Zhong et al., 2011). Our microarray experiment thus reveals two out of three pathways which involve the prominent ERK/MAPK signalling pathway and thereby indicates a role for this pathway in L-plastin Ser5 phosphorylation. In

addition, the *in vitro* kinase assay screen carried out in parallel identified the ERK/MAPK pathway downstream kinases RSK1 and RSK2 as the most prominent candidate kinases for L-plastin Ser5 phosphorylation. This kinase screening was performed on N-terminal L-plastin peptides with the initiator methionine removed and the subsequent alanine acetylated as this co-translational modification was described by the UniProtKB/Swiss-Prot database (www.uniprot.org). Nevertheless we also included non-modified peptides in order to make sure that this difference does not completely change the ability of the kinases to phosphorylate L-plastin peptides. Indeed a similar ranking was observed for kinases phosphorylating peptides with or without this N-terminal modification. However, peptides containing the initiator methionine displayed much higher radioactivity counts for almost all kinases than peptides without methionine but with acetylated alanine in the N-terminal part. This could be explained by the fact that acetylation of the alanine residue abolishes the amine group at the N-terminus and converts a basic amino acid into a neutral one. Most kinases prefer to have basic amino acids in the -3 position and to a lesser extent in the -2 and -4 positions before the phosphor-acceptor residue (Rust and Thompson, 2011). Even though the methionine is at the -4 position which is less influential, it still exhibits a free amine and a positive charge and might still improve substrate recognition by most protein kinases.

All these findings together with a previous report describing L-plastin as an ERK/MAPK pathway-regulated protein (Lewis et al., 2000) prompted us to proceed to an in-depth investigation of this pathway, whose deregulation has also been associated with breast cancer progression (Whyte et al., 2009). Several approaches were used to unravel the involvement of the ERK/MAPK pathway with its downstream kinases RSK1 and RSK2 in the L-plastin Ser5 phosphorylation event. To trigger this pathway we stimulated the cells with EGF or with PMA, both described as activators of the ERK/MAPK pathway. Evidence for an involvement of the ERK/MAPK pathway downstream kinases RSK1 and RSK2 in L-plastin Ser5 phosphorylation was provided both by an siRNA knockdown approach and by the use of two different RSK inhibitors BI-D1870 and SL0101. This reduces the probability that the observed inhibitor-dependent decrease of phosphorylation is due to off-target effects. Indeed, BI-D1870 and SL0101 have only one common off-target, Aurora B (Bain et al., 2007), which demonstrated considerably weaker potency in phosphorylating L-plastin peptides than RSK1 or RSK2 as shown by the *in vitro* kinase assays from KINEXUS (Table 4.2.3). Most importantly, the two kinases RSK1 as well as RSK2 were able to directly phosphorylate the recombinant L-plastin protein on residue Ser5 in an *in vitro* kinase assay. Further evidence for the importance of the ERK/MAPK pathway is provided by the data

obtained with the MEK inhibitor PD98059 as well as with the clinically used MEK inhibitor Trametinib. Moreover, our finding that L-plastin Ser5 phosphorylation can be mediated by RSK upon activation of the ERK/MAPK pathway was confirmed by our computational model.

The applied PBN modelling approach revealed to be a very useful method to deepen our understanding of signalling pathways upstream of L-plastin Ser5 phosphorylation in our four breast cancer cell lines. This model allowed us to calculate normalised steady-state values that fit our extensive set of normalised experimental data and that give us quantitative information on the importance of all interactions included in our signalling network. This quantitative outcome of the PBN modelling study allowed us to corroborate our initial hypothesis that RSK is an important activator of L-plastin in breast cancer cells and that this signal can be modulated by an upstream crosstalk directed from PKC to PKA.

In an effort to correlate invasiveness and concomitant L-plastin Ser5 phosphorylation with RSK expression and activity, we found that higher RSK1 and RSK2 protein levels in invasive versus non-invasive cells seem to largely correlate with higher baseline L-plastin Ser5 phosphorylation in invasive versus non-invasive cells. However, we were not able to correlate the invasive status of breast cancer cell lines and thus differential L-plastin Ser5 phosphorylation levels with differential RSK activities. Since it is known from the literature that multiple phosphorylation events are required for the activation of RSKs, the antibody used to detect P-RSK was chosen in order to reveal the last phosphorylation step (phosphorylated serine residues 221 and 227 of RSK1 and RSK2 respectively) by PDK1 which is required for full activation of RSK1/2 and subsequent substrate phosphorylation. Even though this antibody is described to recognise phosphorylated forms of RSK1 and RSK2, the company does not specify whether it also recognises the phosphorylated form of RSK3 (RSK4 does not need phosphorylation of this residue to be active). Furthermore, it should be considered that myristoylation of RSK and its translocation to the plasma membrane have also been described to be necessary for maximal activation of RSKs (Richards et al., 2001). These factors should be taken into account when analysing the existence of a correlation between RSK activities and L-plastin Ser5 phosphorylation level. Most importantly, it cannot be excluded that L-plastin might also be phosphorylated by other kinases in addition to RSKs.

Although our results provide strong evidence for a role of the ERK/MAPK pathway with the downstream kinases RSK1 and RSK2 being able to directly phosphorylate L-plastin on

residue Ser5, they do not rule out that L-plastin Ser5 phosphorylation can also be mediated by other pathways. As mentioned before, until now mainly PKA (Janji et al., 2006; Wang and Brown, 1999) and PKC (Al Tanoury et al., 2010; Freeley et al., 2012; Janji et al., 2010; Jones et al., 1998; Lin et al., 1998; Paclet et al., 2004; Pazdrak et al., 2011) have been reported to play a role in L-plastin Ser5 phosphorylation. Even though siRNA-mediated knockdowns of PKCδ (Al Tanoury et al., 2010; Janji et al., 2010) and PKCβII (Pazdrak et al., 2011) reduced L-plastin Ser5 phosphorylation, it has to be taken into account that most studies were based on activation and/or inhibition studies. Strikingly, all inhibitors (H89, GF109203X, Gö6976 and Ro-31-8220) used to demonstrate the involvement of PKA and PKC in L-plastin Ser5 phosphorylation also strongly inhibit RSK2 (Alessi, 1997; Davies et al., 2000). Moreover, PMA used as a PKC activator does not only activate PKC but has also been shown to activate the ERK1/2 pathway either through PKC and c-Src or through RasGRP (Amos et al., 2005; Brose and Rosenmund, 2002; Kazanietz, 2000). Finally, the effect of the PKA activator cAMP on the ERK1/2 pathway appears to depend on the cellular context since cAMP has been demonstrated to activate ERK in a B-Raf dependent manner or to suppress ERK signalling in many cells through its ability to target C-Raf (reviewed in (Dumaz and Marais, 2005)). Altogether these observations imply that findings about L-plastin Ser5 phosphorylation revealed by activation and inhibition studies only, may have to be reconsidered keeping in mind the important off-target effects of the used inhibitors and especially the fact that they all unspecifically inhibit RSK2. In line with this, our computational model suggests that activation of L-plastin by RSK is largely predominant as compared to its activation by PKC or PKA. This result is in line with previous findings of Hagi and collaborators who reported that cAMP stimulation was not able to trigger L-plastin Ser5 phosphorylation in macrophages (Hagi et al., 2006).

Regarding a potential involvement of the PI3K/AKT pathway in the phosphorylation of L-plastin Ser5 in breast cancer cells, future studies which were out of the scope of the present work, have to be dedicated to the investigation of this prominent signalling pathway. Indeed, our *in vitro* kinase screening assays on L-plastin peptides have revealed further kinases, which are downstream effectors of the PI3K/AKT pathway, to be able to phosphorylate L-plastin Ser5. These include serum and glucocorticoid- regulated kinases 2 and 3 (SGK2 and SGK3) as well as p70 ribosomal protein S6 kinase (p70S6K), a kinase with substantial homology to the NTKD of RSK. It is interesting to note that the ERK/MAPK and the PI3K/AKT pathways interact at several levels and cannot be considered as linear signalling pathways (Mendoza et al., 2011). Moreover, this crosstalk has a high significance in cancer therapeutics. As a high proportion of human cancers display oncogenic mutations

in ras (Bos, 1989), the inhibition of the ras downstream target MEK was tested in the clinic and in patient-derived xenograft models with unfortunately deceiving results (Sun et al., 2014). This lack of response is thought to arise from feedback activation of pathways that circumvent the roadblock imposed by the drug. This can occur through loss of negative-feedback regulation which is mediated through direct phosphorylation of almost all components of the RTK-RAS-MAPK cascade by ERK (Lito et al., 2013). In addition, MEK inhibition causes a transcriptional upregulation of both ErbB2 and ErbB3 with the formation of active ErbB1-ErbB3 and ErbB2-ErbB3 complexes that activate downstream PI3K/AKT and ERK/MAPK signalling (Sun et al., 2014). Thus MEK inhibition results on the one hand in a reduction of pERK and on the other hand in an increase of pAKT (Mirzoeva et al., 2009; Sun et al., 2014). As both AKT and ERK routes are involved in the inactivation of pro-apoptotic proteins and thus in proliferation, and as the inhibition of one pathway was shown to result in compensatory activation of the other pathway, the inhibition of only one of these pathways is not sufficient to reduce proliferation (Sun et al., 2014). Combination therapies have notably been shown to have synergistic cellular effects in breast cancer with combined MEK and PI3K inhibition (Mirzoeva et al., 2009) and in non-small cell lung cancer and colorectal cancer with combined MEK and ErbB2 and ErbB1 inhibition (Sun et al., 2014). The effect of such combination therapies in the clinic remains to be tested. It also remains to be investigated whether L-plastin Ser5 phosphorylation is a target of the ERK/MAPK pathway only or also of the PI3K/AKT pathway.

RSKs have been described as versatile regulators controlling migration and invasion downstream of ERK/MAPK activation (Sulzmaier and Ramos, 2013) by altering the transcription of many genes involved in epithelial to mesenchymal transition, by regulating cell adhesion through phosphorylation events with subsequent modulation of integrin activity and/or by remodelling the actin cytoskeleton. Notably, RSK2 expression has been correlated to the expression of the actin-bundling protein fascin in head and neck squamous cell carcinoma and to filopodia formation (Li et al., 2013). RSK2 phosphorylates the transcription factor CREB which upregulates the transcription of fascin and thereby increases filopodia formation and actin-bundling providing a proinvasive and prometastatic advantage to human cancers. In our study, both RSK1 and RSK2 were able to phosphorylate the actin-bundling protein L-plastin and combined knockdown of the two isoforms led to a clear decrease in cell migration and invasion. In addition, we showed that L-plastin phosphorylation and localisation in migratory structures upon EGF stimulation is linked to RSK activity. The identification of the actin-bundling protein L-plastin as a new target of RSK kinases consolidates the role of these kinases in the regulation of the actin cytoskeleton. Our results

extend the findings of Doehn and colleagues, who investigated the effects of RSK1 and RSK2 on migration and invasion in epithelial breast cells and showed that combined knockdown of RSK1 and RSK2 or the use of RSK inhibitors suppressed the ERK pathway-dependent induction of promotile and proinvasive genes (Doehn et al., 2009).

Interestingly, RSK2 has been described to phosphorylate a further actin-binding protein, filamin A (Ohta and Hartwig, 1996), on residue Ser2152 (Woo et al., 2004). This RSK-dependent phosphorylation was shown to promote filamin A binding to β integrin tails (Gawecka et al., 2012) which leads to inhibition of cell adhesion through integrin inactivation (Gawecka et al., 2012; Vial and McKeown-Longo, 2012). Furthermore, the phosphorylation of filamin A and the subsequent inactivation of integrins was shown to be involved in EGF-induced cell migration (Gawecka et al., 2012; Woo et al., 2004). In our work we have revealed that L-plastin is phosphorylated by RSK and that RSK activity is important for the recruitment of L-plastin to migratory structures and for migration and invasion. Overall, we suggest that the effect of RSK knockdown on the promotile capacities of cancer cells may also be due, at least in part, to the decrease of L-plastin phosphorylation on Ser5, comparable to the decrease of filamin A-dependent cell migration observed upon RSK inhibition. We thus speculate whether L-plastin, similarly to filamin A, was able to modulate integrin activation. In this regard it is interesting to note that also L-plastin was described to interact with β1 and β2 integrin subunits (Le Goff et al., 2010). Our preliminary results show that L-plastin indeed reduces integrin activation and we intend to deepen the investigation of L-plastin effects on integrin affinity in future studies (see under 5.2 Perspectives).

To our knowledge our results show the first evidence for the involvement of the ERK/MAPK pathway in L-plastin Ser5 phosphorylation in breast cancer cells. These findings corroborate Ser5 phosphorylated L-plastin as a molecular marker for invasive carcinomas with deregulated ERK/MAPK pathway signalling.

One could also make a slightly more daring consideration regarding a potential therapeutic application of our findings. L-plastin Ser5 phosphorylation was shown to promote invasion in HEK and melanoma cells as well as to increase *in vivo* metastasis formation in melanoma (Janji et al., 2006; Klemke et al., 2007; Riplinger et al., 2014). It remains to be established whether this link is also observed in breast cancer. In cancers where this link between L-plastin Ser5 phosphorylation and cancer cell invasion and metastasis can be confirmed, blocking of L-plastin Ser5 phosphorylation could be a potential cancer therapy. As we have

identified RSK kinases to be responsible for this phosphorylation, inhibition of these kinases could be helpful to reduce L-plastin Ser5 phosphorylation and thereby invasion and metastasis formation. Our identification of a new RSK1 and RSK2 kinase substrate which is involved in invasion and metastasis, consolidates the formerly described role of these kinases in cancer progression (Anjum and Blenis, 2008). In contrast to MEK and Raf, RSKs are not “global regulators” and thus their inhibition by therapeutic drugs may have less severe side effects. Knowing that RSKs are overexpressed in approximately 50% of human breast cancer tissues (Smith et al., 2005), this kinase family could be considered as a highly promising therapeutic drug target in certain invasive carcinomas.

Alternatively, nanobodies could be used to directly inhibit L-plastin Ser5 phosphorylation. Nanobodies are the smallest functional fragment of a naturally occurring single chain antibody (15 kDa) and similarly to conventional antibodies they have high target specificity and affinity and low inherent toxicity. Advantages include their small size, high stability and ease of production. In contrast to knockdown approaches, nanobodies do not eradicate protein expression but only target one specific protein domain and thus only inhibit a particular function. A team of the University of Ghent led by Prof. Gettemans has produced such nanobodies targeting L-plastin and has shown that two nanobodies were able to consistently delay and reduce CD3/CD28-stimulated L-plastin Ser5 phosphorylation in Jurkat T cells (De Clercq et al., 2013b). The same nanobodies however did not affect PMA-stimulated L-plastin Ser5 phosphorylation in THP-1 cells (De Clercq et al., 2013a) indicating that distinct pathways occur in distinct cell types and/or with distinct stimulators. Moreover, one of the nanobodies efficient to block L-plastin Ser5 phosphorylation in Jurkat cells also strongly inhibited actin-bundling by L-plastin which subsequently inhibited filopodia formation, motility, and invasion upon transfection into PC-3 prostate cancer cells (Delanote et al., 2010). In breast cancer cells, the effects of such nanobodies on L-plastin Ser5 phosphorylation, on actin-bundling and on subsequent migration and invasion capacities remain to be investigated. Ideally, nanobodies could be developed further into a therapeutic drug to block L-plastin Ser5 phosphorylation and related invasion. Nanobodies have already proven to be successful in the treatment of diverse diseases including epidermoid carcinoma (Roovers et al., 2007) where intra-peritoneally administered nanobodies directed against the EGFR reduced tumor growth in mice. So far, the use of nanobodies has not yet been approved for disease treatment, but several clinical trials using nanobodies are ongoing in phases I and II (http://ablynx.com/rd-portfolio/overview/).

Another option for targeting L-plastin-dependent invasion could be to inhibit L-plastin-dependent actin-bundling with small molecule inhibitors. A similar strategy targeting another actin-bundling protein, fascin, proved effective for reducing migration and invasion *in vitro* and metastasis formation *in vivo* (Huang et al., 2015). In contrast to microtubule proteins which have been successfully used as drug targets for decades, no actin cytoskeletal protein has yet been used clinically as therapeutic target for cancer treatment. Nevertheless, the study by Huang and colleagues points to the potential of using actin-binding proteins as novel targets for cancer treatment. They identified a small molecule inhibitor against the actin-bundling protein fascin which specifically inhibits the biochemical function of fascin to bundle actin filaments and thereby blocks the formation of filopodia. Similarly to L-plastin, fascin expression is low or absent in normal adult epithelial cells whereas elevated levels of fascin were found in many types of metastatic tumours and are correlated with a clinically aggressive phenotype, poor prognosis and shorter survival (Hashimoto et al., 2011; Machesky and Li, 2010; Tan et al., 2013). This fascin-targeting drug not only reduces breast tumour cell migration and invasion *in vitro* but also lung metastases of 4T1 mouse breast tumour cells and MDA-MB-231 human breast tumour cells *in vivo* by approximately 95% (Huang et al., 2015). This strongly advocates the testing of such inhibitors in clinical trials. L-plastin small molecule inhibitors would need to be identified and to be tested regarding their effect on metastasis reduction *in vivo*. In addition to small molecule inhibitors, the use of the above-described nanobodies targeting L-plastin function could also be of interest as such molecules have been shown to directly inhibit F-actin-bundling or to prevent L-plastin activation (De Clercq et al., 2013a; Delanote et al., 2010).

5.2 Perspectives

Our work has demonstrated that ERK/MAPK signalling leads to Ser5 phosphorylation of L-plastin. Since our *in vitro* kinase assay screening however also indicates that some selected downstream kinases of the PI3K/AKT pathway potentially phosphorylate L-plastin Ser5, it will be interesting to investigate if this phosphorylation can also result from alternative signalling pathways, in particular from the prominent PI3K/AKT signalling pathway. An expanded PBN study will be applied to analyse the role of this pathway in addition to the ERK/MAPK pathway upstream of the L-plastin Ser5 phosphorylation event. EGF, hepatocyte growth factor and insulin-like growth factor or cell adhesion onto fibronectin and collagen via integrins will be used to stimulate the activation of the PI3K/AKT and ERK/MAPK pathways and key signalling molecules of these pathways will be inhibited. Subsequently L-plastin Ser5 phosphorylation will be monitored together with further output nodes such as activated ERK,

RSK, FAK and AKT. Based on the generated data, the model will allow making quantitative predictions on the relevance of interactions within the network leading to the identification and validation of key signalling molecules important for L-plastin Ser5 phosphorylation. Such an approach will allow us to establish whether L-plastin Ser5 phosphorylation, in addition to the ERK/MAPK signalling pathway, is also a target of the PI3K/AKT pathway and will reveal whether Ser5 phosphorylated L-plastin can serve as a molecular marker for the deregulation of only one or of both signalling pathways involved in cancer progression.

Moreover, the L-plastin Ser5 phosphorylation state is planned to be analysed in breast cancer patient tissues to confirm the results obtained in cells and to validate Ser5 phosphorylated L-plastin as a diagnostic or prognostic marker. Immunohistochemistry on breast cancer tissue samples would allow us to analyse the expression of L-plastin, the L-plastin Ser5 phosphorylation state, the presence and activity of key signalling molecules of the signal transduction network and of the candidate kinases for L-plastin Ser5 phosphorylation. These experiments would also enable us to investigate whether a link exists between our results and the molecular subtype and clinicopathological parameters of the analysed breast cancer samples. A collaboration with the Integrated BioBank of Luxembourg has recently been established and the collection of breast cancer tissues is about to be started.

.

Importantly, we also need to check whether the observed effects of RSK knockdown on migration and invasion are indeed due to the decrease in L-plastin Ser5 phosphorylation or due to another RSK-dependent mechanism. A possibility to investigate this would be to use the existing L-plastin-specific nanobodies to block L-plastin Ser5 phosphorylation and to analyse L-plastin Ser5 phosphorylation-dependent migration and invasion in breast cancer cells. This is planned in the framework of a collaboration with Prof. Gettemans from University of Ghent.

A further interesting follow-up of this work would be to test and extend our findings in a mouse model. In this regard we could use human breast tumour cells in which L-plastin or L-plastin Ser5 phosphorylation is inhibited (f.ex. by stable RSK shRNA expression or by stable L-plastin-targeting nanobody expression) and analyse whether they lead to a lower formation of metastatic lesions upon injection in mice. Alternatively, we could treat mice injected with human breast cancer cells with RSK inhibitors, L-plastin targeting nanobodies or small

molecule inhibitors against L-plastin (to be identified) and then monitor metastasis formation compared to non-treated mice.

Moreover, we intend to confirm the results obtained by mass spectrometry by pulldown, immunoprecipitation, GFP-Nanotrap and/or mitochondrial targeting experiments and we also plan to repeat the whole experiment as we had some technical issues preventing us from detecting interaction partners of L-plastinWT.

And finally, as described in the discussion section, we investigated whether L-plastin was able to modulate integrin activity. In order to determine the effect of L-plastin and L-plastin phosphorylation variants on the activation state of integrin αIIbβ3, we took advantage of CHO cells expressing either human αIIbβ3WT at the resting state or mutant human αIIbβ3T562N in a constitutively active state (Kashiwagi et al., 1999; Salsmann et al., 2005). Following transient transfection of GFP, L-plastinWT-GFP, L-plastinS5A-GFP (unphosphorylatable) or L-plastinS5E-GFP (phosphomimic), we compared the binding of the activation-specific mAb PAC-1 as well as of a β3-specific or a αIIbβ3-specific mAb to the transfected cells. As shown in Figure 5.2, neither the transfection of L-plastinWT nor the transfection of the phosphomutants was able to activate integrin αIIbβ3WT. In contrast, the expression of L-plastin considerably reduced PAC-1 binding to CHO αIIbβ3T562N cells, and thus decreased αIIbβ3 integrin activity. The effect was even clearer for the L-plastin phosphomutants than for L-plastinWT. Even though these preliminary results will need to be confirmed, they point to a link between L-plastin expression and the integrin activity state. As a follow-up of this experiment it would be interesting to use other constitutively active integrin variants with mutations in distinct localisations than the extracellular β3 localisation of the αIIbβ3T562N mutant. We could notably use the intracellular αIIbβ3D723A mutation which disturbs salt bridge formation between residues β3D723 and αIIbR995 restraining the integrin in the inactive state. In case of a mutation in this area, the integrin complex is found to be activated. This mutant would be of particular interest with regard to the results of Le Goff et al. reporting an interaction between L-plastin and the cytoplasmic domain of integrin β1 and β2 (Le Goff et al., 2010). Furthermore it would be interesting to use different L-plastin fragments in order to identify which part of L-plastin is required for integrin binding and affinity modulation.

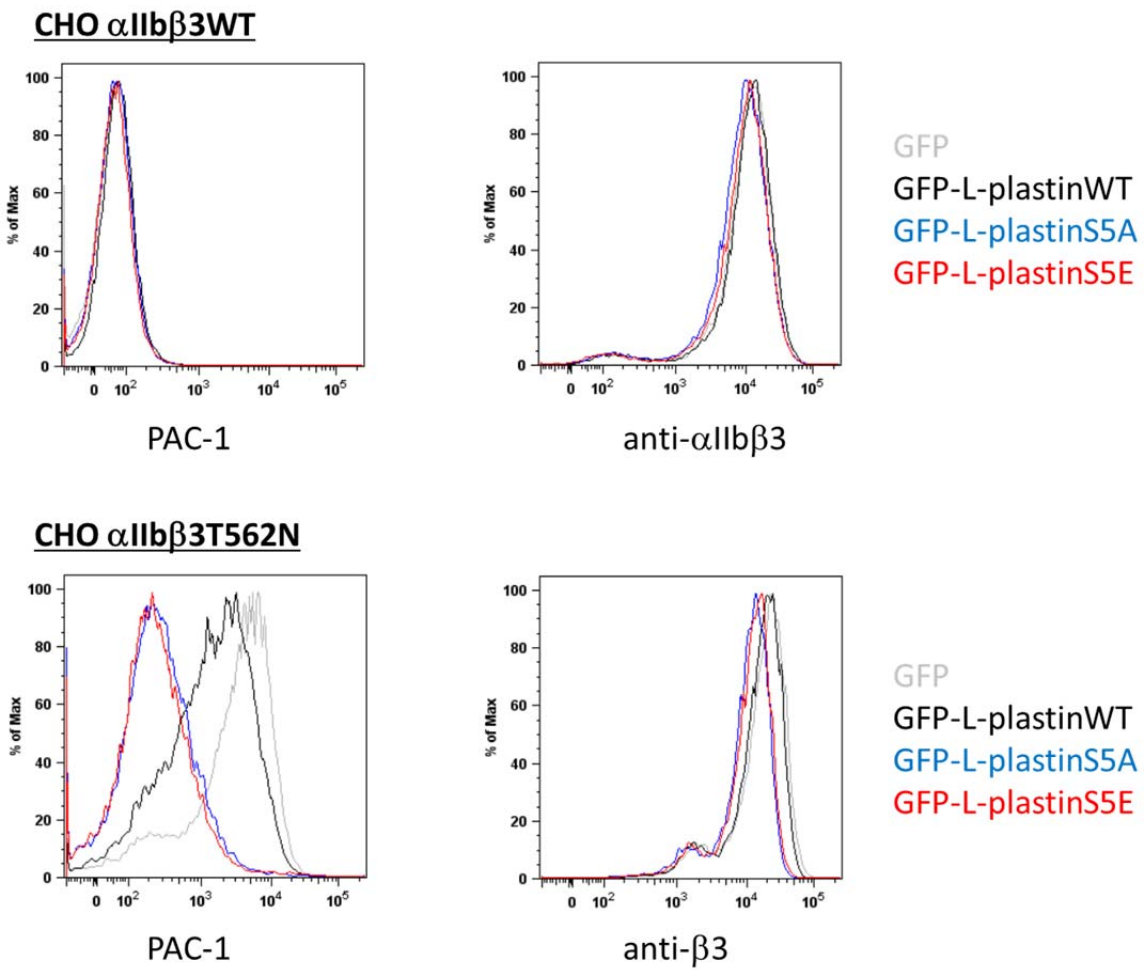

Figure 5.2 The ectopic expression of human L-plastin into CHO cells affects the activity state of a constitutively active αIIbβ3 integrin mutant. CHO cells expressing either human αIIbβ3WT at the resting state or mutant human αIIbβ3T562N in a constitutively active state were transiently transfected with GFP, L-plastinWT-GFP, L-plastinS5A-GFP or L-plastinS5E-GFP. Binding of the activation-specific mAb PAC-1 as well as of a β3-specific or αIIbβ3-specific mAb was measured by flow cytometry.

References

Adams, A.E., W. Shen, C.S. Lin, J. Leavitt, and P. Matsudaira. 1995. Isoform-specific complementation of the yeast sac6 null mutation by human fimbrin. *Molecular and cellular biology*. 15:69-75.

Al Tanoury, Z. 2009. The role of L-plastin in the assembly of the cortical cytoskeleton and progression of cancer cells. *In* Life Sciences Research Unit. University of Strasbourg, University of Luxembourg

Al Tanoury, Z., E. Schaffner-Reckinger, A. Halavatyi, C. Hoffmann, M. Moes, E. Hadzic, M. Catillon, M. Yatskou, and E. Friederich. 2010. Quantitative kinetic study of the actin-bundling protein L-plastin and of its impact on actin turn-over. *PLoS One*. 5:e9210.

Alberts B., A. Johnson, J. Lewis, M. Raff, K. Roberts, and P. Walter. 2008. Molecular Biology of the Cell. Garland Science.

Alessi, D.R. 1997. The protein kinase C inhibitors Ro 318220 and GF 109203X are equally potent inhibitors of MAPKAP kinase-1beta (Rsk-2) and p70 S6 kinase. *FEBS letters*. 402:121-123.

Ammer, A.G., and S.A. Weed. 2008. Cortactin branches out: roles in regulating protrusive actin dynamics. *Cell Motil Cytoskeleton*. 65:687-707.

Amos, S., P.M. Martin, G.A. Polar, S.J. Parsons, and I.M. Hussaini. 2005. Phorbol 12-myristate 13-acetate induces epidermal growth factor receptor transactivation via protein kinase Cdelta/c-Src pathways in glioblastoma cells. *J Biol Chem*. 280:7729-7738.

Ang, C.S., and E.C. Nice. 2010. Targeted in-gel MRM: a hypothesis driven approach for colorectal cancer biomarker discovery in human feces. *J Proteome Res*. 9:4346-4355.

Anjum, R., and J. Blenis. 2008. The RSK family of kinases: emerging roles in cellular signalling. *Nature reviews. Molecular cell biology*. 9:747-758.

Arpin, M., E. Friederich, M. Algrain, F. Vernel, and D. Louvard. 1994. Functional differences between L- and T-plastin isoforms. *J Cell Biol*. 127:1995-2008.

Arteaga, C.L., M.X. Sliwkowski, C.K. Osborne, E.A. Perez, F. Puglisi, and L. Gianni. 2012. Treatment of HER2-positive breast cancer: current status and future perspectives. *Nature reviews. Clinical oncology*. 9:16-32.

Artym, V.V., K. Matsumoto, S.C. Mueller, and K.M. Yamada. 2011. Dynamic membrane remodeling at invadopodia differentiates invadopodia from podosomes. *European journal of cell biology*. 90:172-180.

Artym, V.V., Y. Zhang, F. Seillier-Moiseiwitsch, K.M. Yamada, and S.C. Mueller. 2006. Dynamic interactions of cortactin and membrane type 1 matrix metalloproteinase at invadopodia: defining the stages of invadopodia formation and function. *Cancer Res*. 66:3034-3043.

Babb, S.G., P. Matsudaira, M. Sato, I. Correia, and S.S. Lim. 1997. Fimbrin in podosomes of monocyte-derived osteoclasts. *Cell Motil Cytoskeleton*. 37:308-325.

Bailly, M., and J. Condeelis. 2002. Cell motility: insights from the backstage. *Nat Cell Biol*. 4:E292-294.

Bain, J., L. Plater, M. Elliott, N. Shpiro, C.J. Hastie, H. McLauchlan, I. Klevernic, J.S. Arthur, D.R. Alessi, and P. Cohen. 2007. The selectivity of protein kinase inhibitors: a further update. *Biochem J*. 408:297-315.

Behrens, J., K.M. Weidner, U.H. Frixen, J.H. Schipper, M. Sachs, N. Arakaki, Y. Daikuhara, and W. Birchmeier. 1991. The role of E-cadherin and scatter factor in tumor invasion and cell motility. *Exs*. 59:109-126.

Benjamini, Y., and Y. Hochberg. 1995. Controlling the False Discovery Rate: A Practical and Powerful Approach to Multiple Testing. *Journal of the Royal Statistical Society. Series B (Methodological)*. 57:289-300.

Bhattacharyya, R.P., A. Remenyi, B.J. Yeh, and W.A. Lim. 2006. Domains, motifs, and scaffolds: the role of modular interactions in the evolution and wiring of cell signaling circuits. *Annual review of biochemistry*. 75:655-680.

Biondi, R.M., and A.R. Nebreda. 2003. Signalling specificity of Ser/Thr protein kinases through docking-site-mediated interactions. *Biochem J*. 372:1-13.

Blake, R.A., P. Garcia-Paramio, P.J. Parker, and S.A. Courtneidge. 1999. Src promotes PKCdelta degradation. *Cell growth & differentiation : the molecular biology journal of the American Association for Cancer Research*. 10:231-241.

Block, M.R., C. Badowski, A. Millon-Fremillon, D. Bouvard, A.P. Bouin, E. Faurobert, D. Gerber-Scokaert, E. Planus, and C. Albiges-Rizo. 2008. Podosome-type adhesions and focal adhesions, so alike yet so different. *European journal of cell biology*. 87:491-506.

Bos, J.L. 1989. ras oncogenes in human cancer: a review. *Cancer Res*. 49:4682-4689.

Brandt, D., M. Gimona, M. Hillmann, H. Haller, and H. Mischak. 2002. Protein kinase C induces actin reorganization via a Src- and Rho-dependent pathway. *J Biol Chem*. 277:20903-20910.

Brandt, D.T., A. Goerke, M. Heuer, M. Gimona, M. Leitges, E. Kremmer, R. Lammers, H. Haller, and H. Mischak. 2003. Protein kinase C delta induces Src kinase activity via activation of the protein tyrosine phosphatase PTP alpha. *J Biol Chem*. 278:34073-34078.

Bravo-Cordero, J.J., L. Hodgson, and J. Condeelis. 2012. Directed cell invasion and migration during metastasis. *Current opinion in cell biology*. 24:277-283.

Bretscher, A. 1981. Fimbrin is a cytoskeletal protein that crosslinks F-actin in vitro. *Proc Natl Acad Sci U S A*. 78:6849-6853.

Brose, N., and C. Rosenmund. 2002. Move over protein kinase C, you've got company: alternative cellular effectors of diacylglycerol and phorbol esters. *Journal of cell science*. 115:4399-4411.

Brown, N.R., M.E. Noble, J.A. Endicott, and L.N. Johnson. 1999. The structural basis for specificity of substrate and recruitment peptides for cyclin-dependent kinases. *Nat Cell Biol*. 1:438-443.

Burgess, A.W., H.S. Cho, C. Eigenbrot, K.M. Ferguson, T.P. Garrett, D.J. Leahy, M.A. Lemmon, M.X. Sliwkowski, C.W. Ward, and S. Yokoyama. 2003. An open-and-shut case? Recent insights into the activation of EGF/ErbB receptors. *Molecular cell*. 12:541-552.

Burgstaller, G., and M. Gimona. 2004. Actin cytoskeleton remodelling via local inhibition of contractility at discrete microdomains. *Journal of cell science*. 117:223-231.

Burness, M.L., T.A. Grushko, and O.I. Olopade. 2010. Epidermal growth factor receptor in triple-negative and basal-like breast cancer: promising clinical target or only a marker? *Cancer J*. 16:23-32.

Burns, S., A.J. Thrasher, M.P. Blundell, L. Machesky, and G.E. Jones. 2001. Configuration of human dendritic cell cytoskeleton by Rho GTPases, the WAS protein, and differentiation. *Blood*. 98:1142-1149.

Cai, Z., A. Bettaieb, N.E. Mahdani, L.G. Legres, R. Stancou, J. Masliah, and S. Chouaib. 1997. Alteration of the sphingomyelin/ceramide pathway is associated with resistance of human breast carcinoma MCF7 cells to tumor necrosis factor-alpha-mediated cytotoxicity. *J Biol Chem*. 272:6918-6926.

Cargnello, M., and P.P. Roux. 2011. Activation and function of the MAPKs and their substrates, the MAPK-activated protein kinases. *Microbiology and molecular biology reviews : MMBR*. 75:50-83.

Chafel, M.M., W. Shen, and P. Matsudaira. 1995. Sequential expression and differential localization of I-, L-, and T-fimbrin during differentiation of the mouse intestine and yolk sac. *Dev Dyn*. 203:141-151.

Chaijan, S., S. Roytrakul, A. Mutirangura, and K. Leelawat. 2014. Matrigel induces L-plastin expression and promotes L-plastin-dependent invasion in human cholangiocarcinoma cells. *Oncology letters*. 8:993-1000.

Chambers, A.F. 2009. MDA-MB-435 and M14 cell lines: identical but not M14 melanoma? *Cancer Res*. 69:5292-5293.

Chen, H., A. Mocsai, H. Zhang, R.X. Ding, J.H. Morisaki, M. White, J.M. Rothfork, P. Heiser, E. Colucci-Guyon, C.A. Lowell, H.D. Gresham, P.M. Allen, and E.J. Brown. 2003. Role for plastin in host defense distinguishes integrin signaling from cell adhesion and spreading. *Immunity*. 19:95-104.

Chen, R.H., C. Sarnecki, and J. Blenis. 1992. Nuclear localization and regulation of erk- and rsk-encoded protein kinases. *Molecular and cellular biology*. 12:915-927.

Cohen, P. 2000. The regulation of protein function by multisite phosphorylation--a 25 year update. *Trends in biochemical sciences*. 25:596-601.

Collin, O., S. Na, F. Chowdhury, M. Hong, M.E. Shin, F. Wang, and N. Wang. 2008. Self-organized podosomes are dynamic mechanosensors. *Current biology : CB*. 18:1288-1294.

Collin, O., P. Tracqui, A. Stephanou, Y. Usson, J. Clement-Lacroix, and E. Planus. 2006. Spatiotemporal dynamics of actin-rich adhesion microdomains: influence of substrate flexibility. *Journal of cell science*. 119:1914-1925.

Condeelis, J., R.H. Singer, and J.E. Segall. 2005. The great escape: when cancer cells hijack the genes for chemotaxis and motility. *Annual review of cell and developmental biology*. 21:695-718.

Correia, I., D. Chu, Y.H. Chou, R.D. Goldman, and P. Matsudaira. 1999. Integrating the actin and vimentin cytoskeletons. adhesion-dependent formation of fimbrin-vimentin complexes in macrophages. *J Cell Biol*. 146:831-842.

Dalby, K.N., N. Morrice, F.B. Caudwell, J. Avruch, and P. Cohen. 1998. Identification of regulatory phosphorylation sites in mitogen-activated protein kinase (MAPK)-activated protein kinase-1a/p90rsk that are inducible by MAPK. *J Biol Chem*. 273:1496-1505.

Davies, S.P., H. Reddy, M. Caivano, and P. Cohen. 2000. Specificity and mechanism of action of some commonly used protein kinase inhibitors. *Biochem J*. 351:95-105.

De Antonellis, P., M. Carotenuto, J. Vandenbussche, G. De Vita, V. Ferrucci, C. Medaglia, I. Boffa, A. Galiero, S. Di Somma, D. Magliulo, N. Aiese, A. Alonzi, D. Spano, L. Liguori, C. Chiarolla, A. Verrico, J.H. Schulte, P. Mestdagh, J. Vandesompele, K. Gevaert, and M. Zollo. 2014. Early targets of miR-34a in neuroblastoma. *Molecular & cellular proteomics : MCP*. 13:2114-2131.

de Arruda, M.V., S. Watson, C.S. Lin, J. Leavitt, and P. Matsudaira. 1990. Fimbrin is a homologue of the cytoplasmic phosphoprotein plastin and has domains homologous with calmodulin and actin gelation proteins. *J Cell Biol*. 111:1069-1079.

De Clercq, S., C. Boucherie, J. Vandekerckhove, J. Gettemans, and A. Guillabert. 2013a. L-plastin nanobodies perturb matrix degradation, podosome formation, stability and lifetime in THP-1 macrophages. *PLoS One*. 8:e78108.

De Clercq, S., O. Zwaenepoel, E. Martens, J. Vandekerckhove, A. Guillabert, and J. Gettemans. 2013b. Nanobody-induced perturbation of LFA-1/L-plastin

phosphorylation impairs MTOC docking, immune synapse formation and T cell activation. *Cellular and molecular life sciences : CMLS*. 70:909-922.

Deady, L.E., E.M. Todd, C.G. Davis, J.Y. Zhou, N. Topcagic, B.T. Edelson, T.W. Ferkol, M.A. Cooper, J.T. Muenzer, and S.C. Morley. 2014. L-plastin is essential for alveolar macrophage production and control of pulmonary pneumococcal infection. *Infection and immunity*. 82:1982-1993.

Delanote, V., K. Van Impe, V. De Corte, E. Bruyneel, G. Vetter, C. Boucherie, M. Mareel, J. Vandekerckhove, E. Friederich, and J. Gettemans. 2005a. Molecular basis for dissimilar nuclear trafficking of the actin-bundling protein isoforms T- and L-plastin. *Traffic*. 6:335-345.

Delanote, V., J. Vandekerckhove, and J. Gettemans. 2005b. Plastins: versatile modulators of actin organization in (patho)physiological cellular processes. *Acta Pharmacol Sin*. 26:769-779.

Delanote, V., B. Vanloo, M. Catillon, E. Friederich, J. Vandekerckhove, and J. Gettemans. 2010. An alpaca single-domain antibody blocks filopodia formation by obstructing L-plastin-mediated F-actin bundling. *FASEB J*. 24:105-118.

Denning, M.F., A.A. Dlugosz, M.K. Howett, and S.H. Yuspa. 1993. Expression of an oncogenic rasHa gene in murine keratinocytes induces tyrosine phosphorylation and reduced activity of protein kinase C delta. *J Biol Chem*. 268:26079-26081.

Destaing, O., F. Saltel, J.C. Geminard, P. Jurdic, and F. Bard. 2003. Podosomes display actin turnover and dynamic self-organization in osteoclasts expressing actin-green fluorescent protein. *Mol Biol Cell*. 14:407-416.

Doehn, U., C. Hauge, S.R. Frank, C.J. Jensen, K. Duda, J.V. Nielsen, M.S. Cohen, J.V. Johansen, B.R. Winther, L.R. Lund, O. Winther, J. Taunton, S.H. Hansen, and M. Frodin. 2009. RSK is a principal effector of the RAS-ERK pathway for eliciting a coordinate promotile/invasive gene program and phenotype in epithelial cells. *Molecular cell*. 35:511-522.

dos Remedios, C.G., and D. Chhabra. 2008. Actin-Binding Proteins and Disease. Vol. 8. C.G. Dos Remedios and D. Chhabra, editors. Springer Verlag-New York. 348.

dos Remedios, C.G., D. Chhabra, M. Kekic, I.V. Dedova, M. Tsubakihara, D.A. Berry, and N.J. Nosworthy. 2003. Actin binding proteins: regulation of cytoskeletal microfilaments. *Physiological reviews*. 83:433-473.

Dovas, A., J.C. Gevrey, A. Grossi, H. Park, W. Abou-Kheir, and D. Cox. 2009. Regulation of podosome dynamics by WASp phosphorylation: implication in matrix degradation and chemotaxis in macrophages. *Journal of cell science*. 122:3873-3882.

Dubey, M., A.K. Singh, D. Awasthi, S. Nagarkoti, S. Kumar, W. Ali, T. Chandra, V. Kumar, M.K. Barthwal, K. Jagavelu, F.J. Sanchez-Gomez, S. Lamas, and M. Dikshit. 2015. L-Plastin S-glutathionylation promotes reduced binding to beta-actin and affects neutrophil functions. *Free radical biology & medicine*. 86:1-15.

Dumaz, N., and R. Marais. 2005. Integrating signals between cAMP and the RAS/RAF/MEK/ERK signalling pathways. Based on the anniversary prize of the Gesellschaft fur Biochemie und Molekularbiologie Lecture delivered on 5 July 2003 at the Special FEBS Meeting in Brussels. *The FEBS journal*. 272:3491-3504.

Dummler, B.A., C. Hauge, J. Silber, H.G. Yntema, L.S. Kruse, B. Kofoed, B.A. Hemmings, D.R. Alessi, and M. Frodin. 2005. Functional characterization of human RSK4, a new 90-kDa ribosomal S6 kinase, reveals constitutive activation in most cell types. *J Biol Chem*. 280:13304-13314.

Eccles, S.A. 2011. The epidermal growth factor receptor/Erb-B/HER family in normal and malignant breast biology. *The International journal of developmental biology*. 55:685-696.

Eckert, M.A., T.M. Lwin, A.T. Chang, J. Kim, E. Danis, L. Ohno-Machado, and J. Yang. 2011. Twist1-induced invadopodia formation promotes tumor metastasis. *Cancer cell*. 19:372-386.

El Sayegh, T.Y., P.D. Arora, C.A. Laschinger, W. Lee, C. Morrison, C.M. Overall, A. Kapus, and C.A. McCulloch. 2004. Cortactin associates with N-cadherin adhesions and mediates intercellular adhesion strengthening in fibroblasts. *Journal of cell science*. 117:5117-5131.

Ellison, G., T. Klinowska, R.F. Westwood, E. Docter, T. French, and J.C. Fox. 2002. Further evidence to support the melanocytic origin of MDA-MB-435. *Molecular pathology : MP*. 55:294-299.

Engers, R., and H.E. Gabbert. 2000. Mechanisms of tumor metastasis: cell biological aspects and clinical implications. *Journal of cancer research and clinical oncology*. 126:682-692.

Foley, J., N.K. Nickerson, S. Nam, K.T. Allen, J.L. Gilmore, K.P. Nephew, and D.J. Riese, 2nd. 2010. EGFR signaling in breast cancer: bad to the bone. *Seminars in cell & developmental biology*. 21:951-960.

Foran, E., P. McWilliam, D. Kelleher, D.T. Croke, and A. Long. 2006. The leukocyte protein L-plastin induces proliferation, invasion and loss of E-cadherin expression in colon cancer cells. *Int J Cancer*. 118:2098-2104.

Foulds, L. 1954. The experimental study of tumor progression: a review. *Cancer Res*. 14:327-339.

Frederick, L., X.Y. Wang, G. Eley, and C.D. James. 2000. Diversity and frequency of epidermal growth factor receptor mutations in human glioblastomas. *Cancer Res*. 60:1383-1387.

Freeley, M., F. O'Dowd, T. Paul, D. Kashanin, A. Davies, D. Kelleher, and A. Long. 2012. L-plastin regulates polarization and migration in chemokine-stimulated human T lymphocytes. *J Immunol*. 188:6357-6370.

Fricke, K., A. Heitland, and E. Maronde. 2004. Cooperative activation of lipolysis by protein kinase A and protein kinase C pathways in 3T3-L1 adipocytes. *Endocrinology*. 145:4940-4947.

Frodin, M., and S. Gammeltoft. 1999. Role and regulation of 90 kDa ribosomal S6 kinase (RSK) in signal transduction. *Molecular and cellular endocrinology*. 151:65-77.

Galiegue-Zouitina, S., S. Quief, M.P. Hildebrand, C. Denis, L. Detourmignies, J.L. Lai, and J.P. Kerckaert. 1999. Nonrandom fusion of L-plastin(LCP1) and LAZ3(BCL6) genes by t(3;13)(q27;q14) chromosome translocation in two cases of B-cell non-Hodgkin lymphoma. *Genes, chromosomes & cancer*. 26:97-105.

Galkin, V.E., A. Orlova, O. Cherepanova, M.C. Lebart, and E.H. Egelman. 2008. High-resolution cryo-EM structure of the F-actin-fimbrin/plastin ABD2 complex. *Proc Natl Acad Sci U S A*. 105:1494-1498.

Gaszner, B., M. Nyitrai, N. Hartvig, T. Koszegi, B. Somogyi, and J. Belagyi. 1999. Replacement of ATP with ADP affects the dynamic and conformational properties of actin monomer. *Biochemistry*. 38:12885-12892.

Gatesman, A., V.G. Walker, J.M. Baisden, S.A. Weed, and D.C. Flynn. 2004. Protein kinase Calpha activates c-Src and induces podosome formation via AFAP-110. *Molecular and cellular biology*. 24:7578-7597.

Gawecka, J.E., S.S. Young-Robbins, F.J. Sulzmaier, M.J. Caliva, M.M. Heikkila, M.L. Matter, and J.W. Ramos. 2012. RSK2 protein suppresses integrin activation and fibronectin matrix assembly and promotes cell migration. *J Biol Chem*. 287:43424-43437.

Giganti, A., J. Plastino, B. Janji, M. Van Troys, D. Lentz, C. Ampe, C. Sykes, and E. Friederich. 2005. Actin-filament cross-linking protein T-plastin increases Arp2/3-mediated actin-based movement. *Journal of cell science*. 118:1255-1265.

Gille, H., M. Kortenjann, O. Thomae, C. Moomaw, C. Slaughter, M.H. Cobb, and P.E. Shaw. 1995. ERK phosphorylation potentiates Elk-1-mediated ternary complex formation and transactivation. *EMBO J*. 14:951-962.

Gimona, M., R. Buccione, S.A. Courtneidge, and S. Linder. 2008. Assembly and biological role of podosomes and invadopodia. *Current opinion in cell biology*. 20:235-241.

Goldstein, D., J. Djeu, G. Latter, S. Burbeck, and J. Leavitt. 1985. Abundant synthesis of the transformation-induced protein of neoplastic human fibroblasts, plastin, in normal lymphocytes. *Cancer Res*. 45:5643-5647.

Gould, K.L., J.R. Woodgett, J.A. Cooper, J.E. Buss, D. Shalloway, and T. Hunter. 1985. Protein kinase C phosphorylates pp60src at a novel site. *Cell*. 42:849-857.

Griendling, K.K., T. Tsuda, and R.W. Alexander. 1989. Endothelin stimulates diacylglycerol accumulation and activates protein kinase C in cultured vascular smooth muscle cells. *J Biol Chem*. 264:8237-8240.

Gschwendt, M., K. Kielbassa, W. Kittstein, and F. Marks. 1994. Tyrosine phosphorylation and stimulation of protein kinase C delta from porcine spleen by src in vitro. Dependence on the activated state of protein kinase C delta. *FEBS letters*. 347:85-89.

Gyorffy, B., A. Lanczky, A.C. Eklund, C. Denkert, J. Budczies, Q. Li, and Z. Szallasi. 2010. An online survival analysis tool to rapidly assess the effect of 22,277 genes on breast cancer prognosis using microarray data of 1,809 patients. *Breast cancer research and treatment*. 123:725-731.

Hagi, A., H. Hirata, and H. Shinomiya. 2006. Analysis of a bacterial lipopolysaccharide-activated serine kinase that phosphorylates p65/L-plastin in macrophages. *Microbiology and immunology*. 50:331-335.

Haleem-Smith, H., E.Y. Chang, Z. Szallasi, P.M. Blumberg, and J. Rivera. 1995. Tyrosine phosphorylation of protein kinase C-delta in response to the activation of the high-affinity receptor for immunoglobulin E modifies its substrate recognition. *Proc Natl Acad Sci U S A*. 92:9112-9116.

Halilovic, E., and D.B. Solit. 2008. Therapeutic strategies for inhibiting oncogenic BRAF signaling. *Current opinion in pharmacology*. 8:419-426.

Hanahan, D., and R.A. Weinberg. 2000. The hallmarks of cancer. *Cell*. 100:57-70.

Hanahan, D., and R.A. Weinberg. 2011. Hallmarks of cancer: the next generation. *Cell*. 144:646-674.

Harris, L.D., J. De La Cerda, T. Tuziak, D. Rosen, L. Xiao, Y. Shen, A.L. Sabichi, B. Czerniak, and H.B. Grossman. 2008. Analysis of the expression of biomarkers in urinary bladder cancer using a tissue microarray. *Mol Carcinog*. 47:678-685.

Hashimoto, Y., D.J. Kim, and J.C. Adams. 2011. The roles of fascins in health and disease. *J Pathol*. 224:289-300.

Hasselblatt, M., C. Bohm, L. Tatenhorst, V. Dinh, D. Newrzella, K. Keyvani, A. Jeibmann, H. Buerger, C.H. Rickert, and W. Paulus. 2006. Identification of novel diagnostic markers for choroid plexus tumors: a microarray-based approach. *The American journal of surgical pathology*. 30:66-74.

Henning, S.W., S.C. Meuer, and Y. Samstag. 1994. Serine phosphorylation of a 67-kDa protein in human T lymphocytes represents an accessory receptor-mediated signaling event. *J Immunol*. 152:4808-4815.

Holland, P.M., and J.A. Cooper. 1999. Protein modification: docking sites for kinases. *Current biology : CB*. 9:R329-331.

Hollestelle, A., J.H. Nagel, M. Smid, S. Lam, F. Elstrodt, M. Wasielewski, S.S. Ng, P.J. French, J.K. Peeters, M.J. Rozendaal, M. Riaz, D.G. Koopman, T.L. Ten Hagen, B.H. de Leeuw, E.C. Zwarthoff, A. Teunisse, P.J. van der Spek, J.G. Klijn, W.N. Dinjens, S.P. Ethier, H. Clevers, A.G. Jochemsen, M.A. den Bakker, J.A. Foekens, J.W. Martens, and M. Schutte. 2010. Distinct gene mutation profiles among luminal-type and basal-type breast cancer cell lines. *Breast cancer research and treatment*. 121:53-64.

Hollestelle, A., and M. Schutte. 2009. Comment Re: MDA-MB-435 and M14 cell lines: identical but not M14 Melanoma? *Cancer Res*. 69:7893.

Holt, J.R., and D.P. Corey. 2000. Two mechanisms for transducer adaptation in vertebrate hair cells. *Proc Natl Acad Sci U S A*. 97:11730-11735.

Hoshino, R., Y. Chatani, T. Yamori, T. Tsuruo, H. Oka, O. Yoshida, Y. Shimada, S. Ari-i, H. Wada, J. Fujimoto, and M. Kohno. 1999. Constitutive activation of the 41-/43-kDa mitogen-activated protein kinase signaling pathway in human tumors. *Oncogene*. 18:813-822.

Hu, S., T. Biben, X. Wang, P. Jurdic, and J.C. Geminard. 2011. Internal dynamics of actin structures involved in the cell motility and adhesion: Modeling of the podosomes at the molecular level. *Journal of theoretical biology*. 270:25-30.

Huang, F.K., S. Han, B. Xing, J. Huang, B. Liu, F. Bordeleau, C.A. Reinhart-King, J.J. Zhang, and X.Y. Huang. 2015. Targeted inhibition of fascin function blocks tumour invasion and metastatic colonization. *Nature communications*. 6:7465.

Hubbard, S.R. 1997. Crystal structure of the activated insulin receptor tyrosine kinase in complex with peptide substrate and ATP analog. *EMBO J*. 16:5572-5581.

Huse, M., and J. Kuriyan. 2002. The conformational plasticity of protein kinases. *Cell*. 109:275-282.

Hynes, N.E., and G. MacDonald. 2009. ErbB receptors and signaling pathways in cancer. *Current opinion in cell biology*. 21:177-184.

Janji, B., A. Giganti, V. De Corte, M. Catillon, E. Bruyneel, D. Lentz, J. Plastino, J. Gettemans, and E. Friederich. 2006. Phosphorylation on Ser5 increases the F-actin-binding activity of L-plastin and promotes its targeting to sites of actin assembly in cells. *Journal of cell science*. 119:1947-1960.

Janji, B., L. Vallar, Z. Al-Tanoury, F. Bernardin, G. Vetter, E. Schaffner-Reckinger, G. Berchem, E. Friederich, and S. Chouaib. 2010. The actin filament cross-linker L-plastin confers resistance to TNF-alpha in MCF-7 breast cancer cells in a phosphorylation-dependent manner. *J Cell Mol Med*. 14:1264-1275.

Johnson, L.N. 2009. The regulation of protein phosphorylation. *Biochemical Society transactions*. 37:627-641.

Jones, S.L., and E.J. Brown. 1996. FcgammaRII-mediated adhesion and phagocytosis induce L-plastin phosphorylation in human neutrophils. *J Biol Chem*. 271:14623-14630.

Jones, S.L., J. Wang, C.W. Turck, and E.J. Brown. 1998. A role for the actin-bundling protein L-plastin in the regulation of leukocyte integrin function. *Proc Natl Acad Sci U S A*. 95:9331-9336.

Jura, N., N.F. Endres, K. Engel, S. Deindl, R. Das, M.H. Lamers, D.E. Wemmer, X. Zhang, and J. Kuriyan. 2009. Mechanism for activation of the EGF receptor catalytic domain by the juxtamembrane segment. *Cell*. 137:1293-1307.

Kang, S., H.S. Shim, J.S. Lee, D.S. Kim, H.Y. Kim, S.H. Hong, P.S. Kim, J.H. Yoon, and N.H. Cho. 2010. Molecular proteomics imaging of tumor interfaces by mass spectrometry. *J Proteome Res*. 9:1157-1164.

Kao, J., K. Salari, M. Bocanegra, Y.L. Choi, L. Girard, J. Gandhi, K.A. Kwei, T. Hernandez-Boussard, P. Wang, A.F. Gazdar, J.D. Minna, and J.R. Pollack. 2009. Molecular

profiling of breast cancer cell lines defines relevant tumor models and provides a resource for cancer gene discovery. *PLoS One*. 4:e6146.

Kashiwagi, H., Y. Tomiyama, S. Tadokoro, S. Honda, M. Shiraga, H. Mizutani, M. Handa, Y. Kurata, Y. Matsuzawa, and S.J. Shattil. 1999. A mutation in the extracellular cysteine-rich repeat region of the beta3 subunit activates integrins alphaIIbbeta3 and alphaVbeta3. *Blood*. 93:2559-2568.

Kasza, K.E., F. Nakamura, S. Hu, P. Kollmannsberger, N. Bonakdar, B. Fabry, T.P. Stossel, N. Wang, and D.A. Weitz. 2009. Filamin A is essential for active cell stiffening but not passive stiffening under external force. *Biophysical journal*. 96:4326-4335.

Kazanietz, M.G. 2000. Eyes wide shut: protein kinase C isozymes are not the only receptors for the phorbol ester tumor promoters. *Mol Carcinog*. 28:5-11.

Kenny, P.A., G.Y. Lee, C.A. Myers, R.M. Neve, J.R. Semeiks, P.T. Spellman, K. Lorenz, E.H. Lee, M.H. Barcellos-Hoff, O.W. Petersen, J.W. Gray, and M.J. Bissell. 2007. The morphologies of breast cancer cell lines in three-dimensional assays correlate with their profiles of gene expression. *Molecular oncology*. 1:84-96.

Kim, D.S., Y.P. Choi, S. Kang, M.Q. Gao, B. Kim, H.R. Park, Y.D. Choi, J.B. Lim, H.J. Na, H.K. Kim, Y.P. Nam, M.H. Moon, H.R. Yun, D.H. Lee, W.M. Park, and N.H. Cho. 2010. Panel of candidate biomarkers for renal cell carcinoma. *J Proteome Res*. 9:3710-3719.

Kim, E.K., and E.J. Choi. 2010. Pathological roles of MAPK signaling pathways in human diseases. *Biochim Biophys Acta*. 1802:396-405.

Klein, M.G., W. Shi, U. Ramagopal, Y. Tseng, D. Wirtz, D.R. Kovar, C.J. Staiger, and S.C. Almo. 2004. Structure of the actin crosslinking core of fimbrin. *Structure*. 12:999-1013.

Klemke, M., M.T. Rafael, G.H. Wabnitz, T. Weschenfelder, M.H. Konstandin, N. Garbi, F. Autschbach, W. Hartschuh, and Y. Samstag. 2007. Phosphorylation of ectopically expressed L-plastin enhances invasiveness of human melanoma cells. *Int J Cancer*. 120:2590-2599.

Kobayashi, T., T. Wang, M. Maezawa, M. Kobayashi, S. Ohnishi, K. Hatanaka, S. Hige, Y. Shimizu, M. Kato, M. Asaka, J. Tanaka, M. Imamura, K. Hasegawa, Y. Tanaka, and R.K. Brachmann. 2006. Overexpression of the oncoprotein prothymosin alpha triggers a p53 response that involves p53 acetylation. *Cancer Res*. 66:3137-3144.

Korenbaum, E., and F. Rivero. 2002. Calponin homology domains at a glance. *Journal of cell science*. 115:3543-3545.

Lacroix, M., and G. Leclercq. 2004. Relevance of breast cancer cell lines as models for breast tumours: an update. *Breast cancer research and treatment*. 83:249-289.

Lai, F.P., M. Szczodrak, J. Block, J. Faix, D. Breitsprecher, H.G. Mannherz, T.E. Stradal, G.A. Dunn, J.V. Small, and K. Rottner. 2008. Arp2/3 complex interactions and actin network turnover in lamellipodia. *EMBO J*. 27:982-992.

Lai, F.P., M. Szczodrak, J.M. Oelkers, M. Ladwein, F. Acconcia, S. Benesch, S. Auinger, J. Faix, J.V. Small, S. Polo, T.E. Stradal, and K. Rottner. 2009. Cortactin promotes migration and platelet-derived growth factor-induced actin reorganization by signaling to Rho-GTPases. *Mol Biol Cell*. 20:3209-3223.

Land, H., L.F. Parada, and R.A. Weinberg. 1983. Cellular oncogenes and multistep carcinogenesis. *Science*. 222:771-778.

Lapillonne, A., O. Coue, E. Friederich, A. Nicolas, L. Del Maestro, D. Louvard, S. Robine, and X. Sastre-Garau. 2000. Expression patterns of L-plastin isoform in normal and carcinomatous breast tissues. *Anticancer research*. 20:3177-3182.

Le Goff, E., A. Vallentin, P.O. Harmand, G. Aldrian-Herrada, B. Rebiere, C. Roy, Y. Benyamin, and M.C. Lebart. 2010. Characterization of L-plastin interaction with beta integrin and its regulation by micro-calpain. *Cytoskeleton (Hoboken)*. 67:286-296.

Leavitt, J. 1994. Discovery and characterization of two novel human cancer-related proteins using two-dimensional gel electrophoresis. *Electrophoresis*. 15:345-357.

Lebart, M.C., F. Hubert, C. Boiteau, S. Venteo, C. Roustan, and Y. Benyamin. 2004. Biochemical characterization of the L-plastin-actin interaction shows a resemblance with that of alpha-actinin and allows a distinction to be made between the two actin-binding domains of the molecule. *Biochemistry*. 43:2428-2437.

Lee, J.C., I. Vivanco, R. Beroukhim, J.H. Huang, W.L. Feng, R.M. DeBiasi, K. Yoshimoto, J.C. King, P. Nghiemphu, Y. Yuza, Q. Xu, H. Greulich, R.K. Thomas, J.G. Paez, T.C. Peck, D.J. Linhart, K.A. Glatt, G. Getz, R. Onofrio, L. Ziaugra, R.L. Levine, S. Gabriel, T. Kawaguchi, K. O'Neill, H. Khan, L.M. Liau, S.F. Nelson, P.N. Rao, P. Mischel, R.O. Pieper, T. Cloughesy, D.J. Leahy, W.R. Sellers, C.L. Sawyers, M. Meyerson, and I.K. Mellinghoff. 2006. Epidermal growth factor receptor activation in glioblastoma through novel missense mutations in the extracellular domain. *PLoS medicine*. 3:e485.

Lehmann, B.D., and J.A. Pietenpol. 2014. Identification and use of biomarkers in treatment strategies for triple-negative breast cancer subtypes. *J Pathol*. 232:142-150.

Leighton, I.A., K.N. Dalby, F.B. Caudwell, P.T. Cohen, and P. Cohen. 1995. Comparison of the specificities of p70 S6 kinase and MAPKAP kinase-1 identifies a relatively specific substrate for p70 S6 kinase: the N-terminal kinase domain of MAPKAP kinase-1 is essential for peptide phosphorylation. *FEBS letters*. 375:289-293.

Lenormand, P., C. Sardet, G. Pages, G. L'Allemain, A. Brunet, and J. Pouyssegur. 1993. Growth factors induce nuclear translocation of MAP kinases (p42mapk and p44mapk) but not of their activator MAP kinase kinase (p45mapkk) in fibroblasts. *J Cell Biol*. 122:1079-1088.

Levi, N.L., T. Hanoch, O. Benard, M. Rozenblat, D. Harris, N. Reiss, Z. Naor, and R. Seger. 1998. Stimulation of Jun N-terminal kinase (JNK) by gonadotropin-releasing hormone in pituitary alpha T3-1 cell line is mediated by protein kinase C, c-Src, and CDC42. *Mol Endocrinol*. 12:815-824.

Lewis, A.K., and P.C. Bridgman. 1992. Nerve growth cone lamellipodia contain two populations of actin filaments that differ in organization and polarity. *J Cell Biol*. 119:1219-1243.

Lewis, T.S., J.B. Hunt, L.D. Aveline, K.R. Jonscher, D.F. Louie, J.M. Yeh, T.S. Nahreini, K.A. Resing, and N.G. Ahn. 2000. Identification of novel MAP kinase pathway signaling targets by functional proteomics and mass spectrometry. *Molecular cell*. 6:1343-1354.

Li, D., L. Jin, G.N. Alesi, Y.M. Kim, J. Fan, J.H. Seo, D. Wang, M. Tucker, T.L. Gu, B.H. Lee, J. Taunton, K.R. Magliocca, Z.G. Chen, D.M. Shin, F.R. Khuri, and S. Kang. 2013. The prometastatic ribosomal S6 kinase 2-cAMP response element-binding protein (RSK2-CREB) signaling pathway up-regulates the actin-binding protein fascin-1 to promote tumor metastasis. *J Biol Chem*. 288:32528-32538.

Li, J., and R. Zhao. 2011. Expression and Clinical Significance of L: -Plastin in Colorectal Carcinoma. *J Gastrointest Surg*.

Li, M.X., Z.Q. Xiao, Y.F. Liu, Y.H. Chen, C. Li, P.F. Zhang, M.Y. Li, F. Li, F. Peng, C.J. Duan, H. Yi, H.X. Yao, and Z.C. Chen. 2009. Quantitative proteomic analysis of differential proteins in the stroma of nasopharyngeal carcinoma and normal nasopharyngeal epithelial tissue. *J Cell Biochem*. 106:570-579.

Li, W., H. Mischak, J.C. Yu, L.M. Wang, J.F. Mushinski, M.A. Heidaran, and J.H. Pierce. 1994. Tyrosine phosphorylation of protein kinase C-delta in response to its activation. *J Biol Chem*. 269:2349-2352.

Libermann, T.A., H.R. Nusbaum, N. Razon, R. Kris, I. Lax, H. Soreq, N. Whittle, M.D. Waterfield, A. Ullrich, and J. Schlessinger. 1985. Amplification, enhanced expression and possible rearrangement of EGF receptor gene in primary human brain tumours of glial origin. *Nature*. 313:144-147.

Lin, C.S., R.H. Aebersold, S.B. Kent, M. Varma, and J. Leavitt. 1988. Molecular cloning and characterization of plastin, a human leukocyte protein expressed in transformed human fibroblasts. *Molecular and cellular biology*. 8:4659-4668.

Lin, C.S., R.H. Aebersold, and J. Leavitt. 1990. Correction of the N-terminal sequences of the human plastin isoforms by using anchored polymerase chain reaction: identification of a potential calcium-binding domain. *Molecular and cellular biology*. 10:1818-1821.

Lin, C.S., Z.P. Chen, T. Park, K. Ghosh, and J. Leavitt. 1993a. Characterization of the human L-plastin gene promoter in normal and neoplastic cells. *J Biol Chem*. 268:2793-2801.

Lin, C.S., A. Lau, and T.F. Lue. 1998. Analysis and mapping of plastin phosphorylation. *DNA Cell Biol*. 17:1041-1046.

Lin, C.S., A. Lau, C.C. Yeh, C.H. Chang, and T.F. Lue. 2000. Upregulation of L-plastin gene by testosterone in breast and prostate cancer cells: identification of three cooperative androgen receptor-binding sequences. *DNA Cell Biol*. 19:1-7.

Lin, C.S., T. Park, Z.P. Chen, and J. Leavitt. 1993b. Human plastin genes. Comparative gene structure, chromosome location, and differential expression in normal and neoplastic cells. *J Biol Chem*. 268:2781-2792.

Lin, C.S., W. Shen, Z.P. Chen, Y.H. Tu, and P. Matsudaira. 1994. Identification of I-plastin, a human fimbrin isoform expressed in intestine and kidney. *Molecular and cellular biology*. 14:2457-2467.

Linder, S. 2007. The matrix corroded: podosomes and invadopodia in extracellular matrix degradation. *Trends in cell biology*. 17:107-117.

Linder, S. 2009. Invadosomes at a glance. *Journal of cell science*. 122:3009-3013.

Linder, S., and M. Aepfelbacher. 2003. Podosomes: adhesion hot-spots of invasive cells. *Trends in cell biology*. 13:376-385.

Linder, S., D. Nelson, M. Weiss, and M. Aepfelbacher. 1999. Wiskott-Aldrich syndrome protein regulates podosomes in primary human macrophages. *Proc Natl Acad Sci U S A*. 96:9648-9653.

Linder, S., C. Wiesner, and M. Himmel. 2011. Degrading devices: invadosomes in proteolytic cell invasion. *Annual review of cell and developmental biology*. 27:185-211.

Lito, P., N. Rosen, and D.B. Solit. 2013. Tumor adaptation and resistance to RAF inhibitors. *Nature medicine*. 19:1401-1409.

Lodish, H., A. Berk, C.A. Kaiser, M. Krieger, M.P. Scott, A. Bretscher, H. Ploegh, and P. Matsudaira. 2008. Molecular Cell Biology. W.H. Freeman and Company.

Lollike, K., A.H. Johnsen, I. Durussel, N. Borregaard, and J.A. Cox. 2001. Biochemical characterization of the penta-EF-hand protein grancalcin and identification of L-plastin as a binding partner. *J Biol Chem*. 276:17762-17769.

Lommel, M.J., P. Trairatphisan, K. Gabler, C. Laurini, A. Muller, T. Kaoma, L. Vallar, T. Sauter, and E. Schaffner-Reckinger. 2015. L-plastin Ser5 phosphorylation in breast cancer cells and in vitro is mediated by RSK downstream of the ERK/MAPK pathway. *FASEB J*.

Ma, T., K. Sadashivaiah, N. Madayiputhiya, and M.A. Chellaiah. 2010. Regulation of sealing ring formation by L-plastin and cortactin in osteoclasts. *J Biol Chem*. 285:29911-29924.

Machesky, L.M., and A. Li. 2010. Fascin: Invasive filopodia promoting metastasis. *Communicative & integrative biology*. 3:263-270.

Matsudaira, P.T., and D.R. Burgess. 1979. Identification and organization of the components in the isolated microvillus cytoskeleton. *J Cell Biol*. 83:667-673.

Matsushima, K., Y. Kobayashi, T.D. Copeland, T. Akahoshi, and J.J. Oppenheim. 1987. Phosphorylation of a cytosolic 65-kDa protein induced by interleukin 1 in glucocorticoid pretreated normal human peripheral blood mononuclear leukocytes. *J Immunol*. 139:3367-3374.

Matsushima, K., M. Shiroo, H.F. Kung, and T.D. Copeland. 1988. Purification and characterization of a cytosolic 65-kilodalton phosphoprotein in human leukocytes whose phosphorylation is augmented by stimulation with interleukin 1. *Biochemistry*. 27:3765-3770.

Mau, S.E., T. Saermark, and H. Vilhardt. 1997. Cross-talk between cellular signaling pathways activated by substance P and vasoactive intestinal peptide in rat lactotroph-enriched pituitary cell cultures. *Endocrinology*. 138:1704-1711.

Mendoza, M.C., E.E. Er, and J. Blenis. 2011. The Ras-ERK and PI3K-mTOR pathways: cross-talk and compensation. *Trends in biochemical sciences*. 36:320-328.

Messier, J.M., L.M. Shaw, M. Chafel, P. Matsudaira, and A.M. Mercurio. 1993. Fimbrin localized to an insoluble cytoskeletal fraction is constitutively phosphorylated on its headpiece domain in adherent macrophages. *Cell Motil Cytoskeleton*. 25:223-233.

Mirzoeva, O.K., D. Das, L.M. Heiser, S. Bhattacharya, D. Siwak, R. Gendelman, N. Bayani, N.J. Wang, R.M. Neve, Y. Guan, Z. Hu, Z. Knight, H.S. Feiler, P. Gascard, B. Parvin, P.T. Spellman, K.M. Shokat, A.J. Wyrobek, M.J. Bissell, F. McCormick, W.L. Kuo, G.B. Mills, J.W. Gray, and W.M. Korn. 2009. Basal subtype and MAPK/ERK kinase (MEK)-phosphoinositide 3-kinase feedback signaling determine susceptibility of breast cancer cells to MEK inhibition. *Cancer Res*. 69:565-572.

Mok, T.S. 2011. Personalized medicine in lung cancer: what we need to know. *Nature reviews. Clinical oncology*. 8:661-668.

Moreau, V., F. Tatin, C. Varon, and E. Genot. 2003. Actin can reorganize into podosomes in aortic endothelial cells, a process controlled by Cdc42 and RhoA. *Molecular and cellular biology*. 23:6809-6822.

Morley, S.C., C. Wang, W.L. Lo, C.W. Lio, B.H. Zinselmeyer, M.J. Miller, E.J. Brown, and P.M. Allen. 2010. The actin-bundling protein L-plastin dissociates CCR7 proximal signaling from CCR7-induced motility. *J Immunol*. 184:3628-3638.

Mosoian, A. 2011. Intracellular and extracellular cytokine-like functions of prothymosin alpha: implications for the development of immunotherapies. *Future medicinal chemistry*. 3:1199-1208.

Motzkus, D., E. Maronde, U. Grunenberg, C.C. Lee, W. Forssmann, and U. Albrecht. 2000. The human PER1 gene is transcriptionally regulated by multiple signaling pathways. *FEBS letters*. 486:315-319.

Moyers, J.S., A.H. Bouton, and S.J. Parsons. 1993. The sites of phosphorylation by protein kinase C and an intact SH2 domain are required for the enhanced response to beta-adrenergic agonists in cells overexpressing c-src. *Molecular and cellular biology*. 13:2391-2400.

Murphy, D.A., and S.A. Courtneidge. 2011. The 'ins' and 'outs' of podosomes and invadopodia: characteristics, formation and function. *Nature reviews. Molecular cell biology*. 12:413-426.

Namba, Y., M. Ito, Y. Zu, K. Shigesada, and K. Maruyama. 1992. Human T cell L-plastin bundles actin filaments in a calcium-dependent manner. *Journal of biochemistry*. 112:503-507.

Nicolson, G.L. 1988. Organ specificity of tumor metastasis: role of preferential adhesion, invasion and growth of malignant cells at specific secondary sites. *Cancer metastasis reviews*. 7:143-188.

Nowell, P.C. 1976. The clonal evolution of tumor cell populations. *Science*. 194:23-28.

Ohsawa, K., Y. Imai, Y. Sasaki, and S. Kohsaka. 2004. Microglia/macrophage-specific protein Iba1 binds to fimbrin and enhances its actin-bundling activity. *Journal of neurochemistry*. 88:844-856.

Ohta, Y., and J.H. Hartwig. 1996. Phosphorylation of actin-binding protein 280 by growth factors is mediated by p90 ribosomal protein S6 kinase. *J Biol Chem*. 271:11858-11864.

Orr, F.W., H.H. Wang, R.M. Lafrenie, S. Scherbarth, and D.M. Nance. 2000. Interactions between cancer cells and the endothelium in metastasis. *J Pathol*. 190:310-329.

Otsuka, M., M. Kato, T. Yoshikawa, H. Chen, E.J. Brown, Y. Masuho, M. Omata, and N. Seki. 2001. Differential expression of the L-plastin gene in human colorectal cancer progression and metastasis. *Biochem Biophys Res Commun*. 289:876-881.

Otterbein, L.R., P. Graceffa, and R. Dominguez. 2001. The crystal structure of uncomplexed actin in the ADP state. *Science*. 293:708-711.

Pacaud, M., and J. Derancourt. 1993. Purification and further characterization of macrophage 70-kDa protein, a calcium-regulated, actin-binding protein identical to L-plastin. *Biochemistry*. 32:3448-3455.

Paclet, M.H., C. Davis, P. Kotsonis, J. Godovac-Zimmermann, A.W. Segal, and L.V. Dekker. 2004. N-Formyl peptide receptor subtypes in human neutrophils activate L-plastin phosphorylation through different signal transduction intermediates. *Biochem J*. 377:469-477.

Paez, J.G., P.A. Janne, J.C. Lee, S. Tracy, H. Greulich, S. Gabriel, P. Herman, F.J. Kaye, N. Lindeman, T.J. Boggon, K. Naoki, H. Sasaki, Y. Fujii, M.J. Eck, W.R. Sellers, B.E. Johnson, and M. Meyerson. 2004. EGFR mutations in lung cancer: correlation with clinical response to gefitinib therapy. *Science*. 304:1497-1500.

Parekh, A., N.S. Ruppender, K.M. Branch, M.K. Sewell-Loftin, J. Lin, P.D. Boyer, J.E. Candiello, W.D. Merryman, S.A. Guelcher, and A.M. Weaver. 2011. Sensing and modulation of invadopodia across a wide range of rigidities. *Biophysical journal*. 100:573-582.

Park, T., Z.P. Chen, and J. Leavitt. 1994. Activation of the leukocyte plastin gene occurs in most human cancer cells. *Cancer Res*. 54:1775-1781.

Parsons, J.T., A.R. Horwitz, and M.A. Schwartz. 2010. Cell adhesion: integrating cytoskeletal dynamics and cellular tension. *Nature reviews. Molecular cell biology*. 11:633-643.

Pawson, T., and J.D. Scott. 1997. Signaling through scaffold, anchoring, and adaptor proteins. *Science*. 278:2075-2080.

Pazdrak, K., T.W. Young, C. Straub, S. Stafford, and A. Kurosky. 2011. Priming of eosinophils by GM-CSF is mediated by protein kinase CbetaII-phosphorylated L-plastin. *J Immunol*. 186:6485-6496.

Pinna, L.A., and M. Ruzzene. 1996. How do protein kinases recognize their substrates? *Biochim Biophys Acta*. 1314:191-225.

Pollard, T.D., L. Blanchoin, and R.D. Mullins. 2000. Molecular mechanisms controlling actin filament dynamics in nonmuscle cells. *Annu Rev Biophys Biomol Struct*. 29:545-576.

Pollard, T.D., and J.A. Cooper. 2009. Actin, a central player in cell shape and movement. *Science*. 326:1208-1212.

Rae, J.M., C.J. Creighton, J.M. Meck, B.R. Haddad, and M.D. Johnson. 2007. MDA-MB-435 cells are derived from M14 melanoma cells--a loss for breast cancer, but a boon for melanoma research. *Breast cancer research and treatment*. 104:13-19.

Raman, M., W. Chen, and M.H. Cobb. 2007. Differential regulation and properties of MAPKs. *Oncogene*. 26:3100-3112.

Ranganathan, A., G.W. Pearson, C.A. Chrestensen, T.W. Sturgill, and M.H. Cobb. 2006. The MAP kinase ERK5 binds to and phosphorylates p90 RSK. *Archives of biochemistry and biophysics*. 449:8-16.

Red Brewer, M., S.H. Choi, D. Alvarado, K. Moravcevic, A. Pozzi, M.A. Lemmon, and G. Carpenter. 2009. The juxtamembrane region of the EGF receptor functions as an activation domain. *Molecular cell*. 34:641-651.

Richards, S.A., V.C. Dreisbach, L.O. Murphy, and J. Blenis. 2001. Characterization of regulatory events associated with membrane targeting of p90 ribosomal S6 kinase 1. *Molecular and cellular biology*. 21:7470-7480.

Richards, S.A., J. Fu, A. Romanelli, A. Shimamura, and J. Blenis. 1999. Ribosomal S6 kinase 1 (RSK1) activation requires signals dependent on and independent of the MAP kinase ERK. *Current biology : CB*. 9:810-820.

Riplinger, S.M., G.H. Wabnitz, H. Kirchgessner, B. Jahraus, F. Lasitschka, B. Schulte, G. van der Pluijm, G. van der Horst, G.J. Hammerling, I. Nakchbandi, and Y. Samstag. 2014. Metastasis of prostate cancer and melanoma cells in a preclinical in vivo mouse model is enhanced by L-plastin expression and phosphorylation. *Molecular cancer*. 13:10.

Roovers, R.C., T. Laeremans, L. Huang, S. De Taeye, A.J. Verkleij, H. Revets, H.J. de Haard, and P.M. van Bergen en Henegouwen. 2007. Efficient inhibition of EGFR signaling and of tumour growth by antagonistic anti-EFGR Nanobodies. *Cancer immunology, immunotherapy : CII*. 56:303-317.

Ross, D.T., U. Scherf, M.B. Eisen, C.M. Perou, C. Rees, P. Spellman, V. Iyer, S.S. Jeffrey, M. Van de Rijn, M. Waltham, A. Pergamenschikov, J.C. Lee, D. Lashkari, D. Shalon, T.G. Myers, J.N. Weinstein, D. Botstein, and P.O. Brown. 2000. Systematic variation in gene expression patterns in human cancer cell lines. *Nature genetics*. 24:227-235.

Rothbauer, U., K. Zolghadr, S. Muyldermans, A. Schepers, M.C. Cardoso, and H. Leonhardt. 2008. A versatile nanotrap for biochemical and functional studies with fluorescent fusion proteins. *Molecular & cellular proteomics : MCP*. 7:282-289.

Rust, H.L., and P.R. Thompson. 2011. Kinase consensus sequences: a breeding ground for crosstalk. *ACS chemical biology*. 6:881-892.

Sahai, E. 2005. Mechanisms of cancer cell invasion. *Current opinion in genetics & development*. 15:87-96.

Salsmann, A., E. Schaffner-Reckinger, F. Kabile, S. Plancon, and N. Kieffer. 2005. A new functional role of the fibrinogen RGD motif as the molecular switch that selectively triggers integrin alphaIIbbeta3-dependent RhoA activation during cell spreading. *J Biol Chem*. 280:33610-33619.

Schoumacher, M., R.D. Goldman, D. Louvard, and D.M. Vignjevic. 2010. Actin, microtubules, and vimentin intermediate filaments cooperate for elongation of invadopodia. *J Cell Biol*. 189:541-556.

Schubbert, S., K. Shannon, and G. Bollag. 2007. Hyperactive Ras in developmental disorders and cancer. *Nat Rev Cancer*. 7:295-308.

Schulz, D.M., C. Bollner, G. Thomas, M. Atkinson, I. Esposito, H. Hofler, and M. Aubele. 2009. Identification of differentially expressed proteins in triple-negative breast carcinomas using DIGE and mass spectrometry. *J Proteome Res*. 8:3430-3438.

Schulze, W.X., L. Deng, and M. Mann. 2005. Phosphotyrosine interactome of the ErbB-receptor kinase family. *Molecular systems biology*. 1:2005 0008.

Sellappan, S., R. Grijalva, X. Zhou, W. Yang, M.B. Eli, G.B. Mills, and D. Yu. 2004. Lineage infidelity of MDA-MB-435 cells: expression of melanocyte proteins in a breast cancer cell line. *Cancer Res*. 64:3479-3485.

Serber, Z., and J.E. Ferrell, Jr. 2007. Tuning bulk electrostatics to regulate protein function. *Cell*. 128:441-444.

Serrano-Pertierra, E., E. Cernuda-Morollon, T. Brdicka, V. Hooejsi, and C. Lopez-Larrea. 2014. L-plastin is involved in NKG2D recruitment into lipid rafts and NKG2D-mediated NK cell migration. *Journal of leukocyte biology*. 96:437-445.

Sever, R., and J.S. Brugge. 2015. Signal Transduction in Cancer. *Cold Spring Harbor perspectives in medicine*. 5.

Shaul, Y.D., and R. Seger. 2006. ERK1c regulates Golgi fragmentation during mitosis. *J Cell Biol*. 172:885-897.

Shiau, A.L., P.R. Lin, M.Y. Chang, and C.L. Wu. 2001. Retrovirus-mediated transfer of prothymosin gene inhibits tumor growth and prolongs survival in murine bladder cancer. *Gene therapy*. 8:1609-1617.

Shibata, M., Y. Yamakawa, T. Ohoka, S. Mizuno, and K. Suzuki. 1993. Characterization of a 64-kd protein phosphorylated during chemotactic activation with IL-8 and fMLP of human polymorphonuclear leukocytes. II. Purification and amino acid analysis of phosphorylated 64-kd protein. *Journal of leukocyte biology*. 54:10-16.

Shinomiya, H., A. Hagi, M. Fukuzumi, M. Mizobuchi, H. Hirata, and S. Utsumi. 1995. Complete primary structure and phosphorylation site of the 65-kDa macrophage protein phosphorylated by stimulation with bacterial lipopolysaccharide. *J Immunol*. 154:3471-3478.

Shinomiya, H., M. Shinjo, L. Fengzhi, Y. Asano, and H. Kihara. 2007. Conformational analysis of the leukocyte-specific EF-hand protein p65/L-plastin by X-ray scattering in solution. *Biophys Chem*. 131:36-42.

Shiroo, M., and K. Matsushima. 1990. Enhanced phosphorylation of 65 and 74 kDa proteins by tumor necrosis factor and interleukin-1 in human peripheral blood mononuclear cells. *Cytokine*. 2:13-20.

Siegel, R., E. Ward, O. Brawley, and A. Jemal. 2011. Cancer statistics, 2011: the impact of eliminating socioeconomic and racial disparities on premature cancer deaths. *CA: a cancer journal for clinicians*. 61:212-236.

Smith, J.A., C.E. Poteet-Smith, K. Malarkey, and T.W. Sturgill. 1999. Identification of an extracellular signal-regulated kinase (ERK) docking site in ribosomal S6 kinase, a sequence critical for activation by ERK in vivo. *J Biol Chem*. 274:2893-2898.

Smith, J.A., C.E. Poteet-Smith, Y. Xu, T.M. Errington, S.M. Hecht, and D.A. Lannigan. 2005. Identification of the first specific inhibitor of p90 ribosomal S6 kinase (RSK) reveals an unexpected role for RSK in cancer cell proliferation. *Cancer Res*. 65:1027-1034.

Soh, J.W., E.H. Lee, R. Prywes, and I.B. Weinstein. 1999. Novel roles of specific isoforms of protein kinase C in activation of the c-fos serum response element. *Molecular and cellular biology*. 19:1313-1324.

Steinberg, S.F. 2004. Distinctive activation mechanisms and functions for protein kinase Cdelta. *Biochem J*. 384:449-459.

Steinberg, S.F. 2012. Cardiac actions of protein kinase C isoforms. *Physiology (Bethesda)*. 27:130-139.

Stes, E., M. Laga, A. Walton, N. Samyn, E. Timmerman, I. De Smet, S. Goormachtig, and K. Gevaert. 2014. A COFRADIC protocol to study protein ubiquitination. *J Proteome Res*. 13:3107-3113.

Stetler-Stevenson, W.G., R. Hewitt, and M. Corcoran. 1996. Matrix metalloproteinases and tumor invasion: from correlation and causality to the clinic. *Seminars in cancer biology*. 7:147-154.

Stewart, B.W., and C.B. Wild. 2014. World Cancer Report 2014. World Health Organization.

Straub, F.B. 1942. Actin. *Stud. Inst. Med. Chem. Univ. Szeged*:3-15.

Strickler, A.G., J.G. Vasquez, N. Yates, and J. Ho. 2014. Potential diagnostic significance of HSP90, ACS/TMS1, and L-plastin in the identification of melanoma. *Melanoma research*. 24:535-544.

Subik, K., J.F. Lee, L. Baxter, T. Strzepek, D. Costello, P. Crowley, L. Xing, M.C. Hung, T. Bonfiglio, D.G. Hicks, and P. Tang. 2010. The Expression Patterns of ER, PR, HER2, CK5/6, EGFR, Ki-67 and AR by Immunohistochemical Analysis in Breast Cancer Cell Lines. *Breast cancer : basic and clinical research*. 4:35-41.

Sugita, S., D.A. Baxter, and J.H. Byrne. 1997. Modulation of a cAMP/protein kinase A cascade by protein kinase C in sensory neurons of Aplysia. *The Journal of neuroscience : the official journal of the Society for Neuroscience*. 17:7237-7244.

Sulzmaier, F.J., and J.W. Ramos. 2013. RSK isoforms in cancer cell invasion and metastasis. *Cancer Res*. 73:6099-6105.

Sumandea, M.P., V.O. Rybin, A.C. Hinken, C. Wang, T. Kobayashi, E. Harleton, G. Sievert, C.W. Balke, S.J. Feinmark, R.J. Solaro, and S.F. Steinberg. 2008. Tyrosine phosphorylation modifies protein kinase C delta-dependent phosphorylation of cardiac troponin I. *J Biol Chem*. 283:22680-22689.

Sun, C., S. Hobor, A. Bertotti, D. Zecchin, S. Huang, F. Galimi, F. Cottino, A. Prahallad, W. Grernrum, A. Tzani, A. Schlicker, L.F. Wessels, E.F. Smit, E. Thunnissen, P. Halonen, C. Lieftink, R.L. Beijersbergen, F. Di Nicolantonio, A. Bardelli, L. Trusolino, and R. Bernards. 2014. Intrinsic resistance to MEK inhibition in KRAS mutant lung and colon cancer through transcriptional induction of ERBB3. *Cell reports*. 7:86-93.

Tan, V.Y., S.J. Lewis, J.C. Adams, and R.M. Martin. 2013. Association of fascin-1 with mortality, disease progression and metastasis in carcinomas: a systematic review and meta-analysis. *BMC medicine*. 11:52.

Tarcic, G., R. Avraham, G. Pines, I. Amit, T. Shay, Y. Lu, Y. Zwang, M. Katz, N. Ben-Chetrit, J. Jacob-Hirsch, L. Virgilio, G. Rechavi, G. Mavrothalassitis, G.B. Mills, E. Domany, and Y. Yarden. 2012. EGR1 and the ERK-ERF axis drive mammary cell migration in response to EGF. *FASEB J*. 26:1582-1592.

Tebbutt, N., M.W. Pedersen, and T.G. Johns. 2013. Targeting the ERBB family in cancer: couples therapy. *Nat Rev Cancer*. 13:663-673.

Tinoco, G., S. Warsch, S. Gluck, K. Avancha, and A.J. Montero. 2013. Treating breast cancer in the 21st century: emerging biological therapies. *Journal of Cancer*. 4:117-132.

Trairatphisan, P., A. Mizera, J. Pang, A.A. Tantar, and T. Sauter. 2014. optPBN: an optimisation toolbox for probabilistic Boolean networks. *PLoS One*. 9:e98001.

Trairatphisan, P., A. Mizera, J. Pang, A.A. Tantar, J. Schneider, and T. Sauter. 2013. Recent development and biomedical applications of probabilistic Boolean networks. *Cell communication and signaling : CCS*. 11:46.

Ubersax, J.A., and J.E. Ferrell, Jr. 2007. Mechanisms of specificity in protein phosphorylation. *Nature reviews. Molecular cell biology*. 8:530-541.

Ueda, Y., S. Hirai, S. Osada, A. Suzuki, K. Mizuno, and S. Ohno. 1996. Protein kinase C activates the MEK-ERK pathway in a manner independent of Ras and dependent on Raf. *J Biol Chem*. 271:23512-23519.

Urban, E., S. Jacob, M. Nemethova, G.P. Resch, and J.V. Small. 2010. Electron tomography reveals unbranched networks of actin filaments in lamellipodia. *Nat Cell Biol*. 12:429-435.

Vaidyanathan, H., and J.W. Ramos. 2003. RSK2 activity is regulated by its interaction with PEA-15. *J Biol Chem*. 278:32367-32372.

Vandekerckhove, J., and K. Weber. 1978. At least six different actins are expressed in a higher mammal: an analysis based on the amino acid sequence of the amino-terminal tryptic peptide. *Journal of molecular biology*. 126:783-802.

Vial, D., and P.J. McKeown-Longo. 2012. Epidermal growth factor (EGF) regulates alpha5beta1 integrin activation state in human cancer cell lines through the p90RSK-dependent phosphorylation of filamin A. *J Biol Chem*. 287:40371-40380.

Vivanco, I., H.I. Robins, D. Rohle, C. Campos, C. Grommes, P.L. Nghiemphu, S. Kubek, B. Oldrini, M.G. Chheda, N. Yannuzzi, H. Tao, S. Zhu, A. Iwanami, D. Kuga, J. Dang, A. Pedraza, C.W. Brennan, A. Heguy, L.M. Liau, F. Lieberman, W.K. Yung, M.R. Gilbert, D.A. Reardon, J. Drappatz, P.Y. Wen, K.R. Lamborn, S.M. Chang, M.D. Prados, H.A. Fine, S. Horvath, N. Wu, A.B. Lassman, L.M. DeAngelis, W.H. Yong, J.G. Kuhn, P.S. Mischel, M.P. Mehta, T.F. Cloughesy, and I.K. Mellinghoff. 2012. Differential sensitivity of glioma- versus lung cancer-specific EGFR mutations to EGFR kinase inhibitors. *Cancer discovery*. 2:458-471.

Wabnitz, G.H., P. Lohneis, H. Kirchgessner, B. Jahraus, S. Gottwald, M. Konstandin, M. Klemke, and Y. Samstag. 2010. Sustained LFA-1 cluster formation in the immune synapse requires the combined activities of L-plastin and calmodulin. *Eur J Immunol*. 40:2437-2449.

Wang, C., S.C. Morley, D. Donermeyer, I. Peng, W.P. Lee, J. Devoss, D.M. Danilenko, Z. Lin, J. Zhang, J. Zhou, P.M. Allen, and E.J. Brown. 2011. Actin-bundling protein L-plastin regulates T cell activation. *J Immunol*. 185:7487-7497.

Wang, J., and E.J. Brown. 1999. Immune complex-induced integrin activation and L-plastin phosphorylation require protein kinase A. *J Biol Chem*. 274:24349-24356.

Wang, J., H. Chen, and E.J. Brown. 2001. L-plastin peptide activation of alpha(v)beta(3)-mediated adhesion requires integrin conformational change and actin filament disassembly. *J Biol Chem*. 276:14474-14481.

Wang, W., R. Eddy, and J. Condeelis. 2007a. The cofilin pathway in breast cancer invasion and metastasis. *Nat Rev Cancer*. 7:429-440.

Wang, W., S. Goswami, K. Lapidus, A.L. Wells, J.B. Wyckoff, E. Sahai, R.H. Singer, J.E. Segall, and J.S. Condeelis. 2004. Identification and testing of a gene expression signature of invasive carcinoma cells within primary mammary tumors. *Cancer Res*. 64:8585-8594.

Wang, W., J.B. Wyckoff, S. Goswami, Y. Wang, M. Sidani, J.E. Segall, and J.S. Condeelis. 2007b. Coordinated regulation of pathways for enhanced cell motility and chemotaxis is conserved in rat and mouse mammary tumors. *Cancer Res*. 67:3505-3511.

Wegner, A. 1976. Head to tail polymerization of actin. *Journal of molecular biology*. 108:139-150.

Wegner, A., and J. Engel. 1975. Kinetics of the cooperative association of actin to actin filaments. *Biophys Chem*. 3:215-225.

Wegner, A., and G. Isenberg. 1983. 12-fold difference between the critical monomer concentrations of the two ends of actin filaments in physiological salt conditions. *Proc Natl Acad Sci U S A*. 80:4922-4925.

Whyte, J., O. Bergin, A. Bianchi, S. McNally, and F. Martin. 2009. Key signalling nodes in mammary gland development and cancer. Mitogen-activated protein kinase signalling in experimental models of breast cancer progression and in mammary gland development. *Breast cancer research : BCR*. 11:209.

Woo, M.S., Y. Ohta, I. Rabinovitz, T.P. Stossel, and J. Blenis. 2004. Ribosomal S6 kinase (RSK) regulates phosphorylation of filamin A on an important regulatory site. *Molecular and cellular biology*. 24:3025-3035.

Wu, H., A.B. Reynolds, S.B. Kanner, R.R. Vines, and J.T. Parsons. 1991. Identification and characterization of a novel cytoskeleton-associated pp60src substrate. *Molecular and cellular biology*. 11:5113-5124.

Xue, C., J. Wyckoff, F. Liang, M. Sidani, S. Violini, K.L. Tsai, Z.Y. Zhang, E. Sahai, J. Condeelis, and J.E. Segall. 2006. Epidermal growth factor receptor overexpression results in increased tumor cell motility in vivo coordinately with enhanced intravasation and metastasis. *Cancer Res*. 66:192-197.

Yamaguchi, H., M. Lorenz, S. Kempiak, C. Sarmiento, S. Coniglio, M. Symons, J. Segall, R. Eddy, H. Miki, T. Takenawa, and J. Condeelis. 2005a. Molecular mechanisms of invadopodium formation: the role of the N-WASP-Arp2/3 complex pathway and cofilin. *J Cell Biol*. 168:441-452.

Yamaguchi, H., J. Wyckoff, and J. Condeelis. 2005b. Cell migration in tumors. *Current opinion in cell biology*. 17:559-564.

Yao, L., P. Fan, Z. Jiang, A. Gordon, D. Mochly-Rosen, and I. Diamond. 2008. Dopamine and ethanol cause translocation of epsilonPKC associated with epsilonRACK: cross-talk between cAMP-dependent protein kinase A and protein kinase C signaling pathways. *Molecular pharmacology*. 73:1105-1112.

Yarden, Y., and G. Pines. 2012. The ERBB network: at last, cancer therapy meets systems biology. *Nat Rev Cancer*. 12:553-563.

Yilmaz, M., and G. Christofori. 2009. EMT, the cytoskeleton, and cancer cell invasion. *Cancer metastasis reviews*. 28:15-33.

Yoon, S., and R. Seger. 2006. The extracellular signal-regulated kinase: multiple substrates regulate diverse cellular functions. *Growth Factors*. 24:21-44.

Yuan, C.B., R. Zhao, F.J. Wan, J.H. Cai, X.P. Ji, and Y.Y. Yu. 2010. [Significance of plasmic L-plastin levels in the diagnosis of colorectal cancer]. *Zhonghua wei chang wai ke za zhi = Chinese journal of gastrointestinal surgery*. 13:687-690.

Zajchowski, D.A., M.F. Bartholdi, Y. Gong, L. Webster, H.L. Liu, A. Munishkin, C. Beauheim, S. Harvey, S.P. Ethier, and P.H. Johnson. 2001. Identification of gene expression profiles that predict the aggressive behavior of breast cancer cells. *Cancer Res*. 61:5168-5178.

Zang, Q., P. Frankel, and D.A. Foster. 1995. Selective activation of protein kinase C isoforms by v-Src. *Cell growth & differentiation : the molecular biology journal of the American Association for Cancer Research*. 6:1367-1373.

Zang, Q., Z. Lu, M. Curto, N. Barile, D. Shalloway, and D.A. Foster. 1997. Association between v-Src and protein kinase C delta in v-Src-transformed fibroblasts. *J Biol Chem*. 272:13275-13280.

Zhang, X., J. Gureasko, K. Shen, P.A. Cole, and J. Kuriyan. 2006. An allosteric mechanism for activation of the kinase domain of epidermal growth factor receptor. *Cell*. 125:1137-1149.

Zhao, Y., C. Bjorbaek, S. Weremowicz, C.C. Morton, and D.E. Moller. 1995. RSK3 encodes a novel pp90rsk isoform with a unique N-terminal sequence: growth factor-stimulated kinase function and nuclear translocation. *Molecular and cellular biology*. 15:4353-4363.

Zheng, J., N. Rudra-Ganguly, G.J. Miller, K.A. Moffatt, R.J. Cote, and P. Roy-Burman. 1997. Steroid hormone induction and expression patterns of L-plastin in normal and carcinomatous prostate tissues. *Am J Pathol*. 150:2009-2018.

Zheng, J., N. Rudra-Ganguly, W.C. Powell, and P. Roy-Burman. 1999. Suppression of prostate carcinoma cell invasion by expression of antisense L-plastin gene. *Am J Pathol*. 155:115-122.

Zhong, J.L., L. Yang, F. Lu, H. Xiao, R. Xu, L. Wang, F. Zhu, and Y. Zhang. 2011. UVA, UVB and UVC induce differential response signaling pathways converged on the eIF2alpha phosphorylation. *Photochemistry and photobiology*. 87:1092-1104.

Zhu, H., J.F. Klemic, S. Chang, P. Bertone, A. Casamayor, K.G. Klemic, D. Smith, M. Gerstein, M.A. Reed, and M. Snyder. 2000. Analysis of yeast protein kinases using protein chips. *Nature genetics*. 26:283-289.

Quotation of co-authorship

As already indicated in the corresponding sections, the computational modelling of section 4.2.7 was performed in collaboration with Dr. Panuwat Trairatphisan and Prof. Thomas Sauter (Systems Biology Group, University of Luxembourg), the microarray experiments of section 4.2.2 were performed in collaboration with Dr. Laurent Vallar, Arnaud Muller and Tony Kaoma (Genomics Research Unit, Luxembourg Institute of Health), the two-dimensional gel electrophoresis experiments of section 4.2.6 were performed in collaboration with Prof. Christophe Ampe and Prof. Marleen van Troys (Molecular Cell Biology and Biochemistry of the Actin Cytoskeleton Group, University of Ghent) and the mass spectrometry experiments of section 4.4.2 were performed in collaboration with Prof. Kris Gevaert (Proteomics Lab, University of Ghent) and Prof. Christophe Ampe, financed by a Prime-XS grant.

Affidavit

I hereby confirm that I have cited all sources that were used to write the PhD thesis entitled "Analysis of signal transduction pathways linking L-plastin Ser5 phosphorylation to breast cancer cell invasion" and that the research work described therein has been conducted following "good scientific practice" guidelines.

Luxembourg, 30th October 2015

Maiti Lommel

Appendix

The appendix of this thesis contains the following documents in the order as listed:

- Manuscript recently published in The FASEB Journal (Lommel et al., 2015): L-plastin Ser5 phosphorylation in breast cancer cells and *in vitro* is mediated by RSK downstream of the ERK/MAPK pathway
- Survival curves for L-plastin
- Supplemental *in vitro* kinase assay data

The following documents are available as supplemental Excel files:

- Supplemental microarray data, containing six sheets:
    - ❖ List DEG1 - Comparison of MCF7+PMA and MCF7
    - ❖ List DEG2 - Comparison of SK-BR-3+PMA and PMA
    - ❖ List DEG3 - Intersection of the comparisons of BT-20 vs. MCF7, MDA-MB-435S vs. MCF7, BT-20 vs. SK-BR-3 and MDA-MB-435S vs. SK-BR-3
    - ❖ List CP1 - Canonical pathways identified by IPA for the comparison of MCF7+PMA and MCF7
    - ❖ List CP2 - Canonical pathways identified by IPA for the comparison of SK-BR-3+PMA and SK-BR-3
    - ❖ List CP3 - Canonical pathways identified by IPA for the intersection of the comparisons of BT-20 vs. MCF7, MDA-MB-435S vs. MCF7, BT-20 vs. SK-BR-3 and MDA-MB-435S vs. SK-BR-3
- Supplemental LC-MS/MS data for the L-plastinWT experiment
- Supplemental LC-MS/MS data for the L-plastinSE experiment

The FASEB Journal article fj.15-276311. Published online November 30, 2015.

L-plastin Ser5 phosphorylation in breast cancer cells and *in vitro* is mediated by RSK downstream of the ERK/MAPK pathway

Maiti J. Lommel,* Panuwat Trairatphisan,† Karoline Gäbler,* Christina Laurini,* Arnaud Muller,‡ Tony Kaoma,‡ Laurent Vallar,‡ Thomas Sauter,† and Elisabeth Schaffner-Reckinger*,[1]

*Laboratory of Cytoskeleton and Cell Plasticity and †Systems Biology Group, Life Sciences Research Unit, University of Luxembourg, Luxembourg City, Luxembourg; and ‡Genomics Research Unit, Luxembourg Institute of Health, Luxembourg City, Luxembourg

ABSTRACT **Deregulated cell migration and invasion are hallmarks of metastatic cancer cells. Phosphorylation on residue Ser5 of the actin-bundling protein L-plastin activates L-plastin and has been reported to be crucial for invasion and metastasis. Here, we investigate signal transduction leading to L-plastin Ser5 phosphorylation using 4 human breast cancer cell lines. Whole-genome microarray analysis comparing cell lines with different invasive capacities and corresponding variations in L-plastin Ser5 phosphorylation level revealed that genes of the ERK/MAPK pathway are differentially expressed. It is noteworthy that *in vitro* kinase assays showed that ERK/MAPK pathway downstream ribosomal protein S6 kinases α-1 (RSK1) and α-3 (RSK2) are able to directly phosphorylate L-plastin on Ser5. Small interfering RNA- or short hairpin RNA-mediated knockdown and activation/inhibition studies followed by immunoblot analysis and computational modeling confirmed that ribosomal S6 kinase (RSK) is an essential activator of L-plastin. Migration and invasion assays showed that RSK knockdown led to a decrease of up to 30% of migration and invasion of MDA-MB-435S cells. Although the presence of L-plastin was not necessary for migration/invasion of these cells, immunofluorescence assays illustrated RSK-dependent recruitment of Ser5-phosphorylated L-plastin to migratory structures. Altogether, we provide evidence that the ERK/MAPK pathway is involved in L-plastin Ser5 phosphorylation in breast cancer cells with RSK1 and RSK2 kinases able to directly phosphorylate L-plastin residue Ser5.—Lommel, M. J., Trairatphisan, P., Gäbler, K., Laurini, C., Muller, A., Kaoma, T., Vallar, L., Sauter, T., Schaffner-Reckinger, E. L-plastin Ser5 phosphorylation in breast cancer cells and *in vitro* is mediated by RSK downstream of the ERK/MAPK pathway. *FASEB J.* 30, 000–000 (2016). www.fasebj.org**

Key Words: invasion · migration · signal transduction · actin cytoskeleton

Tumor cell migration and invasion are largely dependent on actin cytoskeleton changes, which are under the control of a plethora of actin-binding proteins, such as cofilin, filamin, fascin, or the plastins (1, 2). In this context, our previous studies have shown that the actin-bundling protein L-plastin regulates the turnover of actin filaments in addition to its cross-linking activities (3). Although L-plastin is typically expressed in hematopoietic cells where it plays a role in the immune response [reviewed in Morley (4)], it is also frequently ectopically expressed in carcinoma cells [reviewed in Shinomiya (5)]. L-plastin localizes to actin-rich structures such as focal adhesions, filopodia, and membrane ruffles, which are involved in adhesion, signaling, or locomotion (6, 7).

L-plastin activity has been shown to be increased following phosphorylation on residue Ser5 *in vitro* and in cells. In leukocytes, phosphorylation of L-plastin is part of the immune response (8, 9). Moreover, F-actin–binding and –bundling activities of L-plastin are increased upon Ser5 phosphorylation, and this phosphorylation is required for its efficient targeting to focal adhesions (7). It is noteworthy that recent findings have demonstrated that L-plastin Ser5 phosphorylation is crucial for *in vitro* invasion (7, 10) and *in vivo* metastasis (11). Distinct protein kinases have been reported to play a role in L-plastin Ser5 phosphorylation, depending on the cell type and environment. Candidate kinases include PKA (7, 12), PKC (3, 13–18), and PI3K (13, 16). Nevertheless, the detailed signaling pathway leading to L-plastin Ser5 phosphorylation remains to be resolved.

Besides the deregulation of the actin cytoskeleton, also the deregulation of signaling pathways is an important feature of many cancers (19). Breast cancers as well as

Abbreviations: AKT, RAC-α serine/threonine-protein kinase; DEG, differentially expressed gene; EGF, epidermal growth factor; EGFR, epidermal growth factor receptor; FDR, false discovery rate; HA, hemagglutinin; HEK, human embryonic kidney; HER, human epidermal growth factor receptor; IPA, ingenuity pathway analysis; LPL, total L-plastin; MSK1, ribosomal protein S6 kinase α-5; MT, mutant;

(*continued on next page*)

[1] Correspondence: Laboratory of Cytoskeleton and Cell Plasticity, Life Sciences Research Unit, University of Luxembourg, Campus Limpertsberg, 162a, Avenue de la Faïencerie L-1511, Luxembourg. E-mail: elisabeth.schaffner@uni.lu

doi: 10.1096/fj.15-276311

This article includes supplemental data. Please visit *http://www.fasebj.org* to obtain this information.

other cancer types frequently display an up-regulation of members of the epidermal growth factor (EGF) receptor (EGFR) family (20). The EGFR [also called HER1 (human epidermal growth factor receptor 1)] and its relatives HER2, HER3, and HER4 are known as oncogenic drivers in various cancers, including lung cancer (21), breast cancer (22), and glioblastoma (23–25). In particular, EGFR and HER2 are mutated to constitutively active forms in a large number of epithelial tumors. Signaling pathways downstream of these receptors that are frequently deregulated in cancer are the Ras/Raf proto-oncogene serine/threonine-protein kinase (Raf)/MEK/ERK and the phosphatase and tensin homolog/PI3K/RAC-α serine/threonine-protein kinase (AKT)/mammalian target of rapamycin pathways [for review, see (26, 27)].

In this study, we investigated the signaling pathways leading to L-plastin Ser5 phosphorylation in breast cancer cells, and we demonstrate that the ERK/MAPK pathway is crucial for L-plastin Ser5 phosphorylation. *In vitro* kinase assays revealed that phosphorylation of L-plastin residue Ser5 can be directly mediated by the ERK/MAPK-activated protein kinases ribosomal protein S6 kinase α-1 (RSK1) and ribosomal protein S6 kinase α-3 (RSK2). Although the presence of L-plastin *per se* does not appear to be required for enabling migration and invasion of the breast cancer cell line MDA-MB-435S, we provide clear evidence that L-plastin, and more precisely Ser5-phosphorylated L-plastin (P-LPL), is redistributed to migratory structures upon ribosomal S6 kinase (RSK) activation.

MATERIALS AND METHODS

Cell culture and transfection

SK-BR-3 and BT-20 cells were grown in McCoy's 5A and Eagle's minimal essential media (Lonza Group, Basel, Switzerland), respectively, and MCF7 and MDA-MB-435S cells were cultured in Roswell Park Memorial Institute medium (Lonza Group). All media were supplemented with 10% fetal bovine serum, 2 mM L-glutamine, and 100 U/ml penicillin and streptomycin (complete medium) (Lonza Group). Cells were grown at 37°C under 5% CO_2 atmosphere. All cells were bought from or authenticated by American Type Culture Collection (Manassas, VA, USA). Transient transfection of MDA-MB-435S or SK-BR-3 cells was performed using Lipofectamine 2000 (Life Technologies, Ghent, Belgium) according to the manufacturer's instructions.

Antibodies, reagents, and cDNA constructs

Mouse monoclonal IgG1 antibody against L-plastin (LPL4A.1, MA5-11921) was purchased from Thermo Scientific (Erembodegem, Belgium). Rabbit polyclonal anti-Ser5-*P* antibody specifically recognizing L-plastin phosphorylated on Ser5 was raised against a peptide encoding L-plastin residues 2–17 in which Ser5 was phosphorylated [ARG**S(*P*)**VSDEEMMELREA] [characterized in (7)]. Rabbit pAbs against RSK1 (sc-231) or RSK2 (#9340) were purchased from Santa Cruz Biotechnology (Heidelberg, Germany) and Cell Signaling Technology (Leiden, The Netherlands), respectively. Mouse anti-β-actin (A5441) and mouse anti-α-tubulin (T5168) antibodies were obtained from Sigma-Aldrich (Diegem, Belgium), mouse anti-HA (hemagglutinin) tag (#2367) and rabbit anti-EGFR (#2232) antibodies were from Cell Signaling Technology, and a rabbit anti-β-tubulin (sc-9104) antibody was from Santa Cruz Biotechnology. Phorbol 12-myristate 13-acetate (PMA), EGF, 8-Bromo-cAMP, H89, and PP2 were obtained from Sigma-Aldrich, GF109203X, SL0101, and BI-D1870 were from Calbiochem Merck Millipore (Nottingham, United Kingdom), and PD98059 was from Cell Signaling Technology. The HA-tagged mouse RSK2 wild-type (RSK2wt) and constitutively active RSK2Y707A constructs were obtained from Joe W. Ramos (University of Hawaii, Honolulu, HI, USA) and originate from the lab of Thomas W. Sturgill (University of Virginia, Charlottesville, VA, USA).

Treatment of cells with pharmacologic agents

Cells were treated with PMA at a concentration of 0.1 μM for 1 h, EGF at 1 ng/ml for 15 min, 8-bromo-cAMP at 1 mM for 1 h, GF109203X at 1 μM for 3 h, H89 at 50 μM for 1 h, PP2 at 10 μM for 1 h, PD98059 at 10 μM for 1 h, BI-D1870 at 5 μM for 30 min, or SL0101 at 80 μM for 4 h. In case of combined treatment with activators and inhibitors, the incubation with the inhibitor was performed before the incubation with the activator. For serum starvation prior to EGF treatment, cells were cultured in the absence of serum for 24 h.

Microarrays

RNA extraction was performed using TRIzol reagent (Thermo Scientific). RNA quality and concentration were evaluated spectroscopically using a NanoDrop 2000c instrument (Thermo Scientific). RNA integrity was subsequently analyzed on an Agilent 2100 Bioanalyzer (Agilent Technologies, Palo Alto, CA, USA). Only good-quality RNA with integrity numbers >9 was used. Transcriptome-profiling assays were performed using the Affymetrix Human GeneChip 1.0 ST arrays (Affymetrix, Santa Clara, CA, USA). Briefly, 250 ng total RNA was reverse transcribed into cDNA, then transcribed into cRNA and labeled into biotinylated cRNA using the GeneChip WT PLUS Reagent kit (Affymetrix) according to the manufacturer's protocols (P/N 4425209 Rev.B 05/2009 and P/N 702808 Rev.6). Labeled cRNA products were randomly fragmented and hybridized onto Affymetrix GeneChips. Arrays were washed and stained with the Affymetrix GeneChip WT Terminal Labeling and Hybridization Kit, before being scanned using a GeneChip Scanner 3000 (Affymetrix). Cell intensity files containing hybridization raw signal intensities were imported into the Partek GS software (Partek, St. Louis, MO, USA) using default options. Resulting expression data (transcript cluster level) were imported into R statistical environment for further analysis. Transcript clusters without chromosome location were removed. Quality of the data was assessed through boxplot, relative log expression, and Pearson correlation. Linear Models for Microarray Data from Bioconductor was used to compare transcript cluster expression between different conditions, according to the author's recommendations (Linear Models for Microarray Data User's Guide section 9.5) (https://bioconductor.org/). Resulting *P* values were adjusted for false discovery rate (FDR) with Benjamini and Hochberg's FDR (28), and transcript clusters with FDR <0.05 and absolute fold change ≥1.5 were considered as significantly differentially expressed and

(*continued from previous page*)

PBN, probabilistic Boolean network; P-LPL, phosphorylated L-plastin; PMA, phorbol 12-myristate 13-acetate; P-PKA, phosphorylated PKA; RAF, RAF proto-oncogene serine/threonine-protein kinase; RSK, ribosomal S6 kinase; RSK1, ribosomal protein S6 kinase α-1; RSK2, ribosomal protein S6 kinase α-3; shRNA, short hairpin RNA; siRNA, small interfering RNA; WT, wild-type

used for further analyses. The Ingenuity Pathway Analysis (IPA) software (Ingenuity Systems, Redwood City, CA, USA; www.ingenuity.com) was used for transcript cluster mapping, which led to the identification of differentially expressed genes (DEGs), and for data mining, including functional analyses and gene network reconstruction. Right-tailed Fisher's exact test was used to calculate a *P* value for functional enrichment analysis: threshold, -log(*P* value) >1.301. Microarray expression data are available in the ArrayExpress database (www.ebi.ac.uk/arrayexpress) under the accession number E-MTAB-3487.

Kinase screening

The phosphorylation prediction algorithm, kinase substrate predictor version 2.0 from Kinexus Bioinformatics Corporation (Vancouver, BC, Canada), identified the 50 best-scored candidate kinases for L-plastin phosphorylation on residue Ser5, out of which 43 were subsequently screened by Kinexus Bioinformatics Corporation. The following peptides corresponding to the L-plastin N terminus and comprising residue Ser5 were chosen to be used in the kinase assays: ARG**S**V**S**-DEERR [wild-type (WT)] and ARG**S**V**A**DEERR [mutant (MT)], both starting with an *N*-acetylalanine (taking into account cotranslational modifications described by the UniProt Knowledgebase/Swiss-Prot database), as well as native MARG**S**V**S**DEERR (M-WT) and MARG**S**V**A**DEERR (M-MT), both still comprising the initial methionine residue. Residue Ser7 was substituted by an alanine in order to be able to distinguish between Ser5 and Ser7 phosphorylation and to exclude false-positives. There were 2 arginine residues added at the C-terminal end of the peptides to ensure adhesion of the peptides to the capture phosphocellulose filter paper following the kinase assay, and placed far enough from the Ser5 site so as not to affect the kinase recognition of this site. In brief, L-plastin peptides were mixed with individual protein kinases in the presence of [$\gamma-^{33}$P]ATP for 20–40 min, depending on the protein kinase tested. The assay was terminated by spotting 10 μl of the reaction mixture onto a multiscreen phosphocellulose P81 plate. After removing unreacted [$\gamma-^{33}$P]ATP from the reaction, radioactivity was quantified in a scintillation counter.

In vitro kinase assays of full-length recombinant L-plastin

A total of 10 μg full-length recombinant L-plastin was incubated with 50 μM ATP and 100 ng recombinant kinase [RSK1, RSK2, or ribosomal protein S6 kinase α-5 (MSK1)] obtained from SignalChem (Richmond, BC, Canada) in a reaction volume of 25 μl, according to the manufacturer's protocol. For the controls, the respective kinase was omitted. Following an incubation of 15 min at 30°C, Laemmli buffer was added, and the samples were boiled at 100°C for 5 min and then analyzed by immunoblotting.

Immunoblotting

Cells were lysed *in situ* in ice-cold lysis buffer [50 mM Tris-HCl (pH 7.5), 150 mM NaCl, 0.1% sodium dodecyl sulfate, 5 mM EDTA, 1% Nonidet P-40, 1% Triton X-100, 1% sodium-deoxycholate, 1 mM Na_3VO_4, 10 mM NaF, 100 μM leupeptin, and 100 μM E64D] containing a cocktail of protease inhibitors (Roche Diagnostics Gesellschaft mit beschränkter Haftung, Mannheim, Germany). Lysates were cleared by centrifugation at 13,200 rpm for 15 min at 4°C. The total protein concentration was determined by Bradford assay (Bio-Rad, Temse, Belgium). Protein separation was performed by SDS-PAGE under reducing conditions, and proteins were transferred onto nitrocellulose membranes by semidry transfer. The membranes were saturated with 1% bovine serum albumin in Tris-buffered saline supplemented with 0.1% Tween for 1 h at room temperature, then incubated with primary antibodies overnight at 4°C and with secondary antibodies coupled to a fluorescent dye for 1 h at room temperature. Antibody incubations were followed by membrane washings with Tris-buffered saline supplemented with 0.1% Tween. Signal intensities were detected by the Odyssey Infrared Image System (LI-COR Biosciences, Westburg, Leusden, The Netherlands). For quantification, the ratio between the intensities obtained for P-LPL [or phosphorylated PKA (P-PKA) substrates] *versus* total L-plastin (LPL) was determined to make individual samples comparable and then normalized to the mean of all the values obtained in one experiment to make blots comparable by accounting for technical day-to-day variability. For representative purposes, data were scaled to the highest signal and are represented as means ± SD. Statistical significance was determined by an unpaired *t* test with Welch's correction. $P < 0.05$ was considered significant.

Small interfering RNA knockdown

Small interfering RNA (siRNA) against RSK1 (Hs_RPS6KA1_10) and RSK2 (Hs_RPS6KA3_5) was purchased from QIAGEN Gesellschaft mit beschränkter Haftung (Venio, The Netherlands). A total of 60 nM siRNA was transfected using Lipofectamine 2000 according to the manufacturer's protocol.

Invasion and migration assays

Cells were seeded in collagen I-coated (200 μg/ml) 96-well plates (Essen ImageLock; Essen Bioscience, Hertfordshire, United Kingdom). At ~90% confluence, a wound was scratched across each well with the CellPlayer 96-well WoundMaker (Essen Bioscience). For siRNA knockdown, cells were transfected with siRNA 24 h before wound scratching. To study invasion, cells were covered with collagen I (1.5 mg/ml) diluted in cell culture medium. To study migration, cell culture medium was added to the cells. Wound confluence was monitored with the IncuCyte LiveCell Imaging System (Essen Bioscience) by measuring cell confluence over a total of 72 h. Graphs depict means ± SEM.

Immunofluorescence assay

Cells were plated on fibronectin-coated (20 μg/ml) glass coverslips. In case of transient transfection, cells were transfected 48 h prior to fixation. In case of treatment, cells were serum starved 24 h prior to treatment. A wound was scratched with a micropipette tip and then the cells were treated with vehicle or EGF (100 ng/ml) with or without prior treatment with BI-D1870 (5 μM). At 1 h following treatment, the cells were fixed with 4% paraformaldehyde for 10 min, permeabilized with 0.5% Triton X-100 in PBS for 5 min, and blocked in 2% bovine serum albumin in PBS-Tween 0.05% for 10 min. Between steps, the cells were washed with PBS-Tween. The cells were stained with phalloidin and antibodies against the HA tag of RSK2 constructs, against L-plastin or Ser5-P-LPL. Imaging was performed on an Andor Spinning Disk Revolution system (CSU-W1; Andor Technology, Belfast, United Kingdom) based on a Nikon Ti microscope (Nikon, Konan, Minato-ku, Tokyo, Japan) with an Andor iXon Ultra EMCCD camera and a ×100-1.4 NA oil objective. Image acquisition was performed using Andor Technology iQ3 software,

and image analysis was performed using ImageJ software (National Institutes of Health, Bethesda, MD, USA).

Modeling

The literature-derived model topology of L-plastin signaling including the interactions between Src, PKC, PKA and the ERK/MAPK pathway was described as Boolean rules with corresponding selection probabilities in the probabilistic Boolean network (PBN) framework [see review in (29)]. The experimental data obtained for ratios of P-LPL:LPL and P-PKA substrates:LPL from the 4 cell lines were used for model contextualization. Normalization of immunoblot data was performed as described above. Data generated from different experimental sets were normalized to the calibrator PMA, subsequently pooled, and scaled to the maximal value. We applied an improved version of the optPBN toolbox (30) to optimize the selection probabilities of the L-plastin signaling model in PBN format. Optimization was performed on a standalone machine (Intel CPU Xeon at 3.50 GHz, 16 GB random-access memory; Intel Corp., Santa Clara, CA, USA) for the different model variants based on random initial conditions. Bootstrapping was performed by randomly sampling 100 artificial data sets based on means and SD as acquired from our experimental data sets. Optimization was performed subsequently 100 times to identify the distribution of the identified selection probabilities.

Generation of stable RSK1, RSK2, and L-plastin knockdown MDA-MB-435S cells

Lentiviral vectors

The packaging vector psPAX2 and the envelope vector pMD2.G were obtained from Addgene (LGC Standards, Middlesex, United Kingdom). The transfer vectors containing short hairpin RNA (shRNA) for L-plastin (GIPZ Lentiviral shRNA Library, pool of clones V2LHS_133928, V2LHS_133929, V2LHS_238253, V2LHS_311716, and V2LHS_311717; Thermo Fisher Scientific, Waltham, MA, USA) as well as the GIPZ nonsilencing lentiviral shRNA control were purchased from GE Dharmacon (Diegem, Belgium).

Lentivirus production

Lentiviral particles were prepared by transient transfection of human embryonic kidney (HEK)293T/17 cells (American Type Culture Collection). In brief, 9×10^6 HEK293T/17 cells was seeded in Iscove's modified Dulbecco's medium (Lonza Group) with 10% fetal bovine serum in T75 cell culture flasks precoated with poly-L-lysine (Sigma-Aldrich). The next day, HEK293T/17 cells were cotransfected with 18 μg transfer vector, 15 μg packaging vector psPAX2, and 5.25 μg envelope vector pMD2.G in 12 ml OptiMEM medium (Thermo Fisher Scientific) using polyethylenimine (Polysciences, Eppelheim, Germany). The transfection mix was replaced by 12 ml Iscove's modified Dulbecco's medium with 2% fetal bovine serum per flask after 7–8 h. The virus-containing supernatant was harvested 40–48 h after medium change, cleared by centrifugation at 2000 rpm and 4°C for 10 min, and filtered through a 0.45 μm filter. Concentration of lentiviral particles was performed by precipitation with PEG10000 (1:5 volume of 40% PEG10000 solution; Sigma-Aldrich) at 4°C overnight followed by centrifugation at 1500 *g* and 4°C for 30 min. Subsequently, the virus was resuspended in 1:100 of the original volume of 50 mM Tris-HCl buffer (pH 7.4), divided in aliquots, and stored at −80°C. For determination of the lentivirus titer, 1×10^5 HT-1080 cells per well was transduced with limiting virus dilutions (1:100 to $1:10^6$) in the presence of 8 μg/ml polybrene (hexadimethrine bromide; Sigma-Aldrich) in a 6-well cell culture plate for 16 h. Transduced cells expressed green fluorescent protein and were quantified by fluorescence-activated cell sorting analysis after 3 d. Titers of concentrated lentivirus were in the range of 35,000 IU/μl.

Transduction of target cells

Ready-to-use lentiviral particles containing shRNA for RSK1 or RSK2 (Thermo Scientific GIPZ Lentiviral shRNA Library, human RPS6KA1, V2LHS_32012, and human RPS6KA3, V2LHS_47382) were obtained from GE Dharmacon. A total of 3.2×10^5 MDA-MB-435S cells in a 6-well cell culture plate was transduced with lentiviral particles containing shRNA for RSK1, shRNA for RSK2, shRNA for RSK1 and RSK2, shRNA for L-plastin (pool), or nonsilencing shRNA as a control (multiplicity of infection, 3) in the presence of 8 μg/ml Polybrene for 16 h. Subsequently, the transduced cells, positive for green fluorescent protein expression, were selected with 0.5 μg/ml puromycin in complete medium.

RESULTS

Invasive breast cancer cell lines display higher baseline L-plastin Ser5 phosphorylation than noninvasive breast cancer cell lines

The 4 breast cancer cell lines MCF7, SK-BR-3, BT-20, and MDA-MB-435S chosen as a working model for this study were carefully selected in order to cover different molecular profiles (31–33) with the main prerequisite being the expression of our protein of interest L-plastin. It is noteworthy however that considerable doubt had been raised about the origin of the cell clone MDA-MB-435S (34). Indeed, evidence was provided that MDA-MB-435S cells and the M14 melanoma cell line are genetically identical, which was confirmed by microsatellite analysis (35, 36). Although the correct origin of the 2 cell lines is still under debate, the most recent findings strongly suggest that both cell lines may be of breast origin (37, 38). For this study, the invasive phenotype of the chosen breast cancer cell lines is of particular importance, with MCF7 and SK-BR-3 being considered as non- or merely weakly invasive cell lines in contrast to BT-20 and MDA-MB-435S, which have been described as invasive cell lines (39, 40). By performing *in vitro* scratch wound assays, we reassessed the invasive capacities of our 4 cell lines. In line with the literature, our results confirmed that MCF7 and SK-BR-3 cells are only weakly invasive, whereas invasiveness was considerably increased in BT-20 and highly increased in MDA-MB-435S cells (**Fig. 1*A***). Because a correlation between the invasive capacity of melanoma cells and the phosphorylation state of L-plastin on Ser5 has been suggested before (10), we continued by investigating L-plastin Ser5 phosphorylation in the 4 breast cancer cell lines. To this end, we used an antibody specifically recognizing Ser5-P-LPL (anti-Ser5-*P* antibody) raised and characterized by our group (3, 7, 14). Although the L-plastin expression level is higher in the invasive compared with the noninvasive cell lines, our results clearly show high-baseline L-plastin Ser5

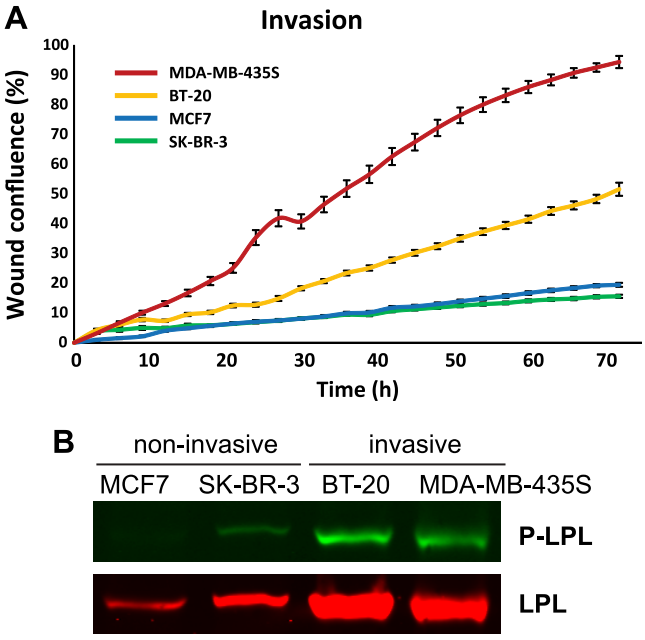

Figure 1. High-baseline L-plastin Ser5 phosphorylation in highly invasive *vs.* low-baseline L-plastin Ser5 phosphorylation in non- or weakly invasive breast cancer cell lines. *A*) There were 4 breast cancer cell lines seeded in collagen I-coated (200 μg/ml) 96-well plates. At ~90% confluence, a wound was scratched across each well with the CellPlayer 96-well WoundMaker. Cells were covered with collagen I (1.5 mg/ml) diluted in cell culture medium. Wound confluence was monitored with the IncuCyte LiveCell Imaging System by measuring cell confluence every 3 h over a total period of 72 h. The graph depicts mean ± SEM from all technical replicates obtained from 3 independent experiments. *B*) Cell extracts were subjected to immunoblot analysis using antibodies specific for Ser5-P-LPL (anti-Ser5-*P* antibody) and LPL.

phosphorylation in the invasive cell lines BT-20 and MDA-MB-435S as compared to absent or extremely weak phosphorylation in the noninvasive cell lines MCF7 and SK-BR-3 (Fig. 1*B*).

The ERK/MAPK pathway is enriched in DEGs when comparing breast cancer cells with differential L-plastin Ser5 phosphorylation

Whole-genome microarray analysis was performed to detect differences in signal transduction pathways leading to differential L-plastin Ser5 phosphorylation in noninvasive breast cancer cells with low-baseline Ser5-P-LPL *versus* invasive breast cancer cells with high-baseline Ser5-P-LPL. In addition, we treated the 2 noninvasive cell lines with PMA because this treatment has been shown previously to increase L-plastin Ser5 phosphorylation in MCF7 cells (3). As expected, PMA treatment led to a considerable increase in L-plastin Ser5 phosphorylation in both cell lines MCF7 and SK-BR-3 as compared to their respective untreated control (**Fig. 2**, left). In order to perform microarray analysis, total RNA was isolated from triplicate cell cultures, and microarray data were obtained using Affymetrix technologies. Lists of differentially expressed transcript clusters were established as described under Materials and Methods, and transcript cluster mapping and analysis were performed using IPA. For the comparison of PMA-treated *versus* untreated controls, we thus obtained a first list of DEGs for MCF7 and a second for SK-BR-3 cells. For the comparison of our 2 model invasive and 2 model noninvasive cancer cell lines, we obtained another 4 lists of differentially expressed transcript clusters (Fig. 2, right), the intersection of which was mapped by IPA to obtain a third list of DEGs. Taking the intersection of the 4 lists enabled us to focus on the genes that are differentially expressed between all comparisons of invasive *versus* noninvasive cells, thus setting a stringent filter. The 3 lists of DEGs can be found in Supplemental Data.

To assess a difference in signaling pathways between the compared conditions, we focused on canonical signaling pathways in IPA. For each of the 3 comparisons of interest, IPA revealed a list of canonical signaling pathways (Supplemental Data) from which we selected those that were significant [-log(*P* value) >1.301] and thus enriched by genes that are significantly differentially expressed. Interestingly, we identified 3 canonical signaling pathways that were common to the 3 lists: ERK/MAPK signaling, UVA-induced MAPK signaling, and role of osteoblasts, osteoclasts and chondrocytes in rheumatoid arthritis (Fig. 2, bottom). These results suggest an involvement of ≥1 of these pathways in L-plastin Ser5 phosphorylation.

RSK1 as well as RSK2 specifically phosphorylate residue Ser5 of recombinant full-length L-plastin *in vitro*

L-plastin peptides were synthesized and screened for Ser5 phosphorylation by 43 candidate kinases identified using the phosphorylation prediction algorithm, kinase substrate predictor version 2.0 from Kinexus Bioinformatics Corporation. In addition to PKA, which was previously shown to be able to phosphorylate L-plastin Ser5 *in vitro* (7, 12), our screening identified RSKs as well as MSK1 as top candidate kinases for phosphorylating this residue. As shown in **Table 1**, these kinases led to high radioactivity counts for the WT L-plastin peptide as well as for the Ser7-to-Ala-mutated peptide (MT), both peptides being devoid of the initiator methionine and acetylated on the N-terminal alanine. The WT peptide displayed higher counts for the named kinases than the MT peptide, indicating that phosphorylation occurs not only on residue Ser5 but also on Ser7. It is however noteworthy that Ser7 phosphorylation is not required for Ser5 phosphorylation by the investigated kinases because strong Ser5 phosphorylation was observed in the absence of Ser7. It is also noteworthy that the same kinases appear in the top positions for both peptides. Validation experiments as well as experiments with the WT and MT peptides still containing the initiator methionine were performed and showed similar rankings (data not shown).

Because the *in vitro* kinase assays performed on L-plastin peptides identified RSK1, RSK2, and MSK1 as candidate kinases (Table 1), we also tested these kinases for their ability to phosphorylate recombinant full-length L-plastin on residue Ser5 *in vitro*. As shown in **Fig. 3**, both RSK1 and RSK2 were able to strongly phosphorylate L-plastin on

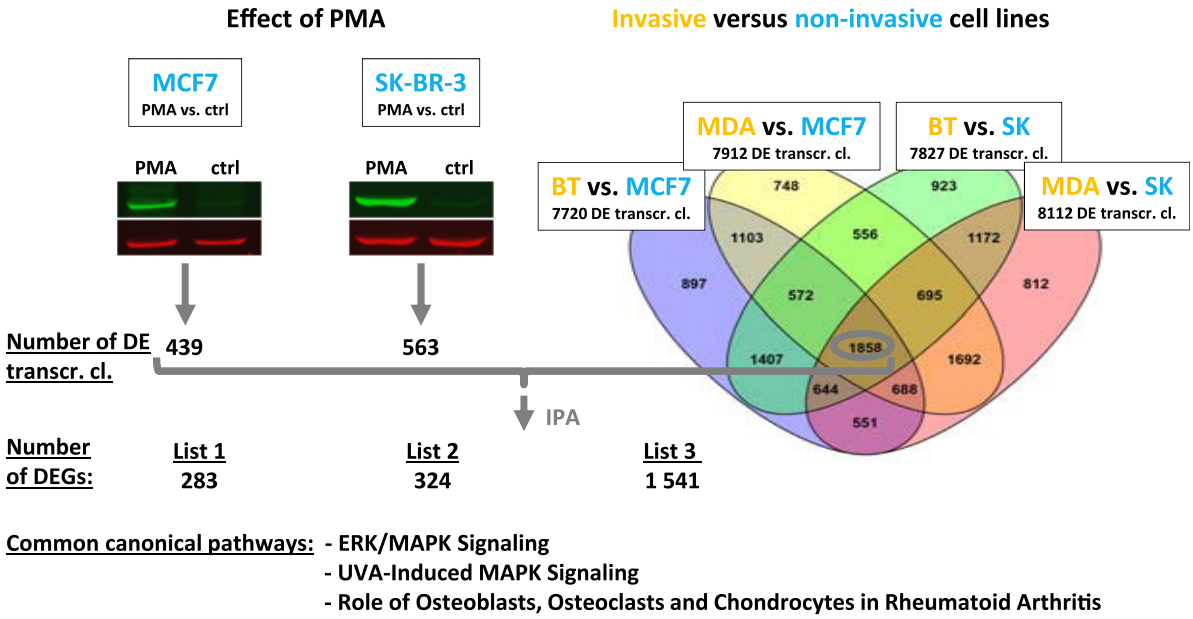

Figure 2. ERK/MAPK pathway enriched by genes that are significantly differentially expressed in breast cancer cells exhibiting differential L-plastin Ser5 phosphorylation levels. Noninvasive cell lines were treated with PMA, and resulting L-plastin Ser5 phosphorylation was determined by immunoblot analysis. Whole-genome microarray analysis was then used to compare breast cancer cells with differential L-plastin Ser5 phosphorylation levels and invasive capacities. There were 3 comparisons analyzed: 1) PMA-treated *vs.* untreated MCF7 cells; 2) PMA-treated *vs.* untreated SK-BR-3 cells; and 3) intersection between comparisons of invasive *vs.* noninvasive cells (BT-20 *vs.* MCF7, MDA-MB-435S *vs.* MCF7, BT-20 *vs.* SK-BR-3, and MDA-MB-435S *vs.* SK-BR-3). Differentially expressed transcript clusters (DE transcr. cl.) were identified for the 3 comparisons and were mapped and analyzed by IPA. For each of the 3 comparisons of interest, IPA revealed a list of canonical signaling pathways (Supplemental Data) from which we selected those that were significant [-log(*P* value) >1.301] and thus enriched by genes that are differentially expressed. There were 3 canonical signaling pathways common to the 3 lists: ERK/MAPK Signaling, UVA-Induced MAPK Signaling, and Role of Osteoblasts, Osteoclasts and Chondrocytes in Rheumatoid Arthritis. ctrl, control.

residue Ser5, whereas MSK1 was merely able to induce a weak L-plastin Ser5 phosphorylation.

The ERK/MAPK pathway and its downstream RSKs are involved in L-plastin Ser5 phosphorylation in breast cancer cells

The 2 newly identified prime candidate kinases capable of phosphorylating L-plastin on Ser5 *in vitro*, RSK1 and RSK2, are downstream effectors of the ERK/MAPK pathway (41). In addition, the results of our microarray experiments have also suggested an involvement of the ERK/MAPK pathway in L-plastin Ser5 phosphorylation. Altogether, these findings prompted us to further investigate the role of the ERK/MAPK pathway in L-plastin Ser5 phosphorylation. In a first step, we inhibited selected signaling molecules of this pathway, and we showed that PKC inhibition with the widely used pan-PKC inhibitor GF109203X, MEK1/MEK2 inhibition with PD98059, as well as RSK inhibition with BI-D1870 decreased baseline L-plastin Ser5 phosphorylation in invasive cells (**Fig. 4*A***).

In a second step, we took advantage of the fact that the ERK/MAPK pathway is one of the major signaling pathways activated upon binding of various growth factors to the corresponding receptor tyrosine kinases. Knowing that the EGFR family, a prominent receptor tyrosine kinase family, plays a key role in normal and malignant breast development (42) and is capable to trigger cell migration through ERK/MAPK pathway signaling (43), we checked for EGFR expression in our 4 model cell lines. As previously described by others (33), both SK-BR-3 and BT-20 cells expressed high levels of EGFR, whereas in MCF7 and MDA-MB-435S cells, the expression was very low or absent (Supplemental Fig. 1*A*). As expected, stimulation with EGF as a key EGFR-binding ligand did not increase L-plastin phosphorylation in the 2 EGFR-negative cell lines MCF7 and MDA-MB-435S, even when stimulated with high EGF concentrations. However, EGF treatment highly increased L-plastin Ser5 phosphorylation in SK-BR-3 and BT-20 cells at all tested concentrations (Supplemental Fig. 1*B*). We have shown previously that treatment with PMA, a well-known activator of PKCs that has also been described to activate the ERK/MAPK pathway (44–46), was able to induce L-plastin Ser5 phosphorylation in MCF7 (3) and SK-BR-3 cells (Fig. 2). Accordingly, PMA treatment of the 2 invasive cell lines BT-20 and MDA-MB-435S, displaying already high-baseline L-plastin Ser5 phosphorylation, was able to further increase this phosphorylation (Fig. 4*B*). Importantly, preincubation with inhibitors of the ERK/MAPK pathway impaired L-plastin phosphorylation upon PMA or EGF stimulation in all tested cell lines (Fig. 4*B*). To exclude off-target effects, we confirmed our results with a second RSK inhibitor, SL0101, which also impaired EGF-triggered L-plastin phosphorylation in SK-BR-3 and BT-20 cells and decreased baseline L-plastin phosphorylation in invasive cell lines (data not shown). Interestingly, the strongest decrease of L-plastin Ser5 phosphorylation was obtained for the combined inhibition of RSK and PKC (Fig. 4*B*).

TABLE 1. In vitro *kinase screening assay for L-plastin Ser5 phosphorylation*

Ranking	Kinases	Cpm ARGSVSDEERR (WT)[a]	Kinases	Cpm ARGSVADEERR (MT)[a]
1	RSK2	116,698	RSK1	55,774
2	PKAca	109,766	PKAca	53,986
3	RSK1	101,952	MSK1	53,254
4	MSK1	86,947	RSK2	48,800
5	RSK3	71,917	PKAcb	34,148
6	PKAcb	54,673	PKAcg	33,572
7	RSK4	45,174	RSK3	32,917
8	PKAcg	40,167	PRKG2	26,041
9	SGK3	32,646	RSK4	22,477
10	SGK2	32,129	SGK2	22,249
11	PRKG2	29,921	SGK3	20,290
12	PKCh	29,273	STK33	10,761
13	p70S6Kb	19,894	PKCh	10,007
14	AURORA B	12,688	AURORA B	9696
15	STK33	9990	PRKG1	9110
16	PKCq	9671	PRKX	8113
17	VRK1	9054	DCAMKL1	5899
18	PRKX	8310	VRK1	5745
19	PRKG1	8189	VRK2	5470
20	CAMK1b	8126	MNK1	5430
21	VRK2	7876	PKCe	5053
22	CAMK4	6955	CAMK4	4668
23	PKCe	6779	DCAMKL2	4447
24	DCAMKL2	5726	p70S6Kb	4242
25	MNK1	5718	CAMK1b	3996
26	DCAMKL1	5437	NDR	3797
27	NDR	5072	PKCq	3589
28	PKCd	4597	IKKe	3422
29	PIM2	4405	NDR2	3284
30	SGK1	4243	ASK1	2771
31	NDR2	3821	SGK1	2540
32	MSK2	3741	PKCd	2329
33	IKKe	3437	AKT1	1920
34	AKT1	3257	p70S6K	1911
35	ASK1	3241	PIM2	1813
36	PIM3	2732	PIM3	1537
37	p70S6K	2454	AKT3	1460
38	AKT3	2196	AKT2	1242
39	AKT2	2142	MSK2	1005
40	PIM1	892	PIM1	922
41	CK2a2	892	AURORA C	663
42	AURORA C	588	CHK1	256
43	CHK1	176	CK2a2	44

For *in vitro* kinase assays on L-plastin peptides, the peptides were mixed with individual protein kinases in the presence of [$\gamma-^{33}$P]ATP for 20–40 min, depending on the protein kinase tested. The assay was terminated by spotting 10 μl of the reaction mixture onto a multiscreen phosphocellulose P81 plate. After removing unreacted [$\gamma-^{33}$P]ATP from the reaction, radioactivity was quantified in counts per minute (Cpm) in a scintillation counter. [a]N-terminal alanine is acetylated.

And finally, trametinib, a clinical MEK inhibitor approved by the U.S. Food and Drug Administration for melanoma treatment (trade name Mekinist), clearly reduced L-plastin Ser5 phosphorylation in invasive cell lines and prevented an EGF-triggered increase in L-plastin Ser5 phosphorylation in SK-BR-3 and BT-20 cells (Fig. 4*C*). Altogether, these results point to a major involvement of the ERK/MAPK signaling pathway in L-plastin Ser5 phosphorylation.

Modeling of the L-plastin signaling pathway with PBNs

The signaling pathways leading to L-plastin Ser5 phosphorylation are not clearly understood, and so far, it was assumed that the identity of the protein kinase responsible for this phosphorylation event depends on the cell type and environment. In addition to reports on the involvement of PKA (7, 12) and PKC (3, 13–18), our results presented here highlight a role of RSKs in this process. In order to obtain a better quantitative understanding of the signaling pathways upstream of L-plastin Ser5 phosphorylation, we applied the optPBN toolbox to further study and analyze these pathways in the PBN framework (30). We built a PBN model that represents the network topology of signaling pathways upstream of L-plastin Ser5 phosphorylation based on literature information and our own findings (**Fig. 5*A***). Our model is mainly focused on the ERK/MAPK pathway

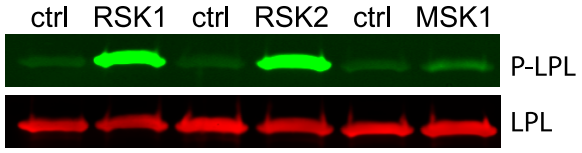

Figure 3. RSK1 and RSK2 are able to directly phosphorylate L-plastin Ser5 *in vitro*. A total of 10 μg recombinant full-length L-plastin was incubated with 100 ng recombinant kinase and with 50 μM ATP in a reaction volume of 25 μl according to the manufacturer's protocol. For each kinase assay, a control (ctrl) was performed by omitting the respective kinase. Samples were incubated for 15 min at 30°C. Following incubation, Laemmli buffer was added, and the samples were boiled at 100°C for 5 min and analyzed by immunoblot visualizing Ser5-P-LPL and LPL.

(downstream of the EGFR) and includes Src, PKC, and PKA kinases, which are known to interact with this pathway. Then, we fitted the PBN model to an extensive data set comprising activation and inhibition of various network nodes that modulate the signals toward the 2 measured output nodes (*i.e.*, L-plastin Ser5 phosphorylation and PKA substrate phosphorylation in 4 breast cancer cell lines). To this end, we took into account the described off-target effects of the inhibitors GF109203X and H89 on RSK (47, 48). As a result, we obtained a model that explained well our experimental data for all 4 cell lines as shown in Fig. 5*B*.

Because we found RSKs to be essential for L-plastin Ser5 phosphorylation, the fitted PBN model was used to investigate whether RSKs have more influence on L-plastin in the 4 cell lines than PKA and PKC. In addition, we checked whether the crosstalk interactions between PKC and PKA suggested in the literature (49, 50) are important to modulate the signal transduction upstream of L-plastin Ser5 phosphorylation. We therefore applied an *in silico* knockout approach where we removed an interaction from the model one at a time and checked if the removal affected the fitting quality. There were 5 interactions situated in close proximity to our output nodes analyzed (*i.e.*, RSK→L-plastin, PKC→L-plastin, PKA→L-plastin, PKC→PKA, and PKA→PKC) (**Table 2**). We found that removing the interactions RSK→L-plastin and PKC→PKA led to a dramatic increase of the model-fitting costs in all 4 cell lines, meaning that the networks missing 1 of these 2 interactions fitted our experimental data less well. The individual knockout of the other 3 interactions only led to minor changes in fitting costs, suggesting that none of these 3 interactions is necessary to explain our experimental data.

We then proceeded by examining the optimized selection probability weights of each interaction and their distributions obtained *via* bootstrapping (see Materials and Methods). A subset of the obtained weight distributions of the interactions is shown in **Table 3**. All weights can be found in Supplemental Fig. 2. Strikingly, in all 4 cell lines, the activation of L-plastin by RSK is largely predominant as compared to its activation by PKC or PKA. In addition, the weights attributed to the investigated interactions indicate that in all 4 cell lines, the crosstalk appears to be directed from PKC to PKA rather than from PKA to PKC. The relatively low SDS on the weights ensured that these findings are robust against experimental variation in the data set.

RSK1 and RSK2 are involved in breast cancer cell migration and invasion and in L-plastin redistribution to migratory structures

Altogether, we provide evidence that RSKs are involved in L-plastin Ser5 phosphorylation by *in vitro* kinase assays, inhibition with 2 different RSK inhibitors, as well as computational modeling. To consolidate our findings, we simultaneously knocked down RSK1 and RSK2 by an siRNA approach. Albeit RSK knockdown was not equally efficient in all the investigated cell lines, we were able to observe a decrease of Ser5-P-LPL in all 4 cell lines following the combined knockdown of RSK1 and RSK2 (**Fig. 6*A***). Comparing P-LPL/LPL between cell lines, it is interesting to note that for SK-BR-3 and MDA-MB-435S for which an efficient RSK knockdown was reached, the decrease in L-plastin Ser5 phosphorylation was more important than for MCF7 and BT-20, with a less-efficient RSK knockdown. The remaining L-plastin Ser5 phosphorylation might be due to residual RSK1 and RSK2 protein presence after knockdown. Altogether, even though phosphorylation was not completely abolished, our data clearly confirm an important role for RSKs in L-plastin Ser5 phosphorylation.

Moreover, we investigated the effect of siRNA-dependent RSK knockdown on migration and invasion in MDA-MB-435S cells. This cell line was selected because it has the highest invasive capacity as shown in Fig. 1*A*. *In vitro* scratch wound assays revealed that the combined knockdown of RSK1 and RSK2 considerably slowed down MDA-MB-435S cell migration and invasion by up to 30% (Fig. 6*B*), whereas cell proliferation remained largely unaffected (data not shown). To further corroborate this finding, we stably knocked down RSK1, RSK2, combined RSK1 and RSK2, or L-plastin in MDA-MB-435S cells using shRNA-expressing lentiviral vectors. Knockdown was more successful for RSK2 than for RSK1, explaining the larger decrease of L-plastin Ser5 phosphorylation in RSK2 knockdown compared to RSK1 knockdown MDA-MB-435S cells (Fig. 6*C*). It is noteworthy that the previously observed siRNA-dependent reduction in migration and invasion (Fig. 6*B*) was confirmed by combined RSK1 and RSK2 knockdown (Fig. 6*D*), whereas knockdown of RSK1 or RSK2 alone was not sufficient to affect migration or invasion (data not shown). Notably, a stable knockdown of L-plastin to an undetectable level on immunoblot (Fig. 6*C*) did not significantly decrease migration and invasion of MDA-MB-435S cells (Fig. 6*D*).

Furthermore, we investigated whether endogenous RSK activity affects actin, L-plastin, and Ser5-P-LPL localization in migrating cells. To this end, SK-BR-3 cells were plated on glass coverslips coated with fibronectin, and at ~90% confluence, a wound was scratched. Immunofluorescent staining of L-plastin, Ser5-P-LPL, and actin was performed after EGF treatment with or without prior treatment with the RSK inhibitor BI-D1870 in cells migrating into the scratched wound. As a result, we observed that EGF treatment led to an increased formation of ruffling membranes, microspikes, and even longer filopodia-like structures embedded in the cortical region of the cell, all of which are

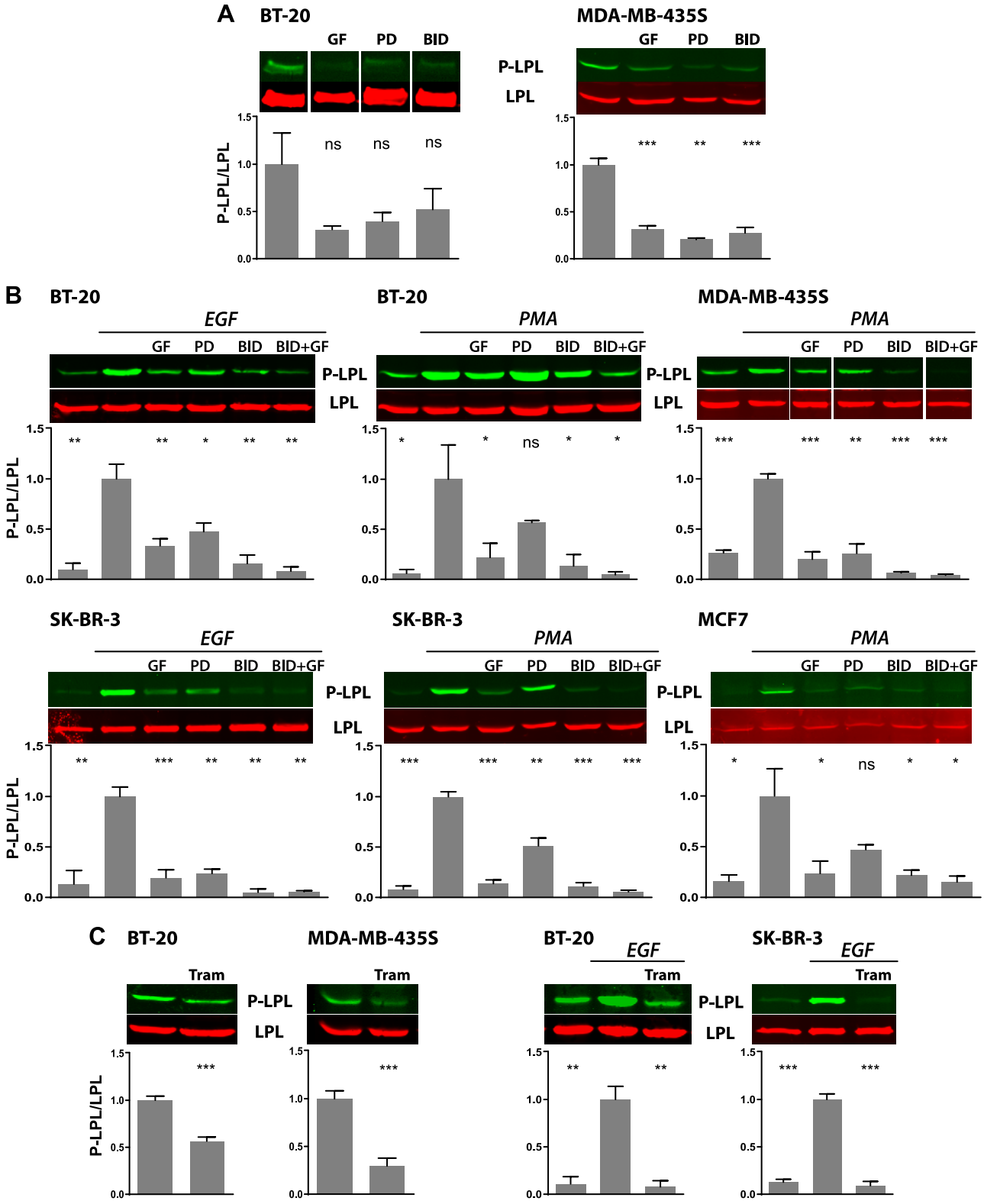

Figure 4. Involvement of the ERK/MAPK pathway in L-plastin Ser5 phosphorylation in breast cancer cells. *A*) Invasive cell lines exhibiting high-baseline L-plastin Ser5 phosphorylation were treated with inhibitors of selected signaling molecules of the ERK/MAPK pathway: GF109203X (GF), PD98059 (PD), and BI-D1870 (BID). Subsequent to inhibitor treatment, residual L-plastin Ser5 phosphorylation was determined by immunoblot analysis. For quantification, the ratio between the intensities obtained for P-LPL *vs.* LPL was determined to make individual samples comparable and then normalized to the mean of all the values obtained in 1 experiment to make blots comparable by accounting for technical day-to-day variability. *B*) Cells were preincubated with inhibitors of the ERK/MAPK pathway and then stimulated with EGF (for the 2 EGFR-expressing cell lines) or PMA (for the 4 cell lines). L-plastin Ser5 phosphorylation was quantified as described under (*A*). *C*) Cells were treated with trametinib (Tram)

(*continued on next page*)

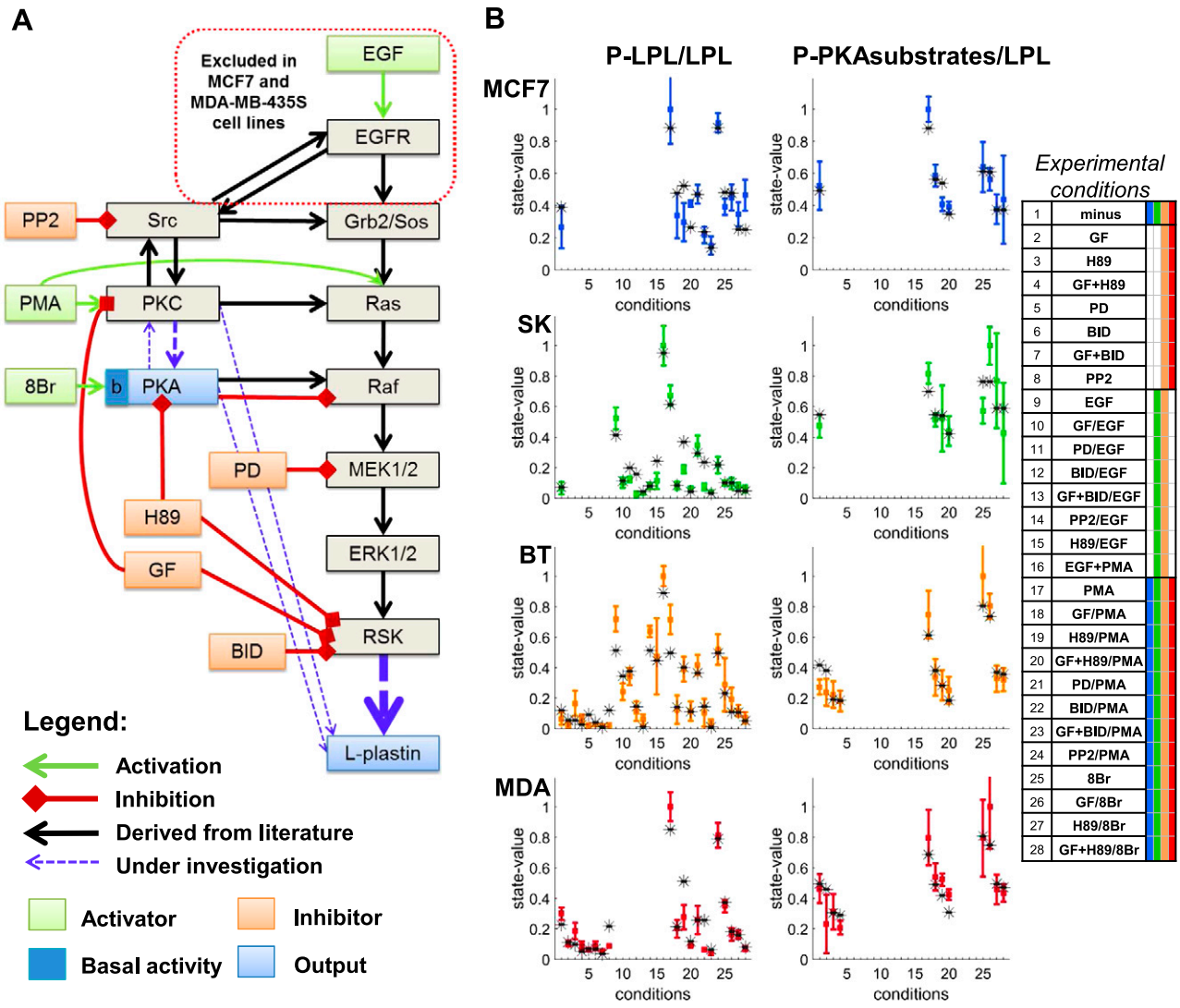

Figure 5. Literature-derived and experiment-based L-plastin signaling network and model-fitting results. *A*) A candidate network for the signaling pathways upstream of L-plastin Ser5 phosphorylation was built based on literature information and our own experimental findings. The network interactions were analyzed by applying a PBN approach taking into account cell line-specific immunoblot-based quantifications of P-LPL and P-PKA substrates. Various conditions were tested in the 4 cell lines MCF7, SK-BR-3 (SK), BT-20 (BT), and MDA-MB-435S (MDA) including activation by EGF, PMA, or 8-Bromo-cAMP (8Br) and/or inhibition by GF109203X (GF), H89, PP2, PD98059 (PD), or BI-D1870 (BID). *B*) PBN model-fitting results in comparison to experimental data for the various tested conditions. Colored bars indicate the conditions tested for the individual cell lines. For quantification, the ratio between the intensities obtained for P-LPL, respectively, P-PKA substrates *vs.* LPL was determined to make individual samples comparable and then normalized to the mean of all the values obtained in 1 experiment to make blots comparable by accounting for technical day-to-day variability. Data generated from different experimental sets were normalized to the calibrator PMA, subsequently pooled, and scaled to the highest signal (of each respective graph) for representative purposes. Means of 10 simulated values from the PBN model (black stars) were compared against the experimental data [multicolored squares (means) and error bars (SD)].

structures playing a role in cell migration (**Fig. 7**). It is noteworthy that L-plastin was highly enriched in these structures. Interestingly, RSK inhibition with BI-D1870 treatment prior to EGF stimulation did not abolish but clearly reduced the formation of these migratory structures and the redistribution of L-plastin to these structures (Fig. 7). Ser5-P-LPL could only be visualized in the cells following EGF treatment and was also found in ruffling membranes and in microspikes. The staining for Ser5-P-LPL disappeared with RSK inhibition (Fig. 7).

with or without subsequent EGF stimulation, and L-plastin Ser5 phosphorylation was quantified as described under (*A*). For each immunoblot shown, samples were run on the same gel, but for BT-20 shown under (*A*) and MDA-MB-435S shown under (*B*), bands were cut and put in another order for representative purposes. For representative purposes, data were scaled to the highest signal and are represented as means ± SD. Statistical significance was determined by an unpaired *t* test with Welch's correction. $P < 0.05$ was considered significant. *$P < 0.05$; **$P < 0.01$; ***$P < 0.001$; n.s., nonsignificant.

TABLE 2. *Model-fitting costs obtained* via in silico *knockout*

Model variant	MCF7	SK-BR-3	BT-20	MDA-MB-435S
Initial model	0.2298	0.2942	0.2961	0.3126
RSK → LPL removed	0.7872	1.0344	0.6921	1.2369
PKC → LPL removed	0.2298	0.2942	0.2962	0.3126
PKA → LPL removed	0.2318	0.2942	0.2966	0.3126
PKC → PKA removed	0.7163	0.4520	0.4245	0.4622
PKA → PKC removed	0.2298	0.2942	0.3045	0.3452

The fitting costs of model variants after removing individual interactions were compared to those of the initial model structure prior to removal. The fitting cost is the sum of squared error between simulated state values and the mean values of the experimental data.

Finally, MDA-MB-435S cells stably knocked down for RSK2 and exhibiting a strong decrease of L-plastin Ser5 phosphorylation were transfected with RSK2wt or constitutively active RSK2Y707A. Notably, both transfections led to a rescue of the level of Ser5-P-LPL to a normal level (Supplemental Fig. 3*A*). In parallel, we analyzed the localization of Ser5-P-LPL by performing immunofluorescence studies. Similar to the effect observed upon EGF treatment in SK-BR-3 cells, the ectopic expression of RSK2wt and RSK2Y707A in MDA-MB-435S cells increased the formation of microspike-like structures with a redistribution of Ser5-P-LPL to these structures (Supplemental Fig. 3*B*). To corroborate our findings, we also performed transient transfection of RSK2wt or RSK2Y707A in SK-BR-3 cells. We observed an increased staining of Ser5-P-LPL in cells overexpressing RSK2wt or RSK2Y707A and, in parallel, the recruitment of Ser5-P-LPL to actin-rich migratory structures (Supplemental Fig. 3*C*).

Altogether, these results indicate a qualitative link between L-plastin Ser5 phosphorylation by RSK and its redistribution to migratory structures.

DISCUSSION

In our previous studies, we have shown that phosphorylation of L-plastin on residue Ser5 plays a critical role in L-plastin activation (3, 7). Here, we have unraveled a major signaling pathway responsible for L-plastin Ser5 phosphorylation in breast cancer cells. We have revealed the involvement of the ERK/MAPK pathway with its downstream target kinases RSK1 and RSK2 being able to directly phosphorylate L-plastin on Ser5. In addition, we have illustrated an RSK-dependent recruitment of L-plastin and, more precisely, Ser5-P-LPL to migratory structures.

In this study, we chose to take a microarray-based gene expression-profiling approach in order to correlate conditions and cell lines presenting differential L-plastin Ser5 phosphorylation levels with patterns of changes in gene expression. In the context of the cofilin pathway in breast cancer invasion and metastasis (51), the authors have pointed out that not only individual genes but whole pathways with differential regulation and activity states of the corresponding molecules should be taken into account for phenotype interpretation. Likewise, in our study, the whole-genome microarray analysis approach allowed us to identify 3 canonical pathways enriched in DEGs, namely ERK/MAPK signaling, UVA-induced MAPK signaling, and role of osteoblasts, osteoclasts and chondrocytes in rheumatoid arthritis, of which the ERK/MAPK pathway is a prominent oncogenic signaling pathway. In addition, the *in vitro* kinase assays carried out in parallel identified the ERK/MAPK pathway downstream kinases RSK1 and RSK2 as the most prominent candidate kinases for L-plastin Ser5 phosphorylation. These findings together with a previous report describing L-plastin as an ERK/MAPK pathway-regulated protein (52) prompted us to proceed to an in-depth investigation of this pathway, whose deregulation has also been associated with breast cancer progression [reviewed in Whyte *et al.* (53)].

Several approaches were used to unravel the involvement of the ERK/MAPK pathway with its downstream kinases RSK1 and RSK2 in the L-plastin Ser5 phosphorylation event. To trigger this pathway, we stimulated the cells with EGF or with PMA, both described as activators of the ERK/MAPK pathway. Evidence for a direct involvement of the ERK/MAPK pathway downstream kinases RSK1 and RSK2 in L-plastin Ser5 phosphorylation was provided both by a knockdown approach and by the use of 2 different RSK inhibitors: BI-D1870 and SL0101. This reduces the probability that the observed inhibitor-dependent decrease of phosphorylation is due to off-target effects. Indeed, BI-D1870 and SL0101 have only 1 common off target, Aurora B (54), which demonstrated considerably weaker potency in phosphorylating L-plastin peptides than RSK1 or RSK2, as shown by the *in vitro* kinase assays from Kinexus Bioinformatics Corporation (Table 1). In line, and most importantly, the 2 kinases RSK1 as well as RSK2 were able to directly phosphorylate the recombinant L-plastin protein on residue Ser5 in an *in vitro* kinase assay. Further evidence for the importance of the ERK/MAPK pathway is provided by the data obtained with the MEK inhibitor PD98059 as well as with the clinically used MEK inhibitor trametinib. Moreover, our finding that L-plastin phosphorylation can be mediated by RSK upon activation of the ERK/MAPK

TABLE 3. *Optimized selection probability weights and their distributions obtained* via *bootstrapping*

Interaction	MCF7	SK-BR-3	BT-20	MDA-MB-435S
RSK → LPL	0.888 (0.081)	1.000 (0.000)	0.948 (0.070)	1.000 (0.000)
PKC → LPL	0.004 (0.023)	0.000 (0.000)	0.025 (0.058)	0.000 (0.000)
PKA → LPL	0.108 (0.073)	0.000 (0.000)	0.027 (0.023)	0.000 (0.000)
PKC → PKA	0.407 (0.060)	0.236 (0.049)	0.262 (0.059)	0.252 (0.093)
PKA → PKC	0.072 (0.112)	0.005 (0.017)	0.256 (0.189)	0.204 (0.068)

The distributions of identified mean weights (SD) obtained *via* bootstrapping are shown for the 5 interactions under investigation in the 4 cell lines.

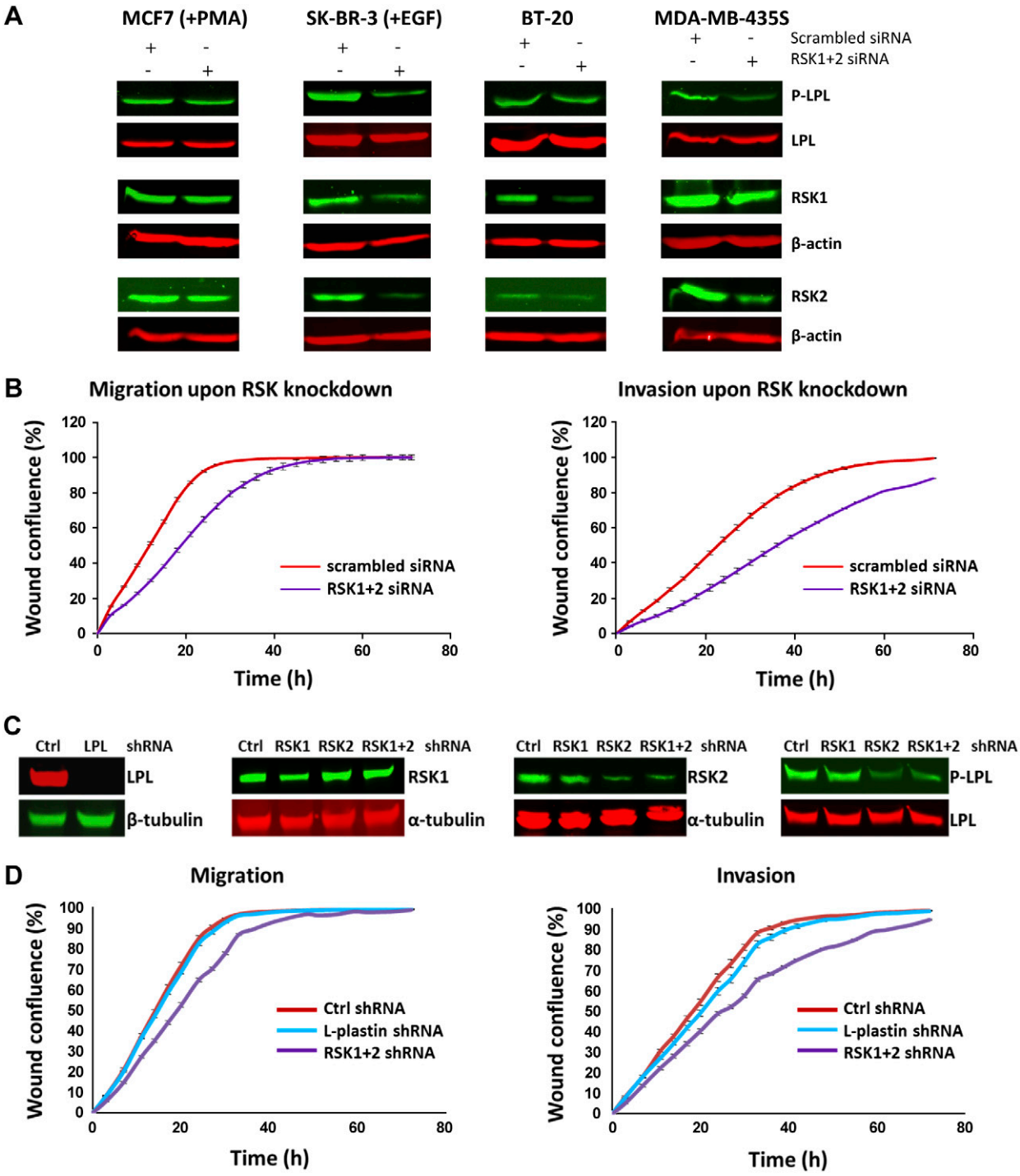

Figure 6. Combined RSK1 and RSK2 knockdown decreases L-plastin Ser5 phosphorylation and impairs migration and invasion, whereas an L-plastin stable knockdown does not affect MDA-MB-435S cell motility. *A*) siRNA against RSK1 and RSK2 or scrambled siRNA was transfected in the 4 cancer cell lines as indicated, and L-plastin Ser5 phosphorylation and RSK1 and RSK2 expression were assessed by immunoblot analysis 72 h posttransfection. Noninvasive cell lines were treated with EGF or PMA as indicated. *B*) MDA-MB-435S cells were seeded in collagen I-coated (200 μg/ml) 96-well plates and transfected with siRNA against RSK1 and RSK2 or with scrambled siRNA. After 24 h, a wound was scratched across each well with the CellPlayer 96-well WoundMaker. To study invasion, cells were covered with collagen I (1.5 mg/ml) diluted in cell culture medium. To study migration, cell culture medium was added to the cells. Migration and invasion were monitored by measuring wound confluence every 3 h for a total of 72 h with the IncuCyte LiveCell Imaging System. Graphs depict means ± SEM from all technical replicates obtained from 3 independent experiments. Efficient knockdown of RSK1 and RSK2 as well as efficient decrease of L-plastin Ser5 phosphorylation were confirmed by immunoblot analysis (quantification included in *A*). *C*) MDA-MB-435S cells were transduced with lentiviral particles containing shRNA for RSK1, RSK2, RSK1 and RSK2, and L-plastin or nonsilencing shRNA as a control (Ctrl). Subsequently, the transduced cells were selected with puromycin in complete medium. RSK1, RSK2, and L-plastin expression as

(*continued on next page*)

pathway was confirmed by our computational model, which suggests that RSK is the most important activator of L-plastin in all 4 cell lines. Our PBN modeling approach proved to be a useful tool to integrate the information from literature together with our vast experimental data set, in particular because signaling tends to occur in complex networks.

Although our results provide strong evidence for a role of the ERK/MAPK pathway with the downstream kinases RSK1 and RSK2 being able to directly phosphorylate L-plastin on residue Ser5, they do not rule out that L-plastin Ser5 phosphorylation can also be mediated by other pathways. So far, only PKA has been reported to directly phosphorylate L-plastin *in vitro* (7, 12), whereas other kinases such as PKCδ, catalytic domain of PKC, casein kinase II, Pak1, PKB, M2K, M3K, and p38-regulated/activated protein kinase failed to directly phosphorylate L-plastin *in vitro* (12, 13). In cells, by contrast, distinct protein kinases have been reported to play a role in triggering L-plastin phosphorylation depending on the cell type and environment. Most frequent are reports of the involvement of PKA (7, 12) and PKC (3, 13–18). PI3K has also been reported to play a role in L-plastin phosphorylation in human neutrophils (13, 16), but not in T lymphocytes (18). Although an siRNA knockdown of PKCδ (3, 14) and PKCβ_{II} (17) reduced L-plastin Ser5 phosphorylation, it has to be taken into account that most reports are based on activation and/or inhibition studies. Strikingly, all inhibitors used to demonstrate the involvement of PKA and PKC (H89, GF109203X, Gö6976, and Ro-31-8220) in L-plastin phosphorylation also strongly inhibit RSK2 (47, 48). Moreover, PMA used as a PKC activator does not only activate PKC but has also been shown to activate the ERK1/2 module either through PKC and c-Src or through RasGRP (44–46). Finally, the effect of the PKA activator cAMP on the ERK1/2 module appears to depend on the cellular context because cAMP has been demonstrated to stimulate ERK in a B-Raf–dependent manner or to suppress ERK signaling in many cells through its ability to target C-Raf [reviewed in Dumaz and Marais (55)]. In the present study, we have demonstrated a clear and direct activity of the kinases RSK1 and RSK2 in L-plastin Ser5 phosphorylation supported by a modeling approach. A potential involvement of the previously described kinases PKA, PKC, and PI3K cannot be ruled out, although in our model, PKA and PKC appear to play a rather indirect role in L-plastin activation. This result is in line with previous findings of Hagi *et al.* (56), who reported that cAMP stimulation was not able to trigger L-plastin Ser5 phosphorylation in macrophages. Regarding a potential involvement of PI3K, future studies that were out of the scope of the present work have to be dedicated to the investigation of the phosphatase and tensin homolog/PI3K/AKT/mammalian target of rapamycin pathway in mediating L-plastin Ser5 phosphorylation.

RSKs have been described as versatile regulators controlling migration and invasion downstream of ERK/MAPK activation (57) by altering the transcription of many genes involved in epithelial-to-mesenchymal transition, regulating cell adhesion through phosphorylation events with subsequent modulation of integrin activity, and/or remodeling the actin cytoskeleton. In this context, the phosphorylation of the RSK1/2 target integrin subunit β4 has been found to play a role in hemidesmosome disassembly regulation and hence in migration (58). It is noteworthy that RSK2 expression has been correlated to the expression of the actin-bundling protein fascin-1 in tumor samples from patients with head and neck squamous cell carcinoma and to filopodia formation in cancer cells (59), suggesting that the RSK2-cAMP response element-binding protein pathway increases proinvasive and prometastatic capacities. Interestingly, RSK2 has been described to phosphorylate a further actin-binding protein filamin A (60) on residue Ser2152 (61). This phosphorylation event is involved in EGF-induced cell migration (61) and inhibition of cell adhesion through integrin inactivation (62). Indeed, RSK-dependent phosphorylation was shown to promote filamin A binding to β integrin tails (63). In this regard, it is interesting to note that also L-plastin was described to interact with β1 and β2 integrin subunits (64) and that L-plastin as well appears to modulate the affinity of integrins (unpublished results). In our study, both RSK1 and RSK2 were able to phosphorylate the actin-binding protein L-plastin, and combined knockdown of the 2 isoforms led to a clear decrease in cell migration and invasion. Surprisingly, however, stable knockdown of L-plastin did not significantly affect migration and invasion of MDA-MB-435S cells, which suggests that the effect of RSK knockdown on the promotile/invasive capacities of these cells is not, or only modestly, mediated through L-plastin. This finding is not in line with the finding that L-plastin knockdown reduced haptotactic migration of the melanoma cell line IF6 (10). Similar contradictory results have been found in PC-3 prostate cancer cells, where one study showed that L-plastin down-regulation decreased migration and invasion rates (65), whereas another study showed that L-plastin down-regulation did not affect filopodia formation and had merely a low effect on motility. The latter study however provided evidence that a nanobody-mediated inhibition of L-plastin bundling led to inhibited filopodia formation and highly decreased migration and invasion of PC-3 cells (66). The authors suggested that the depletion of the L-plastin protein could lead to a compensation of the L-plastin function by a functionally redundant protein. Such a compensatory mechanism might not take place in case of a nanobody-mediated knockout of a specific function of L-plastin (66).

Nevertheless, our results provide evidence for a link between RSK activity and L-plastin phosphorylation and

well as L-plastin Ser5 phosphorylation were determined by immunoblot analysis. *D*) MDA-MB-435S cells with stable knockdown for L-plastin, combined RSK1 and RSK2, or transduced with a nonsilencing control shRNA were seeded in collagen I-coated (200 μg/ml) 96-well plates. A wound was scratched across each well with the CellPlayer 96-well WoundMaker. To study invasion, cells were covered with collagen I (1.5 mg/ml) diluted in cell culture medium. To study migration, cell culture medium was added to the cells. Migration and invasion were monitored by measuring wound confluence over a total of 72 h with the IncuCyte ZOOM LiveCell Imaging System. The graphs depict means ± SEM of at least 10 technical replicates, and shown is 1 representative experiment of 4 independent repeats.

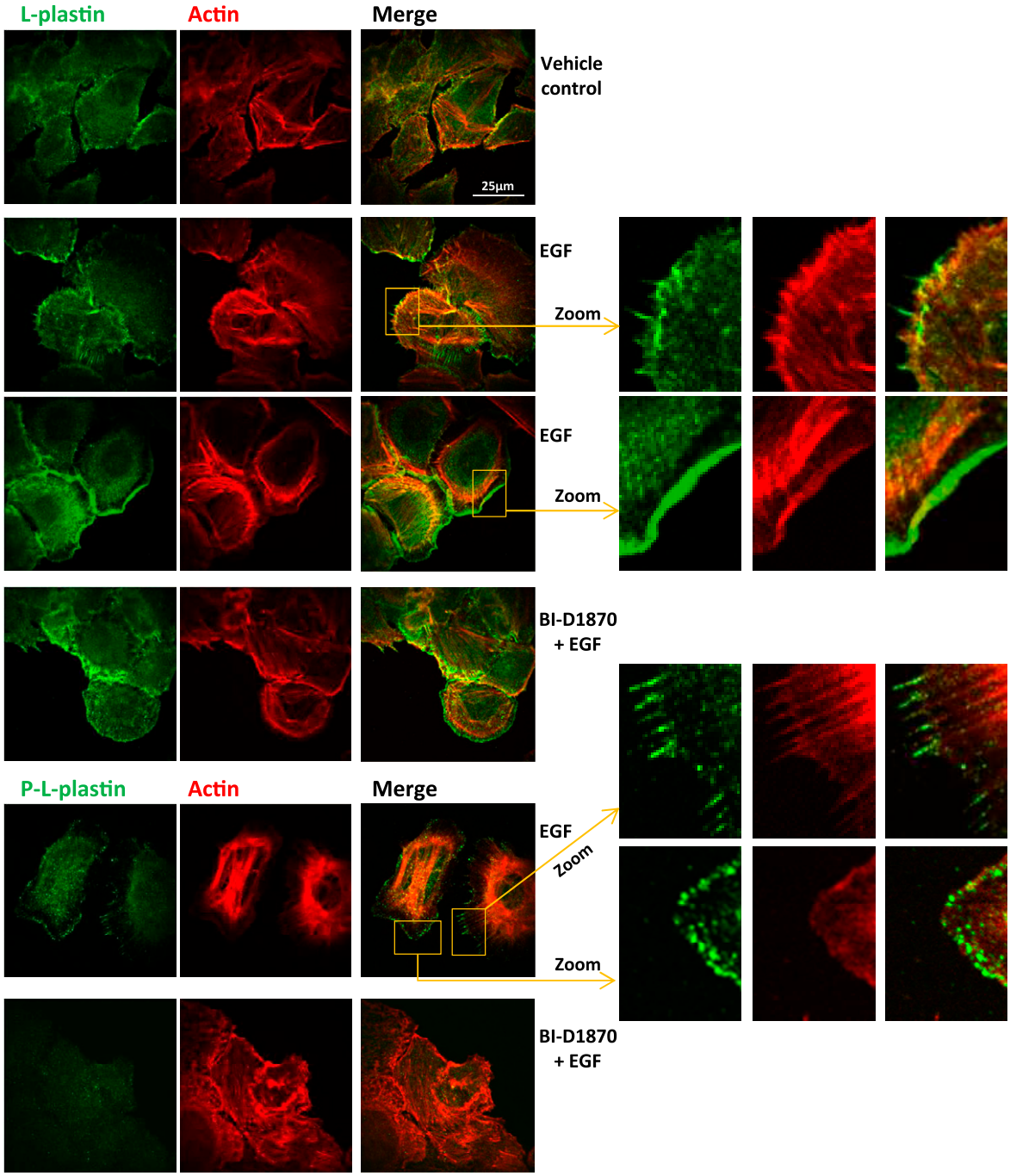

Figure 7. L-plastin Ser5 phosphorylation and localization in migratory structures upon EGF stimulation are dependent on RSK activity. SK-BR-3 cells were plated on fibronectin-coated coverslips and serum starved for 24 h. At ~90% confluence, a wound was scratched with a micropipette tip, and cells were subsequently treated with vehicle or EGF (100 ng/ml) with or without prior treatment with BI-D1870 (5 µM). At 1 h following treatment, the coverslips were fixed and subsequently stained with phalloidin and an antibody specific for L-plastin or Ser5-P-LPL (anti-Ser5-*P* antibody, P-L-plastin) before being analyzed by confocal microscopy.

redistribution to migratory structures formed upon EGF stimulation or RSK2 overexpression. The identification of L-plastin as a new target of RSKs consolidates their role in the regulation of the actin cytoskeleton. Our results extend the findings of Doehn *et al.* (67), who investigated the effects of RSK1 and RSK2 on migration and invasion in epithelial breast cells and showed that combined knockdown of RSK1 and RSK2 or RSK inhibition suppressed the ERK pathway-dependent induction of promotile and proinvasive genes. The detailed functional outcome of L-plastin Ser5 phosphorylation by RSK deserves further in-depth investigation.

Overall, our results show the first evidence, to our knowledge, of the involvement of the ERK/MAPK pathway in L-plastin Ser5 phosphorylation. These findings corroborate Ser5-P-LPL as a molecular marker for invasive carcinomas with deregulated ERK/MAPK pathway signaling. FJ

The authors are grateful to Alexandre Baron (University of Luxembourg, UL) for his meaningful contribution to the revision of this manuscript and to Nicolas Beaume (UL) and Aurélien Ginolhac (UL) for help with statistical data analysis. The authors thank Maria Koffa (Democritus University of Thrace, Alexandroupoli, Greece) and Serge Haan (UL) for proofreading the manuscript and constructive discussions as well as Evelyne Friederich (UL) as an initiator of this research project. The authors also thank François Bernardin (Luxembourg Institute of Health) and Andreas Girod (UL) for assistance with microarray and confocal microscopy experiments, respectively. In addition, the authors thank Joe W. Ramos (University of Hawaii, Honolulu, HI, USA) for providing the ribosomal protein S6 kinase α-3 constructs. This work was supported by a grant from the UL (Internal Research Project: PhosphoPlast). M.J.L. and P.T. are recipients of fellowships allocated by the Fonds National de la Recherche (Aides à la Formation-Recherche Grants 2748401 and 1233900, respectively). The authors declare no conflicts of interest.

REFERENCES

1. Yilmaz, M., and Christofori, G. (2010) Mechanisms of motility in metastasizing cells. *Mol. Cancer Res.* **8**, 629–642
2. Winder, S. J., and Ayscough, K. R. (2005) Actin-binding proteins. *J. Cell Sci.* **118**, 651–654
3. Al Tanoury, Z., Schaffner-Reckinger, E., Halavatyi, A., Hoffmann, C., Moes, M., Hadzic, E., Catillon, M., Yatskou, M., and Friederich, E. (2010) Quantitative kinetic study of the actin-bundling protein L-plastin and of its impact on actin turn-over. *PLoS One* **5**, e9210
4. Morley, S. C. (2012) The actin-bundling protein L-plastin: a critical regulator of immune cell function. *Int. J. Cell Biol.* **2012**, 935173
5. Shinomiya, H. (2012) Plastin family of actin-bundling proteins: its functions in leukocytes, neurons, intestines, and cancer. *Int. J. Cell Biol.* **2012**, 213492
6. Arpin, M., Friederich, E., Algrain, M., Vernel, F., and Louvard, D. (1994) Functional differences between L- and T-plastin isoforms. *J. Cell Biol.* **127**, 1995–2008
7. Janji, B., Giganti, A., De Corte, V., Catillon, M., Bruyneel, E., Lentz, D., Plastino, J., Gettemans, J., and Friederich, E. (2006) Phosphorylation on Ser5 increases the F-actin-binding activity of L-plastin and promotes its targeting to sites of actin assembly in cells. *J. Cell Sci.* **119**, 1947–1960
8. Jones, S. L., and Brown, E. J. (1996) FcgammaRII-mediated adhesion and phagocytosis induce L-plastin phosphorylation in human neutrophils. *J. Biol. Chem.* **271**, 14623–14630
9. Matsushima, K., Kobayashi, Y., Copeland, T. D., Akahoshi, T., and Oppenheim, J. J. (1987) Phosphorylation of a cytosolic 65-kDa protein induced by interleukin 1 in glucocorticoid pretreated normal human peripheral blood mononuclear leukocytes. *J. Immunol.* **139**, 3367–3374
10. Klemke, M., Rafael, M. T., Wabnitz, G. H., Weschenfelder, T., Konstandin, M. H., Garbi, N., Autschbach, F., Hartschuh, W., and Samstag, Y. (2007) Phosphorylation of ectopically expressed L-plastin enhances invasiveness of human melanoma cells. *Int. J. Cancer* **120**, 2590–2599
11. Riplinger, S. M., Wabnitz, G. H., Kirchgessner, H., Jahraus, B., Lasitschka, F., Schulte, B., van der Pluijm, G., van der Horst, G., Hämmerling, G. J., Nakchbandi, I., and Samstag, Y. (2014) Metastasis of prostate cancer and melanoma cells in a preclinical in vivo mouse model is enhanced by L-plastin expression and phosphorylation. *Mol. Cancer* **13**, 10
12. Wang, J., and Brown, E. J. (1999) Immune complex-induced integrin activation and L-plastin phosphorylation require protein kinase A. *J. Biol. Chem.* **274**, 24349–24356
13. Jones, S. L., Wang, J., Turck, C. W., and Brown, E. J. (1998) A role for the actin-bundling protein L-plastin in the regulation of leukocyte integrin function. *Proc. Natl. Acad. Sci. USA* **95**, 9331–9336
14. Janji, B., Vallar, L., Al Tanoury, Z., Bernardin, F., Vetter, G., Schaffner-Reckinger, E., Berchem, G., Friederich, E., and Chouaib, S. (2010) The actin filament cross-linker L-plastin confers resistance to TNF-alpha in MCF-7 breast cancer cells in a phosphorylation-dependent manner. *J. Cell. Mol. Med.* **14**(6A), 1264–1275
15. Lin, C. S., Lau, A., and Lue, T. F. (1998) Analysis and mapping of plastin phosphorylation. *DNA Cell Biol.* **17**, 1041–1046
16. Paclet, M. H., Davis, C., Kotsonis, P., Godovac-Zimmermann, J., Segal, A. W., and Dekker, L. V. (2004) N-Formyl peptide receptor subtypes in human neutrophils activate L-plastin phosphorylation through different signal transduction intermediates. *Biochem. J.* **377**, 469–477
17. Pazdrak, K., Young, T. W., Straub, C., Stafford, S., and Kurosky, A. (2011) Priming of eosinophils by GM-CSF is mediated by protein kinase CbetaII-phosphorylated L-plastin. *J. Immunol.* **186**, 6485–6496
18. Freeley, M., O'Dowd, F., Paul, T., Kashanin, D., Davies, A., Kelleher, D., and Long, A. (2012) L-plastin regulates polarization and migration in chemokine-stimulated human T lymphocytes. *J. Immunol.* **188**, 6357–6370
19. Sever, R., and Brugge, J. S. (2015) Signal transduction in cancer. *Cold Spring Harb. Perspect. Med.* 5:a006098
20. Iqbal, N., and Iqbal, N. (2014) Human epidermal growth factor receptor 2 (HER2) in cancers: overexpression and therapeutic implications. *Mol. Biol. Int.* **2014**, 852748
21. Mok, T. S. (2011) Personalized medicine in lung cancer: what we need to know. *Nat. Rev. Clin. Oncol.* **8**, 661–668
22. Arteaga, C. L., Sliwkowski, M. X., Osborne, C. K., Perez, E. A., Puglisi, F., and Gianni, L. (2011) Treatment of HER2-positive breast cancer: current status and future perspectives. *Nat. Rev. Clin. Oncol.* **9**, 16–32
23. Vivanco, I., Robins, H. I., Rohle, D., Campos, C., Grommes, C., Nghiemphu, P. L., Kubek, S., Oldrini, B., Chheda, M. G., Yannuzzi, N., Tao, H., Zhu, S., Iwanami, A., Kuga, D., Dang, J., Pedraza, A., Brennan, C. W., Heguy, A., Liau, L. M., Lieberman, F., Yung, W. K., Gilbert, M. R., Reardon, D. A., Drappatz, J., Wen, P. Y., Lamborn, K. R., Chang, S. M., Prados, M. D., Fine, H. A., Horvath, S., Wu, N., Lassman, A. B., DeAngelis, L. M., Yong, W. H., Kuhn, J. G., Mischel, P. S., Mehta, M. P., Cloughesy, T. F., and Mellinghoff, I. K. (2012) Differential sensitivity of glioma- versus lung cancer-specific EGFR mutations to EGFR kinase inhibitors. *Cancer Discov.* **2**, 458–471
24. Libermann, T. A., Nusbaum, H. R., Razon, N., Kris, R., Lax, I., Soreq, H., Whittle, N., Waterfield, M. D., Ullrich, A., and Schlessinger, J. (1985) Amplification, enhanced expression and possible rearrangement of EGF receptor gene in primary human brain tumours of glial origin. *Nature* **313**, 144–147
25. Lee, J. C., Vivanco, I., Beroukhim, R., Huang, J. H., Feng, W. L., DeBiasi, R. M., Yoshimoto, K., King, J. C., Nghiemphu, P., Yuza, Y., Xu, Q., Greulich, H., Thomas, R. K., Paez, J. G., Peck, T. C., Linhart, D. J., Glatt, K. A., Getz, G., Onofrio, R., Ziaugra, L., Levine, R. L., Gabriel, S., Kawaguchi, T., O'Neill, K., Khan, H., Liau, L. M., Nelson, S. F., Rao, P. N., Mischel, P., Pieper, R. O., Cloughesy, T., Leahy, D. J., Sellers, W. R., Sawyers, C. L., Meyerson, M., and Mellinghoff, I. K. (2006) Epidermal growth factor receptor activation in glioblastoma through novel missense mutations in the extracellular domain. *PLoS Med.* **3**, e485
26. Hynes, N. E., and MacDonald, G. (2009) ErbB receptors and signaling pathways in cancer. *Curr. Opin. Cell Biol.* **21**, 177–184
27. Dunn, K. L., Espino, P. S., Drobic, B., He, S., and Davie, J. R. (2005) The Ras-MAPK signal transduction pathway, cancer and chromatin remodeling. *Biochem. Cell Biol.* **83**, 1–14
28. Benjamini, Y., and Hochberg, Y. (1995) Controlling the false discovery rate: a practical and powerful approach to multiple testing. *J. R. Stat. Soc. Series B Stat. Methodol.* **57**, 289–300
29. Trairatphisan, P., Mizera, A., Pang, J., Tantar, A. A., Schneider, J., and Sauter, T. (2013) Recent development and biomedical applications of probabilistic Boolean networks. *Cell Commun. Signal.* **11**, 46
30. Trairatphisan, P., Mizera, A., Pang, J., Tantar, A. A., and Sauter, T. (2014) optPBN: an optimisation toolbox for probabilistic Boolean networks. *PLoS One* **9**, e98001
31. Kao, J., Salari, K., Bocanegra, M., Choi, Y. L., Girard, L., Gandhi, J., Kwei, K. A., Hernandez-Boussard, T., Wang, P., Gazdar, A. F., Minna, J. D., and Pollack, J. R. (2009) Molecular profiling of breast cancer cell lines defines relevant tumor models and provides a resource for cancer gene discovery. *PLoS One* **4**, e6146
32. Kenny, P. A., Lee, G. Y., Myers, C. A., Neve, R. M., Semeiks, J. R., Spellman, P. T., Lorenz, K., Lee, E. H., Barcellos-Hoff, M. H., Petersen, O. W., Gray, J. W., and Bissell, M. J. (2007) The morphologies of breast cancer cell lines in three-dimensional assays correlate with their profiles of gene expression. *Mol. Oncol.* **1**, 84–96
33. Subik, K., Lee, J. F., Baxter, L., Strzepek, T., Costello, D., Crowley, P., Xing, L., Hung, M. C., Bonfiglio, T., Hicks, D. G., and Tang, P. (2010) The expression patterns of ER, PR, HER2, CK5/6, EGFR, Ki-67 and

AR by immunohistochemical analysis in breast cancer cell lines. *Breast Cancer (Auckl.)* **4**, 35–41
34. Ross, D. T., Scherf, U., Eisen, M. B., Perou, C. M., Rees, C., Spellman, P., Iyer, V., Jeffrey, S. S., Van de Rijn, M., Waltham, M., Pergamenschikov, A., Lee, J. C., Lashkari, D., Shalon, D., Myers, T. G., Weinstein, J. N., Botstein, D., and Brown, P. O. (2000) Systematic variation in gene expression patterns in human cancer cell lines. *Nat. Genet.* **24**, 227–235
35. Rae, J. M., Creighton, C. J., Meck, J. M., Haddad, B. R., and Johnson, M. D. (2007) MDA-MB-435 cells are derived from M14 melanoma cells–a loss for breast cancer, but a boon for melanoma research. *Breast Cancer Res. Treat.* **104**, 13–19
36. Hollestelle, A., Nagel, J. H., Smid, M., Lam, S., Elstrodt, F., Wasielewski, M., Ng, S. S., French, P. J., Peeters, J. K., Rozendaal, M. J., Riaz, M., Koopman, D. G., Ten Hagen, T. L., de Leeuw, B. H., Zwarthoff, E. C., Teunisse, A., van der Spek, P. J., Klijn, J. G., Dinjens, W. N., Ethier, S. P., Clevers, H., Jochemsen, A. G., den Bakker, M. A., Foekens, J. A., Martens, J. W., and Schutte, M. (2010) Distinct gene mutation profiles among luminal-type and basal-type breast cancer cell lines. *Breast Cancer Res. Treat.* **121**, 53–64
37. Chambers, A. F. (2009) MDA-MB-435 and M14 cell lines: identical but not M14 melanoma? *Cancer Res.* **69**, 5292–5293
38. Hollestelle, A., and Schutte, M. (2009) Comment Re: MDA-MB-435 and M14 cell lines: identical but not M14 Melanoma? *Cancer Res.* **69**, 7893
39. Lacroix, M., and Leclercq, G. (2004) Relevance of breast cancer cell lines as models for breast tumours: an update. *Breast Cancer Res. Treat.* **83**, 249–289
40. Zajchowski, D. A., Bartholdi, M. F., Gong, Y., Webster, L., Liu, H. L., Munishkin, A., Beauheim, C., Harvey, S., Ethier, S. P., and Johnson, P. H. (2001) Identification of gene expression profiles that predict the aggressive behavior of breast cancer cells. *Cancer Res.* **61**, 5168–5178
41. Anjum, R., and Blenis, J. (2008) The RSK family of kinases: emerging roles in cellular signalling. *Nat. Rev. Mol. Cell Biol.* **9**, 747–758
42. Eccles, S. A. (2011) The epidermal growth factor receptor/Erb-B/HER family in normal and malignant breast biology. *Int. J. Dev. Biol.* **55**, 685–696
43. Tarcic, G., Avraham, R., Pines, G., Amit, I., Shay, T., Lu, Y., Zwang, Y., Katz, M., Ben-Chetrit, N., Jacob-Hirsch, J., Virgilio, L., Rechavi, G., Mavrothalassitis, G., Mills, G. B., Domany, E., and Yarden, Y. (2012) EGR1 and the ERK-ERF axis drive mammary cell migration in response to EGF. *FASEB J.* **26**, 1582–1592
44. Amos, S., Martin, P. M., Polar, G. A., Parsons, S. J., and Hussaini, I. M. (2005) Phorbol 12-myristate 13-acetate induces epidermal growth factor receptor transactivation via protein kinase Cdelta/c-Src pathways in glioblastoma cells. *J. Biol. Chem.* **280**, 7729–7738
45. Brose, N., and Rosenmund, C. (2002) Move over protein kinase C, you've got company: alternative cellular effectors of diacylglycerol and phorbol esters. *J. Cell Sci.* **115**, 4399–4411
46. Kazanietz, M. G. (2000) Eyes wide shut: protein kinase C isozymes are not the only receptors for the phorbol ester tumor promoters. *Mol. Carcinog.* **28**, 5–11
47. Davies, S. P., Reddy, H., Caivano, M., and Cohen, P. (2000) Specificity and mechanism of action of some commonly used protein kinase inhibitors. *Biochem. J.* **351**, 95–105
48. Alessi, D. R. (1997) The protein kinase C inhibitors Ro 318220 and GF 109203X are equally potent inhibitors of MAPKAP kinase-1beta (Rsk-2) and p70 S6 kinase. *FEBS Lett.* **402**, 121–123
49. Yao, L., Fan, P., Jiang, Z., Gordon, A., Mochly-Rosen, D., and Diamond, I. (2008) Dopamine and ethanol cause translocation of epsilonPKC associated with epsilonRACK: cross-talk between cAMP-dependent protein kinase A and protein kinase C signaling pathways. *Mol. Pharmacol.* **73**, 1105–1112
50. Sugita, S., Baxter, D. A., and Byrne, J. H. (1997) Modulation of a cAMP/protein kinase A cascade by protein kinase C in sensory neurons of Aplysia. *J. Neurosci.* **17**, 7237–7244
51. Wang, W., Eddy, R., and Condeelis, J. (2007) The cofilin pathway in breast cancer invasion and metastasis. *Nat. Rev. Cancer* **7**, 429–440
52. Lewis, T. S., Hunt, J. B., Aveline, L. D., Jonscher, K. R., Louie, D. F., Yeh, J. M., Nahreini, T. S., Resing, K. A., and Ahn, N. G. (2000) Identification of novel MAP kinase pathway signaling targets by functional proteomics and mass spectrometry. *Mol. Cell* **6**, 1343–1354
53. Whyte, J., Bergin, O., Bianchi, A., McNally, S., and Martin, F. (2009) Key signalling nodes in mammary gland development and cancer. Mitogen-activated protein kinase signalling in experimental models of breast cancer progression and in mammary gland development. *Breast Cancer Res.* **11**, 209
54. Bain, J., Plater, L., Elliott, M., Shpiro, N., Hastie, C. J., McLauchlan, H., Klevernic, I., Arthur, J. S., Alessi, D. R., and Cohen, P. (2007) The selectivity of protein kinase inhibitors: a further update. *Biochem. J.* **408**, 297–315
55. Dumaz, N., and Marais, R. (2005) Integrating signals between cAMP and the RAS/RAF/MEK/ERK signalling pathways. Based on the anniversary prize of the Gesellschaft für Biochemie und Molekularbiologie Lecture delivered on 5 July 2003 at the Special FEBS Meeting in Brussels. *FEBS J.* **272**, 3491–3504
56. Hagi, A., Hirata, H., and Shinomiya, H. (2006) Analysis of a bacterial lipopolysaccharide-activated serine kinase that phosphorylates p65/L-plastin in macrophages. *Microbiol. Immunol.* **50**, 331–335
57. Sulzmaier, F. J., and Ramos, J. W. (2013) RSK isoforms in cancer cell invasion and metastasis. *Cancer Res.* **73**, 6099–6105
58. Frijns, E., Sachs, N., Kreft, M., Wilhelmsen, K., and Sonnenberg, A. (2010) EGF-induced MAPK signaling inhibits hemidesmosome formation through phosphorylation of the integrin beta4. *J. Biol. Chem.* **285**, 37650–37662
59. Li, D., Jin, L., Alesi, G. N., Kim, Y. M., Fan, J., Seo, J. H., Wang, D., Tucker, M., Gu, T. L., Lee, B. H., Taunton, J., Magliocca, K. R., Chen, Z. G., Shin, D. M., Khuri, F. R., and Kang, S. (2013) The prometastatic ribosomal S6 kinase 2-cAMP response element-binding protein (RSK2-CREB) signaling pathway up-regulates the actin-binding protein fascin-1 to promote tumor metastasis. *J. Biol. Chem.* **288**, 32528–32538
60. Ohta, Y., and Hartwig, J. H. (1996) Phosphorylation of actin-binding protein 280 by growth factors is mediated by p90 ribosomal protein S6 kinase. *J. Biol. Chem.* **271**, 11858–11864
61. Woo, M. S., Ohta, Y., Rabinovitz, I., Stossel, T. P., and Blenis, J. (2004) Ribosomal S6 kinase (RSK) regulates phosphorylation of filamin A on an important regulatory site. *Mol. Cell. Biol.* **24**, 3025–3035
62. Vial, D., and McKeown-Longo, P. J. (2012) Epidermal growth factor (EGF) regulates α5β1 integrin activation state in human cancer cell lines through the p90RSK-dependent phosphorylation of filamin A. *J. Biol. Chem.* **287**, 40371–40380
63. Gawecka, J. E., Young-Robbins, S. S., Sulzmaier, F. J., Caliva, M. J., Heikkilä, M. M., Matter, M. L., and Ramos, J. W. (2012) RSK2 protein suppresses integrin activation and fibronectin matrix assembly and promotes cell migration. *J. Biol. Chem.* **287**, 43424–43437
64. Le Goff, E., Vallentin, A., Harmand, P. O., Aldrian-Herrada, G., Rebière, B., Roy, C., Benyamin, Y., and Lebart, M. C. (2010) Characterization of L-plastin interaction with beta integrin and its regulation by micro-calpain. *Cytoskeleton (Hoboken)* **67**, 286–296
65. Zheng, J., Rudra-Ganguly, N., Powell, W. C., and Roy-Burman, P. (1999) Suppression of prostate carcinoma cell invasion by expression of antisense L-plastin gene. *Am. J. Pathol.* **155**, 115–122
66. Delanote, V., Vanloo, B., Catillon, M., Friederich, E., Vandekerckhove, J., and Gettemans, J. (2010) An alpaca single-domain antibody blocks filopodia formation by obstructing L-plastin-mediated F-actin bundling. *FASEB J.* **24**, 105–118
67. Doehn, U., Hauge, C., Frank, S. R., Jensen, C. J., Duda, K., Nielsen, J. V., Cohen, M. S., Johansen, J. V., Winther, B. R., Lund, L. R., Winther, O., Taunton, J., Hansen, S. H., and Frödin, M. (2009) RSK is a principal effector of the RAS-ERK pathway for eliciting a coordinate promotile/invasive gene program and phenotype in epithelial cells. *Mol. Cell* **35**, 511–522

Received for publication May 21, 2015.
Accepted for publication November 16, 2015.

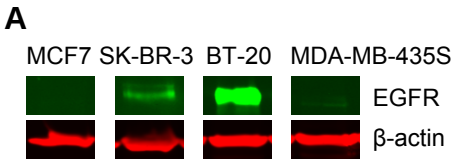

Supplemental Figure 1 Analysis of EGF-dependent L-plastin Ser5 phosphorylation. **A)** EGF receptor (EGFR) is expressed in SK-BR-3 and BT-20 breast cancer cell lines. Cell extracts were subjected to immunoblot analysis using antibodies specific for the EGFR and β-actin, used as a loading control. **B)** Cells were stimulated for 15 min with different EGF concentrations as indicated and cell extracts were subjected to immunoblot analysis using antibodies specific for Ser5 phosphorylated L-plastin or total L-plastin.

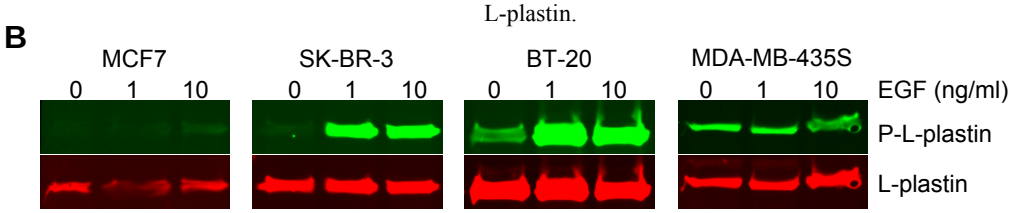

Supplemental Figure 2 Optimized interactions' weights for the L-plastin signaling network. Bootstrapping was performed by randomly sampling 100 artificial data sets based on means and standard deviations as acquired from the experimental data. Optimization was subsequently performed 100 times to identify the distribution of the identified selection probabilities. Means and standard deviations of the interactions' weights were compared among the four cell lines.

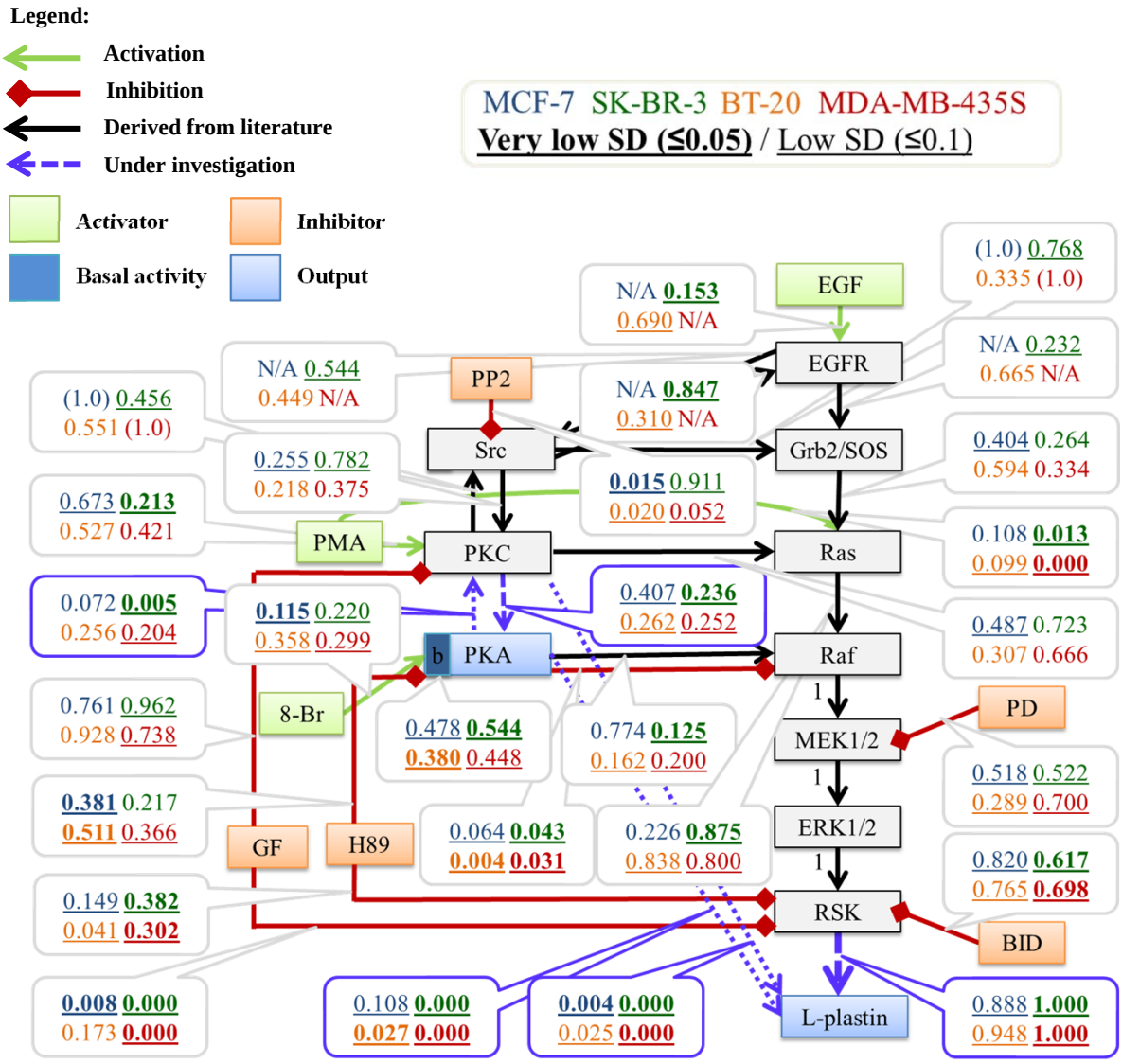

Supplemental Figure 3

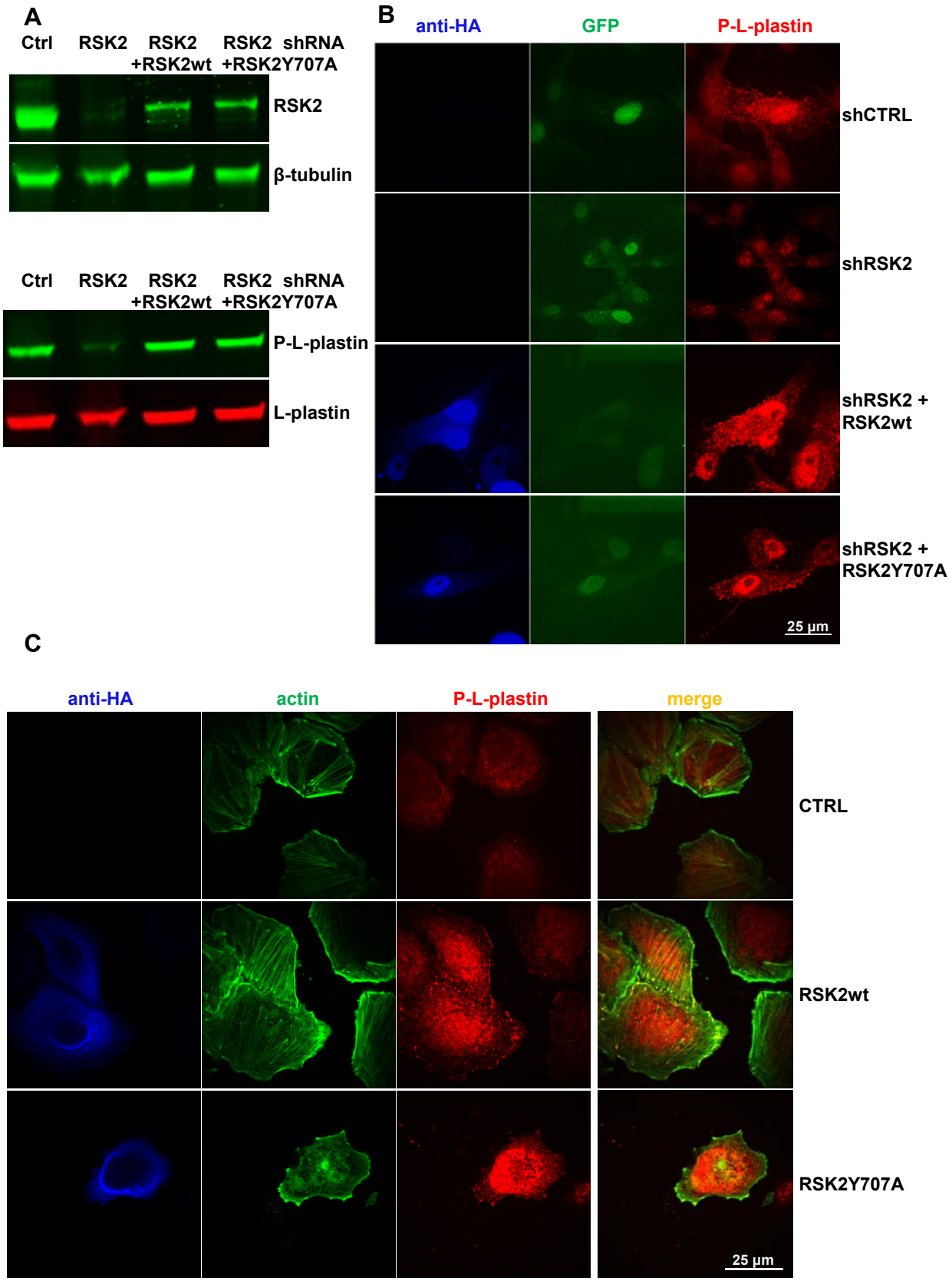

Supplemental Figure 3 Overexpression of RSK2 leads to increased L-plastin Ser5 phosphorylation and to its redistribution to migratory structures. A) MDA-MB-435S cells were transduced with lentiviral particles containing shRNA for RSK2 or non-silencing shRNA as a control. The transduced cells were selected with puromycine in complete medium. Cells were subsequently transfected with RSK2wt or constitutively active RSK2Y707A and the levels of RSK2 and L-plastin Ser5 phosphorylation were determined by immunoblot analysis. B) MDA-MB-435S cells expressing a non-silencing control shRNA or RSK2-targeting shRNA were plated on fibronectin-coated coverslips and transfected with HA-tagged RSK2wt or RSK2Y707A. The coverslips were fixed 48 h after transfection and subsequently stained with an antibody specific for Ser5 phosphorylated L-plastin (anti-Ser5-*P* antibody, P-L-plastin) and with an anti-HA tag antibody to monitor the transfected cells. GFP-positive cells express the corresponding shRNA. Cells were then analyzed by confocal microscopy. The scale bar shown represents 25 μm. C) SK-BR-3 cells were plated on fibronectin-coated coverslips and transfected with HA-tagged RSK2wt or RSK2Y707A. The coverslips were fixed 48 h after transfection and subsequently stained with an antibody specific for Ser5 phosphorylated L-plastin (anti-Ser5-*P* antibody, P-L-plastin), with an anti-HA tag antibody to monitor the transfected cells and with phalloidin. Cells were then analyzed by confocal microscopy. The scale bar shown represents 25 μm.

Survival curves for L-plastin (LCP1)

PhD Thesis - Maiti Lommel

Analysis of signal transduction pathways linking L-plastin Ser5 phosphorylation to breast cancer cell invasion

The following survival curves were generated using the online Kaplan-Meier Plotter tool (www.kmplot.com):

Gyorffy B, Lanczky A, Eklund AC, Denkert C, Budczies J, Li Q, Szallasi Z. An online survival analysis tool to rapidly assess the effect of 22,277 genes on breast cancer prognosis using microarray data of 1809 patients, Breast Cancer Res Treatment, 2010 Oct;123(3):725-31.

Overall survival curves for LCP1, including 1117 patients

P value: 0.063

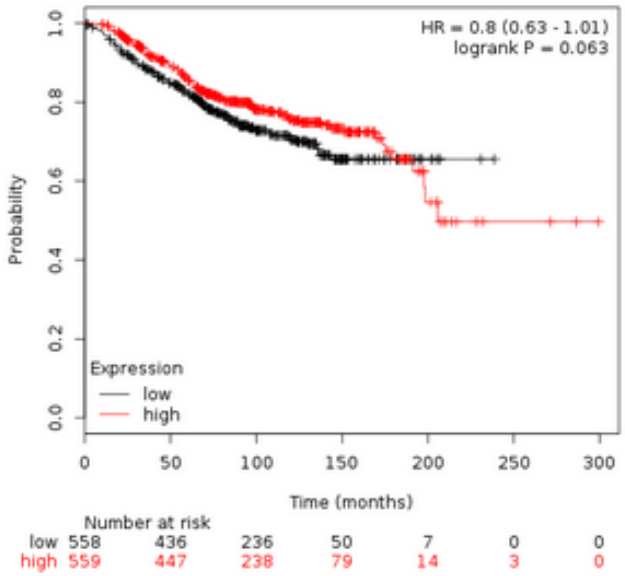

Affymetrix ID:	208885_at	LCP1, CP64, LC64P,
Survival:	OS	
Split patients by:	median	
Follow up threshold:	all	
Censore at threshold:	checked	
Compute median over entire database:	false	
Cutoff value used in analysis:	1049	
Expression range of the probe:	151 - 9043	
Probe set option:	user selected probe set	
Invert HR values below 1:	not checked	

Restrictions

ER status:	all
derive ER status from gene expression data:	not checked
PR status:	all
HER2 status:	all
Lymph node status:	all
Intrinsic subtype:	all
TP53 status:	all
Grade:	all
Use earlier release of the database:	2014 version (n=4142)
Use following dataset for the analysis:	all

Quality control

Remove redundant samples:	checked
Array quality control:	exclude biased arrays
Proportional hazards assumption:	checked

Cohort

Cohorts: not selected

Relapse-free survival curves for LCP1, including 3557 patients

P value: 0.1798

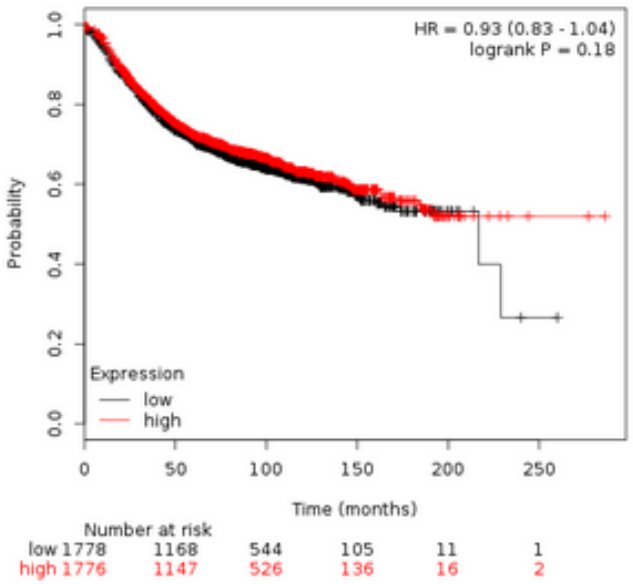

Affymetrix ID:	208885_at	LCP1, CP64, LC64P, ...
Survival:	RFS	
Split patients by:	median	
Follow up threshold:	all	
Censore at threshold:	checked	
Compute median over entire database:	false	
Cutoff value used in analysis:	1018	
Expression range of the probe:	71 - 13217	
Probe set option:	user selected probe set	
Invert HR values below 1:	not checked	

Restrictions

ER status:	all
derive ER status from gene expression data:	not checked
PR status:	all
HER2 status:	all
Lymph node status:	all
Intrinsic subtype:	all
TP53 status:	all
Grade:	all
Use earlier release of the database:	2014 version (n=4142)
Use following dataset for the analysis:	all

Quality control

Remove redundant samples:	checked
Array quality control:	exclude biased arrays
Proportional hazards assumption:	checked

Cohort

Cohorts: not selected

Distant metastasis-free survival curves for LCP1, including 1610 patients

P value: 0.1633

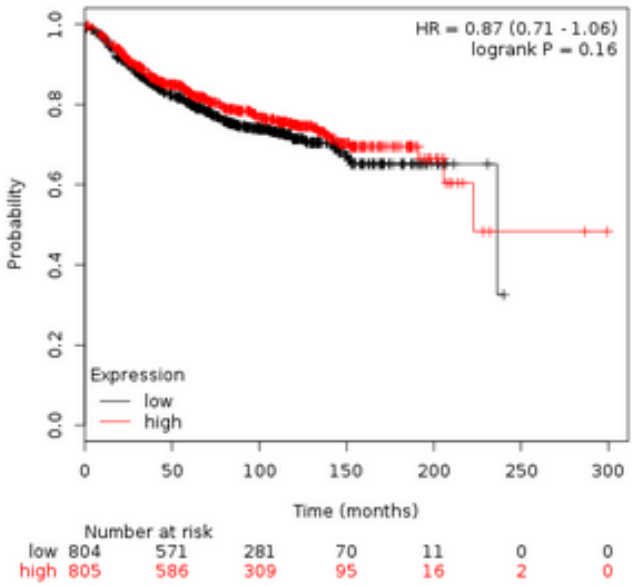

Affymetrix ID:	208885_at	LCP1, CP64, LC64P, ...
Survival:	DMFS	
Split patients by:	median	
Follow up threshold:	all	
Censore at threshold:	checked	
Compute median over entire database:	false	
Cutoff value used in analysis:	1025	
Expression range of the probe:	71 - 13217	
Probe set option:	user selected probe set	
Invert HR values below 1:	not checked	

Restrictions

ER status:	all
derive ER status from gene expression data:	not checked
PR status:	all
HER2 status:	all
Lymph node status:	all
Intrinsic subtype:	all
TP53 status:	all
Grade:	all
Use earlier release of the database:	2014 version (n=4142)
Use following dataset for the analysis:	all

Quality control

Remove redundant samples:	checked
Array quality control:	exclude biased arrays
Proportional hazards assumption:	checked

Cohort

Cohorts: not selected

Supplemental *in vitro* kinase assay data

PhD Thesis - Maiti Lommel

Analysis of signal transduction pathways linking L-plastin Ser5 phosphorylation to breast cancer cell invasion

First run

	Wild type (WT) *ARGSVSDEERR		Mutant (MT) *ARGSVADEERR		Mutant with initiator methionine (M-MT) MARGSVADEERR	
Ranking	Kinases	Counts (cpm)	Kinases	Counts (cpm)	Kinases	Counts (cpm)
1	RSK2	116698	RSK1	55774	RSK1	135794
2	PKAca	109766	PKAca	53986	MSK1	129651
3	RSK1	101952	MSK1	53254	RSK2	115547
4	MSK1	86947	RSK2	48800	PKAca	97124
5	RSK3	71917	PKAcb	34148	PKAcg	94447
6	PKAcb	54673	PKAcg	33572	SGK2	82033
7	RSK4	45174	RSK3	32917	RSK3	81498
8	PKAcg	40167	PRKG2	26041	PKAcb	66998
9	SGK3	32646	RSK4	22477	PRKG2	46081
10	SGK2	32129	SGK2	22249	RSK4	44022
11	PRKG2	29921	SGK3	20290	SGK3	43761
12	PKCh	29273	STK33	10761	AURORA B	26998
13	p70S6Kb	19894	PKCh	10007	PKCh	19741
14	AURORA B	12688	AURORA B	9696	PKCq	18726
15	STK33	9990	PRKG1	9110	PRKG1	17159
16	PKCq	9671	PRKX	8113	STK33	11019
17	VRK1	9054	DCAMKL1	5899	PKCe	10347
18	PRKX	8310	VRK1	5745	PRKX	10004
19	PRKG1	8189	VRK2	5470	PKCd	7763
20	CAMK1b	8126	MNK1	5430	MNK1	7224
21	VRK2	7876	PKCe	5053	CAMK4	6258
22	CAMK4	6955	CAMK4	4668	SGK1	6216
23	PKCe	6779	DCAMKL2	4447	DCAMKL1	6179
24	DCAMKL2	5726	p70S6Kb	4242	p70S6Kb	6088
25	MNK1	5718	CAMK1b	3996	DCAMKL2	5788
26	DCAMKL1	5437	NDR	3797	VRK1	5346
27	NDR	5072	PKCq	3589	AKT1	5038
28	PKCd	4597	IKKe	3422	NDR	4478
29	PIM2	4405	NDR2	3284	CAMK1b	4072
30	SGK1	4243	ASK1	2771	IKKe	3956
31	NDR2	3821	SGK1	2540	NDR2	3458
32	MSK2	3741	PKCd	2329	AKT3	3102
33	IKKe	3437	AKT1	1920	VRK2	3090
34	AKT1	3257	p70S6K	1911	AURORA C	2777
35	ASK1	3241	PIM2	1813	ASK1	2713
36	PIM3	2732	PIM3	1537	MSK2	2496
37	p70S6K	2454	AKT3	1460	PIM3	2139
38	AKT3	2196	AKT2	1242	p70S6K	2075
39	AKT2	2142	MSK2	1005	PIM2	2011
40	PIM1	892	PIM1	922	AKT2	1525

41	CK2a2	892	AURORA C	663	PIM1	1083
42	AURORA C	588	CHK1	256	CHK1	830
43	CHK1	176	CK2a2	44	CK2a2	202

Second run with 12 selected kinases from the first run

	Wild type (WT) *ARGSVSDEERR		Mutant (MT) *ARGSVADEERR		MT with initiator methionine (M-MT) MARGSVADEERR		WT with initiator methionine (M-WT) MARGSVSDEERR	
Ranking	**Kinases**	**Counts (cpm)**	**Kinases**	**Counts (cpm)**	**Kinases**	**Counts (cpm)**	**Kinases**	**Counts (cpm)**
1	RSK1	115889	RSK1	63496	RSK1	141297	RSK1	272191
2	RSK2	70341	PKAca	38409	PKAca	62897	RSK2	153281
3	PKAca	63735	RSK2	27985	RSK2	61065	PKAca	144318
4	PKAcb	52764	PKAcb	27511	PKAcb	54069	PKAcb	106928
5	SGK3	28710	SGK3	19745	SGK3	40186	MSK1	76195
6	RSK3	27353	MSK1	17742	MSK1	39916	SGK3	74101
7	MSK1	25077	RSK3	14042	RSK3	32396	RSK3	59572
8	PKAcg	13848	PKAcg	12524	PKAcg	25959	SGK2	32246
9	SGK2	10796	SGK2	7878	SGK2	21964	PKAcg	31010
10	STK33	7143	STK33	7104	STK33	8209	PKCh	17918
11	VRK2	2065	PKCh	2545	PKCh	2443	STK33	14074
12	PKCh	1631	VRK2	2013	VRK2	2024	VRK2	13082

N.B. The *in vitro* kinase assay screen was performed by KINEXUS